

**ADVANCED
TECHNOLOGY
LABORATORIES**

SEPARABLE CONNECTOR DESIGN HANDBOOK
(TENTATIVE)

EDITED BY
F. O. RATHBUN, JR.

Contract NAS 8-4012

December 1, 1964

277

REPRODUCED BY
NATIONAL TECHNICAL
INFORMATION SERVICE
U. S. DEPARTMENT OF COMMERCE
SPRINGFIELD, VA. 22161

GENERAL  ELECTRIC

(NASA-CR-64944) SEPARABLE CONNECTOR
DESIGN HANDBOOK (TENTATIVE) (General
Electric Co.) 269 p

N74-76953

00/99 Unclas
52401

NOTICE

THIS DOCUMENT HAS BEEN REPRODUCED FROM THE BEST COPY FURNISHED US BY THE SPONSORING AGENCY. ALTHOUGH IT IS RECOGNIZED THAT CERTAIN PORTIONS ARE ILLEGIBLE, IT IS BEING RELEASED IN THE INTEREST OF MAKING AVAILABLE AS MUCH INFORMATION AS POSSIBLE.

SEPARABLE CONNECTOR DESIGN HANDBOOK (TENTATIVE)

CONTRACT NAS 8-4012

Design Criteria
For Zero Leakage Connectors
For Launch Vehicles

Edited by
F. O. Rathbun, Jr.

Prepared for
PROPULSION AND VEHICLE ENGINEERING DIVISION
GEORGE C. MARSHALL SPACE FLIGHT CENTER
NATIONAL AERONAUTICS AND SPACE ADMINISTRATION
HUNTSVILLE, ALABAMA

Prepared by
Advanced Technology Laboratories
General Electric Company
Schenectady, New York

Sponsored by
Missile and Space Division
General Electric Company
Philadelphia, Pennsylvania

NASA Technical Manager
C. C. Wood (M-P&VE-PT)

December 1, 1964

PREFACE

By

L. G. Gitzendanner

The purpose of this handbook is to aid in the design and/or selection of separable fluid connectors. Since fluid connectors must be designed for handling various fluids, for a large range of temperatures, for a range of pressures, and for various environmental conditions, there can be many designs for connectors. However, it is possible to present the basic approach that one may follow in designing or selecting a connector for a particular application. Discussion of the phenomena associated with connectors is included to help the designer avoid oversights, be able to better judge the cause and nature of past difficulties, and, in general, to better appreciate the fundamentals involved.

The Connector Design Handbook is divided into seven chapters. Chapter 1, "Fundamental Considerations of Separable Connector Design," presents a general discussion of the problems to be considered in separable connector design and is based on the laws of physics and an appreciable amount of experimental data.

Chapters 2 and 3, "Flanged Connector Design" and "Threaded Connector Design," give specific design procedures for establishing the geometric dimensions of separable connectors. Design examples, which illustrate the step-by-step mathematical manipulations necessary to finalize a design, are included in each chapter. The design and analysis equations given are based on an elastic stress analysis and have been checked for accuracy within the limitations of the physical assumptions. While ultimate verification of the procedures must await repetitive application of the procedures for a multitude of sizes, pressures, and temperatures, the procedure has been used to effect one threaded connector design (for 4700 psi, 1440°F service) and four possible flange configurations for a ten inch connector (750 psi, 700°F).

Chapter 4, "Pressure-Energized Cantilever Seals and Hollow Metallic O-Rings," also based on elastic stress analyses, gives detailed equations and nomographs for direct and final design of cantilever-type pressure-energized seals. Equations for determining the displacement characteristics of hollow metallic O-rings are also presented.

Chapter 5, "Leakage Measurement Techniques," presents techniques and standards for the determination of the leakage characteristics of fluid connectors under development. The procedures outlined have proven successful over a period of two and one half years in a fluid connector development program.

Material properties useful to a designer are given in Chapter 6, "Material Properties and Compatibility." Included are the mechanical properties of elastomers, plastics, and some structural materials. Compatibility of materials with typical contained fluids is also discussed. This chapter should be a convenient reference for the more commonly required information. All data listed is from accredited sources which are referenced.

Chapter 7, "Catalog of Seals," lists seal configurations and materials particularly applicable to aerospace applications. Each entry is based on experimental results obtained using the leakage test procedures given in Chapter 5. As new configurations are proven and new materials are shown to be successful, additional entries can be made in this catalog.

It is believed that employment of the fundamental considerations listed and use of the analysis and design procedures given will result in connectors which will satisfy most requirements. Where unusually mild or unusually severe environments, or other extreme requirements are included, it may be advantageous or necessary to develop modifications to the equations and procedures, in which case an understanding of the principles underlying the procedures given will be helpful.

The Handbook is at present considered "tentative" in that insufficient use has been given its contents to date. When the applicability and utility of the various procedures have been proven by usage, the volume will be considered "final." Comments pertinent to the contents of the Handbook should be directed to Mr. C.C. Wood, M-P&VE-PT, Marshall Space Flight Center, National Aeronautics and Space Administration, Huntsville, Alabama.

TABLE OF CONTENTS

<u>Section</u>	<u>Page</u>
1	FUNDAMENTAL CONSIDERATIONS OF SEPARABLE CONNECTOR DESIGN . . . 1-1
1.0	Introduction - Formulation of the Fluid Connector Problem 1-1
1.1	Modes of Leakage 1-1
1.2	Surface Deformation of Materials at the Seal Interface 1-4
1.3	Development of Leakage 1-9
1.4	References 1-11
2	FLANGED CONNECTOR DESIGN 2-1
2.0	Introduction 2-1
2.1	Design Procedure 2-5
2.2	Flanges with No Contact Outside the Gasket Circle . . . 2-9
2.3	Integral Flange - Contact Outside Bolt Circle 2-27
2.4	Loose Flange - No Contact Outside Bolt Circle 2-35
2.5	Loose Flange - Contact Outside Bolt Circle 2-43
2.6	Other Configurations 2-47
2.7	Other Analytical Methods 2-49
2.8	References 2-50
2.9	Appendices 2-51
2.10	Design Examples 2-63
2.11	Nomenclature 2-103
3	THREADED CONNECTOR DESIGN 3-1
3.0	Selection of Connector 3-1
3.1	Design Requirements 3-1
3.2	Connector Configuration 3-3
3.3	Seal 3-3
3.4	Attachment to Tubing 3-4
3.5	Flange 3-5
3.6	Union 3-7
3.7	Nut 3-8
3.8	Preload 3-11
3.9	Stress Analysis 3-18
3.10	Testing 3-30
3.11	Appendix 3-30
3.12	References 3-65
3.13	Nomenclature 3-66
4	PRESSURE-ENERGIZED CANTILEVER SEALS AND HOLLOW METALLIC O-RINGS 4-1
4.0	Introduction 4-1
4.1	Types of Seals Considered 4-1
4.2	Details of Design 4-3

<u>Section</u>		<u>Page</u>
4.3	References	4-22
4.4	Nomenclature	4-23
5	LEAKAGE MEASUREMENT TECHNIQUES	5-1
5.0	Introduction	5-1
5.1	Leakage Measurement Requirements	5-1
5.2	Test Apparatus	5-1
5.3	Calibration of Mass Spectrometer Leak Detector	5-4
5.4	Procedures	5-4
5.5	Safety Precautions	5-5
5.6	Other Environments	5-5
5.7	Leakage Detection Testing	5-5
5.8	Other Leak Detection Techniques	5-6
6	MATERIAL PROPERTIES AND COMPATIBILITY	6-1
6.1	References	6-7
7	CATALOG OF SEALS	7-1
7.0	Introduction	7-1
7.1	Seal Classification and Data	7-2

LIST OF TABLES

<u>Table</u>	<u>Page</u>
1.1 Metal Gaskets - Required Sealing Stresses	1-6
1.2 Metal-to-Metal Systems - Required Sealing Stresses	1-7
2.1 Estimation of Bolt Size and Number of Bolts	2-15
2.2 Approximate Friction Coefficients	2-17
2.3 Estimation of Lap and Loose Flange Dimensions	2-36
2A.1 Results - Internal Loads and Displacements	2-100
2A.2 Stresses in Pipe and Hub	2-101
3.1 Recommended Buttress Thread Sizes	3-8
3.2 Format for Compilation of Stress Calculations	3-28
3.3 Format for Optimization of Connector Design for Most Severe Operating Condition	3-29
3.4 Operating Conditions for High-Temperature Connector	3-48
3.5 Approximate Dimensions Used to Initialize the Iterative Design Procedures	3-51
3.6 Dimensions, Physical Constants and Loads Used in the Final Set of Calculations for the Vibration Condition	3-52
3.7 Shell Equation Constants for Use in Coefficient Calculations	3-53
3.8 Coefficients for Nut Spring Constant Calculations	3-53
3.9 Deflections Rotations, Forces, and Moments in Nut Due to a Unit Force	3-54
3.10 Coefficients for Flange and Union Simultaneous Equations	3-55
3.11 Deflections, Rotations, Forces and Moments for the Flange and the Union for Total Stress Calculation	3-56
3.12 Compilation of Stress Calculations for Vibration Test Condition -Total Stresses	3-57
3.13 Compilation of Stress Calculations for Vibration Test Condition - Fatigue Analysis	3-57
6.1 Metallic Material Properties	6-2

<u>Tables</u>		<u>Page</u>
6.2	Organic Material Properties	6-3
6.3	Effect of Temperature on Ultimate Tensile Strength	6-4
6.4	Nominal Chemical Composition	6-5
6.5	Chemical Compatibility of Candidate Tube and Duct Materials with Some Rocket Propellants	6-6

LIST OF ILLUSTRATIONS

<u>Figure</u>	<u>Page</u>
1.1 Typical Leakage -- Sealing Stress Curve	1-7
1.2 Typical Shear Deformation Geometry	1-9
2.1 Bolt Clearances	2-16
2.2 Double-Taper Hub Initial Dimensions	2-16
2.3 Approximate Hub by a Small Number of Cylindrical Segments . .	2-20
2.4 Flange Ring Below Line of Action of Bolt Load	2-22
2.5 Integral Flange Connector with Contact Outside Gasket Circle .	2-28
2.6 Loose Flange - No Contact Outside Bolt Circle	2-36
2.7 Loose Flange - With Contact Outside Bolt Circle	2-44
2.8 Other Connector Configurations	2-48
2A Pipe Deformation Sign Conventions and Symbols	2-51
2B Pipe Segment Sign Conventions and Symbols	2-52
2C Ring Segment Sign Conventions and Symbols	2-53
2D Bolt Geometry, Loads, and Deformations	2-58
2E Gasket Geometry, Loads, and Deformation	2-58
2F Cylindrical Segment Showing Loads and Dimensions	2-61
2G Ring Segment Showing Loads and Dimensions	2-62
2H Bolt Geometry and Loading	2-62
2I Preliminary Design. Integral Flanges - No Contact Outside Bolt Circle	2-68
2J Preliminary Design. Integral Flanges - With Contact Outside Bolt Circle	2-72
2K Preliminary Design. Loose Flanges - No Contact Outside Bolt Circle	2-76
2L Preliminary Design. Loose Flanges - With Contact Outside Bolt Circle	2-80

<u>Figure</u>	<u>Page</u>
2M Preliminary Design. Integral Flanged Connector - No Contact Outside Bolt Circle - Both Flanges Identical	2-82
2N Mathematical Model of Preliminary Flange Design Shown in Figure 2M	2-83
3.1 Typical Connector Configuration	3-3
3.2 Connector-to-tubing Weld	3-4
3.3 Flange Elements	3-6
3.4 Union Dimensions	3-7
3.5 Nut Configuration	3-10
3.6 Separation of Nut for Structural Analysis	3-13
3.7 Separation of Flange and Union for Structural Analysis	3-16
3.8 Location of Flange Stresses Calculated	3-20
3.9 Location of Union Stresses Calculated	3-22
3.10 Location of Nut Stresses Calculated	3-25
3.11 Values of K_1	3-42
3.12 Values of K_2	3-43
3.13 Values of K_3	3-44
3.14 Values of K_4	3-45
3.15 Values of K_5	3-46
3.16 Values of K_6	3-47
3.17 High-temperature Tube Connector	3-60
3.18 Union (Material René 41)	3-61
3.19 Flange (Material René 41)	3-62
3.20 Nut (Material René 41)	3-63
3.21 Triangle Seal (Material Nickel 200)	3-64
4.1 Cantilever Seal Configuration	4-2
4.2 Cantilever Seal - Loaded	4-5

<u>Figure</u>		<u>Page</u>
4.3	Cantilever Seal - Angled	4-6
4.4	Tapered Cantilever Seals	4-8
4.5	Angled Cantilever Seal without Tip	4-9
4.6	Nomograph -- Straight Cantilever Seal Design - $\phi = 0$. . .	4-10
4.7	Nomograph -- Straight Cantilever Seal Design - $\phi = \phi$. . .	4-11
4.8	Nomograph -- Straight Cantilever Seal Design - $\phi = \phi$. . .	4-12
4.9	Nomograph -- Straight Cantilever Seal Design - $\phi = \phi$. . .	4-13
4.10	Nomograph -- Straight Cantilever Seal Design - $\phi = \phi$. . .	4-14
4.11	Nomograph -- Cantilever Seal Design -- Varying Thickness . .	4-15
4.12	Nomograph -- Cantilever Seal Design -- Varying Thickness . .	4-16
4.13	Nomograph -- Cantilever Seal Design -- Varying Thickness . .	4-17
4.14	Nomograph -- Cantilever Seal Design -- Varying Thickness . .	4-18
4.15	O-Ring Designs	4-21
5.1	Tube Vacuum Chamber	5-8
5.2	High-pressure System	5-9
5.3	Leak Detector - Vacuum System	5-10
7.1	Typical Leakage - Normal Stress Response for Superfinished 347 Stainless Steel Seal	7-5
7.2	Load-Deflection Characteristics for Typical Metal Shear O-Ring Seal	7-14
7.3	Typical Leakage - Applied Load Response for Metal Shear O-Ring Seal	7-15
7.4	Load-Deflection Curve for Copper O-Ring	7-18
7.5	Knife-Edge Seal - Load-Deflection Curve for Aluminum Gasket With Inner Space Ring	7-21
7.6	Knife-Edge Seal - Load-Deflection Curve for Aluminum Gasket Without Spacer Ring	7-22
7.7	Triangle Seal - Load-Deflection Curve for Aluminum Gasket . .	7-25

Section 1

FUNDAMENTAL CONSIDERATIONS OF SEPARABLE CONNECTOR DESIGN

by

F. O. Rathbun, Jr.

1.0 Introduction - Formulation of the Fluid Connector Problem

The problems of designing a separable fluid connector are: 1) those of selecting suitable materials and geometry for effecting a seal, and 2) designing a supporting structure which will force the sealing surfaces together, and hold them together under the operating environment and intended life, such that the leakage will remain under a tolerable amount. A given separable fluid connector design can be evaluated by consideration of the following three factors:

1. The leakage rate through the connector under operational conditions.
2. The size and weight of the connector as compared to the pipe section which the connector replaces.
3. The reliability of the connector in maintaining its initial sealing characteristics throughout its operational life.

1.1 Modes of Leakage

The total amount of leakage flow through any separable connector is the sum of the leakage flows by the following three phenomena - permeation through the component materials, flow through component materials having porosity, and flow through the interface between mated components.

1.1.1 Permeation Flow and Porosity

While some gasses will permeate some structural materials which may be used either for piping or tubing or the connector itself, the rate of this flow is usually negligible in connector design. Permeation may be a problem, however, where elastomeric materials or plastics are used to make the seal interface, either as gaskets, or as materials coated on the structural parts. In the case of elastomeric materials, the permeation rate is usually not too severe. Plastics, however, can be subject to significant permeation by several gases. The total permeation flow through the plastic used should be calculated based on the geometry and the permeation constant for that material and gas. The total permeation rate can easily be of the same order of magnitude as the maximum total leakage rate which can be tolerated, in which case it may be desirable or necessary to consider other seal geometries or other gasket materials.

The leakage due to permeation can be calculated from:

$$Q = PA \frac{\Delta p}{L} \quad (1.1)$$

where Q is measured in atm cc/sec, P is a permeation rate constant for the gas and solid material in question ($\text{cm}^3 - \text{mm}/\text{sec} \text{ cm}^2 - \text{atm}$), A is the normal flow area (cm^2), L is the length of flow path, (mm), and Δp is the pressure differential across the seal, (atm). The permeation constant P, which is temperature dependent, is presented for various combinations of gases and solids in Refs. 1.2 and 1.4. Values of P for metals and most gases are below 10^{-8} . Values of P for elastomers and plastics with helium as the gas range from 4×10^{-4} to less than 10^{-7} .

While leakage flow is possible due to porosity of the materials, flow of this kind is not considered as a design parameter. Usually in design, materials are selected which presumably are not porous, or porosity has been sealed off. However, it may be necessary to check for quality; leakage due to porosity can be found where proper care is not taken. For example, welds are designed to be sound metal, but porosity is sometimes found. Laminated materials are often filled or impregnated to avoid leakage due to porosity, but may leak due to poor quality control at some stage.

1.1.2 Flow Through The Sealing Surface Interface

The most serious leakage flow which exists in separable connectors is that which occurs due to a lack of proper mating between the sealing surfaces. A fundamental separable connector design problem is that of insuring that the sealing surfaces are in adequate contact to preclude large rates of flow by this mode.

1.1.2.1 Liquid Interface Leakage Flow

1.1.2.1.1 Viscous Flow

While it is possible for a seal containing a liquid to be subject to a leak path large enough to allow the liquid to flow and reach the external edge of the leak in liquid form, if the rules governing fluid connector design for containment of a gaseous fluid are met, then this problem will not arise.

1.1.2.1.2 Internal Liquid Leaking In Gaseous State

While a tank or a duct may be designed to contain a liquid, that fluid may exist in a gaseous state within the system. Such may exist within the tank or duct during various stages of the fluid consumption or it may exist at various points along the leak path. This phenomenon is dependent on the temperature and the vapor pressure of that fluid. When such is possible, the type gaseous flow possible will be dictated by the size of the leak and of the pressure ratio across the leak path and the flow may be estimated using information given in Section 1.1.2.2.

1.1.2.2 Gaseous Leak Modes

1.1.2.2.1 Molecular Flow

Where the smallest dimension descriptive of the cross-sectional area of a leak path is small in comparison with the mean free path of the gas leaking through the path, then the flow will be molecular. For the dimension representative of the cross-sectional area to be of this magnitude, the leak path cross-section must be extremely small; hence, molecular leakage exists generally for extremely low flow rates. As an order of magnitude molecular flow leakage in practical connector designs could probably be 10^{-6} atm cc/sec or less. During the molecular flow regime, the leakage rate is proportional to the pressure difference existing across the leak path.

At the lower limit of molecular flow, the smallest leak path dimension characterizing the cross-sectional area becomes of the same order of magnitude as the gas molecule. At this point, molecular blockage occurs.

As the smallest leak path dimension becomes large in comparison to the mean free path of the gas in question, viscous flow commences. The regime existing between pure molecular flow and viscous flow is called transition flow.

1.1.2.2.2 Viscous Flow

When the leak path is large enough for viscous flow to exist, the fluid flow through the leak is at first laminar in nature. The flow follows the leak path rather smoothly and is proportional to the difference between the square of the internal pressure and the square of the external pressure. While there is no single leakage rate at which laminar flow begins, generally when the rate reaches 10^{-6} atm cc/sec the flow is laminar.

The flow rate of a gas leaking radially between two flat annular plates, where both laminar and molecular effects are considered, is given by:

$$Q = 13.79 \times 10^{-11} \frac{Wh^3 (\Delta p) \bar{p}}{\mu \ell} \left[1 + 6.383\epsilon \frac{\bar{\lambda}}{h} \right] \quad (1.2)$$

where

- Q = leakage, atm cc/sec
- W = mean perimeter of annulus, inches
- h = clearance between plates, microinches
- Δp = pressure difference across seal, atmosphere
- \bar{p} = mean pressure, $[p_{int} + p_{ext}] / 2$, atmosphere
- μ = absolute viscosity of gas, centipoises
- ℓ = width of the plates (radially), inches
- ϵ = molecular correction factor, dimensionless
(~ 0.9 for a single gas, ~ 0.66 for a mixed gas such as air)
- $\bar{\lambda}$ = mean free path of the gas molecules at the mean pressure, \bar{p} , microinches

Charts showing the clearance h as a function of the pressure differential for several flow rates are given in Ref. 1.3.

For a given gas, as the gas velocity and/or the characteristic dimension of the leak path become larger, the flow ceases to be laminar in nature and becomes turbulent. During this flow regime the flow rate is also proportional to the difference between the internal pressure squared and the external pressure squared, but does not vary with dimensions in the same manner as does laminar flow.

1.2 Surface Deformation of Materials at the Seal Interface

Of the several leakage modes described above, many may occur in series or in parallel in any connector interface. Since each of the materials to be pressed together has a distribution of asperities existing initially on its surface, and since these asperities will be deformed in a manner dependent on the sealing load, the distributions of asperities, the yield stress of the materials in question, and the strain hardening characteristics of the materials, the resultant leak paths at any stage of this compression are extremely difficult to describe and will probably vary in size and shape greatly. The goal in pressing the surfaces together is, of course, to produce a degree of mating such that no leak paths exist when the compression process has been completed. Given that each of the surfaces in question has some asperity distribution on it, each distribution varying in magnitude and direction and type, the exact resultant leak paths for a given set of parameters is impossible to predict. However, some generalities, helpful in the description and understanding of the process, can be made. Metals, plastics, and elastomers behave differently from one another, and must be considered separately.

1.2.1 Metal-to-Metal Sealing

Five regimes of material deformation can be envisioned, and an expected diminution of leakage rate associated with each. Little analytical work has been done on regimes I, III, and V, however; regime II and IV have been investigated. Analytical studies of individual asperity deformation (Refs. 1.5 through 1.8; and studies of bulk flow of compressed materials (Refs. 1.9 and 1.10) have been made.

1.2.1.1 Regime I

Any metal surface, whether it be machined, ground, lapped, or diamond burnished, will have surface asperities existing on it. Most machining or grinding techniques tend to make most of the asperities of generally uniform height. There will always exist, however, a certain number of the asperities that are higher than the mean values. When two surfaces having such distributions are brought together, they will initially touch each other on the higher-than-average asperities. These asperities will be local in nature and will not cause appreciable barriers to fluid flow. As a normal force presses the surfaces together, the stress on the few asperities which are touching will be extremely high and they will deform readily. As the asperities are deformed, initial contact between other asperities occurs until the tops of the asperities of average height have come into contact. The first phase of material deformation, therefore, is the mating and deformation of the extremely high asperities. During this regime of material flow, the two surfaces will move together under extremely low nominal sealing stresses.

During this regime, however, little decrease in fluid flow between the surface can be expected; leakage will generally be excessive for a connector design.

1.2.1.2 Regime II

After the peaks of the most dominant size of asperity on each surface have come into contact, the next increment of material deformation is the plastic deformation of individual asperities as they mate with those asperities immediately opposite. The equilibrium stress level on each asperity during this regime of deformation will be between two and three times the yield stress of the weaker material, depending on the asperity shape. As long as the pile-up of material from one asperity does not significantly interfere with the material pile-up from adjacent asperity deformation, the increase in area of contact between the two surfaces will be linear with the increase in normal load. During this regime of material deformation, it can be expected that the leakage rate will be reduced drastically with the ever increasing area of contact.

1.2.1.3 Regime III

As the load is further increased, the material that is piled-up between asperities radically effects the deformation. As that material pushed to the side from the reduction in height of one asperity interferes with the similar material from the adjoining asperity, a further resistance to material flow occurs. The response of the total deformation process is less the product of asperity deformation than the product of a complex stress field in the bulk material. This complexity is further complicated by whatever strain hardening characteristics the material in question may have. This regime, which is called the transition regime, may occur when stress levels in the bulk material are not high enough to cause bulk flow of the material. It would be expected that during this regime of material flow the increase in area of contact as a function of normal load would be less than that in the previous regime. In common with this, the reduction in leakage may not be as great as in the previous regime.

1.2.1.4 Regime IV

During the previous three regimes of material deformation, stresses in the bulk of the material were not high enough to cause bulk flow of that material. When the stress field in the solid is sufficient to produce yielding in a large portion of the material, drastic geometrical deformations will occur. In the case of flat gaskets, this deformation resembles very closely that of the Prandtl plastic flow problem. Surface shear stresses tend to reduce the bulk flow during this regime. Where the deformable material is in a flat gasket form, or in any shape that will allow the material to slide along the surface with which it is mating, a further decrease in leakage can be expected due to the shear deformation. Where no increase in apparent area is effected by bulk flow of the material, this phenomenon is not useful. Where the materials to be mated are structural parts of the fluid connector, and no replaceable gasket exists, bulk flow of the material should be avoided.

1.2.1.5 Regime V

Where the material in question is a gasket material, the bulk flow will continue without appreciable increases in the ratio of true area of contact to leave in until such time as the stress in the structural sealing surface is enough to cause bulk flow of that material. This case should always be avoided since it will adversely affect the reuseability of the connector. When plastic deformations occur in structural members which may not be mated exactly the same way in a following application, the response of the connector in its second application cannot be expected to be the same as in its first application.

1.2.1.6 Required Sealing Stress

As is indicated in Sections 1.2.1.1 through 1.2.1.5, the mechanism of developing mating between metal surfaces is complex. It has been found, however, that sealing generally occurs within a reasonably predictable range of stress. Even though the leak rate depends on numerous parameters such as seal width, initial roughnesses of the surfaces, properties of the materials, etc., it has been found that the leak rate decreases precipitously as the average stress over the seal area reaches a critical value. For systems having flat metal gaskets pressed between two harder sealing surfaces and systems employing two metal surfaces pressed directly together, the critical value of stress is usually between 1.5 and 2.5 times the yield strength of the softer sealing face material.

Typical values of critical stresses obtained experimentally on a one-inch diameter seal, one-eighth-inch wide are given in Tables 1.1 and 1.2. From the figures given therein, it can be stated that, for most designs, a stress of 2.75 times the yield stress of the softer material would be conservative. Although all data except that associated with the radially ground surface would indicate a lower required stress level, the value of 2.75 is given in that the unintentional radial scratch or scratches would promote a situation much the same as the radially ground case. It is noted that such a surface would never intentionally be produced for a sealing system.

Table 1.1

METAL GASKETS - REQUIRED SEALING STRESSES

Sealing Surface Finish	Required Stress
Diamond Burnished, $\sim 4 \mu$ -in, rms	1.96 σ_y
Radially Ground $\sim 40 \mu$ -in, rms	2.75 σ_y
Fine Circumferential Machining (100 μ -in rms)	1.46 σ_y
Course Circumferential Machining (300 μ -in rms)	1.96 σ_y

Table 1.2

METAL-TO-METAL SYSTEMS - REQUIRED SEALING STRESSES

Sealing Surface	Required Stress
Radially Ground $\sim 40\mu\text{-in, rms}$	$2.3 \sigma_y$
Circumferentially Machined $\sim 100\mu\text{in, rms}$	$0.63 \sigma_y$

While the stress levels appear lower in the case where no gaskets are used, it must be remembered that these stress levels produce local plastic deformations on the surfaces of the materials. Experiments show that, upon re-use, the stress levels required will not be the same as those used initially. In the case of the radial ground surfaces the required sealing stress may reach 2.8 times the yield strength. For the circumferentially machined surface, the second sealing stress may reach 1.3 times the yield strength.

A typical curve of leakage rate versus initial sealing stress is shown in Figure 1.1. The shape and location of the curve is, of course, a function of the material properties and the sealing-surface finish.

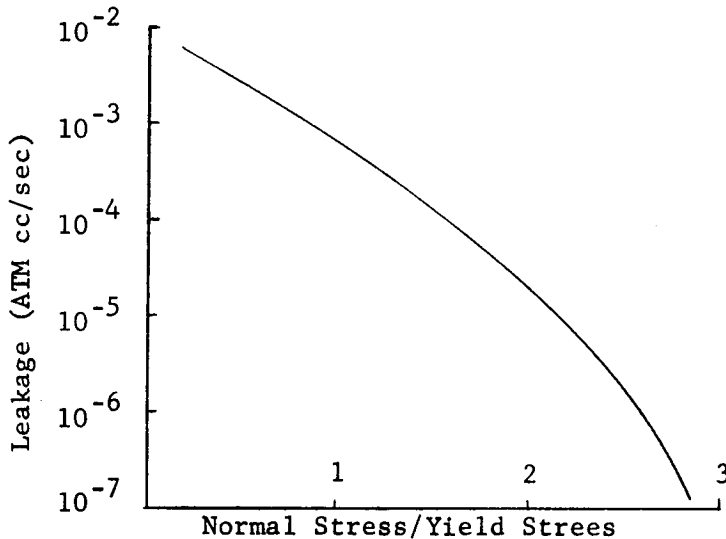


Figure 1.1. Typical Leakage - Sealing Stress Curve.

The stress levels listed in the tables are the result of experiments conducted on flat annular gaskets of a given size. Since the leakage considered covers a range of seven decades, the change in required stress due to change in diameter of the seal is considered negligible. Extrapolation of the data to gasket widths which deviate greatly from one-eighth inch will not completely insure satisfactory sealing. However, for widths less than one-eighth inch, the problem of random scratches across the gasket width arises and the probability that the listed stress levels will be adequate decreases with decreasing gasket widths.

The stress level listed is that stress applied normally to the gasket or sealing surface which will insure a leak rate less than 10^{-6} atm cc/sec across the pressure differential of one atmosphere. The stress levels are completely empirical in nature and are not the results of an elastic or plastic stress analysis. For use with pressure differentials up to eighty atmospheres, it has been experimentally shown that an increase in stress of 25% of the yield strength of the weaker material involved will be adequate.

For the several metal gaskets employed in experiments which yield these results, the sensitivity of the required sealing stress on the strain hardening characteristics of the metals was not significant. If a material which work hardens appreciably, such as soft nickel, is used, a higher factor times initial yield stress may be needed.

1.2.2 Surface Deformation of Soft Plastic Sealing Materials

Whereas in metal gasketing materials, the surface finish is of considerable importance, the surface finish on a soft plastic material to be mated with a metal surface is less important. The loads applied to the plastics are generally such that the plastic will assume the shape of the stronger material very closely. The deformation in the plastic is of a viscoelastic nature to the extent that without proper constraint, the phenomenon of cold flow exists and can cause a design to be unsatisfactory.

The stresses required on plastic gaskets are considerably less than those required on metal gaskets. The reason for this is that a different mode of material deformation takes its place in plastic materials; the material deforms viscoelastically. In general, stress levels of approximately 0.7 times the yield strength of the plastic used will be sufficient to impose a seal. Plastics also are quite insensitive to removal of the normal stress. However, in that the phenomenon of cold flow occurs, (the continuing deformation of the material under stress with time), the reliability a plastic has as a gasketing material can not be assured unless the bulk flow of the gasket is precluded by proper geometric constraints.

1.2.3 Interface Sealing with Elastomeric Materials

Elastomers deform to mate with rigid surfaces by large elastic deformations. Regardless of the surface finish on which the elastomer rests, the required sealing stress is extremely small. Since the deformation of the gasket is almost entirely elastic, the load required to compose a seal must be maintained. If a far greater load than is required is imposed upon the system, then the excess increment of load can be allowed to be lost during the life of the gasket. Where elastomers can be used as gasketing materials, and not precluded for compatibility reasons, they provide seals which require extremely low stresses. Absolute stresses as low as 500 psi are adequate, generally, to effect a seal.

1.2.4 Sealing by Shear Deformation of Elastic-Plastic Materials

The yielding necessary for the production of a seal by putting into extremely close contact two material surfaces is caused, not by a high compressive stress alone, but by a combination of stresses existing in the material to be deformed. If the yield stress condition can be obtained in

a manner that causes the soft material to strain in shear at its surface against the opposite surface, then fresh surfaces on the softer material will be formed and a much tighter mating can be accomplished for a given level of applied force (Figure 1.2). Knife edges, shear O-rings, and geometries of components which cause high stress concentration factors can be used to accomplish this.

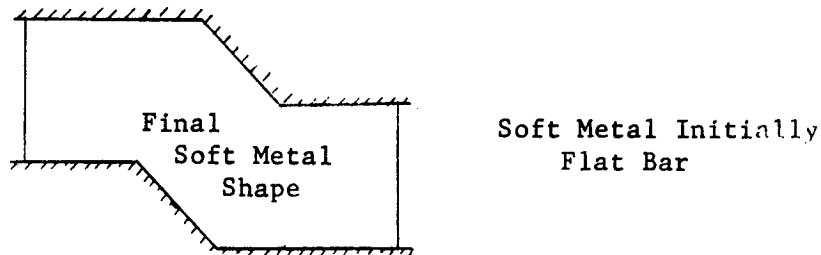


Figure 1.2. Typical Shear Deformation Geometry

1.3 Development of Leakage

Once the problem of achieving two surfaces to be in close enough proximity to close the leakage paths is solved, the problem becomes one of maintaining this state during the life of the connector. In order to design the connector such that leakage will not develop, it is necessary to understand how such leakage could develop in a connector. Basically, two means of leakage development are possible: 1) the reduction of the stress between the mated parts can become so large that a gap opens between the surfaces; or 2) a lateral shift can occur between the sealing surfaces, (thus either shearing off previously mated asperities or laterally moving one asperity away from that with which it was mated).

1.3.1 Reduction of Normal Load

1.3.1.1 Loading on Connector

Loads may be imposed on the connector due to vibration, shock, internal fluid pressure thermal distortion of the system, and initial misalignment. Such loads reduce the effective sealing force and must be considered in calculating whether the minimum permissible sealing force will be met at all times. In general, the more plastic deformation has taken place in the seal interface area, the less sensitive (with regard to leakage) the system is to load removal. In some cases the system is almost completely insensitive to load removal. However, where specific data on load removal sensitivity is not available, as a rule of thumb, the minimum permissible load may be taken as about two-thirds the load required to develop the seal initially.

1.3.1.2 Relaxation

While all stress parts tend to flow and relax the stresses present, at moderate stress levels and in the normal room temperature range, the rate is so small that it is usually neglected. However in a connector, the seal area at least will involve material that is highly stressed, and stress relaxation may become a problem even at normal temperatures. If in addition the connector

is to experience greatly elevated temperatures, then almost certainly relaxation will exist and the life of the connector will be limited.

The problem of estimating relaxation for components subjected to multi-axial stresses, including dynamic as well as static effects, is quite complex.

Dynamic relaxation of stress, caused by the superposition of an alternating stress on an already highly stressed area, can be severe in the seal itself where highly stressed materials are necessary. The amount of relaxation possible due to a vibration environment can be appreciable if the static stress is above the yield stress and the material possesses a stress-strain relationship not completely linear below the yield point. Investigations of this phenomenon are now in progress.

1.3.2 Shifting of Sealing Surfaces

If the two opposing surfaces which are mated to form a seal (or which rest on both sides of a separate gasket) move laterally with respect to one another, the possibility of breaking the seal exists. Either the gasket material will follow its own surfaces in contact with mated surfaces, or sliding will occur at the interface. If sliding occurs, then the microscopic asperity contact which had been effected is lost, at least temporarily. The most probable cause of this negative effect is that of the response of the structural members during a temperature cycle. Should the sealing surfaces each have different coefficients of thermal expansion, then exceedingly high differences in strains will occur and a break in the seal may follow. Should the sealing surfaces be of different temperatures, or merely have different geometries during similar thermal profiles, large differences in strains are possible. Such is true for both quasi-static thermal temperature profiles and thermal transients. Experiments are now being done to investigate this.

1.3.3 Changes in Material Properties

1.3.3.1 Decomposition of Elastomers in High Vacuums

While most elastomers offer excellent properties for fluid seals under many conditions, several elastomers prove extremely unreliable when subjected to a hard vacuum environment over long periods. Hard vacuums cause elastomers to deteriorate and their plasticizers to volatilize. When this occurs, the elastic properties of the material will be lost; at the same time the elastomers lose weight and become porous; the result is that they permanently deform when distorted between surfaces, and can not be used to forcibly close the seal interface between those surfaces. This phenomenon occurs at vacuum levels below 2×10^{-7} mm Hg. It has been noted that butyl rubber loses 31% of its weight at a 2×10^{-8} mm Hg. vacuum over an extended period. Since vacuum levels can reach 10^{-15} mm Hg. in space, each elastomer used must be evaluated with this in mind and a seal life extrapolated from such data (Ref. 1.1).

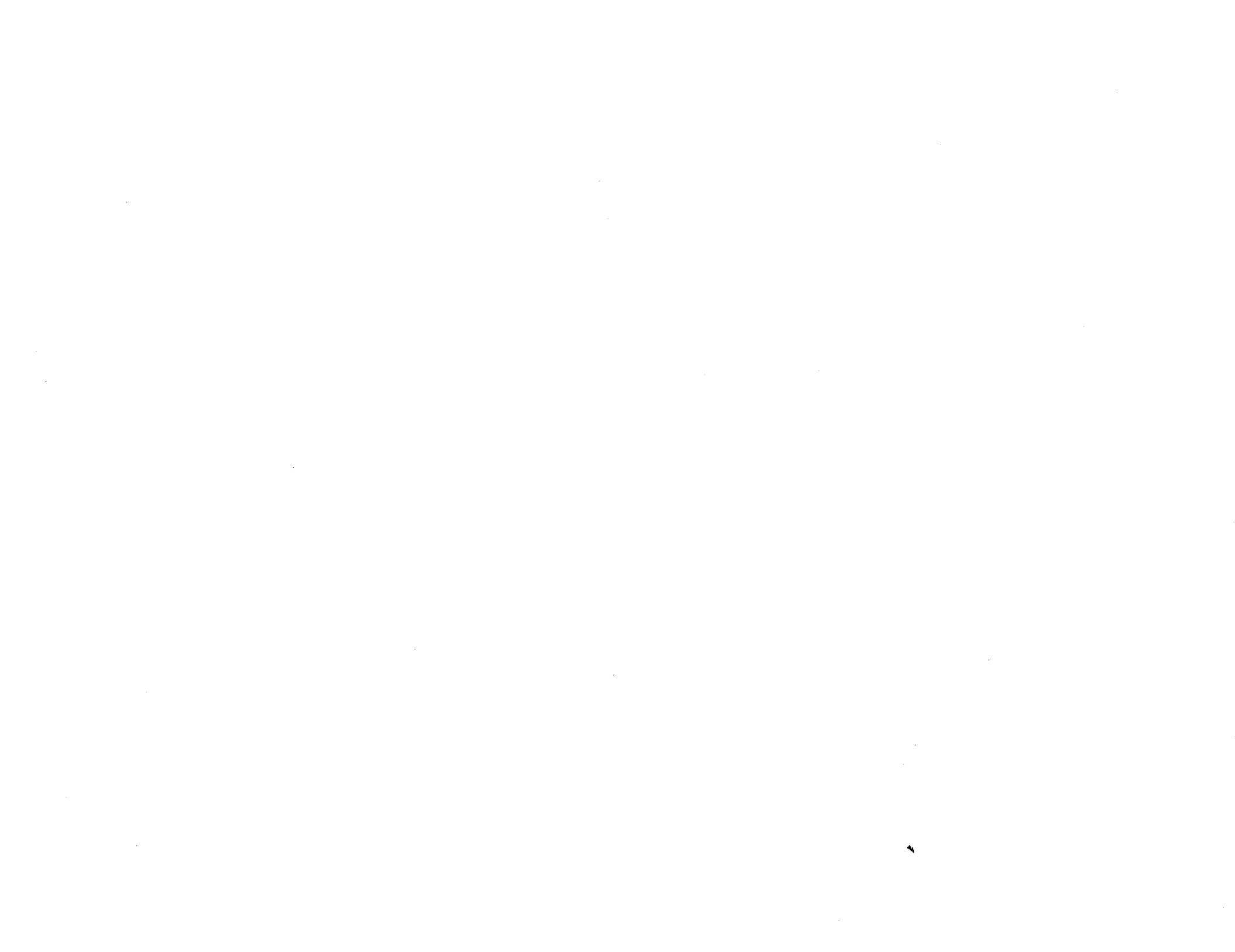
1.3.3.2 Galvanic Corrosion

In the cases where the two connector sealing surfaces or the sealing surfaces and the gasket are made from dissimilar metals, the possibility of galvanic corrosion exists, depending on the relative location of each metal in the electromotive series of metals. One of the metals (the more active)

may go into solution if the interface between the two metals is in the presence of an aqueous solution. In most cases, such would not be intentional. However, each combination used should be evaluated in the light of this possibility, and appropriate steps taken to preclude the phenomenon.

1.4 References

- 1.1 Rosine, L. L., (Editor), Advances in Electronic Circuit Packaging, Volume 3, Plenum Press, New York, 1963.
- 2.1 Rathbun, F.O., Jr., (Editor), "Sealing Action of the Sealing Interface", Design Criteria for Zero-Leakage Connectors for Launch Vehicles, Vol. 3, (NASA Contract Nos. 8-4012, N63-18159, NASA-CR-50559).
- 3.1 Rathbun, F.O., Jr. (Editor), "Fundamental Seal Interface Studies and Design and Testing of Tube and Duct Separable Connectors", Design Criteria for Zero-Leakage Connectors for Launch Vehicles, December 1963, (NASA Contract No. 8-4012).
- 4.1 Elwell, R.C., (Editor), "Studies of Special Topics in Sealing", (NASA Contract Nos. 7-102, N63-19498, NASA-CR-50662), 2 July 1963.
- 5.1 Hill, R., The Mathematical Theory of Plasticity, Oxford Press.
- 6.1 Grunzweig, J., Longman, I.M., and Petch, N.J., "Calculations and Measurements on Wedge-Indentation", Journal of the Mechanics and Physics of Solids, Vol. 2, 1954.
- 7.1 Hill, R., Lee, E.H., and Tupper, S.J., "The Theory of Wedge Indentation of Ductile Materials", Proceedings of the Royal Society, Vol. 188A, 1947.
- 8.1 Hodge, P.G., Jr., "Approximate Solutions of Problems of Plane Plastic Flow", Journal of Applied Mechanics, 1950.
- 9.1 Nye, J.F., "Experiments on the Plastic Compression of a Block Between Rough Plates", Journal of Applied Mechanics, 1952.
- 10.1 Hill, R., Lee, E.H., Tupper, S.J., "A Method of Numerical Analysis of Plastic Flow in Plane Strain and Its Application to the Compression of a Ductile Material Between Rough Plates", Journal of Applied Mechanics, 1951.



Section 2

FLANGED CONNECTOR DESIGN

by

S. Levy

2.0 Introduction

This Section presents a more rigorous way of analyzing flanged connectors than has commonly been used in the past. It obtains a more complete picture of how stresses and deformations are distributed and thus makes possible better optimization. It provides a detailed design procedure for lap flanges. It also makes use of more criteria for acceptability of a particular design than has been done heretofore. Although this portion of the Handbook has been carefully assembled many of the features are new, and therefore should be considered preliminary until experience and use confirm or modify the procedure presented.

The analytical procedures indicate new configurations which show advantages over present configurations for some applications. Some of these configurations are described in Section 2.6, pages 2 - 54.

The basic analytical procedure presented in this Section makes use of equilibrium and compatibility conditions to obtain a solution. In the appendices, Section 2.9, the basic formulas are presented in a form best adapted to connector analysis. These formulas are adapted to either hand or digital computer computation. Where a computer is to be used exclusively, an energy approach is simpler. To this end, Section 2.7 (page 2 - 57) shows techniques for programming a computer for an energy analysis of connectors.

Preliminary design procedures are presented for each basic type of connector so that the trial configuration can be a fair approximation to the final design. Since these procedures necessarily make fixed assumptions regarding the distribution of redundant loads, they must be considered as giving only an approximation to the best configuration, and may indeed be unconservative.

The effects of frictional forces at the gasket, between loose and lap flanges, and elsewhere, are taken into account. Since gasket sliding is a major consideration if "zero leakage" is a design goal, it is felt that this mechanism must be considered. Friction elsewhere has marked effects on the sealing force at the gasket and thus also effects leakage performance.

The effects of eccentric loading on the bolts is included in the analysis. This factor is an important consideration in choosing between flanges having no contact outside the bolt circle and those having such contact.

2.0.1 When To Use Flanged Connectors

Flanged connectors are used for joining larger sizes of pipes while tube connectors are used for smaller sizes. Ordinarily the change over from one type to the other occurs at a diameter of about one inch. The transition is dictated by torque requirements on the bolts. If flanged connectors are used for very small pipes the bolts become too small for reliable torquing. On

the other hand if a tubing connector were used for very large pipes, the wrenches would need to be unreasonably large. In very high-pressure systems the axial loads are so high that the transition from tube to flange connectors might occur at sizes below one inch; while, with very low pressures the size could be somewhat greater than one inch.

2.0.2 Material Choice for Flanged Connectors

Materials for use in flanged connectors must first be selected on the basis of their compatibility with the fluids being transferred. Secondly, they must have an appropriate strength at the temperatures and other environmental conditions to which they will be subjected. Finally, weight, weldability, low expansion coefficient, low creep, corrosion resistance, ease of machining, fatigue strength, ductility, stiffness, etc., may be important material considerations in a particular design. Necessary information on materials of interest in fluid connector design is provided in Section 6 of this Handbook.

Selection of flange materials for connectors used in missiles has in the past largely been limited to stainless steels and aluminum alloys. Bolt and loose flange materials need not have as great a compatibility with missile fluids and therefore offer a greater range of selection.

Where the gasket is not a vendor item, it is recommended that tests be performed to determine the seating and minimum operating gasket forces. Where sealing is the result of plastic flow of the gasketing material, a sealing stress of about 2.75 times the yield stress is indicated in Section 1 (page 1-6), "Fundamental Considerations of Separable Connector Design." To keep bolt forces low, therefore, it is desirable that the gasket be thin. Ordinarily once a "seal" has been made, the gasket force may be reduced up to about half (the exact value of the reduction will depend on the sealing mechanism and is best determined by test) before its ability to maintain "zero leakage" is lost. This consideration governs the seal width since the initial gasket force must be large enough so proof and operating loads do not reduce it below the minimum value permitted.

Where sealing is achieved by mating surfaces whose finish is in the micro-inch range, the material selection should emphasize wear resistance. Thus the loss in finish, with repeated use and with the "working" which accompanies assembly as well as temperature and pressure changes, will be minimized.

Lubricants to reduce the coefficient of friction between bolt and nut, and at other contact points, are important because variability in this factor is a primary source of variability in the force at the gasket to achieve sealing. The lubricant should be selected to be compatible and to give the lowest possible friction coefficients between rubbing parts.

2.0.3 Environmental Conditions

Some of the environmental conditions to which a fluid connector is subjected primarily affect the material properties or the material integrity. These include:

- a. Chemical interaction; i.e., LOX sensitivity or corrosion resistance.
- b. Radiation

- c. Temperature; i.e., change in mechanical properties with temperature or loss of heat treatment, etc.

Other environmental conditions also cause the connector to deform. These include:

- a. Fluid pressure.
- b. Axial load or bending moment on pipe.
- c. Thermal expansion.
- d. Creep
- e. Vibration, shock, water-hammer.

The first group of environmental conditions primarily affect material selection, while the second group primarily affect the detailed geometric design.

2.0.4 Interaction of Flanges and Seal

The choice of a seal determines the assembly preload and the load to be maintained under various operating conditions. Shear O-rings, knife edges, and other wedging-type seals, as compared with flat gaskets, permit about twice as large a ratio between the gasket load at assembly and when operating. Pressure-energized seals, such as the metal O-ring or the Naflex types, are ordinarily contained so that the primary load path bypasses the seal. Such seals place limits on the permissible flange separation at the seal and may also place limits on the permissible relative radial "scrubbing" between flanges.

For flange re-usability it is important that the seal material be softer than the flange material. Surface finish of the flange at the gasket has a moderate effect on the gasket force required for sealing.

Where welding, or some other manufacturing process, is expected to result in a small lack of flange flatness, variable flange rolling or variable gasket compression must make up the difference.

2.0.5 Input Parameters Needed by Flange Designer

The flanges will be subjected to bolt forces, gasket forces, pressure, and pipe forces. The pipe forces include not only the hydrostatic end load from internal pressure but also axial load and bending moment from the pipe supports, Ref 2.3, or from vibration, shock or water-hammer, Ref 2.1. For purposes of design, it will often be adequate to combine the pipe forces into an "equivalent" axisymmetric axial load causing axial pipe stresses equal to the maximum axial fiber stress under the actual axial load (including hydrostatic end load) plus twice the bending moment. (The doubling of the bending effect is an estimate based on the results on pages 47-49 of Ref 2.3 which show a factor of one is unconservative).

In addition to loads, the flange designer must know the operating pressures and temperatures and the time over which satisfactory performance must be maintained.

Combining this information with a knowledge of the fluids, special environmental factors, and re-usability requirements, the flange designer can

select materials and proceed with a detailed design of the flanges.

The input parameters required are therefore:

- a. Pipe size and fluid identification.
- b. Pipe axial load and bending moment.
- c. Fluid pressure-temperature-time history.

2.0.6 Flange Type

A floating (or loose) flange is used when it is necessary to join sections of pipe for which it is not possible to be sure the bolt holes of adjoining flanges will line up.

No contact outside the bolt circle has been standard practice in the ASME codes. Occasionally it is found desirable, however, to have contact outside the bolt circle. Typical cases are:

- a. Where a pressure energized seal is being used and such a configuration provides convenient containment for the seal as well as preventing flange rolling.
- b. Where internal pressure is low and the pipe wall is so thin that it affords little restraint to flange rolling.
- c. Where control of gasket thickness is good enough to provide the planned sharing of bolt load between the gasket and the contact outside the bolt circle.
- d. Where floating flanges might roll excessively.

In the case where the flanges are in contact outside the bolt circle, there is little flange rolling and therefore the bolts are loaded more squarely. This effect permits the use of bolt loads closer to the yield stress times the root cross-sectional area than the 25 percent permitted in the ASME code in the case of flanges with no contact outside the bolt circle. The decreased bolt size permits smaller flange dimensions when there is contact outside the bolt circle.

Present design experience with flanges having contact outside the bolt circle is insufficient to provide a simple guide to predict when they may be preferable to those having no such contact. In the cases listed above it appears to be desirable to perform design studies with both types.

2.0.7 Organization of Section 2

After selecting the flange type, steps in the flange design will be considered in the following sequence:

- a. Selection of materials for the flanges, bolts, and gaskets.
- b. Identification of design values for gasket forces, internal pressure, temperature, and pipe loads for assembly, proof test, and various operating conditions.

- c. Determination of mechanical property values for the materials taking account of the effect of temperature and time under load.
- d. Estimation of a preliminary design layout.
- e. Calculation of stresses and deformations for the preliminary design.
- f. Modification of the design to bring stresses and deformations to design values.

2.0.8 Limitations of Section 2

The analysis is based on linear elastic theory. Therefore, no account is taken of localized yielding which may result from the addition of design stresses to the residual stresses which may have been left during flange manufacture. In the case of ductile materials, it may frequently be desirable to apply initial high bolt forces causing some yielding in the hub region. When the bolt force is released the resulting residual stress pattern may be such that the creep resistance is improved at lower bolt loads, Ref 2.6. The analysis given here applies only after this initial yielding has taken place.

Creep is not considered directly in Section 2. Instead, it is taken into account to a limited degree by using reduced values of allowable stresses. Creep will be more pronounced in highly stressed areas, so that some redistribution of stress will occur. It is recommended that the reduced value of stress, if any, be that for which a 10 percent relaxation of stress will occur during the time the connector is subjected to surge pressure at temperature. Since only localized areas of the connector are at maximum stress, this requirement should result in a much smaller reduction in bolt and gasket loads in the connector, probably less than five percent.

2.1 Design Procedure

Design procedures for axisymmetric flanged connectors are presented in various standards, in ASME papers, Ref 2.4, and in the Taylor Forge Bulletin, Ref 2.2. These procedures embody a number of rational formulas together with design rules and approximations based on past experience.

Perhaps the most significant difference imposed by launch vehicle use is that "zero leakage" must be maintained whereas previously it was sufficient to prevent "large scale leakage". From the point of view of flange design, this means that a substantial gasket load is required even at the highest pressures. A second difference is that the temperature range is wider from cryogenic values to those for hot gases. A third difference is that weight is a far more important requirement for missile applications than it would be for connectors used on the ground. A fourth difference is that dynamic forces in a missile apply substantial loads to the connector. Finally, it is likely to be more difficult to retighten bolts and thus compensate for creep effects.

The design procedure presented herein will have fewer approximations in the formulas than those given previously and will include design rules based on

launch vehicle experience. The computations will determine deformations as well as stresses since in some cases excessive deformation is the reason for poor performance. A detailed design procedure is presented here for lap flanges; whereas, in the past these were frequently "estimated" with resulting excessive deformations and stresses.

2.1.1 Material Properties

Compatibility with the fluid is a primary requisite of the flange material. Table 6.5 in Section 6 of this manual provides information on the chemical compatibility of various flange materials with propellants in a static environment. It can be used as an indicator of the materials having the best probability of being compatible in the presence of abrasion or other severe mechanical environments.

Mechanical properties are given in Tables 6.1 to 6.3 of Section 6. Table 6.3 shows, for example, that in the 1500°F temperature range only nickel alloys and stainless steels have suitable properties. Table 6.1 shows that, at room temperature, aluminum alloys are quite competitive on a strength/weight basis.

Not all materials are suitable for use at cryogenic temperatures since they may become too brittle or experience phase transformations that make them unsuitable. Some steels, for example, become unsuitable at as high a temperature as 0°F, with the 300 series of stainless steels conditionally suitable at cryogenic temperature. Nickel alloys and aluminum alloys are suitable for service at liquid helium temperatures.

2.1.2 Design Loads

Maximum and minimum gasket forces for zero leakage must ordinarily be obtained empirically. If the gasket is a vendor item, the manufacturer can frequently provide values. Factors affecting the gasket force are the gasket material, the surface finish of the flanges, and the flange contour, i.e. flat or knife-edges. On the basis of limited results in Section 1.2.1.6 it appears that flat gaskets require stresses of about 2.75 times the yield stress to achieve "zero leakage". The gasket force can then be reduced roughly a third before the "zero leakage" state is lost. (With knife-edge type gaskets the permissible reduction is closer to two-thirds). The initial gasket load must be large enough so that the application of pressure and pipe loads will not reduce it below the limiting minimum value.

Pressure energized gaskets are usually "contained". As a result there will be flange-to-flange contact. In such a case the force at the flange-to-flange contact can drop to nearly zero without impairing the gasket performance.

Internal pressure is zero during assembly. During proof test it will be 1.5 times the maximum operating pressure, in the absence of other specifications. The connector must also withstand all pressure and temperature combinations anticipated during its service life. Pressure surges can cause increased momentary pressure in the pipe line when valves are opened, Ref 1, Chapter 62. Although these might, under adverse circumstances, double the pressure, it seems that in general a 50 percent increase is a generous design margin for this purpose.

Pipe load is ordinarily considered to be the result of hydrostatic end force in the case of ground installations. In a launch vehicle system, however, it can also be affected by relative displacement of the pipe supports during launch vehicle flexing and by dynamic forces resulting from vibration or shock. Ref 2.1, Chapter 63, shows that dynamic forces of 50 to 100 times the static forces due to gravity can be expected. Thus, it is important to place pipe supports close enough to keep the static forces due to gravity at low levels. In the absence of other specifications, it will be assumed in this handbook that the pipe supports are placed closely enough to prevent the dynamic forces from adding a load having an effect greater than that of the hydrostatic end force. In the absence of specific surge information, fluid surging will be considered able to add 50 percent to the pressure. Thus, the design value of the internal pressure and equivalent pipe load is taken as,

$$p = 1.5 p_{\text{max.oper.}} \text{ during operation with surges (lb/in.}^2\text{)}$$

$$P = 2.5 \pi R^2 p_{\text{max.oper.}} \text{ during operation with surges (lb.)}$$

(Note: In these equations the 0.5 factor is for a nominal surge factor of 50 percent. With specific surge information this factor should be replaced by the actual value)

For pipe with less than 1.5" O.D.

$$p = 2.0 p_{\text{max.oper.}} \text{ during proof test (lb/in.}^2\text{)}$$

$$P = 2.0 \pi R^2 p_{\text{max.oper.}} \text{ during proof test (lb.)}$$

$$p = 4.0 p_{\text{max.oper.}} \text{ during burst test (lb/in.}^2\text{)} \quad (2.1)$$

$$P = 4.0 \pi R^2 p_{\text{max.oper.}} \text{ during burst test (lb.)}$$

For pipe with greater than 1.5" O.D.

$$p = 1.5 p_{\text{max.oper.}} \text{ during proof test (lb/in.}^2\text{)}$$

$$P = 1.5 \pi R^2 p_{\text{max.oper.}} \text{ during proof test (lb.)}$$

$$p = 2.5 p_{\text{max.oper.}} \text{ during burst test (lb/in.}^2\text{)}$$

$$P = 2.5 \pi R^2 p_{\text{max.oper.}} \text{ during burst test (lb.)}$$

$$p_{\text{max.oper.}} = \text{maximum operating internal pressure (lb/in.}^2\text{)}$$

In Eq.2.2, the bending moment effect is doubled in line with the results in Chapter 47 of Ref 2.3.

No additional margin is added above the added 50 percent required for surges during operation and 100 percent (Eq. 2.2) required for dynamic loads. These added loads are present for only a short portion of the life of the connector and thus provide a substantial margin to cover creep, fatigue, thermal transients, etc.

Creep is presently not well understood. It may have a significant effect

when surge pressure is present for long time periods at high temperature. To remove the effects of early creep, the practice of retightening the bolts over a period of several days after initial assembly is recommended. In the case of ductile flange materials it is sometimes advantageous to initially tighten bolts enough to cause some yielding at the hub-flange junction and thereby achieve a more favorable residual stress distribution, Ref 2.6. Such procedures, however, require thorough experimental verification of their effect on creep in a particular installation. Flanges, bolts, and hubs designed by the procedures in this handbook will have stresses below the yield range at all times and therefore will probably have little long-time creep. Excepting for connectors which must operate for long periods of time at high temperatures under their most severe loading conditions, it is recommended that long-time creep be considered negligible for launch vehicle applications. This is done in this handbook. A reduced allowable stress can be used in design if experience indicates creep is significant. This stress should be that for which a 10 percent relaxation in stress will occur during a time equal to the life required under surge pressure conditions at temperature.

2.1.3 Design Requirements

The octahedral stress at any position in the bolts, flanges, or hub is given by

$$\sigma_o = \sqrt{\frac{1}{2} \sqrt{(\sigma_1 - \sigma_2)^2 + (\sigma_2 - \sigma_3)^2 + (\sigma_1 - \sigma_3)^2}}$$

where

$\sigma_1, \sigma_2, \sigma_3$ = hoop, axial and radial stresses respectively.

The requirement to be satisfied is:

$$\sigma_o < \sigma_{\text{allow}} \quad (2.3)$$

where

σ_{allow} = The allowable stress. The yield stress at temperature is taken as σ_{allow} where creep is not important. Where creep is significant, σ_{allow} is taken as the stress for which a 10 percent relaxation in stress will occur during a time equal to the time during which surge pressure is acting at temperature. (It should be noted that standards which permit only 25 percent of the yield stress for bolt materials do not consider bolt bending as is done here. The inclusion of bolt bending is in fact a stricter requirement in many cases). The presence of cyclical loads may require a reduction of allowable stress, however, the margin for surges and dynamic loads in Eq. 2.1 provides substantial fatigue life even when the yield stress is taken as the allowable stress.

The stresses at locations of high stress in a connector are generally a combination of axial and bending stresses. As a result, so long as the connector materials have some ductility, Eq. 2.3 is conservative, since exceeding σ_{allow} moderately merely results in a stress redistribution, rather than failure.

Deformations under load must be such that no interference of parts results. Loose-ring, floating, flanges must be particularly checked for excessive rotation. Lap flanges may also rotate excessively.

The gasket force must always exceed its minimum permitted value.

2.2 Flanges with No Contact Outside the Gasket Circle

The most widely used flanged connector is that having no contact outside the gasket circle. Use will be made of the elastic interaction of the bolts, flanges, hubs, gasket and pipes under the various applied loads to arrive at an optimum design configuration. The design procedure involves selecting a preliminary design layout, analyzing for stresses and deformations under the various loading conditions, using the results to select an improved design layout, reanalyzing, and remodifying until an efficient design is attained. Every effort has been made to make the preliminary design procedure a good one. However, for simplicity, only a few parameters can be considered at a time. Thus, the highly complex interactions of the connector parts can only be accounted for approximately in the preliminary design phase. At least one or two cycles of the analysis-redesign procedure are essential if an optimum configuration is to be achieved.

The detailed design procedure is presented here in a form suitable for hand computation so that the procedures can be clearly understood. It is also in a form which can readily be translated to digital computer language either in part or total. Where many connectors must be designed, use of a digital computer recommends itself both from the point of view of accuracy in the many numerical computations involved as well as cost in repeating computations to achieve an optimum configuration.

2.2.1 Preliminary Design Layout - Integral Flanges

a. Determine the pipe size, wall thickness, and material to either side of the connector. Select materials for the connector halves to be the same as the corresponding pipes except for possible differences in heat treatment or alloying compounds to improve creep, fatigue, or yield strength. Check that the pipe wall thickness satisfies Section 2.4.1 c.

Select a connector sealing system whose maximum permissible load exceeds its minimum permissible load for "zero leakage" by at least $2.5 \pi R_G^2 P_{\max \text{ oper.}}$, the estimated reduction in gasket load during operation.

Determine:

1. Details of the seal -- material, thickness, diameters, etc.
2. Axial load, (G_T) needed to make an effective seal.
3. Axial load, (G_M) needed to maintain a seal at operating temperature

(See Section 2.1.2 for guidance on selecting gasket loads).

b. Determine the initial bolt load, (B_I) , as the greater of the two values:

(G_I) or

$$(G_M) + 2.5 \pi R_G^2 p_{\text{max.oper.}}$$

where R_G is the average radius of the seal and $p_{\text{max.oper.}}$ is the maximum nominal operating pressure (no surges). The factor of 2.5 is an empirical value included to allow for pressure surges, bending moments and axial forces imposed on the system, in addition to bolt load caused by normal pressure.

Select a bolt material and determine its yield stress at maximum operating temperature. In selecting bolt material desirable factors include: high strength, coefficient of expansion compatible with flange material coefficient, and suitability over the entire temperature range low end as well as high end.

Determine (A_B) , the minimum permissible bolt total area at the root of the threads.

$$(A_B) = \frac{5 \cdot (B_I)}{(S_B)}$$

where (S_B) is the yield strength of the bolt material at maximum working temperature. The factor 5 is included to allow for the increase in stress (over that caused by straight tension) due to the normally present bolt bending. For arriving at a preliminary design, it is assumed that the rigidity of the seal system is enough greater than the rigidity of the bolt-flange system that the bolt stress is relatively unaffected by pipe vibration forces and pressure changes and no factor need be included for fatigue.

c. Use Table 2.1, Column 2, to select a bolt size. Enter Column 1, in the appropriate thread-type column, at a value equal to or just larger than the ratio $(A_B)/(R_{BC})$ where (R_{BC}) is an estimated bolt circle radius. The bolt size is given in Column 2. Columns 3 through 7 give other data related to bolt size.

Check to see that the estimated value of (R_{BC}) was reasonable by applying the formula

$$(R_{BC}) = R + (\text{Col. 5}) + (\text{Col. 7}) \times \sqrt{(S_B)/(S_F)}$$

where $(S_B)/(S_F)$ is the ratio of yield stresses for the bolt and flange materials, R is the inner radius of the pipe, and (R_{BC}) is the bolt circle radius. If (R_{BC}) is sufficiently changed that using it in Column 1 of Table 2.1 results in a different bolt size selection, recheck using the new bolt size.

Table 2.1 is based on standard bolts. The use of internal wrenching bolts or special thin-wall wrenches would, generally, result in a design using a larger number of smaller bolts and a reduction in overall connector size and weight.

Select an integral number of bolts, n , such that n is as small as possible while satisfying the relationship:

$$n \geq (A_B)/(\text{Col. 3})$$

Check that (R_{BC}) satisfies the relationship:

$$(R_{BC}) \geq \left(\frac{m}{2\pi}\right) \text{ (Col. 4)}$$

If it does not, it will be necessary to increase (R_{BC}) enough to meet this requirement, while leaving the number and size of bolts unchanged.

d. Select a flange thickness (H_I) and a hub thickness (T_I) based on,

$$(H_I) = \text{(Col. 7)} \times \sqrt{\frac{(S_B)}{(S_F)}} = (T_I)$$

Select a flange outer radius, (R_{OL}) , given by,

$$(R_{OL}) = (R_{BC}) + \text{(Col. 6)}$$

Select a radius for the large end of the hub, (R_{HI}) , given by,

$$(R_{HI}) = R + (T_I)$$

e. Select a hub length (L_I) given by

$$(L_I) = \sqrt{(R/2) [(T_I) + (T_P)]}$$

where (T_P) is pipe wall thickness.

Determine the hub slope (S_H) , given by,

$$(S_H) = (L_I) / [(T_I) - (T_P)]$$

If $(S_H) < 3$, it may be necessary to modify the hub by adding a section with a reduced taper. The details of the reduced taper hub are dictated by welding limitations and should be made to satisfy good welding practice, but not to add unnecessarily to weight. In general, and in the absence of welding information which would be specific or indicate a different design to be better, the hub adjacent to the pipe should have a taper not exceeding 1:3 and a length of at least four pipe wall thicknesses. Thus, in the absence of specific data, make:

$$(L_T) = 4(T_P)$$

$$(R_T) = R + \left(2\frac{1}{3}\right) (T_P)$$

(Refer to Figure 2.2)

Add welding details to drawing.

Add fillet radii to limit stress concentration at:

1. Transition of flange to hub. Make the fillet radius between 0.1 and 0.2 (T_I) .

2. Transition of hub to reduced taper hub, if used, and to pipe.

Make the fillet radius between 0.1 and 0.2 (T_p)

- f. Choose a lubricant for the bolt-nut-flange interfaces to give the lowest possible coefficient of friction.

Specify bolt torque and torquing procedure.

Bolt torque is given approximately by,

$$T = \left(\frac{1}{2} \mu_N + \frac{3}{4} \mu_F \right) d \left[\frac{B \cdot I}{n} \right]$$

where d is the nominal bolt diameter (i.e., 5/8 inch, 1 inch, etc.), μ_N is the coefficient of friction between the bolt and nut, and μ_F is coefficient of friction between flange and nut.

A torquing pattern should be specified which will avoid uneven tightening. A suggested pattern for an eight-bolt assembly is to tighten in the order 1, 5, 3, 7, 2, 6, 4, 8; repeating this pattern for the following loads:

1. Finger tight.
2. Bolt 1 brought to 1/4 rated torque or 1/3 turn increment, whichever is reached first, and all bolts brought to approximately same torque in stated order. If necessary repeat 1/3 turn increments till 1/4 rated torque is reached.
3. Repeat for 1/2 T (but not to exceed 1/6 turn increments).
4. Repeat for 3/4 T (but not to exceed 1/6 turn increments).
5. Repeat for rated torque (but not to exceed 1/6 turn increments) and repeat sequence for rated torque until no bolt continues to tighten when rated torque is applied.

The correct values of μ to use depend on materials and the lubricant, if any, that is used. Guide values are given in Table 2.2. Combinations of materials which may gall should be avoided if possible. It is best to determine the actual relationship between bolt torque and bolt load by test in actual flanges since in use the bolt load is applied eccentrically as a result of flange cocking. In addition the coefficient of friction is variable from one application to another. In some cases bolt load may be set more accurately by tightening the nut an appropriate number of turns, depending on overall connector flexibility.

- g. Select coefficients of friction for the contact between gasket and flange. An approximate value for this is 0.5 if test values are unobtainable.

- h. Add dimensional tolerances in accord with standard shop practice except that sealing face flatness tolerance should not exceed 0.1 times the expected compression of the gasket.

i. Select loading conditions for which a detailed analysis to be described is required. These would normally include,

1. Initial assembly-

Given - Bolt force (B_I)
 Axial load P and internal pressure p are zero
 Temperature is room temperature

Determine - Initial stretch C of bolt-flange-pipe system as well as stresses and deformations

2. Maximum operating conditions

Given - Initial stretch C from above solution

$$p = 1.5 p_{\text{max oper.}}$$

$$P = 2.5\pi R^2 p_{\text{max oper.}}$$

Temperature, operating temperature.

3. Other severe environmental conditions, if present.

Compute the stresses and the deflections that develop in the above trial design for the various loading conditions in accordance with Section 2.2.2. Determine whether any deflection is excessive. Determine whether at any point the octahedral stress, σ_o , multiplied by the appropriate stress concentration factor is either: 1) in excess of the yield stress at maximum temperature reduced by appropriate factors for fatigue and relaxation; or 2) is appreciably lower than this value. (For a few materials yield stress is lower at a lower temperature. In these cases, the lowest yield stress in the intended operating range should be used).

Factors to be used are:

<u>Place</u>	<u>Purpose</u>	<u>Factor</u>
Flange -	For stress concentration at fillet.	1.3
	For fatigue (assuming gasket has appreciably less compliance than bolt-flange system).	1.0
	For stress relaxation.	Select factor based on service life at high temperature. For most designs 1.0 is appropriate. See Section 2.0.8
Hub	For stress concentration at flange fillet	1.3
	Elsewhere on hub	1.0

<u>Place</u>	<u>Purpose</u>	<u>Factor</u>
Hub	For fatigue	Select factor based on material, steady-state stress, alternating component due to vibration and desired life. If not specifically determined use factor of 2.0.
	For stress relaxation.	Select factor based on service life at high temperature. For most designs 1.0 is appropriate. Section 2.0.8.
Bolts	For stress concentration	1.0
	For fatigue (see note for flange)	1.0
	For stress relaxation.	Select factor based on service life at high temperature. For most designs 1.0 is appropriate. See Section 2.0.8.

(Note: Complete steps i through l before attempting to complete a modified design).

j. Check for load on the gasket under design conditions and determine whether this load exceeds (G_M), the gasket load required to maintain a seal. If gasket load drops too much, it is an indication of excessive deformation due to pressure. It can be corrected by using a higher initial gasket load with correspondingly higher initial bolt load. These in turn result in corresponding increases in flange and bolt dimensions. (Complete steps i through (l) before attempting to complete a modified design).

k. If under design loads octahedral stress multiplied by the stress concentration factor is greater than the yield stress reduced by the fatigue and relaxation factors, modify the design as follows:

<u>Overstressed Part</u>	<u>Action</u>
Bolt	Infrequent occurrence. Recheck calculations for error. New trial design if appropriate using more bolt area.
Flange or hub near flange	Increase thickness by a factor equal to half the overstress factor.
Hub, near pipe	Modify hub to join pipe with decreased taper, either by increasing hub length or by using hub with two or more graduated tapers.

l. If octahedral stress is lower than permissible, this indicates the preliminary design is too conservative. The reverse action of step k should be taken.

TABLE 2.1

Estimation of Bolt Size and Number of Bolts*

(1) (Total Bolt Area) (Bolt Circle Radius)			(2) Bolt Size (in)	(3) Root Area			(4) Bolt Spacing** (in)	(5) Radial Eccen. (in)	(6) Edge Distance (in)	(7) Flange Thickness Factor		
Fine (in)	Coarse (in)	8 Thread (in)		Fine (in)	Coarse (in ²)	8 Thread (in ²)				Fine (in)	Coarse (in)	8 Thread (in)
.273	.225	---	1/4	.0326	.0269	---	3/4	1/2	3/8	.161	.147	---
.406	.352	---	5/16	.0524	.0454	---	13/16	9/16	7/16	.209	.379	---
.508	.426	---	3/8	.0809	.0678	---	1	5/8	1/2	.246	.225	---
.609	.521	---	7/16	.1090	.0953	---	1-1/8	11/16	9/16	.283	.262	---
.748	.633	---	1/2	.1486	.126	---	1.25	.81	.62	.340	.313	---
1.007	.845	---	5/8	.2400	.202	---	1.50	.94	.75	.426	.390	---
1.262	1.083	---	3/4	.3513	.302	---	1.75	1.12	.81	.521	.482	---
1.464	1.278	---	7/8	.4805	.419	---	2.06	1.25	.94	.592	.553	---
1.743	1.537	1.537	1	.6245	.551	.551	2.25	1.37	1.06	.676	.634	.634
2.040	1.740	1.828	1-1/8	.8118	.693	.728	2.50	1.50	1.12	.765	.706	.723
2.29	1.988	2.08	1-1/4	1.024	.890	.929	2.81	1.75	1.25	.876	.815	.836
2.69	2.16	2.37	1-3/8	1.260	1.054	1.155	3.06	1.87	1.37	.981	.878	.921
2.94	2.50	2.71	1-1/2	1.521	1.294	1.405	3.25	2.00	1.50	1.058	.976	1.015

*Derived from Ref. 2, page 27, and other sources.

**This spacing can be reduced with internal wrenching bolts or by use of special thin-wall wrenches. When this is done, an appreciable reduction in flange weight is possible since the bolt size can be reduced one or two sizes.

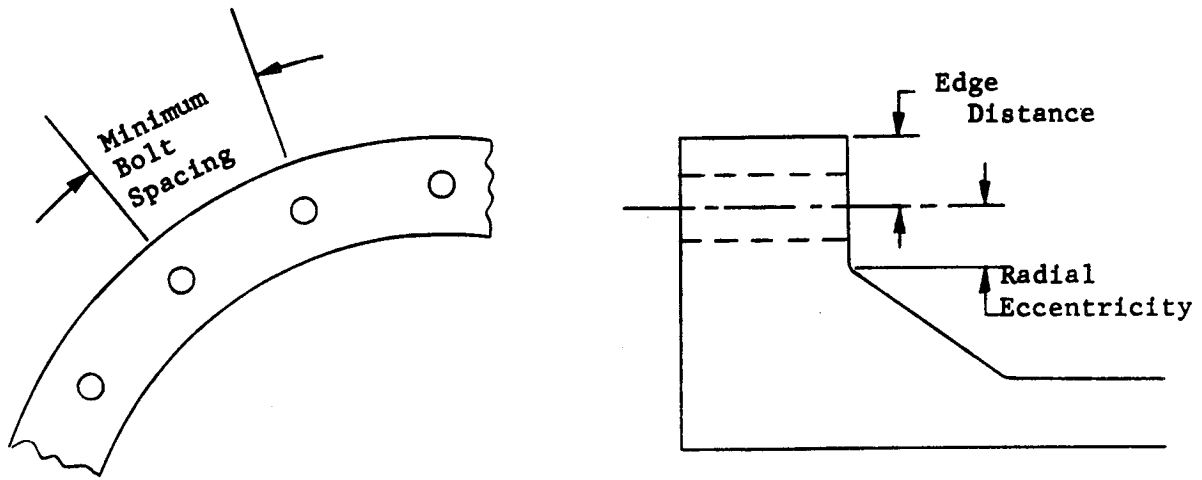


Figure 2.1. Bolt Clearances. See Table 2.1 for Values.

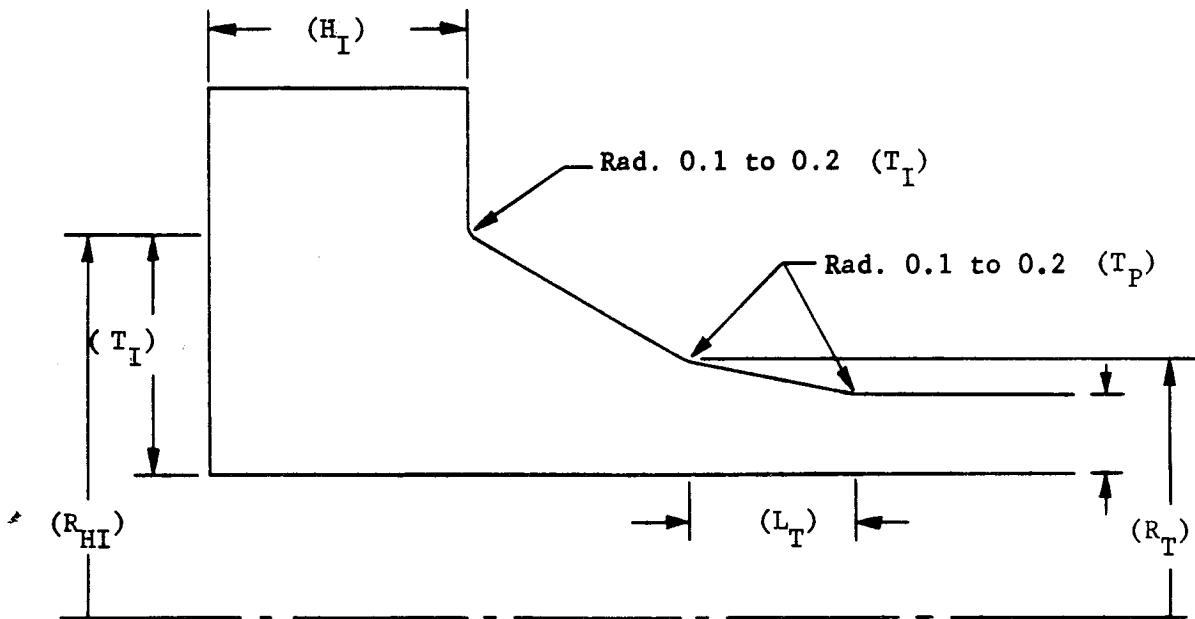


Figure 2.2. Double-Taper Hub Initial Dimensions.

Table 2.2

APPROXIMATE FRICTION COEFFICIENTS

Lubricated Steel on Steel	0.1
Dry Steel on Steel	0.7
Lubricated Aluminum on Steel	0.2
Dry Aluminum on Steel	0.6
Lubricated Aluminum on Aluminum	0.1
Dry Aluminum on Aluminum	1.0

2.2.2 Integral Flanges With No Contact Outside the Gasket Circle Detailed Analysis

An elastic analysis is achieved by satisfying equilibrium and compatibility conditions at the pipe-hub and flange-hub interfaces as well as at the flange-bolt and flange-gasket interfaces. From the elastic analysis, deformations and stresses are obtained at all locations of interest. In the following discussion, the flange is considered to be a plate and the pipe and hub are considered to be cylindrical shells. The bolts are considered to be eccentrically loaded by the flanges at their radially inward side because of flange rotation. The gasket is considered elastic.

The solution in regard to the hub and flange ring is basically a step-by-step process. Thus, the solution of a large number of simultaneous equations is avoided. Starting at the small end of the hub Section 2.2.2.1 proceeds step-wise down the hub. At each step, values are obtained for the wall shear, wall moment, radial deflection, and slope in terms of the wall moment and wall shear at the small end of the hub and the pressure, p , axial load, P , and expansion $\alpha\Delta T$. Then in Section 2.2.2.2 the solution proceeds similarly from the inner to the outer radius of the flange ring. Finally, the wall moment and the wall tension are set to zero at the outer radius of the flange ring and the resulting two simultaneous equations for the moment and shear at the small end of the hub are solved in terms of p , P , $\alpha\Delta T$, $(B \text{ or } C)$ and Q_{gf} .

The solution in regard to the influence of bolt and gasket stiffness is found in Sections 2.2.2.3 and 2.2.2.4. Here three simultaneous equations must be solved. One of these equations involves compatibility of the bolt stretch, gasket compression, and flange ring deflection. The other two equations involve compatibility of the radial displacements of the flange rings and gasket at their points of contact. Solution of these equations gives the values of $(B \text{ or } C)$ and the gasket friction force on each face of the gasket in terms of p , P , $\alpha\Delta T$. With these the hub and flange ring forces are obtained at the small end of the hub and elsewhere and the corresponding stresses are also obtained.

Because of the length of the computation and the fact that it involves the solution of simultaneous equations, it is recommended that five or more

significant figures be maintained in the numerical computation.

2.2.2.1 Pipe Stiffness Including Hub

With cylindrical shell theory, Appendix 2A, it can readily be shown that the deflection and slope of the wall at the end of a long pipe due to wall moment, wall shear, axial force, pressure, and temperature is

$$u = \left(\frac{R\beta^2}{\pi Et}\right) M + \left(\frac{R\beta}{\pi Et}\right) Q + \left(\frac{R^2}{Et}\right) p - \left(\frac{\nu}{2\pi Et}\right) P + R\alpha\Delta T \quad (2.4)$$

$$\theta = \left(\frac{2R\beta^3}{\pi Et}\right) M + \left(\frac{R\beta^2}{\pi Et}\right) Q \quad (2.5)$$

(When the radii to inner and outer pipe walls differs much from R, Eqs. 2A-1 and 2A-2 should be used.)

With cylindrical shell theory for a pipe segment it can be shown (Appendix 2B) that the deflection, slope, wall moment, and wall shear at one end are given in terms of those at the other end and the internal pressure, axial load, and temperature change as

$$Q_r = + K_4 Q_l + 2\beta K_1 M_l + \left(\frac{\pi Et}{R\beta^2}\right) K_2 \theta_l + \left(\frac{2\pi Et}{R\beta}\right) K_3 u_l - \left(\frac{2\pi R}{\beta}\right) p K_3 + \left(\frac{\nu}{R\beta}\right) K_3 P - \left(\frac{2\pi Et}{\beta}\right) \alpha \Delta T K_3 \quad (2.6)$$

$$M_r = -\left(\frac{1}{\beta}\right) K_3 Q_l + K_4 M_l - \left(\frac{\pi Et}{R\beta^3}\right) K_1 \theta_l - \left(\frac{\pi Et}{R\beta^2}\right) K_2 u_l + \left(\frac{\pi R}{\beta^2}\right) K_2 P - \left(\frac{\nu}{2R\beta^2}\right) P K_2 + \left(\frac{\pi Et}{\beta^2}\right) \alpha \Delta T K_2 \quad (2.7)$$

$$\theta_r = -\left(\frac{R\beta^2}{\pi Et}\right) K_2 Q_l + \left(\frac{2\beta^3 R}{\pi Et}\right) K_3 M_l + K_4 \theta_l - 2\beta K_1 u_l + \left(\frac{2\beta R^2}{Et}\right) K_1 P - \left(\frac{\beta \nu}{\pi Et}\right) K_1 P + 2\beta R \alpha \Delta T K_1 \quad (2.8)$$

$$\mu_r = -\left(\frac{R\beta}{\pi Et}\right) K_1 Q_l + \left(\frac{R\beta^2}{\pi Et}\right) K_2 M_l + \left(\frac{1}{\beta}\right) K_3 \theta_l + K_4 u_l + \left(\frac{R^2}{Et}\right) (1-K_4) p - \left(\frac{\nu}{2\pi Et}\right) (1-K_4) P + R (1-K_4) \alpha \Delta T \quad (2.9)$$

Where subscripts "r" and "l" refer to "right" and "left" ends of the segment respectively.

$$\beta^4 = 3(1-\nu^2) / R^2 t^2 \quad (2.10)$$

$$K_1 = \left(\frac{\beta^3 L^3}{3}\right) (1 - \beta^4 L^4 / 210), \beta L < 1 \quad (2.11)$$

$$K_2 = \beta^2 L^2 (1 - \beta^4 L^4 / 90), \beta L < 1 \quad (2.12)$$

$$K_3 = \beta L (1 - \beta^4 L^4 / 30), \beta L < 1 \quad (2.13)$$

$$K_4 = 1 - \beta^4 L^4 / 6 + L^8 / 2520, \beta L < 1 \quad (2.14)$$

Where L = length of pipe segment (in.).

(For values of βL greater than one or for the case where the inner and outer pipe walls have radii much different from R use Appendix 2B).

The theory for tapered hubs is available only for hubs with a linear taper. Even in the case of a linear taper, taking account of all four hub variables, that is, radius, length, and thickness at each end, becomes quite cumbersome. To avoid these difficulties the following procedures will be used:

- a. Divide the hub into a small number of cylindrical segments as shown by the dotted lines in Figure 2.3. The cylinders should approximate the hub dimensions. Three should ordinarily suffice.
- b. Obtain Eqs. 2.6 to 2.14 for each segment.
- c. Use Eqs. 2.4 and 2.5 to obtain the deflection and rotation at the small end of the hub in terms of the wall moment and wall shear at this location.
- d. Take the slope and wall shear obtained in (c) as the values at the left side of the first hub segment from the small end of the hub. Take the moment and deflection obtained in (c) and add to them.

$$\Delta M_1 = (P/2) (\text{thickness of wall of first segment} - \text{thickness of wall of pipe})$$

$$\Delta u_1 = (\alpha \Delta T / 2) (\text{thickness of wall of first segment} - \text{thickness of wall of pipe}).$$

to obtain the moment and deflection at the left side of the first hub segment. (No correction is used for Δu_1 if R is used in place of the mid-thickness radius in Eqs. 2.4 and 2.6 to 2.9).

- e. With the results obtained in (b) for the first hub segment and in (d) for deflection, slope, wall shear, and wall moment at the left side of this segment, corresponding values at the right side of this segment are obtained from Eqs. 2.6 to 2.9.
- f. Take the slope and wall shear obtained in (e) as the values at the left side of the second hub segment. Take the moment and deflection obtained in (e) at the right side of the first segment and add to them

$$\Delta M_2 = (P/2) (\text{thickness of wall of second segment} - \text{thickness of wall of first segment})$$

$$\Delta u_2 = (\alpha \Delta T/2) (\text{thickness of wall of second segment} - \text{thickness of wall of first segment})$$

to obtain the moment and deflection at the left side of the second hub segment.

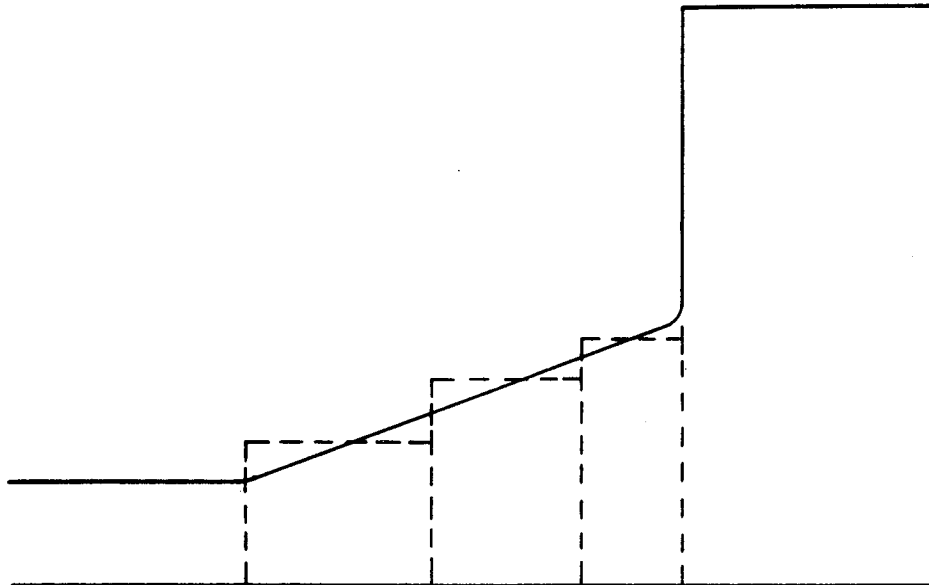


Figure 2.3. Approximate Hub by a Small Number of Cylindrical Segments, shown dotted. (As the number of segments used increases, the wall moment and wall shear as well as the deformations, converge to the values obtained using the theory for a nonuniform wall thickness.)

- g. With the results obtained in (b) for the second hub segment and in (f) for values at the left side of the second segment, values at the right side of the second segment are obtained.
- h. Repeat steps (f) and (g) for the third and any additional segments giving the moment, M_{Hub} , shear, Q_{Hub} , deflection, and slope at the large end of the hub in terms of the moment and shear at the small end of the hub and p , P , $\alpha \Delta T$.

2.2.2.2 Flange Ring Stiffness

Bolt holes reduce the stiffness of the flange ring. In Ref 2.6 it is shown that the increase in flexibility due to the bolt holes is approximately given by

$$f = \frac{1}{1 - nd^2 / \pi (R_{OF}^2 - R^2)} \quad (2.15)$$

Thus, f is equal to the ratio of the flange ring volume without bolt holes to the flange ring volume had the bolt holes been square. Eq. 2.15 is confirmed experimentally in Ref 2.6 for the case of flange rotation.

Regarding stress, it is shown in Ref 2.6 that the weakening effect of the bolt holes occurs at points where the circumferential bending moment is reduced so that there is negligible effect on flange hoop stresses.

All the forces from the hub and gasket are considered, as well as the internal pressure, to cause a resultant radial force, axial force, and moment at the bottom of the flange ring given by,

$$\text{Flange bottom axial force} = \text{bolt pull, } B \quad (2.16)$$

$$\begin{aligned} \text{Flange bottom radial force, } Q_R &= Q_{Hub} + Q_{gf} \\ &\quad - 2\pi Rph \end{aligned} \quad (2.17)$$

$$\begin{aligned} \text{Flange bottom moment, } M_R &= M_{Hub} - G(R_G - R) - t_{Hub} P/2 \\ &\quad + \left(\frac{h}{2}\right) Q_{gf} \\ &\quad - \left(\frac{h}{2}\right) Q_{Hub} - \left(\frac{\pi P}{3}\right)(R_G - R)(2R_G^2 - RR_G - R^2) \end{aligned} \quad (2.18)$$

Where Figure 2.4 gives sign conventions and symbols.

Q_{Hub} is the total circumferential wall shear force in the hub at the hub-flange interface.

M_{Hub} is the total circumferential wall moment in the hub at the hub-flange interface.

t_{Hub} is the hub thickness at the flange.

Q_{gf} is the frictional force applied by the gasket.

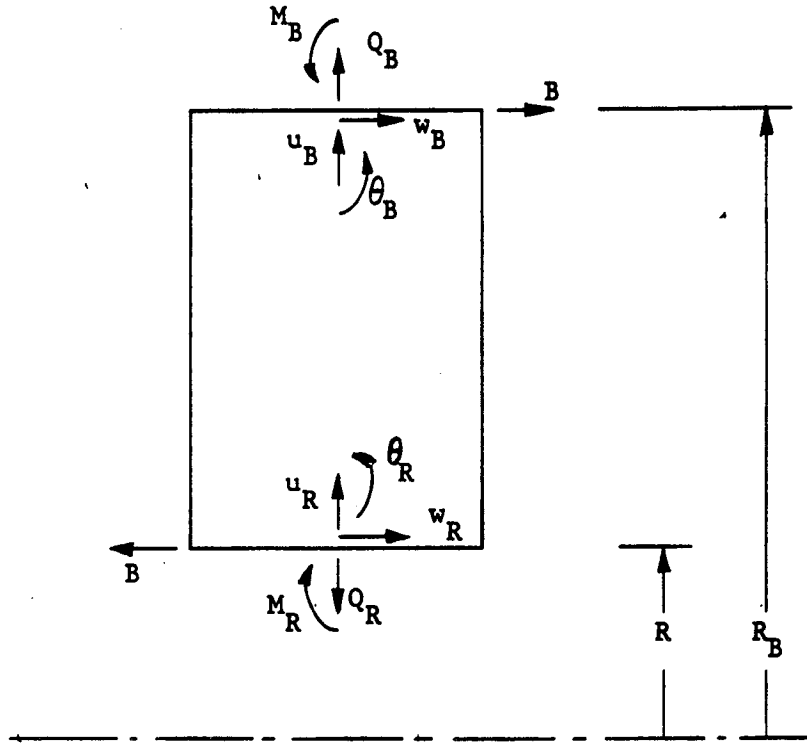


Figure 2.4. Flange Ring Below Line of Action of Bolt Load. (For flanges having no contact outside the bolt circle, R_B is the radius to the circle that is tangent to the inside of the bolts, i.e., the radius to the bolt center minus the bolt radius.

The displacements at the bottom of the flange ring are taken as
 $\theta_R = \theta_{Hub}$, $u_R = u_{Hub} + (h/2) \theta_{Hub} - t_{Hub} \alpha \Delta T / 2$ (2.19)

The last term in Eq 2.19 is omitted if R is used in place of the mid-thickness radius in Eqs. 2.4 and 2.6 to 2.9 .

The corresponding values at the line of action of the bolts are obtained from the values at the flange bottom (Eqs. 2.16 to 2.19) by the use of Appendix 2 C as,

$$Q_B = 1/2 \left[(1 + \nu) \frac{R_B}{R} + (1 - \nu) \frac{R}{R_B} \right] Q_R + \left(\frac{\pi E h}{f} \right) \left(\frac{R_B}{R} - \frac{R}{R_B} \right) u_R - \left(\frac{\pi E h}{f} \right) \left(\frac{R_B}{R} - \frac{R}{R_B} \right) R \alpha \Delta T \quad (2.20)$$

$$M_B = 1/2 \left[(1 + \nu) \frac{R_B}{R} + (1 - \nu) \frac{R}{R_B} \right] M_R + \left(\frac{\pi E h^3}{12 f} \right) \left(\frac{R_B}{R} - \frac{R}{R_B} \right) \theta_R + \left[(1 - \nu) \left(\frac{R_B^2 - R^2}{4 R_B} \right) + \left(\frac{1 + \nu}{2} \right) R_B \log \left(\frac{R_B}{R} \right) \right] B \quad (2.21)$$

$$\theta_B = \left[\frac{3f(1-\nu^2)}{\pi E h^3} \right] \left(\frac{R_B}{R} - \frac{R}{R_B} \right) M_R + 1/2 \left[(1-\nu) \frac{R_B}{R} + (1+\nu) \frac{R}{R_B} \right] \theta_R$$

$$+ \left[\frac{3(1-\nu^2) f R_B}{\pi E h^3} \right] \left[- \left(\frac{R_B^2 - R^2}{2R_B^2} \right) + \log \left(\frac{R_B}{R} \right) \right] B \quad (2.22)$$

$$u_B = \left[\frac{f(1-\nu^2)}{4\pi E h} \right] \left[\frac{R_B}{R} - \frac{R}{R_B} \right] Q_R + 1/2 \left[(1-\nu) \frac{R_B}{R} + (1+\nu) \frac{R}{R_B} \right] u_R$$

$$+ 1/2 (1+\nu) \left[\frac{R_B}{R} - \frac{R}{R_B} \right] R \Delta T \quad (2.23)$$

$$\text{where } B = P + G + \pi p (R_G^2 - R^2) \quad (2.24)$$

R_B = radius to center of bolts minus radius of bolts for flanges which do not touch outside the bolt circle. For flanges that do touch outside the bolt circle, R_B is the radius to the center of the bolts. (2.25)

Proceeding to the top of the flange ring, it is known that the moment and shear at this location are zero. Using the values at the bolt circle given by Eqs. 2.20 to 2.23 in the equations of Appendix 2C, Eqs. 2C.3 and 2C.5 give

$$0 = \left(\frac{\pi E h}{f} \right) \left[\frac{R_{OF}}{R_B} - \frac{R_B}{R_{OF}} \right] u_B + 1/2 \left[(1+\nu) \frac{R_{OF}}{R_B} + (1-\nu) \frac{R_B}{R_{OF}} \right] Q_B \quad (2.26)$$

$$- \left(\frac{\pi E h}{f} \right) \left[\frac{R_{OF}}{R_B} - \frac{R_B}{R_{OF}} \right] R_B \propto \Delta T$$

$$0 = \left(\frac{\pi E h^3}{12f} \right) \left[\frac{R_{OF}}{R_B} - \frac{R_B}{R_{OF}} \right] \theta_B + 1/2 \left[(1+\nu) \frac{R_{OF}}{R_B} + (1-\nu) \frac{R_B}{R_{OF}} \right] M_B \quad (2.27)$$

Equations 2.26 and 2.27 are solved simultaneously to give the pipe wall moment and the pipe wall shear at the hub junction in terms of the bolt load, pressure, temperature change, axial force, and gasket forces. If Eqs. 2.26 and 2.27 are rewritten and denote the coefficients by symbols K_{10} , K_{11} , etc.,

$$0 = K_{10} M + K_{11} Q + K_{12} B + K_{13} p + K_{14} \Delta T + K_{15} P + K_{16} G + K_{17} Q_{gf}$$

$$0 = K_{20} M + K_{21} Q + K_{22} B + K_{23} p + K_{24} \Delta T + K_{25} P + K_{26} G + K_{27} Q_{gf}$$

When these equations are solved simultaneously for M and Q

$$\begin{aligned}
 M &= \left[\frac{K_{21}}{K_{11}K_{20} - K_{10}K_{21}} \right] \left[K_{12}^B + K_{13}^P + K_{14}^{\alpha\Delta T} + K_{15}^P + K_{16}^G + K_{17}^{Q_{gf}} \right] \\
 &- \left[\frac{K_{11}}{K_{11}K_{20} - K_{10}K_{21}} \right] \left[K_{22}^B + K_{23}^P + K_{24}^{\alpha\Delta T} + K_{25}^P + K_{26}^G + K_{27}^{Q_{gf}} \right] \\
 Q &= - \left[\frac{K_{20}}{K_{11}K_{20} - K_{10}K_{21}} \right] \left[K_{12}^B + K_{13}^P + K_{14}^{\alpha\Delta T} + K_{15}^P + K_{16}^G + K_{17}^{Q_{gf}} \right] \\
 &+ \left[\frac{K_{10}}{K_{11}K_{20} - K_{10}K_{21}} \right] \left[K_{22}^B + K_{23}^P + K_{24}^{\alpha\Delta T} + K_{25}^P + K_{26}^G + K_{27}^{Q_{gf}} \right]
 \end{aligned}$$

From the solution for M and Q at the pipe-hub interface, the loads and deformations in the left flange-hub-pipe combination are determined. A similar procedure is used for the right flange-hub-pipe combination starting from the smaller end of the hub and working towards the flange ring top. In the case of the right flange-hub-pipe combination sign conventions are a mirror image of the left flange-hub-pipe combination. As a result, radial displacement is again outward and axial displacement is towards the gasket.

The axial deflection of the flange at the bolts in respect to the gasket circle is obtained from Eq. 2C-9 as

$$\begin{aligned}
 w_B - w_G &= \left[\frac{3fB(1-\nu^2)}{4\pi Eh^3} \right] \left[2R^2 \left(\frac{R_B^2 - R_G^2}{R_B^2 - R^2} \right) \log\left(\frac{R_B}{R}\right) + \left(\frac{3+\nu}{1+\nu}\right)(R_B^2 - R_G^2) \right. \\
 &\quad \left. - 2R_G^2 \log\left(\frac{R_B}{R_G}\right) + 4 \left(\frac{1+\nu}{1-\nu}\right) \left(\frac{R_B^2 R^2}{R_B^2 - R^2}\right) \log\left(\frac{R_B}{R}\right) \log\left(\frac{R_B}{R}\right) \right] \\
 &+ \left[\frac{6fM_R(1-\nu^2)}{\pi Eh^3} \right] \left[\frac{R(R_B^2 - R_G^2)}{2(1+\nu)(R_B^2 - R^2)} + \frac{RR_B^2}{(1-\nu)(R_B^2 - R^2)} \log\left(\frac{R_B}{R_G}\right) \right] \\
 &- \left[\frac{6fM_B(1-\nu^2)}{\pi Eh^3} \right] \left[\frac{R_B(R_B^2 - R_G^2)}{2(1+\nu)(R_B^2 - R^2)} + \frac{R_B R^2}{(1-\nu)(R_B^2 - R^2)} \log\left(\frac{R_B}{R_G}\right) \right] \quad (2.28)
 \end{aligned}$$

The radial displacement of the flange at the gasket is obtained from Eqs. 2C.14 and 2C.15 as

$$\begin{aligned}
 u_G = & \left[\frac{R_G^2 + R^2 - \nu(R_G^2 - R^2)}{2\pi R_G E h (R_B^2 - R^2)} \right] f R_B Q_B - \left[\frac{R_B^2 + R_G^2 + \nu(R_B^2 - R_G^2)}{2\pi R_G E h (R_B^2 - R^2)} \right] f R Q_R \\
 & + R_G \alpha \Delta T - \left[\frac{3R (R_B^2 + R_G^2 + \nu(R_B^2 - R_G^2))}{\pi R_G E h^2 (R_B^2 - R^2)} \right] f M_R \\
 & + \left[\frac{3R_B (R_G^2 + R^2 - \nu(R_G^2 - R^2))}{\pi R_G E h^2 (R_B^2 - R^2)} \right] f M_B \\
 & - \left[\frac{3Bf}{2\pi R_G E h^2} \right] \left[R_G^2 (1 - \nu^2) \log \left(\frac{R_B}{R_G} \right) + R_G^2 (1 - \nu) \right. \\
 & \left. + \frac{R_G^2 (R^2 (1 - \nu^2))}{R_B^2 - R^2} \log \left(\frac{R_B}{R} \right) + \frac{R_B^2 R^2 (1 + \nu)^2}{R_B^2 - R^2} \log \left(\frac{R_B}{R} \right) \right] \quad (2.29)
 \end{aligned}$$

2.2.2.3 Bolt and Gasket Stiffness

The effective bolt shortening is from Eq. 2D-1

$$w_{BB} = \left(\frac{20}{\pi} \right) \left(\frac{L_B}{nEd^2} \right) B + (2h+h_G) \alpha_B \Delta T - C - h \alpha_F \Delta T \quad (2.30)$$

(The last terms in Eqs. (2.30) and (2.31) account for the flange expansion between edge and mid-thickness)

The axial compression of the gasket is from Eq. 2E-1

$$W_{GG} = \left(\frac{hG}{2\pi g R_G E_G} \right) G - h_G \alpha_G \Delta T - h \alpha_F \Delta T \quad (2.31)$$

The radial displacement of the gasket is obtained from Eq. 2E-2 as

$$\begin{aligned}
 u_{GT} = & \left(\frac{R_G}{2\pi g h_G E_G} \right) Q_{gf} \\
 & + \left(\frac{R_G}{2\pi g h_G E_G} \right) Q_{gf} \\
 & + \left[\frac{R_G (R_G - g/2)}{g E_G} \right] P + R_G \alpha_G \Delta T \quad (2.32)
 \end{aligned}$$

Where both right and left gasket frictions are positive outwards in acting on the gasket.

2.2.2.4 Interaction of Flange, Bolts, and Gasket - Integral Flanges.

The sum of the axial deflections of the two flanges, Eq. 2.28, the effective bolt shortening, Eq. 2.30, and the gasket compression, Eq. 2.31, must remain constant in the absence of bolt tightening or creep. This provides an equation involving the initial system extension constant C.

$$w_{BB} + w_{GG} + (w_B - w_G) \text{ Left flange} + (w_B - w_G) \text{ Right flange} = 0 \quad (2.33)$$

Equating the gasket radial displacements, Eq. 2.32, to the corresponding flange values, Eq. 2.29, gives two additional equations.

$$(u_G) \text{ Left flange} = u_{GT} \quad (2.34)$$

$$(u_G) \text{ Right flange} = u_{GT} \quad (2.35)$$

These equations can be solved simultaneously with Eq. 2.33 and Eq. 2.24 to give the gasket force G, bolt pull B (or when initially tightened the constant C) and the gasket friction forces. If the resulting values for gasket friction exceed the gasket friction coefficient times the gasket force, this indicates that sliding actually occurs. In that case, the two radial deflection equations (Eqs. 2.34 and 2.35) are replaced by

$$Q_{gf \text{ left}} = -Q_{gf \text{ right}} = \pm \mu_G G \quad (2.36)$$

the sign depending on the relative direction of sliding.

The value of the constant C is now evaluated at the initial tightening conditions by setting p, P, ΔT equal zero, and $B = (B_I)$. Using this value of C and the design load values, the load distribution in the flange and the hub and the deformations are found.

The bolt stress is given by Eq. 2D.3.

Maximum hoop compressive stresses in the flange ring occur at the inner radius away from the hub. From Eq. 2C.13 we have

$$\sigma_{\text{Hoop, Flange, Max}} = \left[\frac{R_B Q_B}{\pi h} \right] \left[\frac{1}{R_B^2 - R^2} \right] - \frac{Q_R (R_B^2 + R^2)}{2\pi R h (R_B^2 - R^2)} \quad (\text{continue})$$

$$-\left[\frac{3B}{2\pi h^2}\right]\left[(1+\nu)\left(\frac{2R_B^2}{R_B^2-R^2}\right)\log\left(\frac{R_B}{R}\right) + (1-\nu)\right]$$

$$-\left(\frac{3M_R}{\pi R h^2}\right)\left(\frac{R_B^2+R^2}{R_B^2-R^2}\right) + \left(\frac{6R_B M_B}{\pi h^2}\right)\left(\frac{1}{R_B^2-R^2}\right) \quad (2.37)$$

At this location,

$$\sigma_{\text{Axial}} = \sigma_{\text{Radial}} = -p \quad (2.38)$$

The radial stress in the hub and pipe can be taken as zero. The hoop stress in the hub and pipe is given by using Eqs. 2.4 or 2.9 to obtain u (here used to denote radial deflection generally), and substituting in

$$\sigma_{\text{Hoop pipe}} = \left(\frac{E}{R_{\text{mid-thickness}}}\right)\left(u + \frac{\nu}{2\pi Et} P\right) - E\alpha\Delta T \quad (2.39)$$

where t is the actual thickness rather than that of the substitute cylindrical segments. The axial stress in the hub and pipe is given by using Eq. 2.7 to obtain M (here used to denote wall moment generally) and substituting in

$$\sigma_{\text{Axial pipe}} = \left(\frac{P}{2\pi t R_{\text{mid-thickness}}}\right) + \left(\frac{6M}{2\pi t^2 R_{\text{mid-thickness}}}\right) \quad (2.40)$$

(The value will be greatest when the sign before M in Eq. 2.40 is minus since the value of M is ordinarily negative in the hub region when there is no contact outside the bolt circle. The thickness t in Eq. 2.40 is the actual thickness, not that of the substitute segments.)

Comparing the stresses with the allowable values indicates where additional thickness is needed and where thickness can be removed. Since the connector is a redundant structure, additions of material at either hub or flange tend to affect stresses everywhere but have the greatest affect locally. It is recommended that thickness changes be in direct proportion to half the difference of stress from the allowable values. Comparing the gasket load with the minimum permitted indicates whether an increase in initial bolt load or general thickening is needed. Similarly distortion limits may require thickening.

2.3 Integral Flange - Contact Outside Bolt Circle

An integral flange connector with contact at a raised region outside the gasket circle, (Figure 2.5) is frequently applied where the gasket is contained in a pocket. The use of raised regions near the flange edge and the gasket is preferred to a flat flange since it makes the gasket contact stiffer. Use will be made of an elastic analysis to achieve an optimum design configuration.

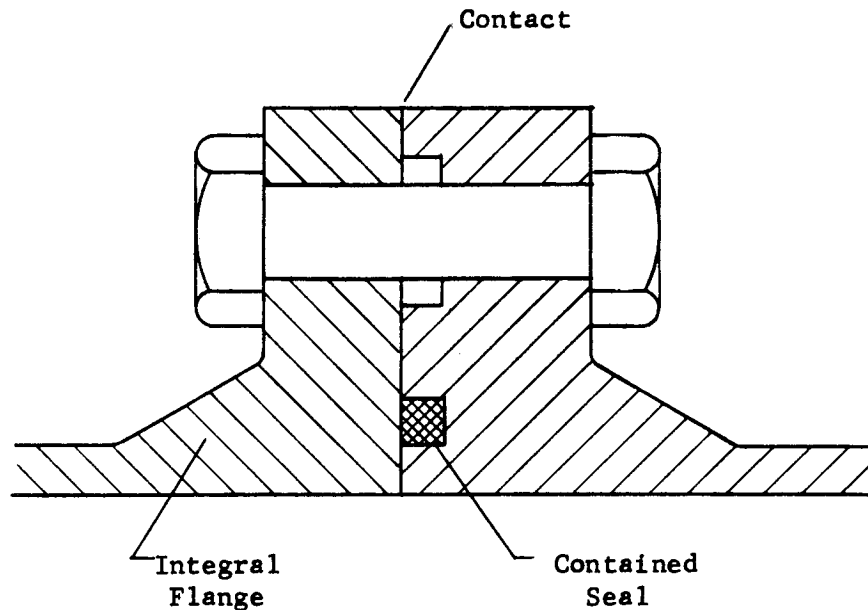


Figure 2.5. Integral Flange Connector with Contact Outside Gasket Circle.

The design procedure involves selecting a preliminary design layout, analyzing for stresses and deformations under the various loading conditions, using the results to select an improved design layout, reanalyzing, and remodeling, until an efficient design is attained. Every effort has been made to make the preliminary design procedure a good one. However, for simplicity, only a few parameters can be considered at a time. Thus, the highly complex interactions of the connector parts can only be accounted for approximately in the preliminary design phase. At least one or two cycles of the analysis-redesign procedure are essential if an optimum configuration is to be achieved.

The detailed design procedure is presented here in a form suitable for hand computation so that the procedures can be clearly understood. It is also in a form which can readily be translated to digital computer language either in part or total. Where many connectors must be designed, use of a digital computer recommends itself both from the point of view of accuracy in the many numerical computations involved as well as cost in repeating computations to achieve an optimum configuration.

2.3.1 Preliminary Design Layout - Contact Outside Bolt Circle

- a. Determine the pipe size, wall thickness, and material to either side of the connector. Select materials for the connector halves to be the same as the corresponding pipes except for possible differences in heat treatment or alloying compounds to improve creep, fatigue, or yield strength.

Select a connector sealing system whose maximum permissible load exceeds its minimum permissible load for "zero leakage" by at

least $2.5 \pi R_G^2 p_{\text{max. oper.}}$, the estimated reduction in gasket load during operation.

- b. Set the initial bolt load (B_I) equal to twice the value in (b) of Section 2.2.1. (This assumes equal load division during assembly between the gasket region and a raised outboard region of the flange. Set the minimum total bolt area (A_B) at the root of the threads equal to the ratio of initial bolt load to yield stress of the bolt material.

$$(A_B) = (B_I) / (S_B)$$

- c. Use Table 2.1 to select the bolt size and number of bolts. Enter this table in Column 1 at a value just larger than the ratio of the minimum total bolt area (A_B) to an estimated bolt circle radius (R_{BC}). The bolt size is given in Column 2. The corresponding number of bolts is obtained by dividing the minimum total bolt area by the root area per bolt, Column 3, and rounding up to a convenient integral number. If this number, when multiplied by the minimum bolt spacing in Column 4, exceeds the bolt circle in circumference, it will be necessary to increase (R_{BC}) slightly keeping the same bolt size and number of bolts.
- d. Select a flange thickness (H_I) from Column 7 of Table 2.1 such that

$$(H_I) = (\text{Col. 7}) \sqrt{3(S_B) / (S_F)}$$

- e. Select a flange outer radius (R_{OL}) given by $(R_{OL}) = 2(R_{BC}) - R$. Provide a raised bearing surface at outer edge of the flange based on Col. 1 of Table 2.1. Let the radial width of this raised surface be $(R_{BS}) = 0.1 \text{ Col. 1}$. Let the height of this raised bearing surface be $(H_B) \geq 0.002 \text{ Col. 1}$. Let the flange be raised at the gasket region to match the raised bearing surface at the outer edge. Contain the gasket.
- f. Select a hub thickness at the flange of $(T_I) = 2.5 R p_{\text{max. oper.}} / \sigma_{\text{allow.}}$

(The value 3.28 in place of 2.5 for the coefficient would be such that if the flange neither deflected radially nor rotated, the maximum axial hub stress at the inside radius would equal the allowable when the internal pressure was $1.5 p_{\text{max. oper.}}$ and the axial load was $2.5 \pi R^2 p_{\text{max. oper.}}$. The reduction to 2.5 gives an adjustment for the fact that the flange ring deflects and rotates somewhat, and the hub tapers more rapidly. Check that $(R_{BC}) > R + 1.2(T_I) + \text{Col. 5}$ of Table 2.1. Increase (R_{BC}) if necessary.)

- g. Same as (e), (f), (g), and (h) Section 2.2.1.
- h. Same as (i), (j), (k), (l), Section 2.2.1, except perform computation in accordance with Section 2.3.2 instead of 2.2.2.

2.3.2 Integral Flanges With Contact Outside the Gasket Circle - Detailed Analysis

The elastic analysis is based on satisfying equilibrium and compatibility conditions at the pipe-hub, flange-hub, flange-gasket, flange-bolt, and flange-flange interfaces. The methods presented in connection with Section 2.2.2 are used here as well. From the analysis deformations and stresses are obtained for all the loading conditions of interest. Usually the bolts are considered to be squarely loaded since flange rolling should be low with contact outside the bolt circle. The gasket is considered contained so there is flange-to-flange contact in the gasket region as well as at the flange edges.

The solution in regard to the hub and flange ring is again a step-by-step process. Thus the solution of a large number of simultaneous equations is avoided. Starting at the small end of the hub, calculations are made stepwise down the hub as described in Section 2.3.2.1. At each step, solutions are obtained for the wall shear, wall moment, radial deflection, and wall slope in terms of the wall moment, M , and wall shear, Q , at the small end of the hub and the pressure, p , the axial load, P , and the local expansion, $\alpha \Delta T$. Then, in Section 2.3.2.2 solutions are obtained similarly from the inner to the outer radius of the flange ring. Finally, the frictional force is balanced at the contacting outer edge of the flanges and the resulting two equations are solved for M and Q in terms of p , P , $\alpha \Delta T$, $(B \text{ or } C)$, F , and the friction forces at the gasket and outer flange regions.

The solution in regard to the influence of bolt and gasket stiffness is found in Sections 2.3.2.3 and 2.3.2.4. Here four simultaneous equations must be solved. Two of these involve compatibility of the bolt stretch and flange ring deformations at the gasket and outer flange regions. The other two involve equilibrium of the frictional forces between the two flanges in the gasket and outer flange regions. Solution of these equations gives the values of $(B \text{ or } C)$ and the normal and friction forces at the gasket and outer flange regions in terms of p , P , and $\alpha \Delta T$. With these M and Q are obtained. Stresses and deformations at all portions of the connector can then be computed.

Because of the length of the computation and the fact that it involves the solution of simultaneous equations, it is recommended that five or more significant figures be maintained in the numerical computation.

2.3.2.1 Pipe and Hub Stiffness

This portion of the analysis is identical with that in Section 2.2.2.1 for flanges with no contact outside the gasket circle.

2.3.2.2 Flange Ring Stiffness

Bolt holes reduce the stiffness of the flange. In the case of a flange having contact outside the bolt circle, the largest flange stresses are radial and are maximum at the bolt circle. In the absence of better data, the increase in flexibility will be considered as being inversely proportional to the uncut circumference at the bolt circle.

$$f = 2\pi R_B / (2\pi R_B - nd) \quad (2.41)$$

where R_B = radius to the circle through the bolt centers for flanges having contact outside the bolt circle.

Regarding radial flange stress, the same factor f will be taken as the ratio of actual stress to that computed neglecting bolt holes. In line with the discussion in Section 2.2.2.2, no factor will be applied to the flange hoop stress.

The forces from the hub and gasket as well as the internal pressure are considered to cause a resultant axial force at the bottom of the flange ring.

Equations 2.16 through 2.23 apply to the case of the flange having contact outside the bolt circle, if B is replaced by (B-F) in Eqs. 2.16, 2.21, and 2.22.

Proceeding now to the flange portion between the bolt circle and the outer edge, it is known that the moment and tension at the outer edge balance the flange friction Q_{OF} at the outer edge. Using Appendix 2C, Eqs. 2C.3 and 2C.5 give

$$Q_{OF} = \left(\frac{\pi E h}{f}\right) \left(\frac{R_{OF}}{R_B} - \frac{R_B}{R_{OF}}\right) u_B + (1/2) \left[(1+\nu) \frac{R_{OF}}{R_B} + (1-\nu) \frac{R_B}{R_{OF}} \right] Q_B - \left(\frac{\pi E h}{f}\right) \left(\frac{R_{OF}}{R_B} - \frac{R_B}{R_{OF}}\right) R_B \alpha \Delta T \quad (2.42)$$

$$\left(\frac{h}{2}\right) Q_{OF} = M_{OF} = \left(\frac{\pi E h^3}{12f}\right) \left(\frac{R_{OF}}{R_B} - \frac{R_B}{R_{OF}}\right) \theta_B + (1/2) \left[(1+\nu) \frac{R_{OF}}{R_B} + (1-\nu) \frac{R_B}{R_{OF}} \right] M_B - \left(\frac{R_B}{4}\right) \left(\frac{R_{OF}}{R_B} - \frac{R_B}{R_{OF}}\right) \left[(1-\nu) + 2(1+\nu) \left(\frac{R_{OF}^2}{R_{OF}^2 - R_B^2}\right) \log\left(\frac{R_{OF}}{R_B}\right) \right] F \quad (2.43)$$

Equations 2.42 and 2.43 are solved simultaneously to give the pipe wall moment and the pipe wall shear at the small end of the hub in terms of the bolt load, pressure, temperature change, axial force, and forces at the flange-to-flange contacts.

From these the loads and deformations in the left flange-hub-pipe combination are determined. From Eq. 2C.9.

$$\begin{aligned}
 (w_B - w_G) = & \left[\frac{3f(1-\nu^2)(B-F)}{4\pi Eh^3} \right] \left[2R^2 \left(\frac{R_B^2 - R_G^2}{R_B^2 - R^2} \right) \log\left(\frac{R_B}{R}\right) + \right. \\
 & \left. \left(\frac{3+\nu}{1+\nu} \right) (R_B^2 - R_G^2) - 2R_G^2 \log\left(\frac{R_B}{R_G}\right) \right. \\
 & \left. + 4 \left(\frac{1+\nu}{1-\nu} \right) \left(\frac{R_B^2 R^2}{R_B^2 - R^2} \right) \log\left(\frac{R_B}{R_G}\right) \log\left(\frac{R_B}{R}\right) \right] \\
 & + \left[\frac{6f(1-\nu^2)MR}{\pi Eh^3} \right] \left[\frac{R(R_B^2 - R_G^2)}{2(1+\nu)(R_B^2 - R^2)} + \frac{RR_B^2}{(1-\nu)(R_B^2 - R^2)} \log\left(\frac{R_B}{R_G}\right) \right] \\
 & - \left[\frac{6f(1-\nu^2)M_B}{\pi Eh^3} \right] \left[\frac{R_B(R_B^2 - R_G^2)}{2(1+\nu)(R_B^2 - R^2)} + \frac{R_B R^2}{(1-\nu)(R_B^2 - R^2)} \log\left(\frac{R_B}{R_G}\right) \right] \quad (2.44)
 \end{aligned}$$

$$\begin{aligned}
 (w_B - w_{OF}) = & \left[\frac{3fF}{4\pi Eh^3} \right] \left[(1-\nu)(3+\nu)(R_{OF}^2 - R_B^2) + 4(1+\nu)^2 \left(\frac{R_{OF}^2 R_B^2}{R_{OF}^2 - R_B^2} \right) \log^2\left(\frac{R_{OF}}{R_B}\right) \right. \\
 & - \left[\frac{3fM_B}{\pi Eh^3} \right] \left[(1-\nu)R_B + 2(1+\nu) \left(\frac{R_B R_{OF}^2}{R_{OF}^2 - R_B^2} \right) \log\left(\frac{R_{OF}}{R_B}\right) \right] \\
 & + \left[\frac{3fQ_{OF}}{2\pi Eh^2} \right] \left[(1-\nu)R_{OF} + 2(1+\nu) \left(\frac{R_B^2 R_{OF}}{R_{OF}^2 - R_B^2} \right) \log\left(\frac{R_{OF}}{R_B}\right) \right] \quad (2.45)
 \end{aligned}$$

The radial displacement of the gasket region of the flange is given by Eq. 2.29 with the term B replaced by (B-F).

The radial displacement of the outer flange region is given by Eqs. 2C-14 and 2C-15.

$$\begin{aligned}
u_{OF} = & \left[\frac{R_{OF}^2 + R_B^2 - \nu (R_{OF}^2 - R_B^2)}{2\pi Eh (R_{OF}^2 - R_B^2)} \right] f_{Q_{OF}} - \left[\frac{R_{OF} R_B}{\pi Eh (R_{OF}^2 - R_B^2)} \right] f_{Q_B} \\
& - \left[\frac{6R_{OF} R_B}{\pi Eh^2 (R_{OF}^2 - R_B^2)} \right] f_{M_B} + 3 \left[\frac{R_{OF}^2 + R_B^2 - \nu (R_{OF}^2 - R_B^2)}{2\pi Eh (R_{OF}^2 - R_B^2)} \right] f_{Q_{OF}} \\
& + \left(\frac{3R_{OF}}{2\pi Eh^2} \right) \left[1 - \nu + 2(1 + \nu) \left(\frac{R_B^2}{R_{OF}^2 - R_B^2} \right) \log \left(\frac{R_{OF}}{R_B} \right) \right] f_{F+R_{OF}\Delta T}
\end{aligned} \tag{2.46}$$

A similar procedure is used for the right flange-hub-pipe combination starting from the smaller end of the hub and working towards the flange ring top. Sign conventions for the right combination are a mirror image of those for the left combination. As a result radial displacement is again outward, and axial displacement is towards the gasket. The friction forces at the outer flange and gasket regions must satisfy the relations,

$$Q_{OF \text{ Left}} + Q_{OF \text{ Right}} = 0 \tag{2.47}$$

$$Q_{gf \text{ Left}} + Q_{gf \text{ Right}} = 0 \tag{2.48}$$

2.3.2.3 Bolt and Gasket Stiffness

The axial extension of the bolt and gasket regions is from Eq. 2D.2 and 2E.1.

$$w_{BB} = \left(\frac{4}{\pi} \right) \frac{L_B B}{nEd^2} + 2 h \alpha_B \Delta T - C - h \alpha_F \Delta T \tag{2.49}$$

$$w_{GG} = - h \alpha_F \Delta T$$

The last term in Eq. 2.49 accounts for the expansion of the flange between edge and midthickness.

2.3.2.4 Interaction of Bolts and Flanges - Contact Outside the Gasket Circle.

The sum of the axial deflections of the two flanges between the gasket and the bolt circle plus the bolt stretch must remain constant in the absence of bolt tightening or creep. Similarly, the sum of the axial deflections of the two flanges between the flange edge and the bolt circle plus the bolt stretch must remain constant. These two equations involve the initial system tightening constant, C, and the force, F, at the flange edge. Thus

$$w_{GG} + w_{BB} + (w_B - w_G)_{\text{Left Flange}} + (w_B - w_G)_{\text{Right Flange}} = 0 \quad (2.50)$$

$$w_{GG} + w_{BB} + (w_B - w_{OF})_{\text{Left Flange}} + (w_B - w_{OF})_{\text{Right Flange}} = 0 \quad (2.51)$$

If there is no slipping between gasket regions of the two flanges,

$$u_G \text{ Left Flange} = u_G \text{ Right Flange} \quad (2.52)$$

If there is no slipping in the outer flange region,

$$u_{OF} \text{ Left Flange} = u_{OF} \text{ Right Flange} \quad (2.53)$$

Solving simultaneously Eqs. 2.50, 2.51, 2.52, 2.53 and

$$B = G + F + P + \pi(R_G^2 - R^2)p \quad (2.54)$$

gives the gasket force, G, the bolt pull, B (or when initially tightened the constant C), the outer flange force, F, and the friction forces in the "gasket area" and the "outer edge of flange" area. If the resulting values for either friction force exceed the coefficient of friction times the corresponding normal force, G or F, this is an indication that sliding actually occurs in this area. In case sliding occurs at the gasket area, replace Eq. 2.52 by

$$Q_{gf} \text{ Left} = - Q_{gf} \text{ Right} = \pm \mu G \quad (2.55)$$

and repeat the computations, the sign in Eq. 2.55 depending on the relative direction of sliding. In case sliding occurs in the outer flange region, replace Eq. 2.53 by

$$Q_{OF} \text{ left} = - Q_{OF} \text{ right} = \pm \mu F \quad (2.56)$$

and repeat the computation,

where again the sign depends on the relative direction of sliding.

The value of the constant, C , is evaluated at the initial tightening condition by setting p , P , ΔT equal to zero and $B = (B_T)$. Using this value of C and the design load values, the load and deformation distributions in the flanges and hub are obtained.

The bolt stress is given by Eq. 2D.4.

The maximum hoop stress in the flange is given by one of the Eqs. 2C.10 to 2C.13. However, it is likely to be quite small so it may be taken as zero for conventional designs.

The radial stress in the flange at the bolt circle is given by either Eqs. 2C.16 or 2C.17 as

$$\sigma_{\text{Radial}} = \left[\frac{Q_B}{2\pi R_B h} + \frac{3M_B}{\pi R_B h^2} \right] f \quad (2.57)$$

where the sign is chosen to give the largest value of the radial stress and the multiplying factor f is obtained from Eq. 2.41.

The hoop and axial stresses in the hub and pipe are given by Eqs. 2.39 and 2.40. In the case of flanges contacting outside the bolt circle, the sign before M in Eq. 2.40 is most critical when it is positive.

Comparing the stresses with the allowable values indicates where additional thickness is needed and where thickness can be removed. If the gasket load drops below the minimum permitted, an increase in initial bolt load or general thickening may be beneficial. Similarly distortion limits may require thickening. Where increased thickening is used, the change in thickness should be in proportion to half the difference between values obtained and allowable values.

2.4 Loose Flange - No Contact Outside Bolt Circle

A widely used form of flange connector is one having one integral flange and one loose flange Figure 2.6. The loose flange permits bolt holes to be matched more readily than with two integral flange connectors. The loose flange in turn bears on a lap flange (ferrule). Use will be made of the elastic interaction of the bolts, flanges, hubs, gasket and pipes under the various applied loads to arrive at an optimum design configuration.

The design procedure involves selecting a preliminary design layout, analyzing for stresses and deformations under the various loading conditions, using the results to select an improved design layout, reanalyzing, and remodeling until an efficient design is attained. Every effort has been made to make the preliminary design procedure a good one. However, for simplicity, only a few parameters can be considered at a time. Thus, the highly complex interactions of the connector parts can only be accounted for approximately in the preliminary design phase. At least

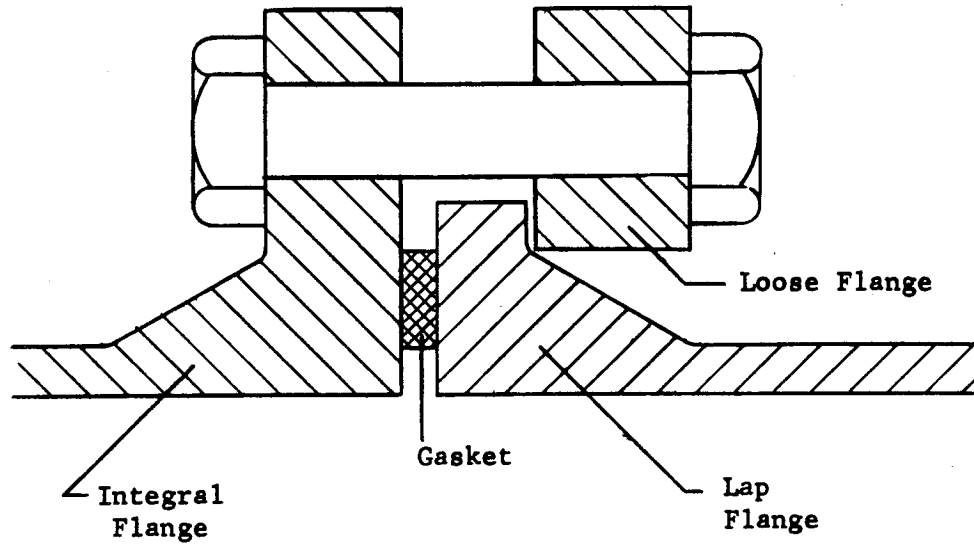


Figure 2.6. Loose Flange - No Contact Outside Bolt Circle.

Table 2.3

ESTIMATION OF LAP AND LOOSE FLANGE DIMENSIONS

1	2	3	4	5	6
<u>Pipe wall thickness</u> Inner pipe radius	<u>Hub thickness at flange(lap)</u> Pipe wall thickness	<u>Outer flange (lap) radius</u> Inner pipe radius	<u>Max. Oper. Pressure</u> Allowable stress in pipe wall	<u>Hub length (lap)</u> Inner pipe radius	<u>Loose flange inner radius</u> Inner pipe radius
0.01	5.60	1.077	0.0072	0.183	1.067
0.03	5.40	1.225	0.0216	0.318	1.195
0.05	5.24	1.364	0.0362	0.409	1.314
0.07	5.08	1.496	0.0507	0.485	1.426
0.09	4.96	1.626	0.0655	0.550	1.536
0.11	4.84	1.749	0.080	0.611	1.64
0.13	4.74	1.871	0.095	0.665	1.74
0.15	4.66	1.988	0.110	0.717	1.84
0.17	4.58	2.09	0.125	0.766	1.92
0.19	4.51	2.20	0.140	0.812	2.01
0.21	4.44	2.32	0.155	0.857	2.11
0.23	4.37	2.44	0.170	0.898	2.21
0.25	4.31	2.55	0.186	0.942	2.30
0.27	4.25	2.65	0.200	0.98	2.38
0.29	4.20	2.76	0.216	1.02	2.47
0.31	4.16	2.86	0.231	1.06	2.55
0.33	4.12	2.97	0.246	1.10	2.64
0.35	4.08	3.06	0.262	1.13	2.71
0.37	4.04	3.16	0.277	1.17	2.79
0.39	4.00	3.26	0.292	1.20	2.87

one or two cycles of the analysis-redesign procedure are essential if an optimum configuration is to be achieved.

The detailed design procedure is presented here in a form suitable for hand computation so that the procedures can be clearly understood. It is also in a form which can readily be translated to digital computer language either in part or total. Where many connectors must be designed, use of a digital computer recommends itself both from the point of view of accuracy in the many numerical computations involved as well as cost in repeating computations to achieve an optimum configuration.

2.4.1 Preliminary Design Layout - Integral and Loose Flanges - No Contact Outside Bolt Circle.

A preliminary design layout is selected as follows:

- a. Proceed with steps (a) to (d) of Section 2.2.1 for the bolts and integral flange portion of the connector.
- b. Choose a lubricant and friction coefficient for the contact between loose flange and lap flange. Some approximate friction coefficients are given in Table 2.2. A low friction coefficient will usually be preferable.
- c. Check the pipe wall thickness at the small end of the hub* from Table 2.3 by entering in Col. 4 with the ratio of maximum operating pressure to allowable stress in the pipe and setting

$$(T_P) = R \text{ Col. 1}$$

Take the hub thickness at the junction with the lap flange as

$$(T_L) = (T_P) \text{ Col. 2}$$

Take the outer flange radius of the lap flange as

$$(R_{OL}) = R \text{ Col. 3}$$

Take the thickness of the lap flange as

$$(H_L) = (T_P) \text{ Col. 2}$$

Let the fillet at the junction of hub and lap flange have a radius of 0.1 to 0.2 (T_L), and the fillet at the junction of hub and pipe have a radius of 0.1 to 0.2 (T_P).

Take the basic hub length as

$$(L_H) = R \text{ Col. 5}$$

* Exceeds by a small margin the value obtained.

This will generally give a hub having a greater slope than 3:1 so a welding taper as described in Section 2.2.1, e should be added.

d. Same as 2.2.1,h.

e. Take the inner radius of the loose flange from Table 2.3 as

$$(R_{ILF}) = R \text{ Col. 6}$$

f. Take the outer radius of the loose flange from the value for the integral flange as (R_{OF}) .

g. Using the values determined for the integral flange of the connector of

$$\begin{aligned} (B_I) &= \text{initial bolt load} \\ (R_{BC}) &= \text{radius to bolt center} \\ d &= \text{bolt diameter} \end{aligned}$$

determine the loose flange thickness as

$$(H_F) = \sqrt{\frac{(B_I)}{(S_{FL})} \left[\frac{(R_{BC}) - (R_{ILF}) - (d-t)/2}{(R_{OF}) - (R_{ILF})} \right]}$$

where (S_{FL}) is the allowable stress in the loose flange material.. (Since the loose flange is not in contact with the fluid, it may be of higher strength material than the "integral" or "lap stub" flanges).

Ordinarily the loose flange dimensions will be such that the bolt clearance makes a hub inappropriate. The "loose" flange "lap" "stub" combination should be checked to assure satisfaction of the bolt clearance requirement, Col. 5 of Table 2.1. If necessary, increase the loose flange thickness above the value computed here to satisfy the clearance requirement.

2.4.2 Loose Flange - No Contact Outside Bolt Circle - Detailed Analysis

The elastic analysis is based on satisfying equilibrium and compatibility conditions at the various interfaces. The methods in Section 2.2 are used. From the analysis, deformations and stresses are obtained for all the loading conditions of interest. The bolts in this case are eccentrically loaded because of flange rolling.

The solution in regard to the integral hub and flange ring is basically a step-by-step process. Starting at the small end of the hub, solutions are obtained stepwise down the hub and up the flange ring as described in Section 2.3.2.1. Setting the wall moment and wall tension to zero at the outer radius of the flange ring, the resulting two simultaneous equations are solved for the moment and shear in the pipe wall at its junction with the integral flange hub in terms of p , P , $\alpha\Delta T$, $(B \text{ or } C)$, and Q_{gf} .

the integral flange hub in terms of p , P , $\alpha\Delta T$, $(B \text{ or } C)$, and $Q_{\text{Gasket friction}}$

The solution in regard to the lap flange is similar. Starting at the small end of the lap-flange hub, solutions are obtained stepwise along the hub to the lap flange and then up the lap-flange ring as described in Section 2.4.2.2. Placing the forces between lap and loose flanges in equilibrium, the resulting two simultaneous equations are solved for the moment and shear in the pipe wall at its junction with the lap-flange hub in terms of p , P , $\alpha\Delta T$, $(B \text{ or } C)$, Q_{gf} , and the friction forces between the loose and lap flanges.

The solution in regard to the loose flange is based on the assumption of no loose-flange hub. (Lap flanges designed as described here make loose-flange hubs inappropriate). Starting at the inner radius of the loose flange the solution in Section 2.4.2.4 proceeds stepwise to the outer radius. Placing the wall moment and wall tension to zero and solving the resulting two simultaneous equations, gives the radial displacement and rotation of the inner radius of the loose-flange ring in terms of $(B \text{ or } C)$, $\alpha\Delta T$, and the friction force between loose and lap flanges.

The solutions in regard to bolt and gasket stiffness are given in Section 2.4.2.3.

In Section 2.4.2.5 the interaction of the various connector parts is considered by solving four simultaneous equations. The first involves compatibility of the bolt stretch, gasket compression, and flange ring deflections. The other three involve equilibrium of frictional forces at the two flange-gasket contacts and at the contact of lap and loose flanges. Solution of these equations gives the values of $(B \text{ or } C)$ and the three friction forces. With these the stresses and deformations are also obtained.

2.4.2.1 Pipe, Hub, and Flange Stiffness of Integral Flange.

The flexibility of the integral pipe-hub-flange combination is computed by using Sections 2.2.2.1 and 2.2.2.2 directly. These give the deformations and stresses for this portion in terms of the bolt load, pressure, temperature change, axial force and gasket frictional force.

2.4.2.2 Pipe, Hub, and Flange Stiffness of Lap Flange

A similar procedure to Sections 2.2.2.1 is applied starting from the smaller end of the flange hub and working towards the larger end. For the lap-flange ring, the procedure in Section 2.2.2.2, Eqs. 2.15 to 2.19, is followed, except for the following difference. Since the lap-flange ring has no holes, in place of Eq. 2.15

$$f = 1 \quad (2.58)$$

At the outer radius of the lap flange, the axial force, P_R , equals the bolt force B and the radial force is

$$Q_{OL} = -Q_{LF} \quad (2.59)$$

and the moment is

$$M_{OL} = \left(\frac{h}{2}\right) (Q_{LF}) \quad (2.60)$$

Usually the loose flange rolls inward with respect to the lap flange so

$$Q_{LF} = \mu_{OL} B \quad (2.61)$$

Using Appendix 2C

$$Q_{OL} = (\pi Eh) \left[\frac{R_{OL}}{R} - \frac{R}{R_{OL}} \right] u_R + 1/2 \left[(1+\nu) \frac{R_{OL}}{R} + (1-\nu) \frac{R}{R_{OL}} \right] Q_R - (\pi Eh) \left[\frac{R_{OL}}{R} - \frac{R}{R_{OL}} \right] R \alpha \Delta T \quad (2.62)$$

$$M_{OL} = \left(\frac{\pi Eh^3}{12}\right) \left[\frac{R_{OL}}{R} - \frac{R}{R_{OL}} \right] \Theta_R + 1/2 \left[(1+\nu) \frac{R_{OL}}{R} + (1-\nu) \frac{R}{R_{OL}} \right] M_R + \left[\frac{R_{OL}}{R} - \frac{R}{R_{OL}} \right] \left[1 - \nu + 2(1+\nu) \left(\frac{R_{OL}^2}{R_{OL}^2 - R^2} \right) \log \left(\frac{R_{OL}}{R} \right) \right] B \quad (2.63)$$

Equations 2.59 to 2.63 are solved simultaneously to give the wall moment and wall shear at the small end of the hub. The values are obtained in terms of the bolt load, pressure, temperature change, axial force, gasket force, and frictional forces.

2.4.2.3 Bolt and Gasket Stiffness

The axial extension of the bolt is obtained from Eq. 2D.1 as

$$w_{BB} = \left(\frac{20}{\pi}\right) \left[\frac{L_B}{nEd^2} \right] B - C + \left[h_G + (H_I) + (H_L) + (H_F) \right] \alpha_B \Delta T - \left[(H_L) + (H_I)/2 + (H_F)/2 \right] \alpha_F \Delta T \quad (2.64)$$

The axial compression of the gasket is obtained from Eq. 2E.1 as

$$w_{GG} = \left[\frac{h_G}{2\pi g R_G E_G} \right] G - \left[(H_L) + (H_I)/2 + (H_F)/2 \right] \alpha_F \Delta T - h_G \alpha_G \Delta T \quad (2.65)$$

The radial gasket displacement is given by Eq. 2.32.

2.4.2.4 Loose Flange Stiffness

The loose flange stiffness is obtained similarly to the integral flange stiffness. Assuming no hub, subscript ILF is taken to indicate the inner radius of the loose flange and set

$$\text{Loose-flange-bottom axial force} = \text{bolt pull, } B \quad (2.66)$$

$$\text{Loose-flange-bottom radial force, } Q_{ILF} = -Q_{LF} \quad (2.67)$$

$$\text{Loose-flange-bottom moment, } M_{ILF} = -(1/2)(H_F)(Q_{LF}) - B(R_{OL} - R_{ILF}) \quad (2.68)$$

The displacements at the bottom of the loose-flange ring are taken as

$$\Theta_{ILF}, \quad u_{ILF}$$

The corresponding values at the line of action of the bolts are given by use of Appendix 2C. In this case, the flexibility factor due to the bolt holes is

$$f = 1 / \left[1 - nd^2 / \pi (R_{OF}^2 - R_{ILG}^2) \right] \quad (2.69)$$

Equations 2.20 to 2.25 of Section 2.2.2.2 apply, except R_{ILF} replaces R , Q_{ILF} replaces Q_R , u_{ILF} replaces u_R , Θ_{ILF} replaces Θ_R , and M_{ILF} replaces M_R .

Equations 2.26 and 2.27 apply directly and are solved simultaneously to give the radial wall displacement and wall rotation at the inner radius of the loose flange in terms of the bolt load, temperature change, and loose-flange friction. From these the loads and deformations in the loose flange are determined.

2.4.2.5 Interaction of Flanges, Bolts and Gasket - Loose Flange Without Contact Outside Bolt Circle.

The sum of the axial deflections of the flanges, the bolt stretch, Eq. 2.30 and the gasket compression, Eq. 2.31 must remain constant in the absence of bolt tightening or creep. This provides an equation involving the initial system extension C.

$$\begin{aligned}
 (w_{BB} + w_{GG}) + (w_B - w_G)_{\text{Integral Flange}} + (w_{OL} - w_G)_{\text{Lap flange}} \\
 + (w_B - w_{OL})_{\text{Loose flange}} = 0 \qquad (2.70)
 \end{aligned}$$

In this expression the first term is obtained from Eqs. 2.64 and 2.65. The second term is obtained from Eq. 2.28 with f from Eq. 2.15, M_R for the integral flange, and h equal (H_I). The third term is obtained from Eq. 2.28 with f equal one, subscript OL replacing subscript B, h equal (H_L), and M_R for the lap flange. The last term is obtained from Eq. 2.28 with h equal (H_F), subscript OL replacing subscript G, subscript ILF replacing subscript R, R_{ILF} replacing R, and f obtained from Eq. 2.69.

The radial displacement of the integral flange at the gasket is obtained from Eq. 2.29 with f given by Eq. 2.15, h equal (H_I), and Q_R, M_R, M_B the values for the integral flange. Equating this to the value in Eq. 2.32 gives an equation applying when there is no gasket slip.

$$u_G(\text{Integral}) = u_{GT} \qquad (2.71)$$

The radial displacement of the lap flange at the gasket is obtained from Eq. 2.29 with f equal one, h equal (H_L), M_R and Q_R the values for the lap flange, and subscript OL replacing subscript B. Equating this to the value in Eq. 2.32 gives another equation applying when there is no gasket slip.

$$u_G(\text{Lap}) = u_{GT} \qquad (2.72)$$

The two equations 2.71 and 2.72 involving gasket frictions are solved simultaneously with Eq. 2.70 to give the bolt pull, B, (or when initially tightened the constant C) and the gasket friction forces. The gasket force is obtained from Eq. 2.25. If the resulting values for gasket friction exceed the friction coefficient times the gasket force, G, this indicates that sliding actually occurs. In that event, one or both equations involving radial displacement are replaced by Eqs. 2.36.

The radial displacement of the loose flange at the point of contact with the lap flange is obtained from Eq. 2.29 with h equal (H_F) , subscript OL replacing subscript G, subscript ILF replacing subscript R, R_{ILF} replacing R, and using the value of f in Eq. 2.69.

The radial displacement of the lap flange at the point of contact with the loose flange is obtained from Eq. 2.29 with h equal (H_L) , subscript OL replacing subscripts G and B, f equal one, and reversing the signs of the last three terms in Eq. 2.29 involving B and the two moments.

If these two radial deflections do not show a relative radial displacement inwards of the loose flange with respect to the lap flange, the value of the frictional force between them will be less than μB and is found by equating the radial deflections of the loose and lap flanges at their point of contact and solving the simultaneous equations again for the value of Q_{LF} .

The value of the constant C is now evaluated at the initial tightening conditions by setting p , P , $\Delta T=0$, and $B=G=(B_T)$. Using this value of C and the load values corresponding to proof test and various operating conditions, the load distribution in the flanges, hubs, bolts, etc. are found. Deformations are also found and should be checked to see that rolling of the loose or lap flanges is not excessive and that the proper assumptions regarding friction (sliding or not) have been used for all loadings.

The bolt stress is given by Eq. 2D.3. The maximum stress in the integral flange is given by Eq. 2.37 and 2.38. For the loose flange the maximum hoop stress is given by Eq. 2.37 with R replaced by R_{ILF} and subscript R replaced by subscript ILF. The axial and radial stresses in the loose flange are usually negligible. For the lap flange the maximum stress is given by Eq. 2.37 and 2.38 with subscript B replaced by subscript OL. The hoop stress in the hub and pipe for the integral and lap flanges is given by Eq. 2.39. Axial stress in the hubs and pipe is given by Eq. 2.40.

Comparing the stresses and deformations with allowable values indicates where thickness changes may be desirable. Comparing the gasket loads with the minimum permitted values indicates when a higher initial bolt load may be required. In general the thickness changes should be in proportion to half the desired stress or deformation changes.

2.5 Loose Flange - Contact Outside Bolt Circle

Where contact outside the bolt circle is desirable it may be necessary to provide a loose flange so that bolt holes can be aligned. Such a connector design is considered in Figure 2.7. The lap flange should always be checked for excessive rolling in such a design.

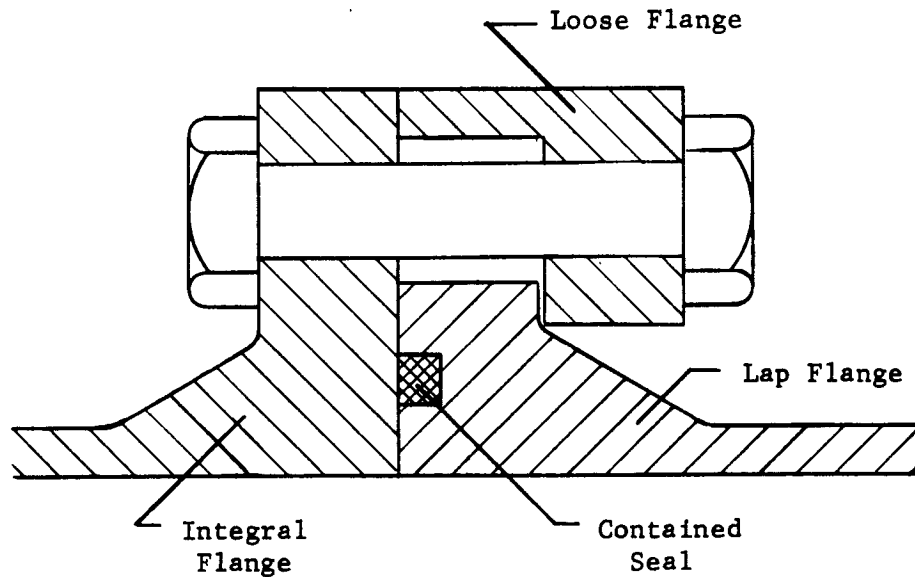


Figure 2.7. Loose Flange - With Contact Outside Bolt Circle

The design procedure involves selecting a preliminary design layout, analyzing for stresses and deformations under the various loading conditions using the results to select an improved design layout, reanalyzing, and remodeling until an efficient design is attained. Every effort has been made to make the preliminary design procedure a good one. However, for simplicity, only a few parameters can be considered at a time. Thus, the highly complex interactions of the connector parts can only be accounted for approximately in the preliminary design phase. At least one or two cycles of the analysis-redesign procedure are essential if an optimum configuration is to be achieved.

The detailed design procedure is presented here in a form suitable for hand computation so that the procedures can be clearly understood. It is also in a form which can readily be translated to digital computer language either in part or total. Where many connectors must be designed, use of a digital computer recommends itself both from the point of view of accuracy in the many numerical computations involved as well as cost in repeating computations to achieve an optimum configuration.

2.5.1 Preliminary Design Layout - Loose Flange - Contact Outside Bolt Circle

- (a) For the integral flange and bolts and gasket, steps (a) through (f) of Section 2.3.1 and steps (e) through (l) of Section 2.2.1 are followed, except perform detailed computations as described in Section 2.5.2.
- (b) For the lap flange, follow steps (b) through (d) of Section 2.4.1.

- c. For the loose flange, let the outer radius be the same as that of the integral flange. Provide a lip at the outer radius whose depth is sufficient to reach the integral flange and whose inner radius clears the bolt. Let the inner radius of the loose flange clear the lap flange hub. Take the thickness equal to that of the integral flange.

2.5.2 Detailed Analysis - Loose Flange - Contact Outside Bolt Circle

2.5.2.1 Integral Flange, Hub and Pipe

These are treated exactly as described in Sections 2.3.2.1 and 2.3.2.2.

2.5.2.2 Lap Flange, Hub and Pipe

These are treated exactly as described in Section 2.4.2.2.

2.5.2.3 Bolt and Gasket Deformation

The axial extension of the bolt is obtained from Eq. 2D.2 as (considering the gasket contained),

$$w_{BB} = \left(\frac{4}{\pi}\right) \left[\frac{L_B}{nEd^2}\right]_{B-C} + \left[(H_I) + (H_L) + (H_F) \right] \alpha_B \Delta T - \left[(H_L) + (H_I)/2 + (H_F)/2 \right] \alpha_F \Delta T \quad (2.73)$$

The axial compression of the gasket is obtained from Eq. 2E.1 (considering the gasket contained) as,

$$w_{GG} = - \left[(H_L) + (H_I)/2 + (H_F)/2 \right] \alpha_F \Delta T \quad (2.74)$$

2.5.2.4 Loose Flange Stiffness

Assuming no hub, subscript ILF is taken to indicate the inner radius of the loose flange and set

$$\text{Loose flange bottom axial force} = B-F \quad (2.75)$$

$$\text{Loose flange bottom radial force} = Q_{ILF} = -Q_{LF} \quad (2.76)$$

$$\text{Loose flange bottom moment} = M_{ILF} = -(1/2)(H_F)(Q_{LF}) \quad (2.77)$$

Take θ_{ILF} and u_{ILF} as the inner displacements.

The flexibility factor is given by Eq. 2.41. The values at the bolt circle are obtained from Eqs. 2.20 to 2.24 with R_{ILF} replacing R , $(B-F)$ replacing B , subscript ILF replacing subscript R , and h equal (H_F) .

Proceeding now to the flange portion between the bolt circle and the outer edge, the only force at the outer edge is the flange friction. Eqs. 2.42 and 2.43 apply directly with h equal (H_F) and f given by Eq. 2.41.

2.5.2.5 Interaction of Bolts and Flanges - Loose Flange with Contact Outside Bolt Circle

The axial deflections of the flanges and bolts must remain compatible. In the absence of bolt tightening, Eq. 2.70 applies directly. In this expression, w_{BB} is obtained from Eq. 2.73 and w_{GG} from Eq. 2.74. The second term is obtained from Eq. 2.44 with f from Eq. 2.41, M_R for the integral flange, and h equal (H_I) . The third term is obtained from Eq. 2.28 with f equal one, subscript OL replacing subscript B, (B-F) replacing B, M_R for the lap flange, and h equal (H_L) . The last term is obtained from Eq. 2.28 with f from Eq. 2.41, (B-F) replacing B, subscript OL replacing subscript G, subscript ILF replacing subscript R, R_{ILF} replacing R, and h equal (H_F) .

Similarly Eq. 2.51 for compatibility at the outer flange region applies directly. Again w_{BB} is obtained from Eq. 2.73 and w_{GG} from Eq. 2.74. The third term in this expression is obtained from Eq. 2.45 with f given by Eq. 2.41, M_B the value for the integral flange, and h equal (H_I) . The last term in the expression is given by Eq. 2.45 with f given by Eq. 2.41, M_B the value for the loose flange, and h equal (H_F) .

The radial displacement compatibility in the outer flange regions is expressed by Eq. 2.53. The term on the left side of this expression is obtained from Eq. 2.46 using Q_B and M_B for the integral flange, f from Eq. 2.41, and h equal (H_I) . The term on the right side of Eq. 2.53 is obtained from Eq. 2.46 using Q_B and M_B for the loose flange, f from Eq. 2.41, and h equal (H_F) .

The radial displacement compatibility in the gasket region is expressed by Eq. 2.52. The term on the left side of this expression is obtained from Eq. 2.29 with M_B , Q_B , M_R , Q_R the values for the integral flange, (B-F) replacing B, f given by Eq. 2.41, and h equal (H_I) . The term on the right side of Eq. 2.52 is given by Eq. 2.29 with f equal one, subscript OL replacing subscript B, (B-F) replacing B, M_R and Q_R for the lap flange, and h equal (H_L) .

The gasket force is given by Eq. 2.54. The loose-flange frictional force will ordinarily be inwards with respect to the lap flange so

$$Q_{1f} = \mu_{OL} (B-F) \quad (2.78)$$

Using Eqs. 2.51, 2.52, 2.53, 2.70 and 2.78 simultaneously makes it possible to solve for (B or C), F, G, and the three frictional forces. If the resulting value of Q_{gf} exceeds $\mu_G G$, the corresponding compatibility equation is replaced by Eq. 2.55 with appropriate sign. If the resulting value of Q_{OF} exceeds $\mu_{OF} F$, the corresponding compatibility equation is replaced by Eq. 2.56 with appropriate sign.

Equation 2.78 applies if there is relative inward sliding of the loose flange on the lap flange. A check should be made to assure that this occurs by computing the radial displacements of the two flanges at their points of contact. The radial displacement of the lap flange is obtained from Eq. 2.29 by replacing B by (B-F), replacing subscripts G and B by subscript OL, setting f equal one, h equal (H_L), reversing the signs of the last three terms involving (B-F), M_{OL} , M_R , and using the values of M_R and Q_R for the lap flange. The radial displacement of the loose flange u_{OL} (Loose) is obtained from Eq. 2.29 by replacing subscript G with subscript OL, subscript R with subscript ILF, R with R_{ILF} , B with (B-F), and using h equal (H_F), f from Eq. 2.41, M_B , Q_B for the loose flange. In the event the relative sliding is not as assumed, Eq. 2.78 is replaced by

$$u_{OL} \text{ (Lap)} = u_{OL} \text{ (Loose)} \quad (2.79)$$

The value of the constant, C, is now evaluated at the initial tightening conditions by setting p, P, $\Delta T=0$, and $B = (B_I)$. Using this value of C and the design load, stress and deformation distributions in the connector are found. At this point, it is again desirable to check that the proper assumptions on friction (sliding or not) have been used.

The bolt stress is given by Eq. 2D.4 . The hoop stress in the flanges is given by one of Eqs. 2C.10 to 2C.13. However, it is likely to be quite small. The radial flange stress is given by Eq. 2.57. The hoop and axial stresses are given for the hubs and pipes by Eqs. 2.39 and 2.40. In the case of the integral flange, Eq. 2.40 is most critical with the sign before M positive, while for the lap flange the negative sign is more critical.

Comparing stresses with allowable values indicates where thickness changes are needed. If the gasket load drops below the minimum permissible value, an increase in bolt load, an increase in flange height, or a general thickening would be beneficial. If the lap flange has greater roll than the gasket can tolerate, the roll can be reduced by increasing the thickness of the lap flange and its hub.

Each set of changes in geometry must be reanalyzed until a satisfactory configuration is found.

2.6 Other Configurations

The methods presented here are suitable for analyzing connectors which are different from the conventional ones considered in the previous sections. Some of these are sketched in Figure 2.8. Their possible advantages and disadvantages are discussed below.

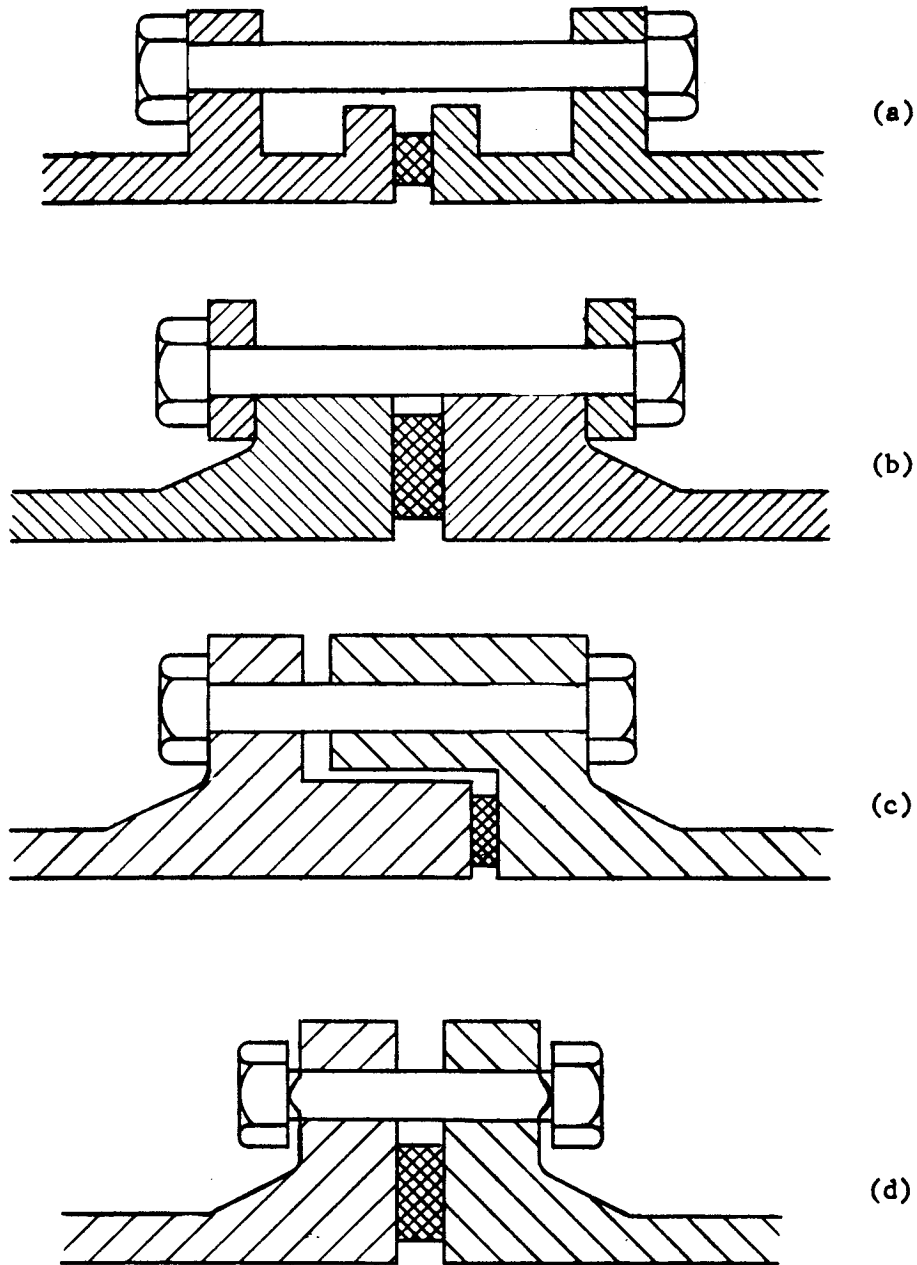


Figure 2.8. Other Connector Configurations

- (a) This configuration restrains flange rolling by having the pipe to both sides of each flange. "Barrelling" should be materially less. Thermal effects may be increased somewhat because of the increased bolt length. Weight is saved in flange width but lost again in increased bolt length.
- (b) This configuration recognizes that the bolts bear only near their inner side when the flanges can roll. This design increases flange thickness while reducing flange height, thus saving weight for the same stiffness and stress levels. The increased bolt length counterbalances this weight saving. The purpose of a "loose" flange is achieved without the flexibility of "loose" flanges.
- (c) Interlocked flanges increase the rolling stiffness of each flange without any overall weight increase. For the same strength and stiffness weight can be saved. The joint loses symmetry however and is somewhat more difficult to machine.
- (d) By providing a slight protuberance on the flange at the bolt-center-line circle, it is possible to load the bolts more squarely, even in the presence of flange rolling, than would otherwise be possible. Bolt stresses would thereby be substantially reduced. Bearing stresses under the bolt head and nut would be large, however, high bearing stresses also occur with eccentric loading by a flange which has rolled. The reduction in bolt area permits the use of smaller bolts and thus reduces the overall flange dimensions.

2.7 Other Analytical Methods

Connectors of the types described above can also be analyzed by Castigliano's Theorem. In this approach the strain energy of all the component elements is determined in terms of the applied and redundant loads. The component strain energies are then summed giving a quadratic function in the loads. The derivatives of this function with respect to the redundant loads, when set equal to zero, give a set of simultaneous equations which can be solved for the redundant loads. The derivatives with respect to the applied loads give the deflections at these loads. This approach can readily be adapted to include friction and temperature effects. Appendices 2F, 2G, and 2H give expressions for the energy in cylindrical and ring segments and in the bolts.

To include friction effects where no sliding is anticipated, the friction force is allowed to be a redundant load. To include friction where sliding is anticipated, the friction force is taken as the friction coefficient times the normal force. In each case, the original assumption can be checked by comparing the force with the maximum possible where no sliding is assumed, or by checking the direction of sliding where sliding has been assumed.

The application of Castigliano's Theorem is simple in principle for a structure made up of cylindrical and ring elements. However, it involves a large amount of numerical computation both in obtaining the energies and in solving the resulting simultaneous equations. Therefore, it is particularly

well suited to machine computation where simplicity in formulation is of prime importance, whereas drudgery in computation is of no moment since it can be accomplished by machine.

2.8 References

- 2.1 Levy, S., ed., "Environmental Effects", Design Criteria for Zero-Leakage Connectors for Launch Vehicles, Vol. 6, TIS Report No. 63GL46, (NASA Contract NAS 8-4012), March 15, 1963.
- 2.2 "Modern Flange Design", Taylor Forge Bulletin 502, (4th Edition), 1961.
- 2.3 Levy, S., ed., "Design of Connectors", Design Criteria for Zero-Leakage Connectors for Launch Vehicles, Vol. 4, TIS Report No. 63GL44, (NASA Contract NAS 8-4012), March 15, 1963.
- 2.4 "Pressure Vessels and Piping Design Collected Papers 1927-1959", ASME
- 2.5 Goodman, T.P., ed., "Summary, Conclusions, and Design Examples", Design Criteria for Zero-Leakage Connectors for Launch Vehicles, Vol.1, TIS Report No. 63GL41, (NASA Contract NAS 8-4012), March 15, 1963
- 2.6 Bernhard, H. J., "Flange Theory and the Revised Standard B.S. 10:1962-Flanges and Bolting for Pipes, Valves and Fittings", (paper presented to the Institution of Mechanical Engineers in London) October 1963.
- 2.7 McCalley, R.B., Jr., and Kelly, R.G., "Tables of Functions for Short Cylindrical Shells", Paper No. 56-F-5, (presented at ASME Fall Meeting in Denver, Colorado, 1956. (Can be consulted at Engineering Societies' Library).
- 2.8 Timoshenko, S., Theory of Elasticity, McGraw-Hill Book Co., 1934.
- 2.9 Timoshenko, S., Theory of Plates and Shells, McGraw-Hill Book Co., 1940.
- 2.10 Tentative Structural Design Basis for Reactor Pressure Vessels and Directly Associated Components, distributed by OTS, Department of Commerce, PB151987, 1 December 1958, Revision with Addendum No. 1, 27 February 1959, (See also NR-S-1 issued March 1961).

2.9 Appendices

Appendix 2A - Long Pipe Theory

With pages 41 through 47 of Ref. 2.3 and consideration of the growth due to thermal expansion

$$u = \left(\frac{a\beta^2}{\pi Et} \right) M + \left(\frac{a\beta}{\pi Et} \right) Q + \left(\frac{aR}{Et} \right) P - \left(\frac{\nu}{2\pi Et} \right) P + a\alpha \Delta T \quad (2A-1)$$

$$\Theta = \left(\frac{2a\beta^3}{\pi Et} \right) M + \left(\frac{a\beta^2}{\pi Et} \right) Q \quad (2A-2)$$

where sign conventions are shown in Figure 2A and

- R = Inner radius of pipe (in.)
- u = Radial displacement outward (in.)
- Θ = Angular rotation (radian)
- M = Total bending moment around circumference (lb.in.). Equal to $2\pi a$ times the bending moment per inch.
- Q = Total shear around circumference (lb.)
- p = Internal pressure (lb/in.²)
- P = Total axial load around circumference (lb.)
- $a\Delta T$ = Unit expansion due to temperature
- a = Distance from pipe axis to wall midthickness (in.)
- ν = Poisson's ratio
- E = Young's modulus (lb/in.²)
- t = Wall thickness (in.)
- $\beta^4 = 3(1-\nu^2)/a^2t^2$

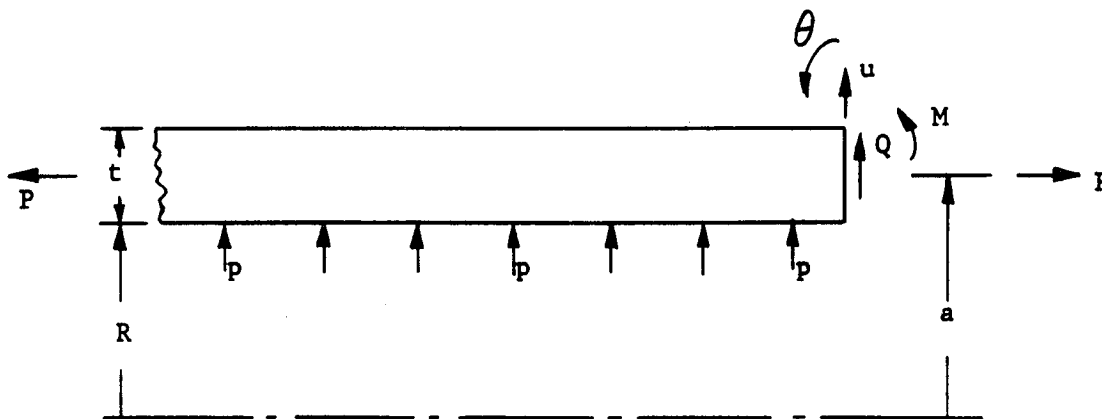


Figure 2A. Pipe Deformation Sign Conventions and Symbols.

Appendix 2B - Pipe Segment Theory

In Ref. 2.7, dealing with the analysis of a short cylindrical shell, a variety of interrelations between the various parameters are presented. From these it is found that Eqs. 2.6 to 2.14 can be derived with the following changes if more precise relationships are required.

- a. Replace "R" by "a" (Figure 2.B) in Eqs. 2.6 to 2.10, except leave R in the coefficient of the p term of Eqs. 2.6 and 2.7 and use aR for R² in the coefficient of the p term in Eqs. 2.8 and 2.9.
- b. For the K coefficients, Eqs. 2.11 and 2.14, use

$$K_1 = (1/2) (\cosh \beta L \sin \beta L - \sinh \beta L \cos \beta L) \quad (2B.2)$$

$$K_2 = \sinh \beta L \sin \beta L \quad (2B.3)$$

$$K_3 = (1/2) (\cosh \beta L \sin \beta L + \sinh \beta L \cos \beta L) \quad (2B.4)$$

$$K_4 = \cosh \beta L \cos \beta L \quad (2B.5)$$

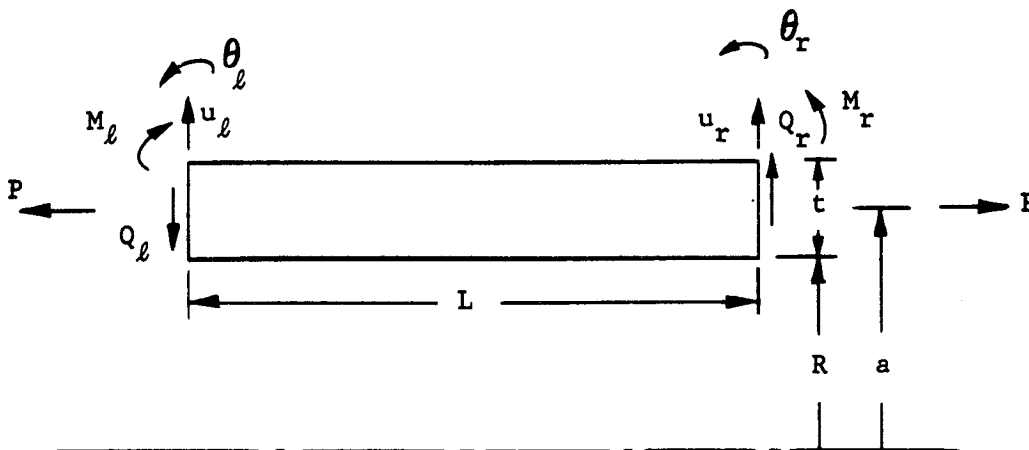


Figure 2B. Pipe Segment Sign Conventions and Symbols.

Appendix C - Flange Plate Equations

Using the equations for plane stress, Eqs. 41 and 49 of Ref. 2.8 give the relationship between radial forces and radial displacement. In terms of the symbols and sign conventions in Figure 2C

$$Q_b - \left(\frac{\pi E h}{f}\right) \left(\frac{a}{b} - \frac{b}{a}\right) u_a + 1/2 \left[(1-\nu) \frac{a}{b} + (1+\nu) \frac{b}{a} \right] Q_a + \left(\frac{\pi E h}{f}\right) \left(\frac{a}{b} - \frac{b}{a}\right) a \alpha \Delta T \quad (2C.1)$$

$$u_b = 1/2 \left[(1+\nu) \frac{a}{b} + (1-\nu) \frac{b}{a} \right] u_a - \left(\frac{f}{4\pi E h} \right) (1-\nu^2) \left(\frac{a}{b} - \frac{b}{a} \right) Q_a - 1/2 (1+\nu) \left(\frac{a}{b} - \frac{b}{a} \right) a \alpha \Delta T \quad (2C.2)$$

$$\text{or, } Q_a = \left(\frac{\pi E h}{f} \right) \left(\frac{a}{b} - \frac{b}{a} \right) u_b + 1/2 \left[(1+\nu) \frac{a}{b} + (1-\nu) \frac{b}{a} \right] Q_b - \left(\frac{\pi E h}{f} \right) \left(\frac{a}{b} - \frac{b}{a} \right) b \alpha \Delta T \quad (2C.3)$$

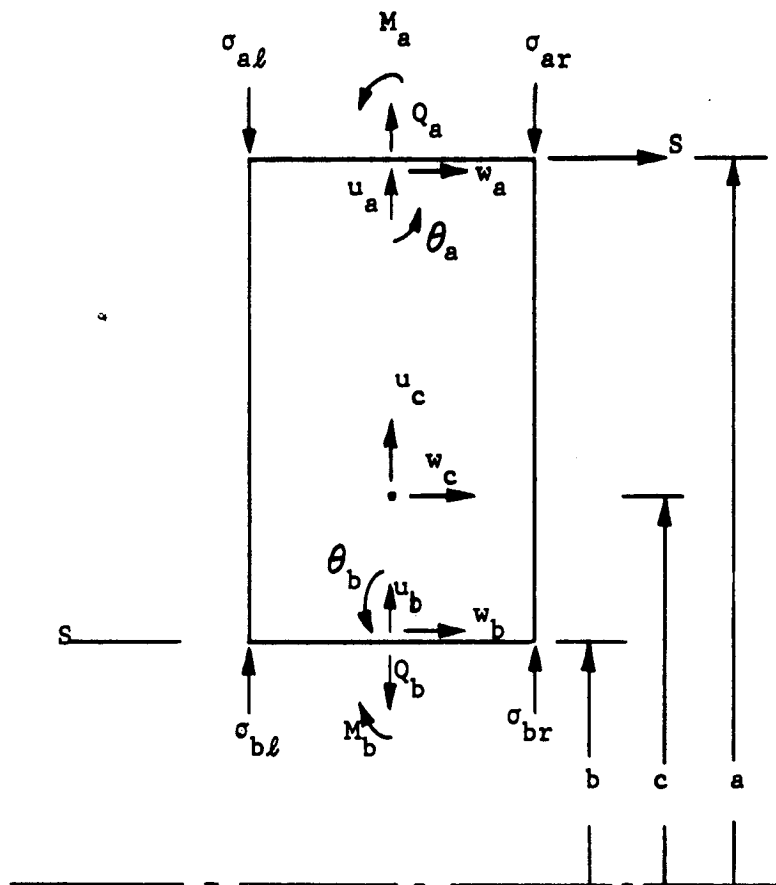


Figure 2C. Ring Segment Sign Conventions and Symbols. (Subscripts "r" and "l" refer to "right" and "left" sides of flange.)

$$u_a = 1/2 \left[(1-\nu) \frac{a}{b} + (1+\nu) \frac{b}{a} \right] u_b + \left(\frac{f}{4\pi E h} \right) (1-\nu^2) \left(\frac{a}{b} - \frac{b}{a} \right) Q_b$$

$$+ 1/2 (1+\nu) \left(\frac{a}{b} - \frac{b}{a} \right) b \alpha \Delta T. \quad (2C.4)$$

Using the plate equations in Ref. 2.9, particularly Eq. 73 page 64, Eq. j page 65, Eq. b page 63, and Eq. f page 65, relationships are obtained for the axial displacements of the flange plate and for the angular rotations of the flange. In terms of the sign conventions and symbols in Figure 2C,

$$M_a = \left(\frac{\pi E h^3}{12f} \right) \left(\frac{a}{b} - \frac{b}{a} \right) (\theta_b - \theta_b^*) + 1/2 \left[(1+\nu) \frac{a}{b} + (1-\nu) \frac{b}{a} \right] M_b \quad (2C.5)$$

$$\theta_a = \theta_a^* + 1/2 \left[(1-\nu) \frac{a}{b} + (1+\nu) \frac{b}{a} \right] (\theta_b - \theta_b^*) + \left(\frac{3f(1-\nu^2)}{\pi E h^3} \right)$$

$$\left(\frac{a}{b} - \frac{b}{a} \right) M_b \quad (2C.6)$$

$$\text{where, } \theta_a^* = - \left[\frac{3(1-\nu^2) f a}{\pi E h^3} \right] \left[\frac{1}{1+\nu} + \left(\frac{2}{1-\nu} \right) \left(\frac{b^2}{a-b} \right) \log \left(\frac{a}{b} \right) \right] S \quad (2C.7)$$

$$\theta_b^* = - \left[\frac{3(1-\nu^2) f b}{\pi E h^3} \right] \left[\frac{1}{1+\nu} + \left(\frac{2}{1-\nu} \right) \left(\frac{a^2}{a-b} \right) \log \left(\frac{a}{b} \right) \right] S \quad (2C.8)$$

The difference in axial displacement between an intermediate radius "c" in Figure 2C, and the radius "a" is given by

$$w_a - w_c = \left(\frac{3fS(1-\nu^2)}{4\pi E h^3} \right) \left[2b^2 \left(\frac{a^2 - c^2}{a^2 - b^2} \right) \log \left(\frac{a}{b} \right) + \left(\frac{3+\nu}{1+\nu} \right) (a^2 - c^2) \right.$$

$$\left. - 2c^2 \log \left(\frac{a}{c} \right) + 4 \left(\frac{1+\nu}{1-\nu} \right) \left(\frac{a^2 b^2}{a^2 - b^2} \right) \log \left(\frac{a}{c} \right) \log \left(\frac{a}{b} \right) \right]$$

$$+ \left(\frac{6M f (1-\nu^2)}{\pi E h^3} \right) \left[- \frac{a(a^2 - c^2)}{2(1+\nu)(a^2 - b^2)} - \left(\frac{ab^2}{(1-\nu)(a^2 - b^2)} \right) \log \left(\frac{a}{c} \right) \right] \quad (2C.9)$$

$$+ \left(\frac{6M_b f (1-\nu^2)}{\pi E h^3} \right) \left[\frac{b(a^2 - c^2)}{2(1+\nu)(a^2 - b^2)} + \frac{ba^2}{(1-\nu)(a^2 - b^2)} \log \left(\frac{a}{c} \right) \right]$$

The hoop stresses at the four corners of the flange ring are given by

$$\begin{aligned} \sigma_{al} = & \left(\frac{Q_a}{2\pi ah} \right) \left(\frac{a^2 + b^2}{a^2 - b^2} \right) - \left(\frac{Q_b}{\pi h} \right) \left(\frac{b}{a^2 - b^2} \right) \\ & + \left(\frac{3S}{2\pi h^2} \right) \left[(1+\nu) \left(\frac{2b^2}{a^2 - b^2} \right) \log \left(\frac{a}{b} \right) + (1-\nu) \right] \\ & + \left(\frac{6bM_b}{\pi h^2} \right) \left(\frac{1}{a^2 - b^2} \right) - \left(\frac{3M_a}{\pi ah^2} \right) \left(\frac{a^2 + b^2}{a^2 - b^2} \right) \end{aligned} \quad (2C.10)$$

$$\begin{aligned} \sigma_{ar} = & \left(\frac{Q_a}{2\pi ah} \right) \left(\frac{a^2 + b^2}{a^2 - b^2} \right) - \left(\frac{Q_b}{\pi h} \right) \left(\frac{b}{a^2 - b^2} \right) \\ & - \left(\frac{3S}{2\pi h^2} \right) \left[(1+\nu) \left(\frac{2b^2}{a^2 - b^2} \right) \log \left(\frac{a}{b} \right) + (1-\nu) \right] \\ & - \left(\frac{6bM_b}{\pi h^2} \right) \left(\frac{1}{a^2 - b^2} \right) + \left(\frac{3M_a}{\pi ah^2} \right) \left(\frac{a^2 + b^2}{a^2 - b^2} \right) \end{aligned} \quad (2C.11)$$

$$\begin{aligned} \sigma_{bl} = & \left(\frac{aQ_a}{\pi h} \right) \left(\frac{1}{a^2 - b^2} \right) - \left(\frac{Q_b}{2\pi bh} \right) \left(\frac{a^2 + b^2}{a^2 - b^2} \right) \\ & + \left(\frac{3S}{2\pi h^2} \right) \left[(1+\nu) \left(\frac{2a^2}{a^2 - b^2} \right) \log \left(\frac{a}{b} \right) + (1-\nu) \right] \\ & + \left(\frac{3M_b}{\pi bh^2} \right) \left(\frac{a^2 + b^2}{a^2 - b^2} \right) - \left(\frac{6aM_a}{\pi h^2} \right) \left(\frac{1}{a^2 - b^2} \right) \end{aligned} \quad (2C.12)$$

$$\begin{aligned} \sigma_{br} = & \left(\frac{aQ_a}{\pi h} \right) \left(\frac{1}{a^2 - b^2} \right) - \left(\frac{Q_b}{2\pi bh} \right) \left(\frac{a^2 + b^2}{a^2 - b^2} \right) \\ & - \left(\frac{3S}{2\pi h^2} \right) (1+\nu) \left(\frac{2a^2}{a^2 - b^2} \right) \log \left(\frac{a}{b} \right) + (1-\nu) \\ & - \left(\frac{3M_b}{\pi bh^2} \right) \left(\frac{a^2 + b^2}{a^2 - b^2} \right) + \left(\frac{6aM_a}{\pi h^2} \right) \left(\frac{1}{a^2 - b^2} \right) \end{aligned} \quad (2C.13)$$

The angular rotation at an intermediate radius is

$$\begin{aligned}
 \theta_c = & \left(\frac{-6bM_b f}{\pi c E h^3 (a^2 - b^2)} \right) (a^2 + c^2 + \nu (a^2 - c^2)) \\
 & + \left(\frac{6aM_a f}{\pi c E h^3 (a^2 - b^2)} \right) [b^2 + c^2 - \nu (c^2 - b^2)] \\
 & - \left(\frac{3Sf}{\pi c E h^3} \right) \left[+ c^2 (1 - \nu^2) \log\left(\frac{a}{c}\right) + c^2 (1 - \nu) + \left(\frac{c^2 b^2 (1 - \nu^2)}{a^2 - b^2} \right) \log\left(\frac{a}{b}\right) \right. \\
 & \left. + \left(\frac{a^2 b^2 (1 + \nu)^2}{a^2 - b^2} \right) \log\left(\frac{a}{b}\right) \right]
 \end{aligned} \tag{2C.14}$$

and the radial displacement at the midthickness is

$$u_c = \left[\frac{c^2 + b^2 - \nu (c^2 - b^2)}{2\pi c E h (a^2 - b^2)} \right] f a Q_a - \left[\frac{a^2 + c^2 + \nu (a^2 - c^2)}{2\pi c E h (a^2 - b^2)} \right] f b Q_b + \alpha \Delta T \tag{2C.15}$$

The radial stresses at the four corners of the ring are

$$\sigma_{al} \text{ radial} = \left(\frac{Q_a}{2\pi a h} \right) - \left(\frac{3M_a}{\pi a h^2} \right) \tag{2C.16}$$

$$\sigma_{ar} \text{ radial} = \left(\frac{Q_a}{2\pi a h} \right) + \left(\frac{3M_a}{\pi a h^2} \right) \tag{2C.17}$$

$$\sigma_{bl} \text{ radial} = \left(\frac{Q_b}{2\pi b h} \right) - \left(\frac{3M_b}{\pi b h^2} \right) \tag{2C.18}$$

$$\sigma_{br \text{ radial}} = \left(\frac{Q_b}{2\pi bh} \right) + \left(\frac{3M_b}{\pi bh^2} \right) \quad (2C.19)$$

Appendix 2.D - Bolt Analysis

In connectors which do not have flange-to-flange contact outside the bolt circle, flange rotation under load is such that the bolt heads and nuts bear only on the side towards the hub. Local yielding at the area of contact moves the effective line of action closer to the bolt center. The bolt load will arbitrarily be considered to act at a distance equal to the bolt radius inwards of the bolt center. The bolt load thus acts at a circle that is tangent to the inside of the bolts when there is no flange contact outside the bolt circle.

The bolt length is taken as one diameter longer than the actual free length to compensate for the additional flexibility at the head and nut. Referring to Figure 2D, the bolt deformation is given by

$$(w_2 - w_1) = \left(\frac{20}{\pi} \right) \left(\frac{L_B B}{nE_B d^2} \right) + (2h + h_G) \alpha_B \Delta T - C - h \alpha_F \Delta T \quad (2D.1)$$

(eccentrically loaded)

where the constant C accommodates the initial tightening and is the travel of the nut down the bolt. The last term represents the flange expansion from side to midthickness. It should be noted that the eccentricity of bolt loading increased the flexibility five-fold, since for squarely loaded bolts

$$(w_2 - w_1) = \left(\frac{4}{\pi} \right) \left(\frac{L_B B}{nE_B d^2} \right) + (2h + h_G) \alpha_B \Delta T - C - h \alpha_F \Delta T \quad (2D.2)$$

(squarely loaded)

The stresses in the bolt are

$$\sigma_{Bi} = \left(\frac{20B}{\pi nd^2} \right) f_B; \quad \sigma_{Bo} = - \left(\frac{12B}{\pi nd^2} \right) f_B \quad (\text{Eccentrically loaded}) \quad (2D.3)^*$$

*See page 2-59.

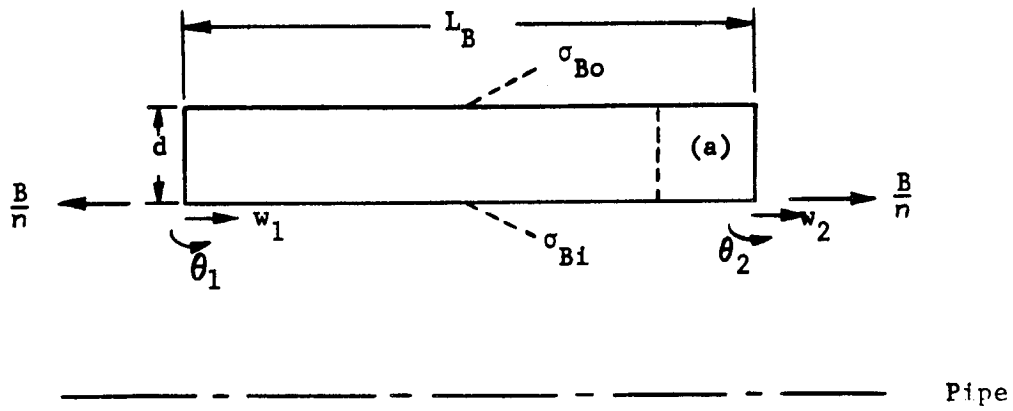


Figure 2D. Bolt Geometry, Loads, and Deformation. (The portion (a) is added to the free length to compensate for end effects at the two ends.)

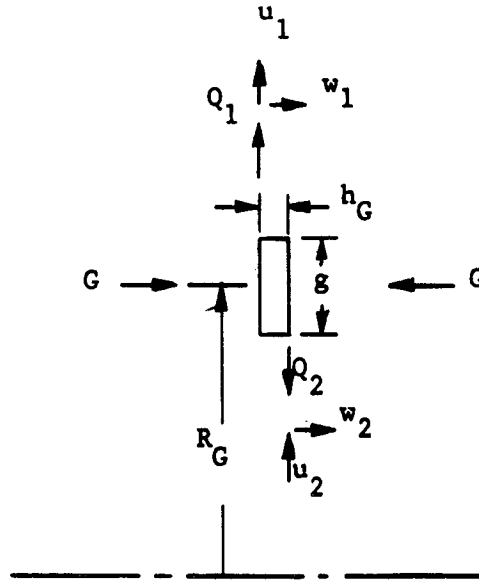


Figure 2E. Gasket Geometry, Loads and Deformation.

Again the eccentricity of loading increases the stress five-fold since for squarely loaded bolts

$$\sigma_{B1} = \sigma_{B0} = \left(\frac{4B}{\pi n d^2} \right) f_B \text{ (squarely loaded)} \quad (2D.4)^*$$

(* In Eqs. 2D.3 and 2D.4 account has been taken of the stress concentration at the threads and the reduced cross section there by a factor f_B . Its value is approximately $(\pi d^2/4)/(\text{root area})$ where Table 2.1 is used to obtain the root area. Tests would be needed for a better value.)

The change in slope from bolt head to nut for the eccentrically loaded bolt is

$$(\theta_2 - \theta_1) = \left(\frac{32}{\pi} \right) \left(\frac{L_B B}{n E_B d^3} \right) \quad (2D.5)$$

In the case of flanges which are not in contact outside the bolt circle the change of slope given by Eq. 2D.5 is nearly always less than the sum of the flange slopes. As a result, the bolt is eccentrically loaded.

Appendix 2E - Gasket Stiffness

The gasket geometry and loads are shown in Fig. 2.E. The deformation across the gasket is

$$(w_2 - w_1) = - \frac{G h_G}{2 \pi g R_G E_G} + h_G \alpha_G \Delta T + h_F \alpha_F \Delta T \quad (2E.1)$$

The last term represents the flange expansion from side to midthickness. Ordinarily the deformation across the gasket will be much smaller than the bolt or flange deformation so long as h_G is small.

A radial friction force on the gasket acts with pressure and temperature to cause radial displacements

$$u_1 = u_2 = \frac{R_G (Q_1 - Q_2)}{2 \pi E_G h_G g} + \frac{\rho (R_G - g/2) R_G}{E_G g} + R_G \alpha_G \Delta T \quad (2E.2)$$

(These equations assume the flanges restrain gasket rolling and that shear in the gasket causes negligible deflection).

Appendix 2F - Cylindrical Segment Energy

$$\begin{aligned}
 \text{Energy *} = & \frac{aRp}{Et} (Q_r - Q_\ell) + \frac{vP}{2\pi Et} (Q_\ell - Q_r) + a\alpha\Delta T (Q_r - Q_\ell) \\
 & + \left(\frac{a}{\pi LEt}\right) \left[(\bar{K}_1)(Q_\ell^2 + Q_r^2) + \bar{K}_4 Q_\ell Q_r \right] \\
 & + \frac{3a}{\pi L^2 Et} \left[\bar{K}_2 (M_r Q_r - M_\ell Q_\ell) + \bar{K}_5 (M_r Q_\ell - M_\ell Q_r) \right] \\
 & + \frac{3a}{\pi L^3 Et} \left[\bar{K}_3 (M_r^2 + M_\ell^2) - 2\bar{K}_6 M_r M_\ell \right] + LP (\alpha\Delta T) \\
 & + \left(\frac{\pi aLR^2}{Et}\right) P^2 + \left(\frac{L}{4\pi aEt}\right) P^2 - v\left(\frac{RL}{Et}\right) pP + 2\pi aRLp (\alpha\Delta T)
 \end{aligned} \tag{2F.1}$$

Where,

$$\begin{aligned}
 \bar{K}_1 &= 1 + 0.0095 (\beta L)^4 - 0.000562 (\beta L)^8 \dots \\
 \bar{K}_2 &= 1 + 0.0349 (\beta L)^4 - 0.000182 (\beta L)^8 \dots \\
 \bar{K}_3 &= 1 + 0.1237 (\beta L)^4 - 0.000416 (\beta L)^8 \dots \\
 \bar{K}_4 &= 1 - 0.0143 (\beta L)^4 + 0.000110 (\beta L)^8 \dots \\
 \bar{K}_5 &= 1 - 0.0206 (\beta L)^4 + 0.000168 (\beta L)^8 \dots \\
 \bar{K}_6 &= 1 - 0.0428 (\beta L)^4 + 0.000386 (\beta L)^8 \dots
 \end{aligned} \tag{2F.2}$$

*Fictitious temperature change terms have been added to give the change in energy due to temperature changes after the loads have been applied.

$$\beta^4 = 3(1 - \nu^2)/a^2 t^2 \quad (2F.3)$$

(Note: \bar{K} here is different from K in Appendix 2B)

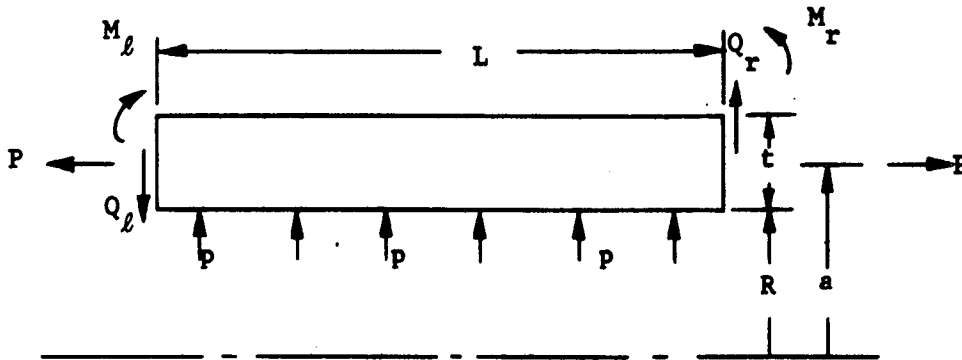


Figure 2F. Cylindrical Segment Showing Loads and Dimensions.

Appendix 2G - Energy Stored in a Ring Section

$$\begin{aligned} \text{Energy} * &= \left(\frac{3S^2}{2\pi Eh^3} \right) \left[(a^2 - b^2) \left(\frac{3+\nu}{4} \right) (1-\nu) + (1+\nu)^2 \left(\frac{a^2 b^2}{a^2 - b^2} \right) \log^2 \left(\frac{a}{b} \right) \right] \\ &+ \left(\frac{3M_b^2}{\pi Eh^3} \right) \left(\frac{a^2 + b^2}{a^2 - b^2} + \nu \right) + \left(\frac{3M_a^2}{\pi Eh^3} \right) \left(\frac{a^2 + b^2}{a^2 - b^2} - \nu \right) \\ &+ \left(\frac{3bSM_b}{\pi Eh^3} \right) \left(1 - \nu + \frac{2(1+\nu)a^2}{a^2 - b^2} \log \left(\frac{a}{b} \right) - \left(\frac{3aSM_a}{\pi Eh^3} \right) \left(1 - \nu + \frac{2(1+\nu)b^2}{a^2 - b^2} \right) \log \left(\frac{a}{b} \right) \right) \\ &- \left(\frac{12abM_a M_b}{\pi Eh^3 (a^2 - b^2)} \right) - \left(\frac{abQ_a Q_b}{\pi Eh (a^2 - b^2)} \right) + (aQ_a - bQ_b) \alpha \Delta T \\ &+ \left(\frac{a^2 + b^2}{4\pi Eh (a^2 - b^2)} \right) (Q_a^2 + Q_b^2) - \left(\frac{\nu}{4\pi Eh} \right) (Q_a^2 - Q_b^2) \end{aligned}$$

*Fictitious temperature change terms have been added to give the change in energy due to temperature changes after the loads have been applied and represent the work done by the loads during expansion.

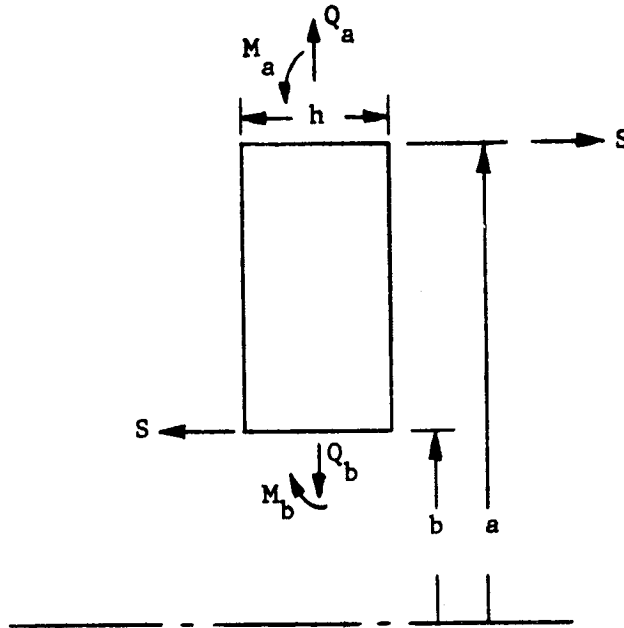


Figure 2G. Ring Segment Showing Loads and Dimensions.

Appendix 2H - Energy Stored in Bolts

$$\text{Energy}^* = \frac{B^2 L_B}{2\pi n E d^2} (4 + 64e^2) + BL_B \alpha \Delta T - BC$$

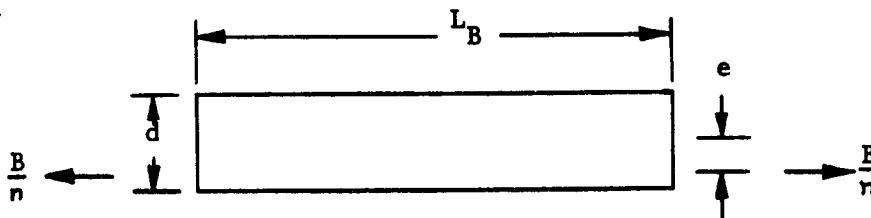


Figure 2H. Bolt Geometry and Loading.

where

- n = Number of bolts
- L_B = Effective length (in.)
- e = Eccentricity of loading (in.)
- B = Total bolt load around circumference (lb.)
- d = Bolt diameter (in.)
- $L_B \alpha \Delta T$ = Bolt expansion (in.)
- C = Tightening of nut on bolt (in.)

* Fictitious temperature change and bolt tightening terms have been added and represent the work done during expansion and tightening by the bolt load.

2.10 Design Examples

2.10.1 Preliminary Design Layouts

2.10.1.1 Integral Flanges - No Contact Outside Bolt Circle

The following preliminary design is accomplished by following, step by step, the procedure of Section 2.2.1. The alphabetic and numerical designation of the calculations agree with those listed in Section 2.2.1

a. Design conditions

$P_{\text{max. oper.}} = 750 \text{ psi}$
Temperature = 700°F
Pipe size, 10 in. I.D. x 0.0625 in. wall
Material, 347 Stainless Steel

1. Gasket Parameters

Width $g = 0.2 \text{ in.}$
Thickness $h = 0.05 \text{ in.}$
Modules, $E_g = 1 \times 10^6 \text{ psi}$
Radius at gasket circle, $R_g = 5.4 \text{ ins.}$
Gasket force required to seal = 2000 lbs/in.
Gasket force to maintain seal = 1000 lbs/in.

2. Axial load (G_I) needed to make an effective seal = $2000 \times 2\pi R_g = 68,000 \text{ lbs.}$
3. Axial load (G_M) needed to maintain a seal at operating temperature after it has been made = $1000 \text{ lb/in.} \times 2\pi \times 5.4 = 34,000 \text{ lbs.}$

- b. The initial bolt load (B_I) is the greater of the following two values.

$$(G_I) = 68,000 \text{ lbs.}$$

or

$$(G_M) + 2.5\pi R_G^2 P_{\text{max. oper.}} = 34,000 + 2.5 \times \pi \times (5.4)^2 (750) = 34,000 + 172,000 = 206,000 \text{ lbs.}$$

Therefore, the initial bolt load must be 206,000 lbs (B_I)

Selection of bolt material -

Yield stress (S_B) of this material at 700°F is 100,000 psi.

The minimum permissible bolt total area at the root of the threads is

$$(A_B) = \frac{5 \cdot (S_I)}{(S_B)} = \frac{5 \times 206,000}{100,000} = 10.3 \text{ ins.}^2$$

c. Estimate of bolt circle radius $(R_{BC}) = 6.5$ inches

Use fine thread

$$\frac{(A_B)}{(R_{BC})} = \frac{10.3}{6.5} = 1.584$$

Enter Column 1 of Table 2.1 under fine thread at a value equal to or larger than $\frac{(A_B)}{(R_{BC})}$, in this case 1.743.

The bolt size, given in Column 2 is 1 inch.

Next check to see that estimated value of (R_{BC}) was reasonable.

$$(R_{BC}) = R + (\text{Col. 5}) + (\text{Col. 7}) \times \sqrt{\frac{(S_B)}{(S_F)}}$$

$$R = 5.0$$

$$\text{Col. 5} = 1.37$$

$$\text{Col. 7} = 0.676$$

$$(S_B) = \text{yield stress for bolt material} = 100,000 \text{ psi.}$$

$$(S_F) = \text{yield stress for flange material} = 100,000 \text{ psi.}$$

$$\begin{aligned} (R_{BC}) &= 5 + 1.37 + 0.676 \sqrt{1} \\ &= 7.046 \text{ ins.} \end{aligned}$$

Dividing (A_B) by this new bolt circle radius gives

$$\frac{10.3}{7.046} = 1.460$$

Comparing this with the values in Column 1, one can see that the ratio $\frac{(A_B)}{(R_{BC})}$ is less than 1.464 so that a bolt size of 7/8 in. (in

Column 2) can be used.

Rechecking the (R_{BC}) using the 7/8-in. bolts yields

$$(R_{BC}) = R + (\text{Col. 5}) + (\text{Col. 7}) \sqrt{\frac{(S_B)}{(S_F)}}$$

$$R = 5$$

$$\text{Col. 5} = 1.25$$

$$\text{Col. 7} = 0.592$$

$$\frac{(S_B)}{(S_F)} = 1$$

$$(R_{BC}) = 5 + 1.25 + 0.592\sqrt{1}$$

$$(R_{BC}) = 6.842 \text{ ins.}$$

The number of bolts is given by

$$n \geq \frac{(A_B)}{(\text{Col. 3})} = \frac{10.3}{0.4805} = 21.4$$

$$n = 22 \text{ bolts}$$

Checking to see that R_{BC} satisfies the relationship $(R_{BC}) \geq \left(\frac{n}{2\pi}\right)$ (Col. 4) on page 2-15

$$6.842 \geq \left(\frac{22}{2\pi}\right) \quad (2.06)$$

$$6.842 < 7.22$$

Since 6.842 is less than 7.22 the bolt circle radius (R_{BC}) will have to be increased to 7.22 ins. to allow adequate bolt spacing.

d. Selection of flange thickness (H_I) and a hub thickness (T_I)

$$\begin{aligned} (H_I) &= (\text{Col. 7}) \times \sqrt{(S_B)/(S_F)} = (T_I) \\ &= 0.592 \times \sqrt{\frac{100,000}{100,000}} = 0.592 \text{ in.} \end{aligned}$$

$$\text{Flange thickness } (H_I) = 0.592 \text{ in.}$$

$$\text{Hub thickness } (T_I) = 0.592 \text{ in.}$$

The flange outer radius (R_{OF}) is given by $(R_{BC}) + (\text{Col. 6})$

$$\text{Flange outer radius} = 7.22 + 0.94 = 8.16 \text{ ins.}$$

$$\text{Flange outer radius } (R_{OF}) = 8.16 \text{ ins.}$$

The large end of the hub has a radius $(R_{HI}) = R + (T_I) = 5.00 + 0.592 = 5.592$ ins.

$$\boxed{\text{Large end of hub radius } (R_{HI}) = 5.592 \text{ ins.}}$$

e. The hub length (L_I) is given by $\sqrt{(R/2) [(T_I) + (T_P)]}$

where T_P is pipe wall thickness

$$\begin{aligned} L_I &= \sqrt{\frac{5}{2} [0.592 + 0.0625]} \\ &= \sqrt{1.64} = 1.28 \text{ ins.} \end{aligned}$$

$$\boxed{\text{Hub Length } (L_I) = 1.28 \text{ ins.}}$$

$$\text{Hub slope } (S_H) = \frac{L_I}{[(T_I) - (T_P)]}$$

$$\text{Hub slope} = \frac{1.28}{0.592 - 0.0625} = 2.42$$

$$\boxed{\text{Hub slope } (S_H) = 2.42}$$

Since this slope is less than three the hub will be modified by adding a section with a reduced taper. In the absence of additional welding specifications the dimensions of this reduced taper are

$$\begin{aligned} \text{Length } (L_T) &= 4 (T_P) \\ &= 4 (0.0625) = 0.250 \text{ in.} \end{aligned}$$

Outer radius at taper intersection (R_T)

$$\begin{aligned} &= R + (2 \frac{1}{3}) (T_P) \\ &= 5 + (2 \frac{1}{3}) (0.0625) \end{aligned}$$

$$\boxed{(R_T) = 5.146 \text{ ins.}}$$

Add fillet radius at transition between hub and flange

$$0.1 (T_I) < \text{radius} < 0.2 (T_I)$$

$$0.0592 < \text{radius} < 0.1184 \text{ in.}$$

Add fillet radius at transition between hub and reduced taper hub

$$0.1 (T_p) < \text{fillet radius} < 0.2 (T_p)$$

$$(0.00625) < \text{fillet radius} < (0.0125) \text{ in.}$$

f. Lubricant

Assume coefficient of friction = 0.5

$$\mu_N = \mu_F = 0.5$$

Calculation of required bolt torque

$$T = \left(\frac{1}{2} \mu_N + \frac{3}{4} \mu_F \right) d \left[\frac{B_I}{n} \right]$$

$$T = \left[\frac{1}{2} (0.5) + \frac{3}{4} (0.5) \right] \left(\frac{7}{8} \right) \left[\frac{206,000}{22} \right]$$

$$T = [0.25 + 0.375] [0.875] [9,370]$$

$$T = 5120 \text{ in.-lbs}$$

g. Coefficient of friction for contact between gasket and flange is 0.5.

h. Add dimensional tolerances.

The dimensioned flange design is illustrated in Figure 2I.

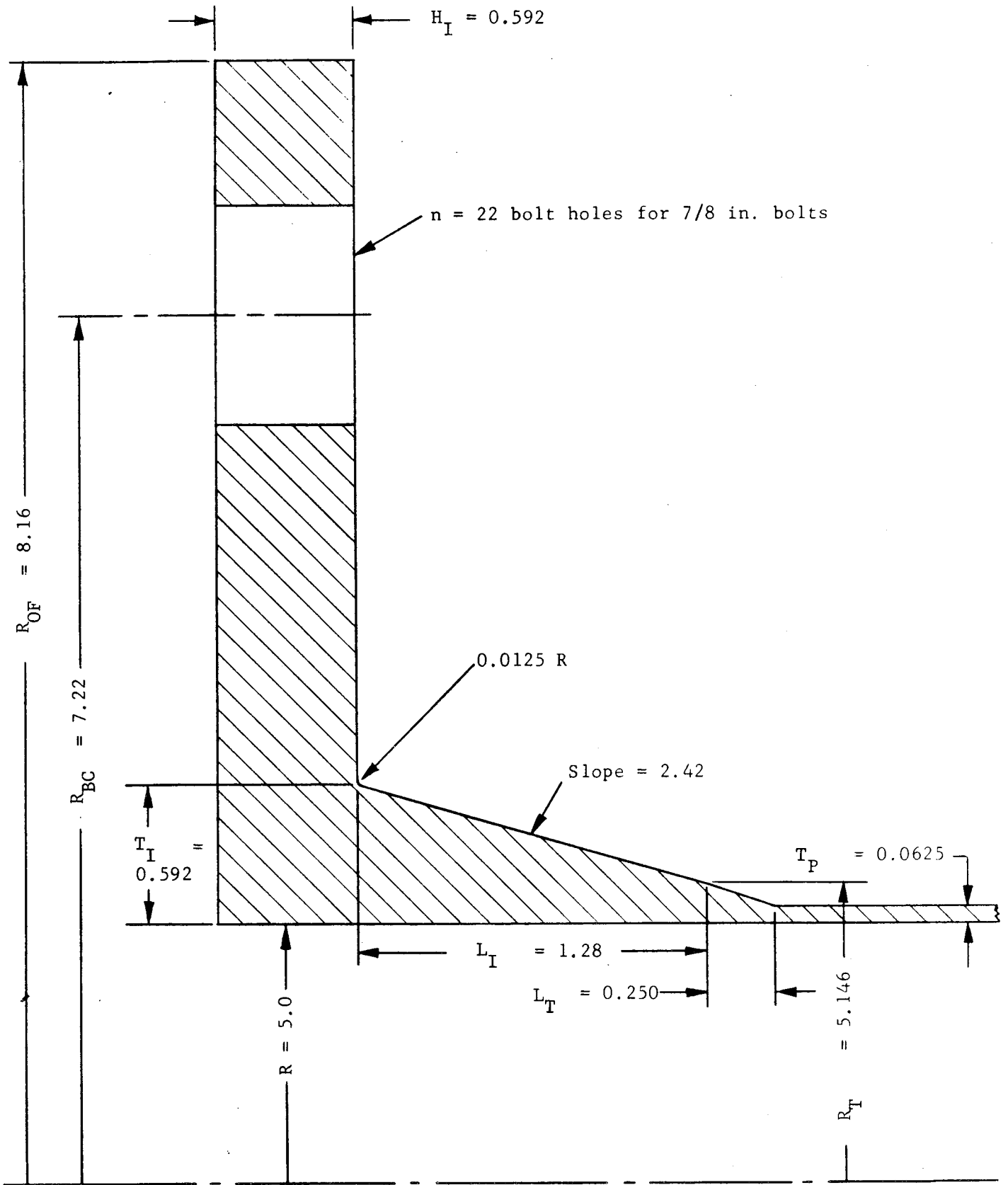


Figure 2I. Preliminary Design. Integral Flanges - No Contact Outside Bolt Circle.

2.10.1.2 Integral Flange - Contact Outside Bolt Circle

Following the design procedure of Section 2.3.1 gives the following results.

a. Design conditions

$P_{\text{max.oper.}} = 750 \text{ psi}$
Temperature = 700°F
Pipe size, 10 in. O.D. x 0.0625 in. wall
Material, 347 Stainless Steel

1. Gasket parameters

Width, $g = 0.2 \text{ in.}$
Thickness, $hg = 0.05 \text{ in.}$
Modulus, $E_g = 1 \times 10^6 \text{ psi}$
Radius, $R_g = 5.4 \text{ ins.}$
Force required to seal initially = 2000 lbs/in.
Force to maintain seal = 1000 lbs/in.

2. Axial force (G_I) needed to make an effective seal =
 $2000 \times 2\pi R_g = 68,000 \text{ lbs.}$

3. Axial force (G_M) needed to maintain a seal = $1000 \times 2\pi \frac{R}{g} =$
 $34,000 \text{ lbs.}$

Set the initial bolt load (B_I)

$$B_I = 2 G_I = 136,000 \text{ lbs.}$$

or

$$B_I = 2 \left[G_M + 2.5\pi R_g^2 P_{\text{max.oper.}} \right]$$

$$B_I = 2 \left[34,000 + 2.5\pi(5.4)^2 (750) \right]$$

$$B_I = 412,000 \text{ lbs.}$$

since this is the larger of the above two values.

The minimum total bolt area,

$$A_B = B_I / (S_B)$$

$$A_B = \frac{412,000}{100,000} = 4.12 \text{ ins.}^2$$

- c. Estimate of bolt circle radius (R_{BC}) is 6.5 ins.

$$\frac{A_B}{R_{BC}} = \frac{4.12}{6.5} = 0.633$$

Entering Table 2.1, Column 1 under Fine Threads, the next larger number is 0.748, indicating a bolt size of 1/2 in. in Column 2.

$$\text{Number of bolts } n = \frac{4.12}{0.1486(\text{Column 3})} = \boxed{28 \text{ bolts}}$$

Multiplying this number by the minimum bolt spacing (Col. 4)

$$28 \times 1.25 = 35 \text{ ins.}$$

Comparing this with the bolt circle circumference

$$2\pi (R_{BC}) = 2\pi (6.5) = 40.8 \text{ ins.}$$

one sees that the spacing will be adequate with a 6.5 in. bolt circle radius.

- d. The flange thickness (H_I) is

$$(H_I) = (\text{Col. 7}) \sqrt{3(S_B)/(S_F)}$$

$$(H_I) = 0.340 \sqrt{3 \frac{100,000}{100,000}}$$

$$(H_I) = \boxed{0.589 \text{ in.}}$$

- e. The flange outer radius (R_{OF}) is given by (R_{OF}) = 2 (R_{BC}) - R according to paragraph e, pages 2 through 34.

$$R_{OF} = 2 \times 6.5 - 5 = 8 \text{ ins.}$$

The radial width of the raised bearing surface at the outer edge is

$$R_{BS} = 0.1 [\text{Col. 1}]$$

$$R_{BS} = 0.1 \cdot 0.748 = \boxed{0.0748}$$

The height of this surface is

$$H_B \geq 0.002 \text{ Col. 1}$$

$$H_B \geq \boxed{0.001496}$$

- f. The hub thickness is

$$T_I = \frac{2.5 R P_{\text{max.oper.}}}{\sigma_{\text{allow.}}}$$

$$T_I = \frac{2.5 \times 5 \times 750}{40,000} = \boxed{0.234 \text{ in.}}$$

Next check that

$$(R_{BC}) > R + 1.2(T_I) = \text{Col. 5}$$

$$6.5 \stackrel{?}{>} 5 + 1.2(0.234) + 0.81$$

$$6.5 > 6.091$$

The bolt circle radius of 6.5 in. is therefore large enough.

g. Follow steps (e), (f), (g) and (h) of Section 2.2.1.

$$(L_I) = \sqrt{R/2 [(T_I) + T_P]}$$

$$= \sqrt{5/2 [(0.234 + 0.0625)]}$$

$$(L_I) = \boxed{0.862}$$

$$(S_H) = (L_I) / [(T_I) + (T_P)]$$

$$(S_H) = \frac{0.862}{0.234 + 0.0625}$$

$$(S_H) = 5.02$$

Since $(S_H) > 3$ it will not be necessary to modify the hub by adding a reduced taper.

Make fillets between flange and hub and between hub and reduced taper hub = $0.2(T_P) = 0.0125$ in.

The coefficient of friction is 0.5 for μ_N and μ_F .

Therefore the bolt torque is approximately

$$T = \left(\frac{1}{2} \mu_N + \frac{3}{4} \mu_F\right) d \left[\frac{B_I}{n}\right]$$

$$T = (0.25 + 0.375) \frac{1}{2} \left[\frac{412,000}{28}\right]$$

$$T = 4580 \text{ in.-lbs.}$$

Select the coefficient of friction between gasket and flange. In this example 0.5 will be used.

Add tolerances to dimensions of connector. The dimension flange design from Example 2 is shown in Figure 2J.

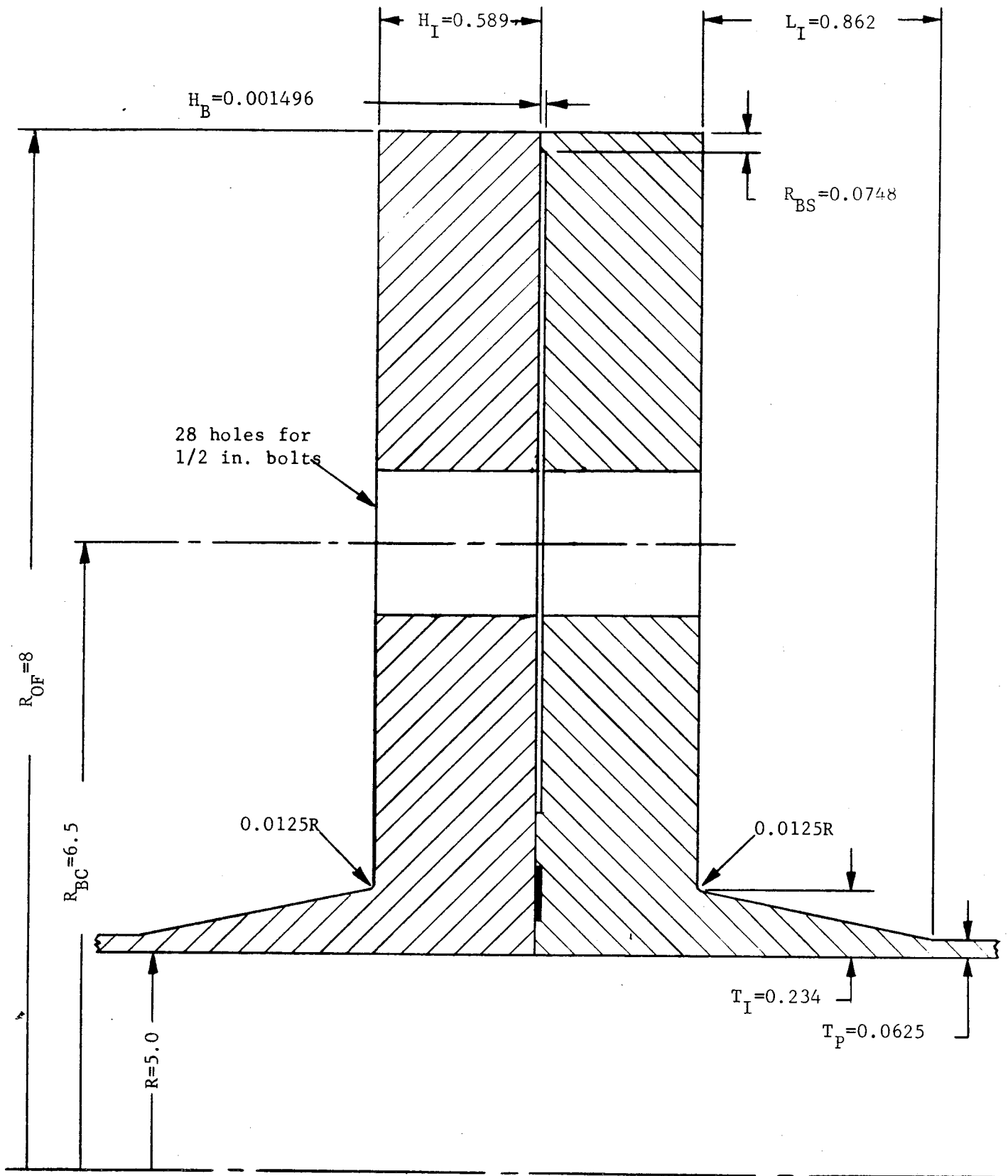


Figure 2J. Preliminary Design. Integral Flanges with Contact Outside Bolt Circle.

2.10.1.3 One Loose Flange - No Contact Outside Bolt Circle

Following the design procedure of Section 2.4 gives the following results.

Design Conditions

$P_{\text{max.oper.}} = 750 \text{ psi}$
Temperature = 700°F
Pipe size = 10 in. I.D. x 0.0625 in. wall
Material, 347 stainless steel

1. Gasket parameters

Width, $g = 0.2 \text{ in.}$
Thickness, $h = 0.05 \text{ in.}$
Modulus, $E_g = 1 \times 10^6 \text{ in.}$
Radius at gasket circle, $R_g = 5.4 \text{ in.}$
Gasket force required to seal = 2000 lb/in.
Gasket force to maintain seal = 1000 lb/in.

- a. The design of the bolts and integral flange portion of the connector is identical to that given in Example 1.

Thus

$$G_I = 68,000 \text{ lbs.}$$

$$G_M = 34,000 \text{ lbs.}$$

$$B_I = 206,000 \text{ lbs.}$$

$$A_B = 10.3 \text{ ins.}^2$$

$$\frac{A_B}{R_{BC}} = 1.584$$

$$d = \boxed{7/8}$$

$$R_{BC} = \boxed{7.22 \text{ ins.}}$$

$$n = \boxed{22 \text{ bolts}}$$

$$H_I = \boxed{0.592 \text{ in.}}$$

$$T_I = \boxed{0.592 \text{ in.}}$$

$$R_{OF} = \boxed{8.16 \text{ ins.}}$$

$$R_{HI} = \boxed{5.592 \text{ ins.}}$$

$$L_I = \sqrt{2.5 (0.592 + 0.15)} = \boxed{1.36}$$

$$S_H = 1.36 / (0.592 - 0.15) = 3.08$$

Fillet between flange and hub = $\boxed{0.1184 \text{ in. R}}$

T = 5120 in.-lbs.

Coefficient of friction between gasket and flange = 0.5.

b. Coefficient of friction between loose flange and lap flange = 0.5.

$$c. \frac{P_{\text{max. oper.}}}{\sigma_{\text{allow}}} = \frac{750}{40,000} = 0.0188$$

Entering Column 4 of Table 2.3 the next larger number is 0.0216 corresponding to a ratio of pipe wall thickness to inner pipe radius of 0.03.

$$T_P = R \text{ Col. 1}$$

$$T_P = \boxed{0.15 \text{ in.}}$$

The hub thickness at the junction with the lap flange is

$$(T_L) = (T_P) \text{ Col. 2}$$

$$(T_L) = 0.15 \times 5.40 = \boxed{0.810}$$

The outer radius of the lap flange is

$$(R_{OL}) = R \text{ Col. 3} = 5 \times 1.225$$

$$(R_{OL}) = \boxed{6.13}$$

The thickness of the lap flange (H_L) is

$$(T_P) \text{ Col. 2}$$

$$(H_L) = (0.15) (5.40) = \boxed{0.810}$$

Fillet at junction of hub and lap flange is 0.2 (T_L) or

$$0.2 \times 0.810 = 0.162 \text{ in. radius}$$

Fillet at junction of hub and pipe is 0.2 (T_P) = 0.03 in.

Hub length

$$(L_H) = R \text{ Col. 5}$$

$$= 5 (0.318)$$

$$(L_H) = \boxed{1.590 \text{ ins.}}$$

Hub slope is

$$\frac{(T_L) - (T_P)}{(L_H)}$$

$$S_H = \frac{0.810 - 0.15}{1.590} = \frac{0.66}{1.590} = \frac{1}{2.41}$$

Since this is less than 1:3 a reduced tapered hub will have to be added. The length of this reduced taper will be, according to paragraph 2.2.1,e,

$$(L_T) = 4 (T_P) = \boxed{0.60 \text{ in.}}$$

$$(R_T) = R + 2 \frac{1}{3} (T_P)$$

$$= 5 + 2 \frac{1}{3} (0.15)$$

$$(R_T) = \boxed{5.35}$$

- d. Coefficient of friction for the bolt-nut-flange interfaces will be 0.5 in this example.

The bolt torque is therefore

$$T = \left[\frac{1}{2}(0.5) + (0.5) \right] d \left[\frac{(B_I)}{n} \right]$$

$$T = \left[0.25 + 0.375 \frac{7}{8} \right] \left[\frac{206,000}{22} \right]$$

$$T = 5120 \text{ in.-lbs.}$$

- e. Inner radius of loose flange

$$(R_{ILF}) = R \text{ (Col. 6)}$$

$$= 5 (1.195)$$

$$(R_{ILF}) = \boxed{5.98 \text{ ins.}}$$

- f. Outer radius of the loose flange is equal to (R_{OF}) for the integral flange or $\boxed{8.16 \text{ ins.}}$

- g. Loose flange thickness

$$(H_F) = \sqrt{\frac{(B_I)}{(S_{FL})} \left[\frac{(R_{BC}) - (R_{ILF}) - (d-t)/2}{(R_{OF}) - (R_{ILF})} \right]}$$

S_{FL} is the allowable stress in the loose flange material. For Example 3 this is 40,000 psi.

Therefore

$$(H_F) = \sqrt{\frac{(206.000)}{(40,000)} \left[\frac{(7.22) - (5.98) - (0.875 - 0.15)/2}{(8.16) - (5.98)} \right]}$$

$$(H_F) = \sqrt{5.15 \left[\frac{0.8775}{2.18} \right]} = \boxed{1.44 \text{ ins.}}$$

A drawing of this design is shown in Figure 2K.

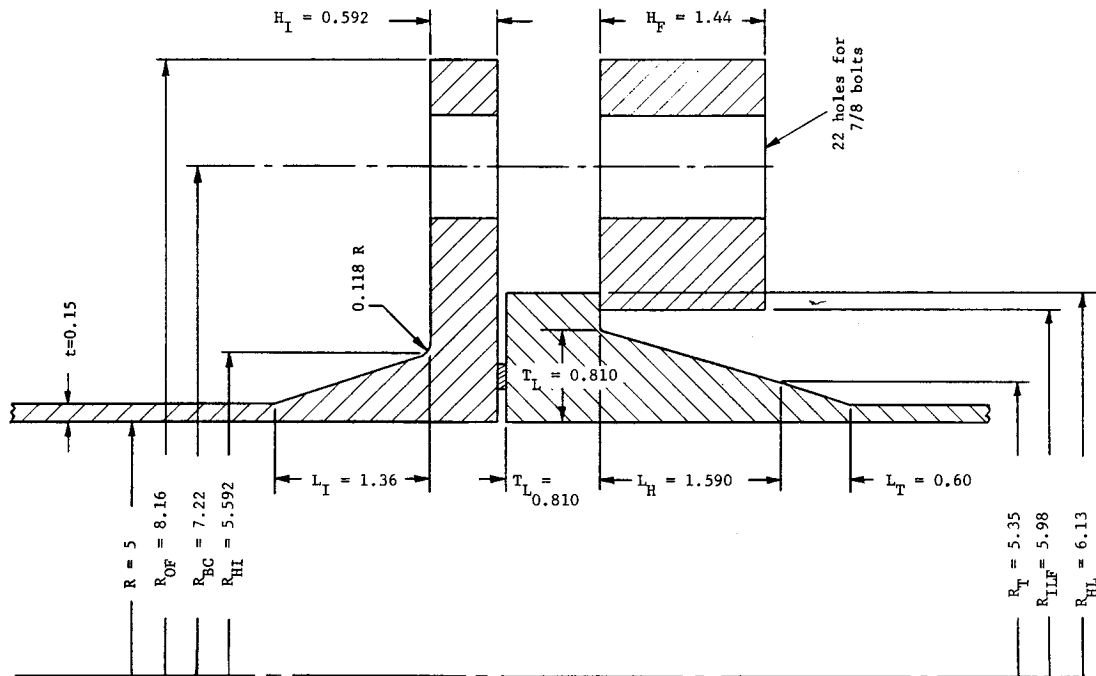


Figure 2K. Preliminary Design. Loose Flange - No Contact Outside Bolt Circle.

2.10.1.4 One Flange - Contact Outside Bolt Circle

Following the design procedure of Section 2.5.1 produces the following results.

Design Conditions:

$$\begin{aligned}P_{\text{max.oper.}} &= 750 \text{ psi} \\ \text{Temperature} &= 700^{\circ}\text{F} \\ \text{Pipe size} &= 10 \text{ in. I.D.} \times 0.0625 \text{ in. wall} \\ \text{Material, 347 stainless steel} \\ (\sigma_{\text{allow}} &= 40,000 \text{ psi})\end{aligned}$$

Gasket parameters

$$\begin{aligned}\text{Width } g &= 0.2 \text{ in.} \\ \text{Thickness } h &= 0.05 \text{ in.} \\ \text{Modulus } E_g &= 1 \times 10^6 \text{ in.} \\ \text{Radius at gasket circle} &= 5.4 \text{ ins.} \\ \text{Gasket force to seal} &= 2000 \text{ lbs/in.} \\ \text{Gasket force to maintain seal} &= 1000 \text{ lbs/in.}\end{aligned}$$

- a. The design of the integral flange and bolts is the same as that determined in steps (a) through (f) of Section 2.3.1 and steps (e) through (l) of Section 2.2.1.

Therefore the design parameters are

$$G_I = 68,000 \text{ lbs.}$$

$$G_M = 34,000 \text{ lbs.}$$

$$B_I = 5\pi R_G^2 P_{\text{max.oper.}} = 412,000 \text{ lbs.}$$

$$A_B = (B_I)/(S_B) = 412,000/100,000 = 4.12 \text{ ins.}^2$$

$$R_{BC} = \boxed{6.5}$$

$$\frac{A_B}{R_{BC}} = \frac{4.12}{6.5} = 0.633$$

$$d = \text{Col. 2, Table 2.1} = \boxed{1/2 \text{ in.}}$$

$$n = \frac{A_B}{\text{Col. 3}} = \frac{4.12}{0.1486} = \boxed{28 \text{ bolts}}$$

$$n \times \text{Col. 4} = 28 \times 1.25 = 35$$

$$2\pi (R_{BC}) = 2\pi (6.5) = 40.8$$

Thus (R_{BC}) is large enough

$$(H_I) = \text{Col. 7 } \sqrt{3} = 0.340 \sqrt{3} = \boxed{0.589 \text{ in.}}$$

$$(R_{OF}) = 2 (R_{BC}) - R = 13 - 5 = \boxed{8 \text{ ins.}}$$

$$(R_{BS}) = 0.1 \text{ Col. 1} = \boxed{0.075}$$

$$(H_B) \geq 0.002 \text{ Col. 1} = \boxed{0.0015}$$

$$(T_I) = 2.5 R_{P_{\text{max.oper.}}} / \sigma_{\text{allow}} = \boxed{0.234 \text{ in.}}$$

Is $(R_{BC}) > R + 1.2 (T_I) + \text{Col. 5, Table 2.1} ?$

$$6.5 \stackrel{?}{>} 5 + 1.2 (0.234) + 0.81$$

$$6.5 > 6.09$$

$$L_I = \sqrt{\left(\frac{R}{2}\right) [(T_I) + (T_P)]}$$

$$= \sqrt{2.5 [0.234 + 0.15]}$$

$$L_I = \sqrt{0.96} = \boxed{0.98 \text{ in.}}$$

$$S_H = \frac{0.98}{0.234 - 0.15} = 11.66$$

No reduced taper hub is required.

$$T = \left(\frac{1}{2} \mu_N + \frac{3}{4} \mu_F\right) d \left(\frac{B_I}{n}\right)$$

$$\mu_N = \mu_F = 0.5$$

$$T = (0.625) \frac{1}{2} \left(\frac{412,000}{28}\right) = 4590 \text{ in.-lbs.}$$

b. The design of the lap flange follows steps (b) through (d) of Section 2.4.1.

Friction coefficient between loose and lap flanges = 0.5

$$\frac{P_{\text{max.oper.}}}{\sigma_{\text{allow}}} = \frac{750}{40,000} = 0.0188$$

$$(T_P) = R \text{ Col. 1} = 5 \times 0.03 = \boxed{0.15 \text{ in.}}$$

$$(T_L) = (T_P) \text{ Col. 2} = 0.15 (5.40) = \boxed{0.81 \text{ in.}}$$

$$(R_{OL}) = R \text{ Col. 3} = 5 \times 1.225 = \boxed{6.125}$$

$$H_L = (T_P) \text{ Col. 2} = 0.81 \text{ in.}$$

Fillet at junction of hub and lap flange has a radius of

$$0.2 (T_L) = 0.162$$

Fillet at junction of hub and pipe has a radius of $0.2 (T_P) = 0.03$

$$(L_H) = R \text{ Col. 5} = 5 \times 0.318 = \boxed{1.59}$$

$$\begin{aligned} \text{Hub slope} &= \frac{(T_L) - (T_P)}{(L_H)} = \frac{0.81 - 0.15}{1.59} \\ &= \frac{1}{2.65} \end{aligned}$$

Since this slope is greater than $1/3$, a welding taper described in Section 2.2.1, e must be added.

$$(L_T) = 4 (T_P) = \boxed{0.6}$$

$$\begin{aligned} (R_T) &= R + 2 \frac{1}{3} (T_P) \\ &= 5 + 2 \frac{1}{3} (0.15) = \boxed{5.35} \end{aligned}$$

Fillet between reduced taper hub and hub is $0.2 (T_P) = 0.03$

c. Loose flange design

$$\text{Outer radius} = \boxed{8 \text{ ins.}}$$

$$\text{Thickness} = \boxed{0.589 \text{ in.}}$$

A drawing of the above design is shown in Figure 2L.

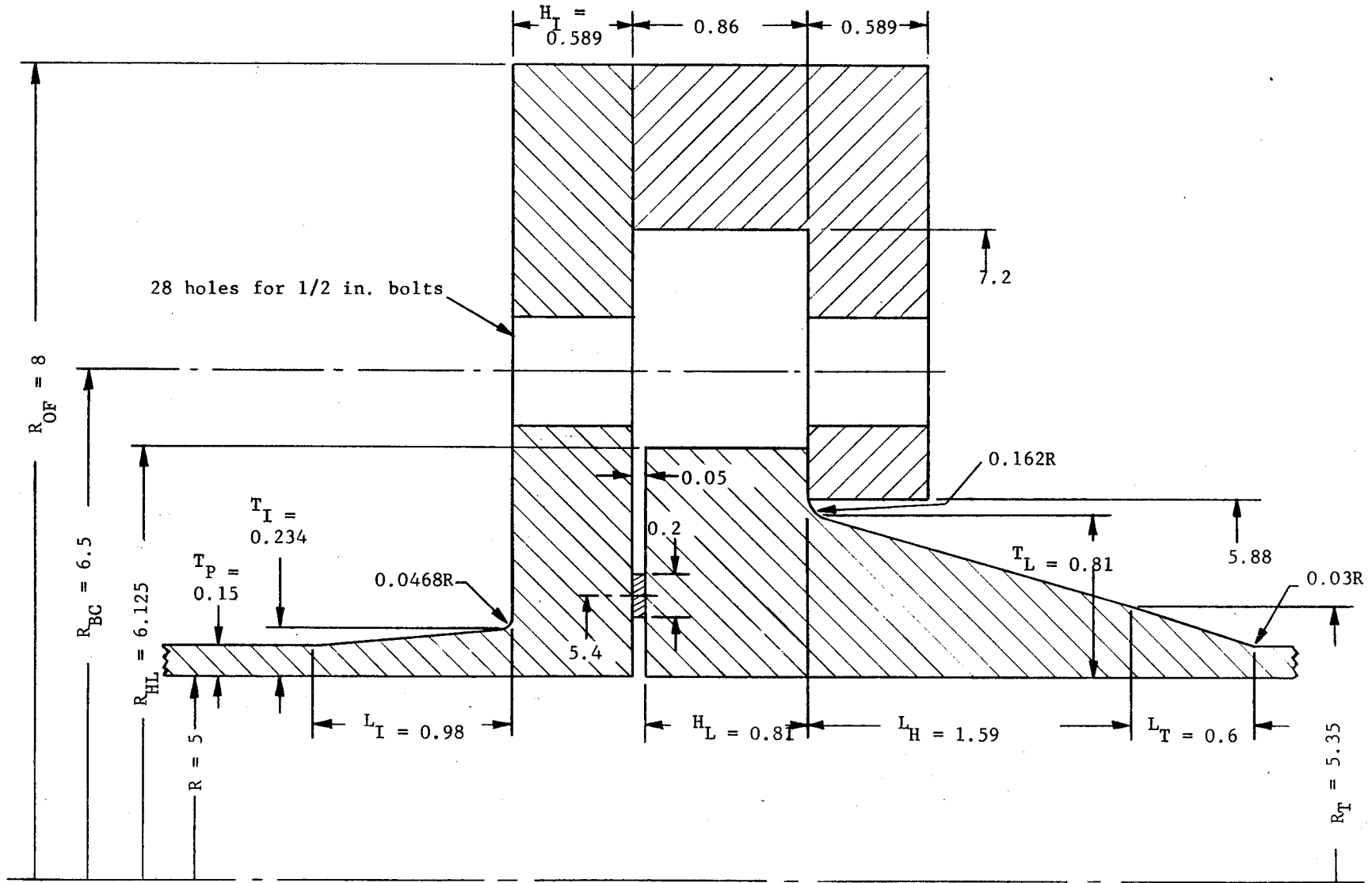


Figure 2L. Preliminary Design. Loose Flange with Contact Outside Bolt Circle

2.10.2 Detailed Analysis - Integral Flanges - No Contact Outside Bolt Circle

2.10.2.1 Design Information - Preliminary Design

Designed for 700°F temperature and 750 psi internal pressure, a 347 stainless steel 10-inch inside diameter flanged connector is as shown in Figure 2M.* The stresses and deformations existing in this connector under operating and initial conditions will be found using the procedure outlined in Section 2.2.2., without regard for the means used in obtaining the preliminary design. Reference will be made herein to section numbers and equation numbers listed in the design procedures. Equations denoted as (2.XX) refer to the design manual; equations denoted (2-XX) refer to those in the design example.

2.10.2.2 Mathematical Model

As per Section 2.2.2.1. a and Figure 2.3, the design shown in Figure 2M is broken into appropriately sized cylinders and plates as shown in Figure 2N. Letters and subscripts A, B, C, and D denote cylindrical elements of the hub; the subscripts L and R refer to the left- and right-hand ends of each segment. For linearly increasing hubs (as is called for in this example), equal length cylinders are chosen for the model. Equivalent thicknesses may be picked based on average hub thickness across the cylinder lengths. In this case, four cylinders have been used; three may also suffice for short stubby hubs.

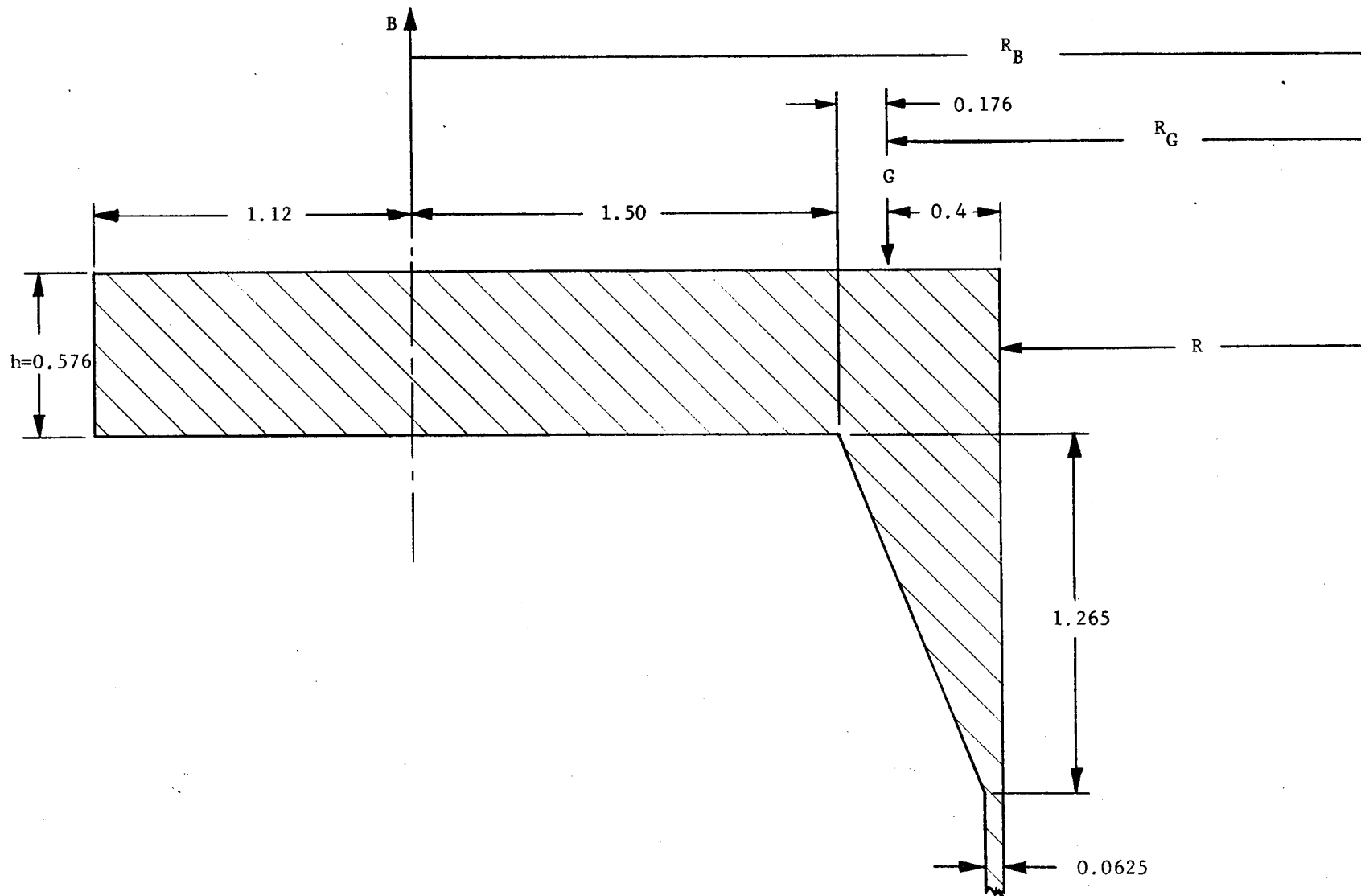
2.10.2.3 Analysis

Matrix arithmetic will be used to illustrate simplicity of procedure and to facilitate bookkeeping of numerical calculations. In this particular example, a digital computer was used for arithmetic calculations; eight digit accuracy was used. It is also possible to utilize a desk calculator; a minimum of five significant figures must be carried.

In the analysis, Eqs 2.4 through 2.14 would ordinarily be used for determining the pipe and hub behavior. In this example, however, to achieve greater precision, the more exact equations in Appendices 2A and 2B have been used as suggested in the comments following Eqs. 2.5 and 2.14 in the design procedure.

1. In preparation for use of equations in Appendices 2A and 2B, the following dimensional parameters are tabulated for the pipe and the four cylinders increments.

* The design sealing loads are an initial 2000-lb/in. minimum, and an operating 1000-lb/in. minimum; the total initial bolt load is 178,587 lbs. Both flanges in the joint are identical in this case.



2-82

Figure 2M. Preliminary Design. Integral Flanged Connector - No Contact Outside Bolt Circle - Both Flanges Identical

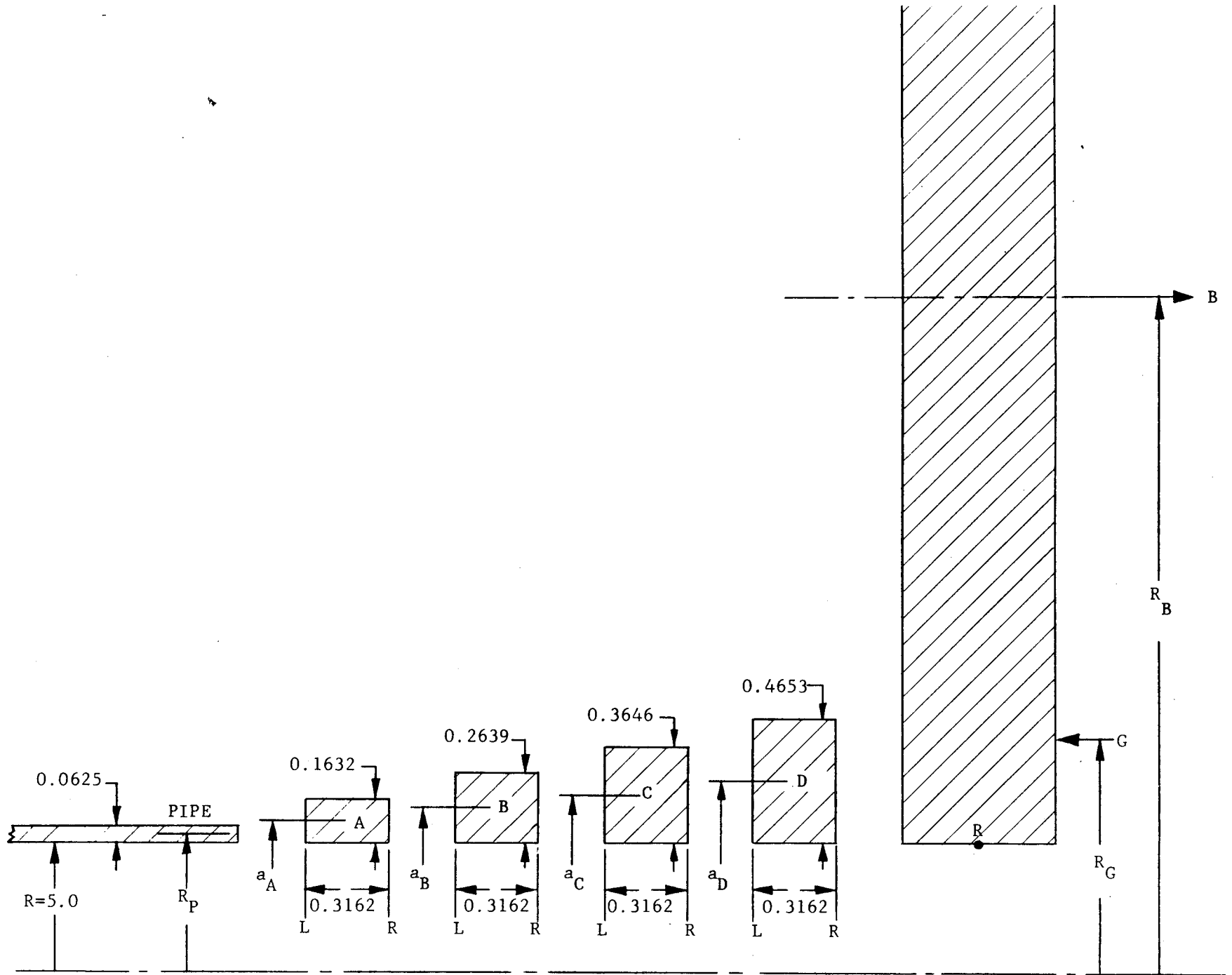


Figure 2N. Mathematical Model of Preliminary Flange Design Shown in Figure 2M.

	a (in.)	t (in.)	Δt (in.)	z (in.)	E (psi)	ν
Pipe	5.03125	0.0625	---	Semi- infinite	26×10^6	0.32
A	5.0816	0.1632	0.1007	0.3162	26×10^6	0.32
B	5.1320	0.2639	0.1007	0.3162	26×10^6	0.32
C	5.1823	0.3646	0.1007	0.3162	26×10^6	0.32
D	5.2327	0.4653	0.1007	0.3162	26×10^6	0.32

where $a = 5,000 + \frac{t}{2}$

= radius to mid-thickness of wall.

2. From Eqs. 2.10 and 2B-2 through 2B-5, for use in the analysis, the following are calculated.

	β Eq. 2.10	βL	β^2	K_1 Eq. 2B-2	K_2 Eq. 2B-3	K_3 Eq. 2B-4	K_4 Eq. 2B-5
Pipe	2.284	---	5.217	---	---	---	---
A	1.406	0.4445	1.978	0.0292	0.1970	0.4434	0.9936
B	1.101	0.3481	1.212	0.0140	0.1211	0.3378	0.9979
C	0.932	0.294	0.8685	0.0085	0.0833	0.2939	0.99876
D	0.821	0.2596	0.6745	0.0059	0.0676	0.2600	0.9992

3. Equations 2A-1 and 2A-2 (instead of 2.4 and 2.5 when R is used) are written for the pipe end; the displacement u at the left end of increment A is written in terms of the displacement at the right end of the pipe through use of Section 2.2.2.1, d. (Since the midthickness radius was used, rather than R, the correction of ΔW is needed.) Similarly, the moment at the left hand end of the segment A is written in terms of the moment at the right end of the pipe. (Section 2.2.2.1, d.) These equations, along with the identities concerning slope and shear (Section 2.2.2.1, d), and the one-to-one relationships between pressure p , load P , and $\alpha \Delta T$ are written in matrix form. The matrix relating the load and displacement parameters across the joint between the pipe and segment A will be called K_a .

Hence,

$$\begin{bmatrix} Q_{LA} \\ M_{LA} \\ \Theta_{LA} \\ u_{LA} \\ P \\ P \\ \alpha \Delta T \end{bmatrix} = K_a \begin{bmatrix} Q_{RP} \\ M_{RP} \\ P \\ P \\ \alpha \Delta T \end{bmatrix} \quad (2-1)$$

where

$$K_a = \begin{bmatrix} 1 & 0 & 0 & 0 & 0 & 0 \\ 0 & 1 & 0 & \frac{\Delta t_A}{2} & 0 & 0 \\ \frac{a\beta^2}{\pi Et} & \frac{2a\beta^3}{\pi Et} & 0 & 0 & 0 & 0 \\ \frac{a\beta}{\pi Et} & \frac{a\beta^2}{\pi Et} & \frac{aR}{Et} & \frac{-\nu}{2\pi Et} & a & 0 \\ 0 & 0 & 1 & 0 & 0 & 0 \\ 0 & 0 & 0 & 1 & 0 & 0 \\ 0 & 0 & 0 & 0 & 0 & 1 \end{bmatrix} \quad (2-2)$$

In terms of the particular parameters at hand,

$$K_a = \begin{bmatrix} +1 & 0 & 0 & 0 & 0 & 0 \\ 0 & +1 & 0 & +.0503 & 0 & 0 \\ +5.1466(10^{-6}) & +23.5200(10^{-6}) & 0 & 0 & 0 & 0 \\ +2.2523(10^{-6}) & +5.1460(10^{-6}) & +15.5775(10^{-6}) & -.0314(10^{-6}) & +5.0816 & 0 \\ 0 & 0 & +1 & 0 & 0 & 0 \\ 0 & 0 & 0 & +1 & 0 & 0 \\ 0 & 0 & 0 & 0 & 0 & +.1 \end{bmatrix} \quad (2-3)$$

4. From Appendix 2B (instead of Section 2.2.2.1, b), Eqs. 2.6 through 2.14, applicable when a is approximated by R , along with the one-to-one identities of p , P , and $\alpha\Delta T$ are written in matrix form for segment A. The transfer matrix relating loads and deflections across segment A will be called K_A . Hence,

$$\begin{bmatrix} Q_{RA} \\ M_{RA} \\ \Theta_{RA} \\ u_{RA} \\ P \\ P \\ \alpha\Delta T \end{bmatrix} = K_A \begin{bmatrix} Q_{LA} \\ M_{LA} \\ \Theta_{LA} \\ u_{LA} \\ P \\ P \\ \alpha\Delta T \end{bmatrix} \quad (2-4)$$

where

$$K_A = \begin{bmatrix} +K_4 & +2\beta K_1 & \frac{+\pi Et K_2}{a\beta^2} & \frac{+2\pi Et K_3}{a\beta} & \frac{-2\pi a K_3}{\beta} & \frac{+\nu K_3}{a\beta} & \frac{-2\pi Et K_3}{\beta} \\ \frac{-K_3}{\beta} & +K_4 & \frac{-\pi Et K_1}{a\beta^3} & \frac{-\pi Et K_2}{a\beta^2} & \frac{+\pi a K_2}{\beta^2} & \frac{-\nu K_2}{2a\beta^2} & \frac{\pi Et K_2}{\beta^2} \\ -a\beta^2 K_2 & \frac{+2a\beta^3 K_3}{\pi Et} & K_4 & -2\beta K_1 & \frac{2\beta a R K_1}{Et} & \frac{-\nu K_1}{\pi Et} & +2\beta a K_1 \\ \frac{-a\beta K_1}{\pi Et} & \frac{a\beta^2 K_2}{\pi Et} & \frac{K_3}{\beta} & K_4 & \frac{aR(1-K_4)}{Et} & \frac{-\nu(1-K_4)}{2\pi Et} & +a(1-K_4) \\ 0 & 0 & 0 & 0 & 1 & 0 & 0 \\ 0 & 0 & 0 & 0 & 0 & 1 & 0 \\ 0 & 0 & 0 & 0 & 0 & 0 & 1 \end{bmatrix} \quad (2-5)$$

In terms of the geometry of segment A.

$$K_A = \begin{bmatrix} +9.9348(10^{-1}) & +8.2504(10^{-2}) & +2.6203(10^{+5}) & +1.6560(10^{+6}) & -1.008(10^{+1}) & +1.9886(10^{-2}) & -8.4149(10^{+6}) \\ -3.1579(10^{-1}) & +9.9348(10^{-1}) & -2.7625(10^{+4}) & -2.6203(10^{+5}) & +1.5946 & -3.1487(10^{-3}) & +1.3316(10^{+6}) \\ -1.4924(10^{-7}) & +9.4312(10^{-7}) & +9.9348(10^{-1}) & -8.2504(10^{-2}) & +5.0209(10^{-7}) & -9.9077(10^{-10}) & +4.1925(10^{-1}) \\ +1.5733(10^{-8}) & +1.4824(10^{-7}) & +3.1579(10^{-1}) & +9.9348(10^{-1}) & +3.9694(10^{-8}) & -7.8328(10^{-11}) & +3.3145(10^{-2}) \\ 0 & 0 & 0 & 0 & 1 & 0 & 0 \\ 0 & 0 & 0 & 0 & 0 & 1 & 0 \\ 0 & 0 & 0 & 0 & 0 & 0 & 1 \end{bmatrix} \quad (2-6)$$

5. With the two matrices K_a and K_A known, the loads and displacements at the right end of segment A can be written in terms of the loads on the pipe.

$$\begin{bmatrix} Q_{RA} \\ M_{RA} \\ \Theta_{RA} \\ u_{RA} \\ P \\ P \\ \alpha\Delta T \end{bmatrix} = K_A \cdot K_a \begin{bmatrix} Q_{RP} \\ M_{RP} \\ P \\ P \\ \alpha\Delta T \end{bmatrix} \quad (2-7)$$

6. In this manner, the loads and deflections at the right-hand end of each segment, up to the right end of segment D can be written in terms of the pipe loads.

$$\begin{bmatrix} Q_{RD} \\ M_{RD} \\ \Theta_{RD} \\ u_{RD} \\ P \\ P \\ \alpha\Delta T \end{bmatrix} = K_D \cdot K_d \cdot K_C \cdot K_c \cdot K_B \cdot K_b \cdot K_A \cdot K_a \begin{bmatrix} Q_{RP} \\ M_{RP} \\ P \\ P \\ \alpha\Delta T \end{bmatrix} \quad (2-8)$$

Similarly, at any point between the right end of the pipe and the right end of Section D, the same quantities can be found by exclusion of the appropriate matrices.

Each K with a capital letter subscript is written generically in the form of Equation 2-5. In terms of the geometries in the present design.

$$K_B = \begin{bmatrix} -9.9755(10^{-1}) & -3.0940(10^{-2}) & +4.1967(10^{+5}) & +2.6536(10^{+6}) & -1.0186(10^{+1}) & +1.9707(10^{-2}) & -1.3618(10^{+7}) \\ -3.1605(10^{-1}) & +9.9755(10^{-1}) & -4.4237(10^{+4}) & -4.1967(10^{+5}) & +1.6109 & -3.1166(10^{-3}) & -2.1538(10^{+6}) \\ -3.4958(10^{-8}) & +2.2104(10^{-7}) & +9.9755(10^{-1}) & -3.0940(10^{-2}) & +1.1876(10^{-7}) & -2.2977(10^{-10}) & +1.5878(10^{-1}) \\ -3.6849(10^{-9}) & +3.4958(10^{-8}) & +3.1605(10^{-1}) & +9.9755(10^{-1}) & +9.3884(10^{-9}) & +1.8164(10^{-11}) & -1.2552(10^{-2}) \\ 0 & 0 & 0 & 0 & 1 & 0 & 0 \\ 0 & 0 & 0 & 0 & 0 & 1 & 0 \\ 0 & 0 & 0 & 0 & 0 & 0 & 1 \end{bmatrix} \quad (2-9)$$

$$K_C = \begin{bmatrix} +9.9874(10^{-1}) & +1.5897(10^{-2}) & +5.7423(10^{+5}) & +3.6314(10^{+6}) & -1.0288(10^{+1}) & +1.9520(10^{-2}) & -1.8819(10^{+7}) \\ -3.1612(10^{-1}) & +9.9874(10^{-1}) & -6.0526(10^{+4}) & -5.7423(10^{+5}) & +1.6268 & -3.0866(10^{-3}) & +2.9758(10^{+6}) \\ -1.3129(10^{-8}) & +8.3025(10^{-8}) & +9.9874(10^{-1}) & -1.5897(10^{-2}) & +4.5036(10^{-8}) & -8.5449(10^{-11}) & +8.2381(10^{-2}) \\ -1.3838(10^{-9}) & +1.3129(10^{-8}) & +3.1612(10^{-1}) & +9.9874(10^{-1}) & +3.5602(10^{-9}) & -6.7548(10^{-12}) & +6.5123(10^{-3}) \\ 0 & 0 & 0 & 0 & 1 & 0 & 0 \\ 0 & 0 & 0 & 0 & 0 & 1 & 0 \\ 0 & 0 & 0 & 0 & 0 & 0 & 1 \end{bmatrix} \quad (2-10)$$

$$K_D = \begin{bmatrix} +9.9924(10^{-1}) & +9.5735(10^{-3}) & +7.2579(10^{+5}) & +4.5902(10^{+6}) & -1.0389(10^{+1}) & +1.9334(10^{-2}) & -2.4019(10^{+7}) \\ -3.1615(10^{-1}) & +9.9924(10^{-1}) & -7.6501(10^{+4}) & -7.2579(10^{+5}) & +1.6427 & -3.0570(10^{-3}) & +3.7979(10^{+6}) \\ -6.2557(10^{-9}) & +3.9564(10^{-8}) & +9.9924(10^{-1}) & -9.5735(10^{-3}) & +2.1668(10^{-8}) & -4.0323(10^{-11}) & +5.0095(10^{-2}) \\ -6.5937(10^{-10}) & +6.2557(10^{-9}) & +3.1615(10^{-1}) & +9.9924(10^{-1}) & +1.7129(10^{-9}) & -3.1876(10^{-12}) & +3.9601(10^{-3}) \\ 0 & 0 & 0 & 0 & 1 & 0 & 0 \\ 0 & 0 & 0 & 0 & 0 & 1 & 0 \\ 0 & 0 & 0 & 0 & 0 & 0 & 1 \end{bmatrix} \quad (2-11)$$

The transfer matrices between cylinder segments, K_b , K_c , and K_d are of identical form, generically,

$$K_{b,c,d} = \begin{bmatrix} 1 & 0 & 0 & 0 & 0 & 0 & 0 \\ 0 & 1 & 0 & 0 & 0 & \frac{\Delta t_A}{2} & 0 \\ 0 & 0 & 1 & 0 & 0 & 0 & 0 \\ 0 & 0 & 0 & 1 & 0 & 0 & \frac{\Delta t_A}{2} \\ 0 & 0 & 0 & 0 & 1 & 0 & 0 \\ 0 & 0 & 0 & 0 & 0 & 1 & 0 \\ 0 & 0 & 0 & 0 & 0 & 0 & 1 \end{bmatrix} \quad (2-12)$$

and result from equating the one-to-one identities of Q , Θ , p , P , and $\alpha \Delta T$ across the interfaces between segments, along with the relationship between M and u across the interfaces suggested by Section 2.2.2.1, f. Since, in this case, the Δt 's have been chosen to be identical, are in numerical form,

$$K_{b,c,d} = \begin{bmatrix} 1 & 0 & 0 & 0 & 0 & 0 & 0 \\ 0 & 1 & 0 & 0 & 0 & 0.05035 & 0 \\ 0 & 0 & 1 & 0 & 0 & 0 & 0 \\ 0 & 0 & 0 & 1 & 0 & 0 & 0.05035 \\ 0 & 0 & 0 & 0 & 1 & 0 & 0 \\ 0 & 0 & 0 & 0 & 0 & 1 & 0 \\ 0 & 0 & 0 & 0 & 0 & 0 & 1 \end{bmatrix} \quad (2-13)$$

Equation 2-8 denotes the final result of carrying out steps 2.2.2.1, a through 2.2.2.1, h. Numerically, this result is:

$$\begin{bmatrix} Q_{RD} \\ M_{RD} \\ \Theta_{RD} \\ u_{RD} \\ p \\ P \\ \alpha\Delta T \end{bmatrix} = \begin{bmatrix} +0.72054(10^2) & +0.82584(10^3) & +0.14045(10^3) & +0.18455 & 0 \\ -0.31380(10^2) & -0.11007(10^3) & -0.70278(10^2) & +0.20314 & 0 \\ +0.26152(10^{-5}) & +0.17680(10^{-4}) & -0.60689(10^{-5}) & +0.97032(10^{-7}) & 0 \\ +0.75033(10^{-5}) & +0.33134(10^{-4}) & +0.12581(10^{-4}) & +0.50546(10^{-7}) & +0.52328(10^1) \\ 0 & 0 & 1 & 0 & 0 \\ 0 & 0 & 0 & 1 & 0 \\ 0 & 0 & 0 & 0 & 1 \end{bmatrix} \begin{bmatrix} Q_{RP} \\ M_{RP} \\ p \\ P \\ \alpha\Delta T \end{bmatrix} \quad (2-14)$$

At the right ends of segments A, B, and C

$$\begin{bmatrix} Q_{RA} \\ M_{RA} \\ \Theta_{RA} \\ u_{RP} \\ p \\ P \\ \alpha\Delta T \end{bmatrix} = \begin{bmatrix} +0.60718(10^1) & +0.14764(10^2) & +0.15718(10^2) & -0.27886(10^{-1}) & 0 \\ -0.10482(10^1) & -0.10043(10^1) & -0.24872(10^1) & +0.55092(10^{-1}) & 0 \\ +0.47770(10^{-5}) & +0.23875(10^{-4}) & -0.78312(10^{-6}) & +0.49082(10^{-7}) & 0 \\ +0.38470(10^{-5}) & +0.12685(10^{-4}) & +0.15516(10^{-4}) & -0.23717(10^{-7}) & +0.50816(10) \\ 0 & 0 & 1 & 0 & 0 \\ 0 & 0 & 0 & 1 & 0 \\ 0 & 0 & 0 & 0 & 1 \end{bmatrix} \begin{bmatrix} Q_{RP} \\ M_{RP} \\ p \\ P \\ \alpha\Delta T \end{bmatrix} \quad (2-15)$$

$$\begin{bmatrix} Q_{RB} \\ M_{RB} \\ \Theta_{RB} \\ u_{RB} \\ p \\ P \\ \alpha\Delta T \end{bmatrix} = \begin{bmatrix} +0.18238(10^2) & +0.58378(10^2) & +0.46260(10^2) & -0.47186(10^{-1}) & 0 \\ -0.47904(10) & -0.12048(10^2) & -0.12315(10^2) & +0.11866 & 0 \\ +0.42023(10^{-5}) & +0.22686(10^{-4}) & -0.22417(10^{-5}) & +0.73748(10^{-7}) & 0 \\ +0.52883(10^{-5}) & +0.20110(10^{-4}) & +0.15095(10^{-4}) & -0.43761(10^{-6}) & +0.51319(10) \\ 0 & 0 & 1 & 0 & 0 \\ 0 & 0 & 0 & 1 & 0 \\ 0 & 0 & 0 & 0 & 1 \end{bmatrix} \begin{bmatrix} Q_{RP} \\ M_{RP} \\ p \\ P \\ \alpha\Delta T \end{bmatrix} \quad (2-16)$$

and

$$\begin{bmatrix} Q_{RC} \\ M_{RC} \\ \Theta_{RC} \\ u_{RC} \\ P \\ P \\ \alpha\Delta T \end{bmatrix} = \begin{bmatrix} +0.39756(10^2) & +0.14417(10^3) & +0.89247(10^2) & +0.15372(10^2) & 0 \\ -0.13822(10^2) & -0.43338(10^2) & -0.33776(10^2) & +0.17866 & 0 \\ +0.34758(10^{-5}) & +0.20571(10^{-4}) & -0.40636(10^{-5}) & +0.88291(10^{-7}) & 0 \\ +0.65220(10^{-5}) & +0.27017(10^{-4}) & +0.14145(10^{-4}) & +0.21220(10^{-7}) & +0.51823(10) \\ 0 & 0 & 1 & 0 & 0 \\ 0 & 0 & 0 & 1 & 0 \\ 0 & 0 & 0 & 0 & 1 \end{bmatrix} \begin{bmatrix} Q_{RP} \\ M_{RP} \\ P \\ P \\ \alpha\Delta T \end{bmatrix} \quad (2-17)$$

Equation 2-14 is the numerical form of equation (2-7).

7. Calculation is now begun of the flange ring stiffness (Section 2.2.2.2). First, the parameters Q_R , M_R , Θ_R , and u_R (at the bottom of the flange, point R, Figure 2N) must be written in terms of similar parameters at the right end of the hub, location RD, and the applied forces. This gives:

$$\begin{bmatrix} Q_R \\ M_R \\ \Theta_R \\ u_R \end{bmatrix} = \begin{bmatrix} Q_{RD} \\ M_{RD} \\ \Theta_{RD} \\ u_{RD} \end{bmatrix} + \begin{bmatrix} 1 & -2\pi hR & 0 & 0 & 0 \\ \frac{h}{2} & \frac{-\pi(R_G^2 - R^2)(R_G - R)}{2} & -(R_{hub} - R) & -(R_G - R) & 0 \\ 0 & 0 & 0 & 0 & 0 \\ 0 & 0 & 0 & 0 & -(R_{hub} - R) \end{bmatrix} \begin{bmatrix} Q_{gf} \\ P \\ P \\ G \\ \alpha\Delta T \end{bmatrix} + \begin{bmatrix} 0 \\ -\frac{h}{2} Q_{RD} \\ 0 \\ \frac{h}{2} \Theta_{RD} \end{bmatrix} \quad (2-18)$$

The top equation, for Q_R , is given by Eq. 2.17, the second, for M_R , by Eq. 2.18, and the last two, for Θ_R and u_R , by Eq. 2.19.

In numerical form, Eq. 2-18 becomes:

$$\begin{bmatrix} Q_R \\ M_R \\ \Theta_R \\ u_R \end{bmatrix} = \begin{bmatrix} Q_{RD} \\ M_{RD} \\ \Theta_{RD} \\ u_{RD} \end{bmatrix} + \begin{bmatrix} 1 & -18.1864 & 0 & 0 & 0 \\ .288 & -2.6125 & -.2328 & -.4 & 0 \\ 0 & 0 & 0 & 0 & 0 \\ 0 & 0 & 0 & 0 & -.2328 \end{bmatrix} \begin{bmatrix} Q_{gf} \\ p \\ P \\ G \\ \alpha DT \end{bmatrix} + \begin{bmatrix} 0 \\ -.288 Q_{RD} \\ 0 \\ .288 \Theta_{RD} \end{bmatrix} \quad (2-19)$$

In that all equations prior to this stage were in the form of Eq. 2-8, i.e. all parameters written in terms of Q_{RP} , M_{RP} , p , P , and $\alpha\Delta T$, it is advisable for arithmetic manipulations to change Eq. 2-18 to a similar form. First, the terms $\{Q_{RD}, M_{RD}, \Theta_{RD}, u_{RD}\}$ are known from Eq. 2-14, and can be inserted directly into the first term of Eq. 2-19, which then becomes:

$$\begin{bmatrix} Q_R \\ M_R \\ \Theta_R \\ u_R \\ B \\ \alpha\Delta T \end{bmatrix} = \begin{bmatrix} 7.2054(10^1) & 2.8259(10^2) & 1.2236(10^2) & 1.8455(10^{-1}) & 0 & 0 & 1 & 0 \\ -3.1380(10^1) & -1.1007(10^2) & -7.2891(10^1) & -2.9624(10^2) & 0 & 0 & .288 & -.4 \\ 2.6152(10^{-6}) & 1.7680(10^{-5}) & -6.0689(10^{-6}) & 9.7032(10^{-8}) & 0 & 0 & 0 & 0 \\ 7.5033(10^{-6}) & 3.3134(10^{-5}) & 1.2581(10^{-5}) & 5.0546(10^{-8}) & 5 & 0 & 0 & 0 \\ 0 & 0 & 0 & 0 & 0 & 1 & 0 & 0 \\ 0 & 0 & 0 & 0 & 1 & 0 & 0 & 0 \end{bmatrix} \begin{bmatrix} Q_{RP} \\ M_{RP} \\ p \\ P \\ \alpha\Delta T \\ B \\ Q_{gf} \\ G \end{bmatrix} + \begin{bmatrix} 0 \\ -.288 Q_{RD} \\ 0 \\ .288 \Theta_{RD} \\ 0 \\ 0 \end{bmatrix} \quad (2-20)$$

The bolt pull, B (Eq. 2-16), and the parameter $\alpha\Delta T$ have been included as one-to-one identities in the above equation for ease in future computations. Next, the right-hand column $\{0, -0.288 Q_{RD}, 0, +0.288 \Theta_{RD}, 0, 0\}$, by means of matrix manipulations and the use of Eq. 2-14, is incorporated into the first term of Eq. 2-20. This is accomplished by multiplying the first and third rows of the matrix in Eq. 2-14 by 0.288 and then subtracting the first row, term by term, from the first five terms of the second row of the matrix in Eq. 2-20, and by adding the third row, term by term, to the first five terms of the fourth row of the Eq. 2-20 matrix. For example, the first term of the second row at the resulting matrix will be

$$-3.1380(10^1) - (0.288) (0.72054(10^2)) = -5.2132(10^1) \quad (2-21)$$

The resulting equation is

$$\begin{bmatrix} Q_R \\ M_R \\ \Theta_R \\ u_R \\ B \\ \alpha\Delta T \end{bmatrix} = \begin{bmatrix} 7.2054(10^1) & 2.8259(10^2) & 1.2236(10^2) & 1.8455(10^{-1}) & 0 & 0 & 1 & 0 \\ -5.2132(10^1) & -1.9145(10^2) & -1.1334(10^2) & -8.2775(10^2) & 0 & 0 & .288 & -.4 \\ 2.6152(10^{-6}) & 1.7680(10^{-5}) & -6.0689(10^{-6}) & 9.7032(10^{-8}) & 0 & 0 & 0 & 0 \\ 8.2564(10^{-6}) & 3.8226(10^{-5}) & 1.0833(10^{-5}) & 7.8491(10^{-8}) & 5 & 0 & 0 & 0 \\ 0 & 0 & 0 & 0 & 0 & 1 & 0 & 0 \\ 0 & 0 & 0 & 0 & 1 & 0 & 0 & 0 \end{bmatrix} \begin{bmatrix} Q_{RP} \\ M_{RP} \\ P \\ P \\ \alpha\Delta T \\ B \\ Q_{gf} \\ G \end{bmatrix} \quad (2-22)$$

Thus, parameters at the bottom of the flange are in terms of pipe parameters Q_{RP} and M_{RP} , along with the applied loads and three new unknowns, B , Q_{gf} , and G . The above matrix will be designated as K_f which includes $K_D^{gf}, K_d, \dots, K_a$.

8. The stiffness of the flange, from the flange bottom to the bolt circle, is calculated. Equations 2-20 through 2-23 are written in matrix form, along with the one-to-one identity $\alpha\Delta T$.

$$\begin{bmatrix} Q_B \\ M_B \\ \Theta_B \\ u_B \\ \alpha\Delta T \end{bmatrix} = K_{F1} \begin{bmatrix} Q_R \\ M_R \\ \Theta_R \\ u_R \\ B \\ \alpha\Delta T \end{bmatrix} \quad (2-23)$$

where

$$K_{F1} = \begin{bmatrix} \frac{1}{2} \left[(1-\nu) \frac{R_B}{R} + (1-\nu) \frac{R}{R_B} \right] & 0 & 0 & \frac{Eh}{T} \left(\frac{R_B}{R} - \frac{R}{R_B} \right) & 0 & \frac{Eh}{T} \left(\frac{R_B}{R} - \frac{R}{R_B} \right) R \\ 0 & \frac{1}{2} \left[(1-\nu) \frac{R_B}{R} + (1-\nu) \frac{R}{R_B} \right] & \frac{Eh^3}{12T} \left(\frac{R_B}{R} - \frac{R}{R_B} \right) & 0 & \left[(1-\nu) \left(\frac{R_B^2 - R^2}{4R_B} \right) + \left(\frac{1+\nu}{2} \right) R_B \right] \left(\frac{R}{R} \right) & 0 \\ 0 & \frac{3(1-\nu^2)}{Eh^3} \left(\frac{R_B}{R} - \frac{R}{R_B} \right) & \frac{1}{2} \left[(1-\nu) \frac{R_B}{R} + (1-\nu) \frac{R}{R_B} \right] & 0 & \left[\frac{3(1-\nu^2)R}{Eh^3} \right] \left[\frac{R_B^2 - R^2}{2R_B} + \left(\frac{R}{R} \right) \right] & 0 \\ \frac{(1-\nu^2)}{4Eh} \left(\frac{R_B}{R} - \frac{R}{R_B} \right) & 0 & 0 & \frac{1}{2} \left[(1-\nu) \frac{R_B}{R} + (1-\nu) \frac{R}{R_B} \right] & 0 & \frac{1}{2} \left[(1-\nu) \left(\frac{R_B}{R} - \frac{R}{R_B} \right) R \right] \\ 0 & 0 & 0 & 0 & 0 & 1 \end{bmatrix} \quad (2-24)$$

In numerical form, for this example,

$$K_{F1} = \begin{bmatrix} 1.1208 & 0 & 0 & 2.2275 & 0 & -1.1138(10^6) \\ 0 & 1.1208 & 6.1587(10^5) & 0 & 1.5916 & 0 \\ 0 & 1.0431(10^{-7}) & 9.4956(10^{-1}) & 0 & 7.5012(10^{-8}) & 0 \\ 2.8841(10^{-9}) & 0 & 0 & 9.4956(10^{-1}) & 0 & 1.7657 \\ 0 & 0 & 0 & 0 & 0 & 1 \end{bmatrix} \quad (2-25)$$

9. Now, the parameters at the bolt circle can be written in terms of the pipe parameters by replacing, in Eq.2-23, the column $\{Q_R, M_R, \Theta_R, u_R, B, \alpha\Delta T\}$ by the matrix equation 2-22. Hence,

$$\begin{bmatrix} Q_B \\ M_B \\ \Theta_B \\ u_B \\ \alpha\Delta T \end{bmatrix} = K_{F1} \cdot K_f \begin{bmatrix} Q_{RP} \\ M_{RP} \\ P \\ P \\ \alpha\Delta T \\ B \\ Q_{gf} \\ G \end{bmatrix} \quad (2-26)$$

Numerically, this yields

$$\begin{bmatrix} Q_B \\ M_B \\ \Theta_B \\ u_B \\ \alpha\Delta T \end{bmatrix} = \begin{bmatrix} 2.2467(10^2) & 1.1682(10^3) & 3.7845(10^2) & 1.9553 & 0 & 0 & 1.1208 & 0 \\ -5.6818(10^1) & -2.0369(10^2) & -1.3077(10^2) & -3.3012(10^2) & 0 & 1.5916 & 3.2278(10^{-1}) & -4.4331(10^{-1}) \\ -2.9549(10^{-6}) & -3.11829(10^{-6}) & -1.7586(10^{-5}) & 8.3503(10^{-8}) & 0 & 7.5012(10^{-8}) & 3.0042(10^{-8}) & -4.1725(10^{-8}) \\ 8.0478(10^{-6}) & 3.7113(10^{-5}) & 1.0640(10^{-5}) & 7.5064(10^{-8}) & 6.5135 & 0 & 2.8841(10^{-9}) & 0 \\ 0 & 0 & 0 & 0 & 1 & 0 & 0 & 0 \end{bmatrix} \begin{bmatrix} Q_{RP} \\ M_{RP} \\ P \\ P \\ \alpha\Delta T \\ B \\ Q_{gf} \\ G \end{bmatrix} \quad (2-27)$$

10. The zero values of shear and moment at the top of the flange are now used to gain two simultaneous equations in Q_{RP} and M_{RP} . Writing Eqs. 2-26 and 2.27 in matrix form,

$$\begin{bmatrix} 0 \\ 0 \end{bmatrix} = K_{F2} \begin{bmatrix} Q_B \\ M_B \\ \Theta_B \\ u_B \\ \alpha\Delta T \end{bmatrix} \quad (2-28)$$

where

$$K_{F2} = \begin{bmatrix} \frac{1}{2} \left[(1+\nu) \frac{R_{OF}}{R_B} + (1-\nu) \frac{R_B}{R_{OF}} \right] & 0 & 0 & \frac{\pi E h}{t} \left(\frac{R_{OF}}{R_B} - \frac{R_B}{R_{OF}} \right) & -\frac{\pi E h}{t} \left(\frac{R_{OF}}{R_B} - \frac{R_B}{R_{OF}} \right) R_B \\ 0 & \frac{1}{2} \left[(1+\nu) \frac{R_{OF}}{R_B} + (1-\nu) \frac{R_B}{R_{OF}} \right] & \frac{\pi E h^3}{12t} \left(\frac{R_{OF}}{R_B} - \frac{R_B}{R_{OF}} \right) & 0 & 0 \end{bmatrix} \quad (2-29)$$

Numerically,

$$K_{F2} = \begin{bmatrix} 1.1007 & 0 & 0 & 1.9300(10^7) & -1.2571(10^8) \\ 0 & 1.1007 & 5.3361(10^5) & 0 & 0 \end{bmatrix} \quad (2-30)$$

Since $\{Q_B, M_B, \Theta_B, u_B, \alpha\Delta T\}$ are known in terms of pipe parameters from Eq. 2-27, substitution into Eq. 2-30 yields

$$\begin{bmatrix} 0 \\ 0 \end{bmatrix} \begin{bmatrix} 4.4665(10^2) & 2.0021(10^3) & 6.2191(10^2) & 3.6009 & 0 & 0 & 1.2893 & 0 \\ -6.4115(10^1) & -2.2590(10^2) & -1.5332(10^2) & 812217(10^{-3}) & 0 & 1.7919 & 3.7136(10^{-1}) & -5.1572(10^{-1}) \end{bmatrix} \begin{bmatrix} Q_{RP} \\ M_{RP} \\ P \\ P \\ \alpha\Delta T \\ B \\ Q_{Rf} \\ G \end{bmatrix} \quad (2-31)$$

11. Matrix Eq. 2-31, representing two simultaneous equations in terms of eight parameters, is solved for Q_{RP} and M_{RP} .

$$Q_{RP} = -6.0597 p + 3.0208(10^{-2}) P + 3.7662(10^{-2}) Q_{gf} - 3.7584(10^{-2}) G \\ + 1.3059(10^{-1}) B \quad (2-32)$$

$$M_{RP} = 1.0412 p - 8.5374(10^{-3}) P - 9.0457(10^{-3}) Q_{gf} + 8.3844(10^{-3}) G \\ - 2.9132(10^{-2}) B \quad (2-33)$$

A simple means of solving the simultaneous equations is shown on pages 2-26 and 2-27.

12. The values of shear and moment in the flange at the bolt circle and at the flange bottom, needed for determining the flange deflections, are now found.

By substituting Eqs. 2-32 and 2-33 into the right-hand column of Eq. 2-22, the first two rows of Eq. 2-22 yield

$$Q_R = -20.0311 p - 0.0515 P + 1.1574 Q_{gf} - 0.3387 G + 1.1769 B \quad (2-34)$$

$$M_R = 3.2228 p - 0.0231 P + 0.0564 Q_{gf} - 0.0459 G - 1.2495 B \quad (2-35)$$

Similarly, substituting Eqs. 2-32 and 2-33 into Eq. 2-27,

$$Q_B = -9.0233 p - 0.02317 P + 0.5211 Q_{gf} - 0.1526 G + 0.5302 B \quad (2-36)$$

$$M_B = 1.4517 p - 0.0104 P + 0.0255 Q_{gf} - 0.0207 G + 0.1057 B \quad (2-37)$$

13. The axial flange displacement at the bolt circle with respect to the gasket circle, $w_B - w_G$, and the radial displacement of the flange at the gasket, u_G , are now found by direct substitution of M_R and B into Eq. 2-28 and Q_R , Q_B , and M_R , and M_B into Eq. 2-29, which are of the form,

$$w_B - w_G = C_1 B + C_2 M_R - C_3 M_B; \quad (2-38)$$

and

$$u_G = C_4 Q_B - C_5 Q_R + R_G \alpha \Delta T - C_6 M_R + C_7 M_B - C_8 B. \quad (2-39)$$

The numerical results are:

$$w_B - w_G = 3.5076(10^{-6}) p - 0.0251(10^{-6}) P + 0.2046(10^{-6}) B \\ + 0.0613(10^{-6}) Q_{gf} - 0.0499(10^{-6}) G \quad (2-40)$$

$$u_G = -0.3873(10^{-6})p + 0.0083(10^{-6})P - 0.0499(10^{-6})Q_{gf} \\ + 0.0234(10^{-6})G - 0.0819(10^{-6})B + 5.4\alpha\Delta T \quad (2-41)$$

Equations 2-40 and 2-41 are written for the flange shown in Figures 2M and 2N, which will be called the left flange. All calculations to this stage of analysis are generally repeated for both mating flanges. In this case, because the flanges have been assumed identical, not only are the equations parametrically the same, but also numerically the same.

14. The bolt and gasket deflections are calculated (Section 2.2.2.3). In terms of the flange parameters, Eqs. 2.30, 2.31, and 2.32 become

$$w_{BB} = 3.8713(10^{-8})B + (1.202\alpha_B - 0.576\alpha)\Delta T - C \quad (2-42)$$

$$w_{GG} = 7.3720(10^{-9})G - (0.05\alpha_G + 0.576\alpha)\Delta T \quad (2-43)$$

$$u_G = 85.987(10^{-6})Q_{gf(\text{left})} + 85.987(10^{-6})Q_{gf(\text{right})} \\ + 143.100(10^{-6})p + 5.4\alpha_G\Delta T \quad (2-44)$$

In these calculations, a gasket with the following properties has been assumed: gasket width, $g = 0.2$ in., gasket thickness, $h_g = 0.05$ in., gasket modulus, $E_g = 10^6$ psi. The effective bolt length, L_B , has been assumed to be 2.4. The gasket coefficient of thermal expansion α_G is assumed to be the same as that of 347 stainless steel.

It will be noted here that, since the bolts and gasket involve interaction between the flanges, the shear force on the left side of the gasket $Q_{gf\ell}$ may, in general, vary from the right side, Q_{gfr} . Of course, w_{BB} and w_{GG} are common values.

15. The compatibility of displacements between the two flanges (Section 2.2.2.4) is now called upon. Substitution of Eq. 2-40, (written twice, once for the left flange and once for the right flange), Eq. 2-42 and Eq. 2-43 into Eq. 2-33, yields

$$C = 7.0153(10^{-6})p - 0.0502(10^{-6})P + 0.4479(10^{-6})B + 0.0613(10^{-6})Q_{fr} \\ + 0.0613(10^{-6})Q_{f\ell} - 0.0925(10^{-6})G \\ + \Delta T [1.202\alpha_B - 0.05\alpha_G - 1.152\alpha] \quad (2-45)$$

Substitution of Eq. 2-41 written for the left flange, along with Eq. 2-44, into Eq. 2.34 yields

$$\begin{aligned}
 & 85.987(10^{-6}) Q_{gf(\text{left})} + 85.987(10^{-6}) Q_{gf(\text{right})} + 143.100(10^{-6}) p \\
 & + 5.4 \alpha_G \Delta T = 0.387344(10^{-6}) p + 0.00834162(10^{-6}) P - 0.0499203(10^{-6}) Q_{gf(\text{left})} \\
 & + 0.0233664(10^{-6}) G - 0.0818531(10^{-6}) B + 5.4 \alpha \Delta T \quad (2-46)
 \end{aligned}$$

Similarly, substitution of Eq. 2-41, written for the right flange, along with Eq. 2-44, into Eq. 2.35 yields

$$\begin{aligned}
 & 85.987(10^{-6}) Q_{gf(\text{left})} + 85.987(10^{-6}) Q_{gf(\text{right})} + 143.100(10^{-6}) p \\
 & + 5.4 \alpha_G \Delta T = .387344(10^{-6}) p + 0.00834162(10^{-6}) P - 0.0499203(10^{-6}) Q_{gf(\text{left})} \\
 & + 0.0233664(10^{-6}) G - 0.0818531(10^{-6}) B + 5.4 \alpha \Delta T \quad (2-47)
 \end{aligned}$$

It will be noted that Eqs. 2-46 and 2-47 are identical. The left sides of the equations will always be the same; in general, the right sides will vary, in which case, the equations may be solved for Q_{gfl} in terms of Q_{gfr} . In this case, it is obvious, by equating the right sides, that

$$Q_{gfl} = Q_{gfr} = Q_{gf} \quad (2-48)$$

Substitution of the above into either of Eqs. 2-46 or 2-47 yields

$$\begin{aligned}
 Q_{gf} = & -0.834107 p + 48.49076(10^{-6}) P + 0.1358314(10^{-3}) G \\
 & - 0.4758205(10^{-3}) B + 0.0313908 (\alpha - \alpha_G) \Delta T \quad (2-49)
 \end{aligned}$$

Substitution of Eq. 2-49 into Eq. 2-45 gives

$$\begin{aligned}
 C = & 6.912934(10^{-6}) p - 0.0501727(10^{-6}) P - 0.0925074(10^{-6}) G \\
 & + 0.4477936(10^{-6}) B + \Delta T [1.202 \alpha_B - 0.0538 \alpha_G - 1.1482 \alpha] \quad (2-50)
 \end{aligned}$$

16) Using the initial flange tightened conditions that p , P , and ΔT all equal zero, and that the bolt load B equals the gasket load Q at that time, (page 2-26, following Eq. 2.36) Eq. 2-50 is solved for

$$C = 0.355286(10^{-6}) B_{\text{initial}} = 0.063449 \quad (2-51)$$

The parameter C is the initial change in bolt length due to travel of the nut along the bolt during tightening.

17. The operational condition relationship between B and Q, Eq. 2.24 is called upon, yielding

$$G = B - P - 13.0624 p. \quad (2-52)$$

Substitution of Eq. 2-52 into Eq. 2-50, along with Eq. 2-51 yields

$$B = -22.85848 p - 0.1191566 P + 2.814631(10^6) C \\ - 2.814631(10^6) \Delta T [1.202 \alpha_B - 0.0538 \alpha_G - 1.1482 \alpha] \quad (2-53)$$

18. Operating bolt load and gasket load are found by substituting the design vales of p and ΔT , and a calculated end load P based on pressure (Eq. 2-1) into Eqs. 2-52 and 2-53.

$$B_{\text{operating}} = 151059 \text{ lbs} \quad (2-54)$$

$$G_{\text{operating}} = 52950 \text{ lbs} \quad (2-55)$$

19. Q_{gf} , M_{RP} , and Q_{RP} are now calculated for both operational and initial conditions by substitution of the appropriate values of p, P, ΔT , B, and G, first into Eq. 2-49 and then into Eqs. 2-32 and 2-33.

$$Q_{gf_{\text{op}}} = -686 \text{ lbs}, Q_{gf_{\text{init}}} = -61 \text{ lbs}. \quad (2-56)$$

$$M_{RP_{\text{op}}} = -3906 \text{ in.lbs}, M_{RP_{\text{init}}} = -3705 \text{ in.lbs}. \quad (2-57)$$

$$Q_{RP_{\text{op}}} = 15834 \text{ lbs}, Q_{RP_{\text{init}}} = 16607 \text{ lbs}, \quad (2-58)$$

20. Moments, shear forces, rotations Θ , and displacements u are now calculated for several locations along the flange. (See Eqs. 2-27, 2-22, 2-15 through 2-17, 2A-1 and 2A-2. The results are shown in Table 2A.1.

Table 2A.1

RESULTS - INTERNAL LOADS AND DISPLACEMENTS

	Q (lb)		M (in. lb)		Θ (rad)		u (in.)	
	initial	operating	initial	operating	initial	operating	initial	operating
Pipe	16,607	15,834	-3,705	-3,906	-0.001649	-0.010400	0.0183428	0.051460
Right End "A"	46,136	47,800	-13,686	-9,674	-0.009124	-0.013868	0.016888	0.0481188
Right End "B"	86,585	91,281	-34,917	-27,549	-0.014262	-0.017238	0.0133148	0.0436009
Right End "C"	126,084	133,445	-68,981	-59,139	-0.018491	-0.0205638	0.0082113	0.0379731
Right End "D"	149,599	158,732	-113,335	-101,724	-0.022074	-0.0236321	0.0018442	0.0313052
Flange Bottom	149,537	144,481	-227,872	-191,331	-0.022074	-0.0236321	-0.0045131	0.0232528
Bolt Circle	67,064	83,472	15,250	11,431	-0.031334	-0.0310673	-0.0038542	0.0319519

21. The bending, axial, and radial stresses are now found. In the flange, the maximum hoop stress from Eq. 2.37 is:

$$\sigma_{\text{hoop, max}_{\text{init}}} = -89,384 \text{ psi} \quad (2-59)$$

$$\sigma_{\text{hoop, max}_{\text{operating}}} = -80,246 \text{ psi} \quad (2-60)$$

In the pipe, and at the right-hand end of each hub segment (the critical stress area), Eqs. 2.39 and 2.40, along with Eq. 2A-1 for the pipe and Eq. 2.9 for the hub segments, yield, for σ_H and σ_A , those stresses shown in Table 2A.2.

Table 2A.2
STRESSES IN PIPE AND HUB

	σ_{hoop}		σ_{axial}	
	initial	operating	initial	operating
Pipe	94,790	141,014	180,113	234,611
Right "A"	86,407	112,395	96,610	85,247
Right "B"	67,456	84,985	93,341	84,026
Right "C"	41,196	53,666	95,669	89,462
Right "D"	9,163	18,165	95,580	91,564

The stresses in the bolts, given by Eq. 2D-3, are:

$$\sigma_{\text{Bi}_{\text{initial}}} = 91668 \text{ psi} \quad (2-61)$$

$$\sigma_{\text{Bi}_{\text{operating}}} = 77,532 \text{ psi} \quad (2-62)$$

$$\sigma_{\text{Bo}_{\text{initial}}} = -55000 \text{ psi} \quad (2-63)$$

$$\sigma_{\text{Bo}_{\text{operating}}} = -46,519 \text{ psi} \quad (2-64)$$

22. Utilizing the axial and hoop stresses in the hub, pipe, and flange, and letting σ_{radial} equal zero, (Section 2.2.2.4), a check is made on incipient yielding through use of Section 2.1.3.

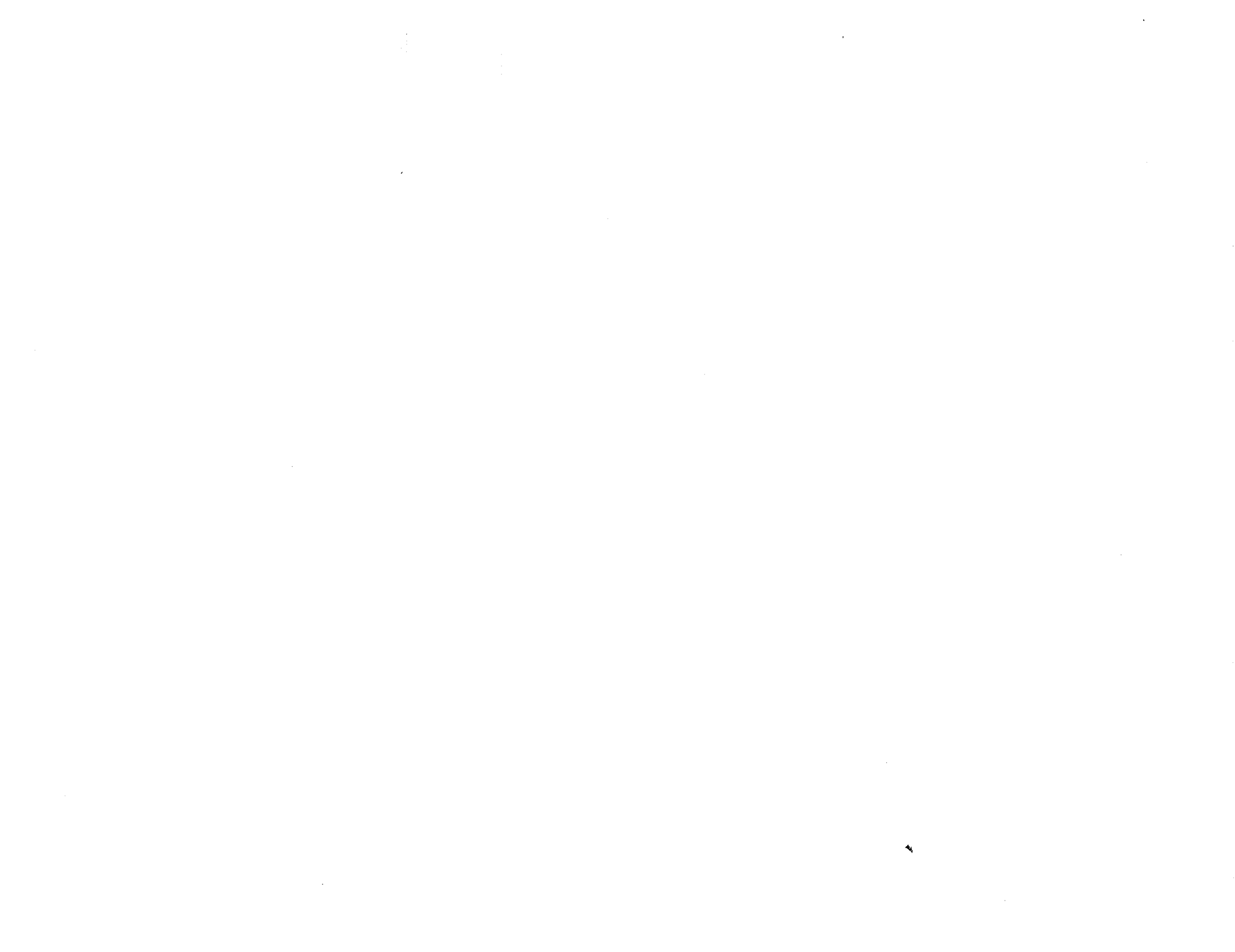
23. Depending on the results of a comparison at each location of the octahedral stress and the allowable stress, the deformations and the allowable deformations, and the gasket loads and the allowable gasket loads changes are made in the preliminary design configuration through use of the rules given in Section 2.2.2.4, (following Eq. 2-40) A modified version of the flange shown in Figure 2M will result. Reanalysis by the procedure shown herein will yield new stresses and deformations. These will more nearly meet requirements. Successive perturbations on the design and analysis are performed until the resulting design meets all requirements.

2.11 Nomenclature

A	Area at root of bolt threads times number of bolts (in. ²)
A _B	Minimum permissible total bolt area for strength (in. ²)
B	Total bolt load as a function of pressure and temperature (lb).
B _I	Initial bolt load (lb)
C	Initial tightening of bolts (in.)
d	Nominal bolt diameter (in.)
E	Modulus of elasticity (lb/in. ²)
f	Flange flexibility factor (see Eqs. 2.15, 2.41 and 2.69).
f _B	Stress concentration factor for bolts (Eq. 2D-4)
F	Total contact force at outer edge of flange (lb)
g	Gasket width (in.)
G	Total axial load at gasket as a function of pressure and temperature (lb)
G _I	Initial gasket load required to make seal (lb)
G _M	Minimum gasket load required to maintain seal (lb)
h	Flange thickness (in.)
h _G	Gasket thickness (in.)
H _B	Height of raised bearing surface at outer edge of contacting flange (in.)
H _L	Lap flange thickness (in.)
H _I	Integral flange thickness (in.)
H _F	Loose flange thickness (in.)
K ₁ , K ₂ , K ₃ , K ₄	Coefficients in cylindrical shell equations (2.11 to 2.14)
$\bar{K}_1, \bar{K}_2, \bar{K}_3, \bar{K}_4, \bar{K}_5, \bar{K}_6$	Coefficients in cylindrical segment energy (Eq. 2F-2)
L	Length of hub segment (in.)
L _B	Effective length of bolt (in.)
L _I	Hub length for integral flange (in.)
L _H	Hub length for lap flange (in.)
L _T	Double taper, length of portion having 3:1 slope (in.)
M	Total wall moment around circumference at pipe-hub interface (lb/in)
M _{Hub}	Wall moment at large end of hub (lb in.)
M _{ILF}	Moment at inner wall of loose flange (lb in.)
M _{OL}	Moment at outer radius of lap flange (lb in.)
M _R	Moment at inner radius of integral and lap flanges (lb in.)
n	Number of bolts
p	Design value of internal pressure in pipe, usually 1.5 p _{max. oper.} : (lb/in. ²)
P _{max. oper.}	Maximum operating pressure in pipe (does not include surges) (lb/in. ²)
P	Design value of total equivalent axial load on pipe usually $2.5 \pi R_G^2 p_{\text{max. oper.}}$ (lb)
Q	Total wall shear at pipe-hub interface (lb)
Q _{gf}	Shear due to gasket friction (lb)

Q_{Hub}	Wall shear at large end of hub (lb)
Q_{ILF}	Radial force (positive tension) at inner radius of loose flange (lb)
Q_{LF}	Loose flange friction
Q_{OL}	Radial force (positive tension) at outer radius of lap flange (lb)
Q_R	Radial force (positive tension) at inner radius of integral or lap flanges (lb)
R	Radius at inner pipe wall (in.)
R_B	Radius at line of action of bolt load (in.)
R_G	Radius at gasket circle (in.)
R_{BC}	Radius to bolt center (in.)
R_{OF}	Outer radius of integral and loose flanges (in.)
R_{HI}	Hub outer radius at integral flange (in.)
R_{HL}	Hub outer radius at lap flange (in.)
R_T	Double taper hub, outer radius at taper intercepts (in.)
R_{BS}	Radial width of bearing surface for flange contact outside the bolt circle (in.)
R_{OL}	Outer radius of lap flange (in.)
R_{ILF}	Inner radius of loose flange (in.)
S_B	Allowable stress in bolt material (lb/in. ²)
S_F	Allowable stress in integral and lap flange materials (lb/in. ²)
S_{FL}	Allowable stress in loose flange material (lb/in. ²)
S_H	Hub slope, (dimensionless)
t	Wall thickness (in.)
t_{Hub}	Hub thickness at flange (in.)
T_I	Hub thickness at integral flange (in.)
T_L	Hub thickness at lap flange (in.)
T_P	Pipe wall thickness (in.)
T	Bolt torque (lb/in.)
w	Axial displacement (in.)
w_B	Axial flange displacement at line of action of bolt force (in.)
w_G	Axial flange displacement at line of action of gasket force (in.)
w_{BB}	Effective bolt shortening due to bolt load (in.)
w_{GG}	Gasket compression due to gasket load (in.)

w_{OF}	Axial displacement of integral or loose flanges at outer edges (in)
w_{OL}	Axial displacement at lap flange outer edge (in)
u	Radial displacement (positive outward) at mid-thickness of pipe wall at pipe-hub interface (in)
u_r, u_ℓ	Radial displacements at right and left ends respectively of pipe segment (in)
u_R	Radial displacement at inner radius at mid-thickness of integral or lap flange wall (in)
u_B	Radial displacement at line of bolt force action at mid-thickness of integral or loose flange wall (in)
u_{ILF}	Radial displacement at inner wall, mid-thickness of loose flange (in)
u_G	Radial displacement of flange adjacent to gasket (in)
u_{GT}	Radial displacement of gasket (in)
u_{OLP}	Radial displacement of lap flange at contact with loose flange (in)
u_{OLL}	Radial displacement of loose flange at contact with lap flange (in)
$\alpha_B \Delta T$	Unit expansion of bolt due to temperature change
$\alpha_F \Delta T$	Unit expansion of flange due to temperature change
β	Factor in cylindrical shell theory (Eq. 2.10)
Θ	Angular rotation (positive counterclockwise for left half of connector, positive clockwise for right half of connector) at pipe-hub interface (rad)
Θ_R	Rotation at inner wall of integral and loose flanges (rad)
Θ_r, Θ_ℓ	Rotations at right and left ends respectively of pipe segment (rad)
Θ_B	Rotation at line of bolt action for integral and loose flanges (rad)
Θ_{ILF}	Rotation at inner wall of loose flange (rad)
σ_o	Octahedral stress at any point (lb/in ²)
$\sigma_1, \sigma_2, \sigma_3$	Circumferential, axial, and radial stresses respectively at any point (lb/in ²)
σ_{allow}	Allowable value of octahedral stress (lb/in ²)
ν	Poisson's ratio
μ	Coefficient of friction
μ_F	Coefficient of friction between flange and nut
μ_G	Coefficient of friction at gasket
μ_{OF}	Coefficient of friction at outer flange contact.
μ_{OL}	Coefficient of friction at loose and lap flange contact
μ_N	Coefficient of friction between bolt and nut



Section 3

THREADED CONNECTOR DESIGN

by

John Wallach

3.0 Selection of Connector

The selection of the correct connector for a given application is not only a question of choosing a connector to meet all of the technical design requirements, but also a question of the time and money available. This section is primarily concerned with the design of a technically optimized connector. It is a custom designed connector for a particular application and requires more time and money than an "off-the-shelf" standard connector. Therefore, whenever a standard connector will meet all the design requirements it should be used.

The current commercial connectors can usually be grouped as flared-tube connectors, swaged-tube connectors, or flanged-tube connectors. The flared-tube connector is subject to leakage unless a soft gasket is used, to gross deformation due to an excessive hoop stress in the union if it is overtorqued, and to fatigue failure at the root of the flare. The swaged-tube connector is subject to leakage unless a gasket is used and to fatigue failure in the swage. The flanged-tube connector is subject to leakage unless a gasket is used and to fatigue failure where the flanged section is attached to the tubing. Each type of connector has many advantages, some of which are peculiar to a certain connector design. The listing necessary to point out these features is too long to include here. Also, some connectors seal effectively with the use of ultrafine machined sealing surfaces rather than a soft gasket. However, the latter method of sealing is considered more reliable.

In case a standard connector will not meet the design requirements, a custom connector can be designed using the design procedure given in this Section. This will result in a technically optimized connector for the particular application. However, if over a period of time a large number of custom designed connectors are required, the design procedure can be automated by the use of a digital computer. Also, if the connectors required can be grouped according to their design requirements, it is possible to design a number of standard connectors so that one standard connector will meet the design requirements of a particular grouping. The use of standard connectors makes possible the stocking of connectors for immediate use.

3.1 Design Requirements

The threaded connector design begins with an accurate statement of the design requirements. These are the input quantities to the design procedure. At this stage of the design, it has already been decided that a separable connector is to be used and that a threaded connector rather than a flanged connector is applicable. The threaded connector is chosen when the tubing

outside diameter is one inch or less and the assembly torque required is not excessively large (under 2400 inch pounds).

The detailed design input requirements are:

a. Tubing

Material

Outside diameter, D_t

Inside diameter, d_t

b. Fluid contained in the tubing

Name and chemical composition

Operating pressure, P_o

Constant pressure, P_k

Cyclical pressure, P_c

Number of cycles of pressure, N_p

Temperature, T_g

c. Environmental conditions

Surrounding fluid

Ambient pressure, P_a

Ambient temperature, T_a

d. External loads

Constant force, F_k

Cyclical force, F_c

Number of cycles of force, N_f

Constant transverse moment, m_k

Cyclical transverse moment, m_c

Number of cycles of moment, N_m

e. Allowable leakage level

These design requirements are determined for each critical operating condition, both steady state and transient. A table of operating conditions and input parameters helps to keep the operating conditions separate. For each operating condition, a check of each parameter is necessary so that the value of the parameter in the table is the correct one for that condition.

In the following sections, reference is usually made to only one operating condition. This condition is very general and includes all of the design input parameters. Based on these parameters, a set of formulas have been derived for the determination of the connector dimensions.

By repeated use of the design procedure for each operating condition and the selection of the most conservative design, a connector design meeting all of the design requirements is generated. Wherever possible, the prior elimination of those operating conditions leading to nonconservative designs will greatly reduce the design effort.

3.2 Connector Configuration

The connector consists of a flange, union, seal and nut. The typical connector configuration is illustrated in Figure 3.1.

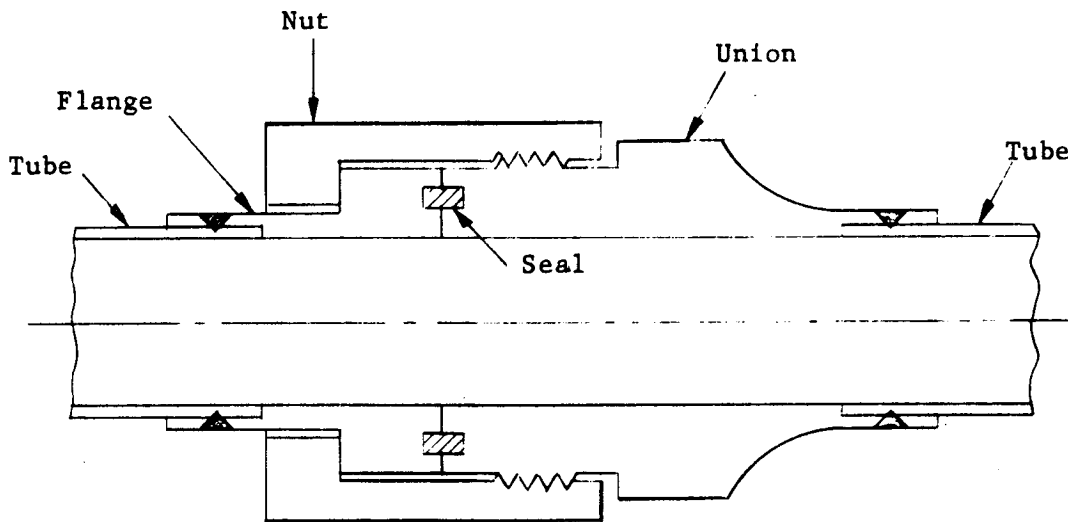


Figure 3.1 Typical Connector Configuration

The connector design separates the various connector functions. The attachments to the tube are made between the flange and the tube, and the union and the tube by welding. The separable part of the connector consists of the flange, nut, and union. Flats are provided on the nut and the union for wrench jaws. The seal is placed between the flange and the union. The compressive load path is from the flange to the union (not through the seal), and the tensile load path is through the nut.

3.3 Seal

The seal consists of either two flange and union surfaces properly prepared or a removable gasket and its companion sealing surfaces on the flange and the union. There is no one seal that can be successfully used in every application. However, certain types of seals can be used in specific

environments. Most of the gaskets for these seals are commercially available, and the seal can be designed from the manufacturer's catalog. A complete discussion of seals is included in Sections 1 and 4 of this Handbook.

3.4 Attachment to Tubing

The attachment of the connector to the tube must be structurally sound, leakproof, and compatible with the fluid contained. The method which best fits these requirements is welding. Swaging is not reliably leak-proof and brazing is limited because of compatibility and temperature problems. Welding, in general, also presents many problems when used in launch vehicle systems. However, a great deal of effort has already gone into the solution of these problems and satisfactory methods are being developed.

One such welding method, which has been developed and is recommended for use in this connector design, is discussed in Refs. 1 and 2. The method described is a tube-to-tube connection, but is applicable to the connector-to-tube connection shown in Figure 3.2. The tubing is slid into the connector

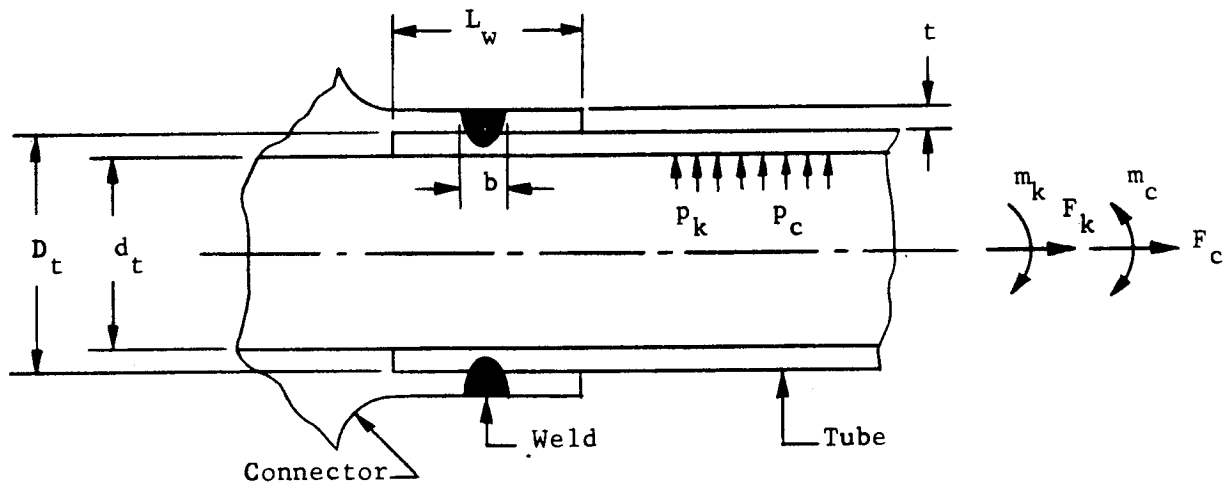


Figure 3.2 Connector-to-tubing Weld

socket and swaged into the socket. The weld is formed by melting the connector and tube materials together. The radial thickness of the socket is assumed equal to the tube thickness. However, the thickness and length, L_w , of the socket are determined by the materials to be welded, the type of weld, and the loading.

The structural integrity of the weld is so largely dependent on the type of weld, welding procedure, and connector and tube materials, that a separate yield strength, B_y , fracture strength, B_u , and fatigue strength, B_n , are determined for the weld. The strengths are expressed in pounds per linear inch of weld circumference. With these strengths known for the critical operating conditions (the strengths are temperature dependent) the structural integrity of the weld can be checked.

To prevent yielding.

$$\frac{H_m}{D_t} \left[0.3183(F_k + F_c) + 0.25d_t^2(P_k + P_c) + \frac{1.273}{D_t} (m_k + m_c) \right] \leq B_y \quad (3.1)$$

To prevent fracture.

$$\frac{H_m}{D_t} \left[0.3183(F_k + F_c) + 0.25d_t^2(P_k + P_c) + \frac{1.273}{D_t} (m_k + m_c) \right] \leq B_u \quad (3.2)$$

To prevent fatigue failure.

$$\frac{H_f}{D_t} \left[0.3183 \left(\frac{F_k}{B_u} + \frac{F_c}{B_u} \right) + 0.25d_t^2 \left(\frac{P_k}{B_u} + \frac{P_c}{B_n} \right) + \frac{1.273}{D_t} \left(\frac{m_k}{B_u} + \frac{m_c}{B_n} \right) \right] \leq 1 \quad (3.3)$$

There is no inconsistency between Eqs. 3.1 and 3.2, because only one of these equations will be used for any one operating condition.

3.5 Flange

3.5.1 Flange Configuration

The flange consists of three elements. The socket is provided for the mechanical attachment of the tube to the flange. A hub increases the distance between the weld and the seal in order to prevent thermal distortion of the flange ring during welding and to provide a smoother transition between the flexible socket and the rigid flange ring. The flange ring provides a bearing surface for the nut, an interface between the flange and the union for the seal and compressive load, and the structural rigidity to maintain the seal. The three elements and the nomenclature associated with the detailed dimensions of each element are shown in Figure 3.3.

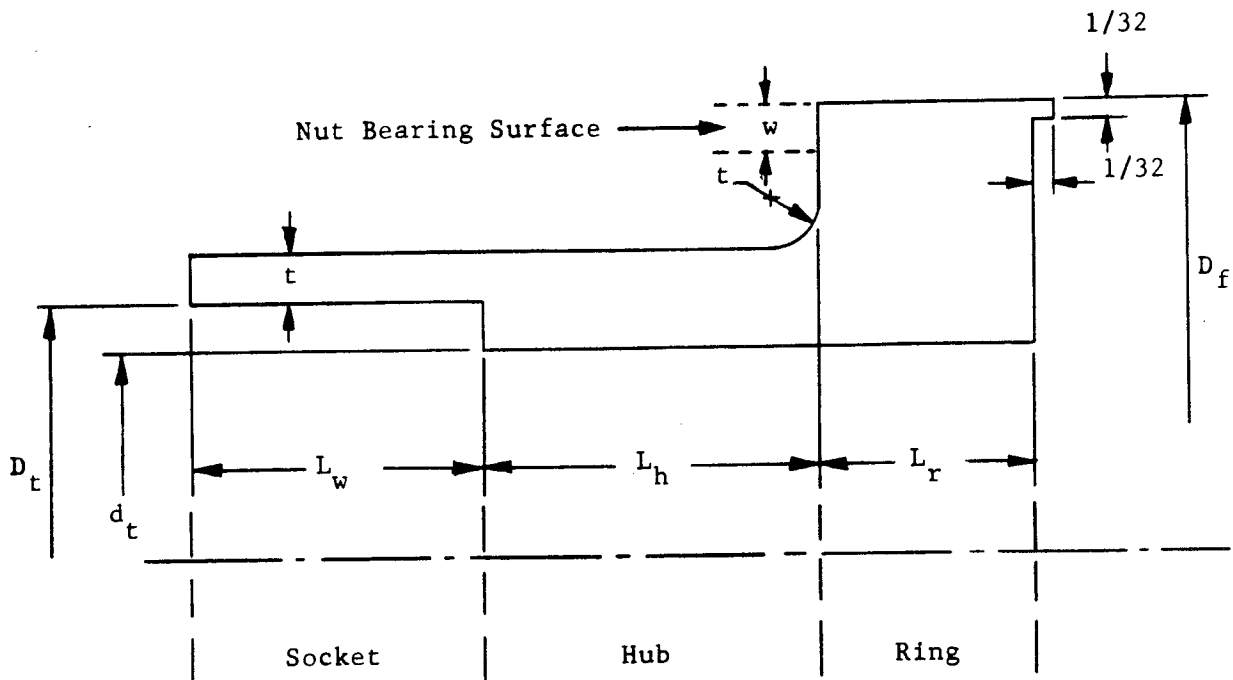


Figure 3.3 Flange Elements

All of the dimensions are chosen on the basis of a thorough stress and vibration analysis. This analysis is done in two steps and possibly a number of iterations. The structural analysis depends on the prior knowledge of the preload applied when tightening the nut. However, the preload depends on prior determination of the structural response of the connector by a structural analysis. Therefore, it is necessary to make an initial estimate of the connector dimensions. Then the preload is determined using these dimensions. The dimensions are then calculated on the basis of a thorough structural analysis using the calculated preload, and the preload is recalculated using the more accurate dimensions. This iterative calculation of connector dimensions and preload is continued until the change in dimensions and preload is negligible. If the second of two consecutive preload calculations results in a preload within five percent of the previous calculation, then the connector is adequately designed for the second preload and the calculations may be stopped.

3.5.2 Approximate Flange Dimensions

The following dimensions are necessary for the calculation of the preload. As stated above, the preload must be calculated before a final determination of flange dimensions is possible.

The length of the transition section of the flange is

$$L_h = 1.5 (D_t + 2t - d_t) \quad (3.4)$$

The outside diameter of the flange ring, D_f , is the largest of the following:

$$(D_f)_1 = D_t + 6t$$

$$(D_f)_2 = D_t + 4t + 1/8$$

$$(D_f)_3 = D_g + 2t + 1/16$$

$$(D_f)_4 = D_g + 3/16 \quad (3.5)$$

$$D_f = \text{the largest of } (D_f)_1, (D_f)_2, (D_f)_3, \text{ or } (D_f)_4$$

The length of the flange ring is approximated by making it equal to the radial width.

$$L_r = 1/2 (D_f - d_t) \quad (3.6)$$

The radial bearing length of the nut on the flange, w , is equal to t or $1/16''$, whichever is larger.

$$w = \text{larger of } (t \text{ or } 1/16'') \quad (3.7)$$

3.6 Union

3.6.1 Union Configuration

The union provides the seal interface, the threads to engage the nut, a set of wrenching flats, and a tube socket. The seal configuration and dimensions are in accordance with Sections 1 or 4. The union configuration and dimensions are given in this section. Figure 3.4 shows the details and dimensional nomenclature for the union. The outside and inside diameters (D_g and d_g) and axial length (L_g) of the seal are shown for reference.

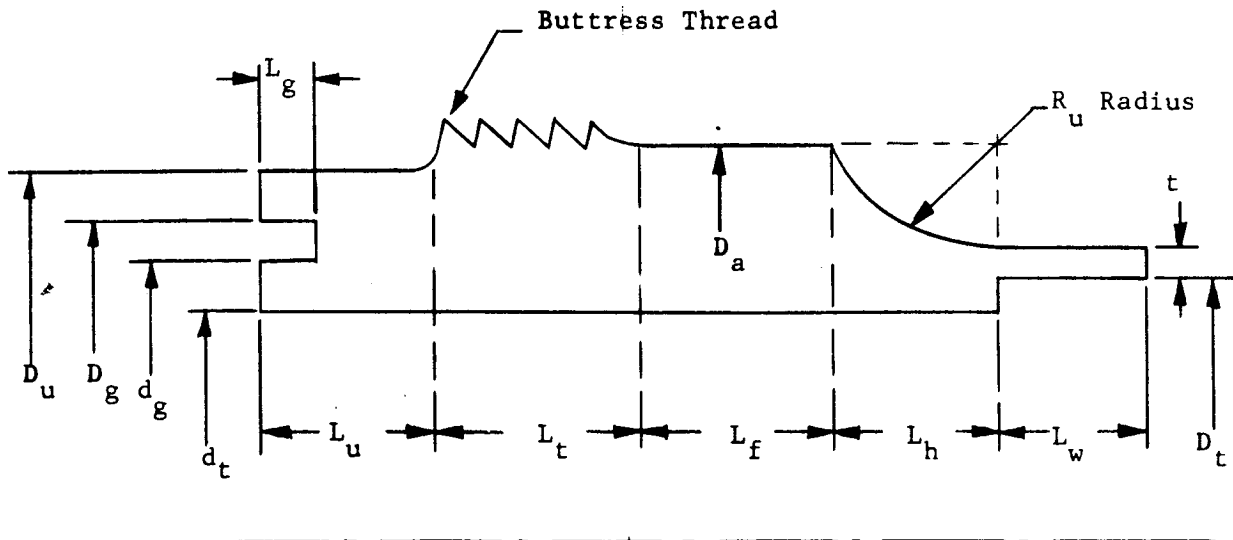


Figure 3.4 Union Dimensions

3.6.2 Union Dimensions

The union dimensions are determined by the mating parts and by the loads imposed. As the loading is not known until the preload has been calculated, the union dimensions and those of the mating parts can not be finalized at this stage of the design. In this Section the union dimensions are determined without a thorough stress analysis. In Section 3.10, after a complete structural analysis the dimensions will be checked.

The union diameter, D_u , is to be a snug sliding fit inside the lip on the flange face. In this way the union is located on the flange and radial motion between the two is prevented.

$$D_u = D_f - 1/16 \quad (3.8)$$

The length, L_u , is to be long enough so that the load on the threads is distributed uniformly over the union-to-flange contact area. So L_u is taken equal to the depth of the seal recess, L_g .

$$L_u = L_g \quad (3.9)$$

The union and nut thread is an American standard buttress screw thread (ASA B 1.9-1953). The nominal size of the thread, D_b , is chosen so that the minimum minor diameter of the nut is larger than D_f , and the nut will freely slide over the flange.

$$D_b \geq D_f + 1.2/n \quad (3.10)$$

The recommended thread sizes, number of threads, lengths of thread engagement, and lengths of threads are given in Table 3.1. These recommendations are based on a structural analysis of the Buttress thread using the formulas of Ref. 3.

Table 3.1

RECOMMENDED BUTTRESS THREAD SIZES

Nominal Size Inch D_b		Number of Threads Per Inch n	Length of Engagement Inch L_e	Length of Thread Inch L_t
From	To			
0	1/2	20	1/4	5/16
1/2	3/4	16	5/16	3/8
3/4	1	12	3/8	7/16
1	1-1/4	10	7/16	1/2
1-1/4	2	8	9/16	5/8
2	3	8	11/16	3/4

The next portion of the union provides a place to put a wrench so that the nut can be tightened on the union. In order to facilitate cutting of the threads, the diameter across corners of the wrenching flats is taken slightly less than the minor diameter of the thread on the union. The diameter across flats, D_a , is given by the following inequality:

$$D_t + 2t \leq D_a \leq 0.866 D_b - \frac{1.219}{n} - 0.017 \quad (3.11)$$

The largest D_a which satisfies Eq. 3.11 and is a standard size for an open end or ^acamloc wrench is chosen. Then L_f is chosen equal to the thickness of the wrench head.

The next section of the union provides a transition between the wrenching flats and the tube socket. A radius, R_u , is used to reduce the stress concentration.

$$R_u = 1/2 (D_a - D_t) - t \quad (3.12)$$

The tube socket on the union is identical to that on the flange. The same final dimensions are used for both. The flange tube socket is discussed in Sections 3.5 and 3.9..

3.7 Nut

3.7.1 Nut Configuration

The nut provides the tension necessary to compress the seal at assembly and to maintain this compression under all operating conditions. The ring of the nut bears on the ring of the flange, and the threads on the nut engage the threads of the union. Wrenching flats are provided on the outside diameter of the nut. Figure 3.5 shows the details and dimensional nomenclature for the nut.

3.7.2 Nut Dimensions

Most of the nut dimensions have been determined in the preceding sections. All of the nut dimensions except the outside diameter, D_n , and length of the ring, L_n , are determined by the mating parts. These remaining dimensions are estimated in this section so that the preload can be calculated. Then the dimensions are checked on the basis of a structural analysis, Section 3.9..

The nominal size of the thread, number of threads per inch, length of thread engagement, and length of thread are the same as for the union, Section 3.6.2. Based on these dimensions the inside diameter of the nut, d_n , is chosen equal to the maximum major diameter of the thread.

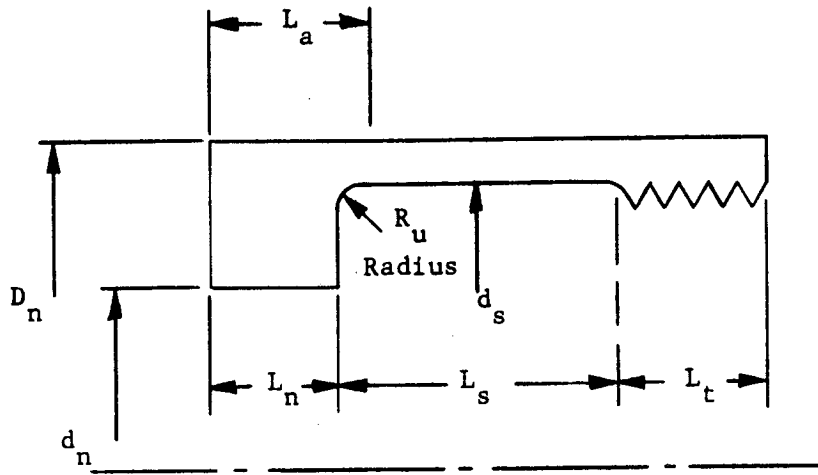


Figure 3.5 Nut Configuration

$$d_s = D_b + \frac{0.208}{n} + 0.014 \quad (3.13)$$

The length of the shell part of the nut is determined by the mating parts.

$$L_s = L_r + L_u + L_e - L_t \quad (3.14)$$

The inner diameter of the ring part of the nut is determined by the flange dimensions.

$$d_n = D_f - 2w \quad (3.15)$$

The small radius, R_n , is used to decrease the stress concentration.

$$R_n = 1/2(d_s - D_f) \quad (3.16)$$

The basic outside diameter of the nut, D_n , is also the diameter across flats of the wrenching flats provided on the nut. The value of D_n

$$D_n \geq d_s + D_u - d_t \quad (3.17)$$

chosen is the smallest standard diameter across the flats for a nut that satisfies Eq. 3.17. The wrenching flats are located at the ring end of the nut and the length of the flats, L_a , is taken equal to the thickness of a standard wrench head.

The length of the ring, L_n , is taken equal to the radial thickness.

$$L_n = 1/2 (D_n - d_n) \quad (3.18)$$

3.8 Preload

Preloading of the connector at assembly is essential to proper operation of the connector. Too small a preload in the connector will result in leakage and too large a preload will result in overstressing the connector. The use of the proper preload is also important in the stress calculations. The use of too small a preload in the calculations will result in a leaky connector and the use of too large a preload will result in an over-designed and overweight connector.

The preloading of a connector at assembly can be considered a two-step operation. First, the nut is tightened until the seal is sufficiently compressed and the flange and union come into contact. The axial force necessary is referred to as the seating force, F_s . At this point a seal has been effected. That is, the seal is designed so that the compressive force to bring the flange and union into contact is more than adequate to make the seal leak-tight.

The second step of the connector preloading is to increase the flange-to-union contact force to a value large enough to maintain the flange-to-union contact during all operating conditions. As the flange and union remain in contact at all times, the only axial movement the seal experiences is the elastic deformation of the flange and union faces. The seal is also protected from relative radial motions as long as the friction force between the flange and the union is not exceeded by the radial forces occurring during operation of the connector. For this reason, a minimum compressive force between the flange and union is maintained at all times.

3.8.1 Seal Force

Two forces are important to the seal. These are the force to effect a leak-tight seal at assembly and the minimum allowable force that will assure a leak-tight connector during operation. Sometimes an amount of compression rather than the force is specified. For instance, a rubber O-ring vendor usually recommends the amount of compression to effect the initial seal. In this case the force is very small, and it is more meaningful to specify the compression. However, in cases where the force to effect the seal is not negligible with respect to the preload, the force must be considered.

The connector being designed depends on a direct flange-to-union contact to carry the major portion of the compressive load. Only during assembly, before the union seats on the flange, does the seal take all the compressive load. Once the union seats on the flange, practically all of the increase in compressive load is taken by the union to flange interface. Therefore, the load on the seal when the flange is just touching the union must be large enough to effect a seal. However, the force should be only as large as necessary to reliably effect a seal at each assembly. Also, the force should be larger than the minimum allowable force for maintaining a leak-tight seal. This is usually the case. That is, for nearly all seals, the force to effect the seal is larger than the force to maintain the seal.

Thus, the sealing forces can be reduced to one force, the seating force F_s . This is the force necessary to bring the flange and union into direct contact. In the succeeding design procedure it is assumed that F_s is just large enough to reliably effect a seal at each assembly and is larger than the force necessary to maintain the seal during operation. The determination of F_s may be by analysis, test, or experience, depending upon the seal. For some seals the vendor will recommend the force to effect the seal and the force necessary to maintain the seal. In case the compression rather than the force is specified and the force is significant the force is determined from the compression. If the force is insignificant, as for a rubber O-ring, F_s is set equal to zero and the connector is designed only in accordance with the necessary compression.

3.8.2 Preload Calculation

The assembly preload, F_p , is chosen so that the load on the seal, F_s is always equal to or greater than the seating force, F_s . To choose the preload, first the axial spring constant, G_n , for the nut is calculated. Then the force on the seal is calculated for each critical operating condition, and from these results the necessary preload is calculated.

3.8.2.1 Spring Constant for the Nut

The spring constant for the nut is calculated on the basis of a thorough structural analysis. Because of the complexity of the analysis and the need to determine the forces and moments at the critical nut locations in order to calculate the stresses, the spring constant is calculated from a set of linear simultaneous equations. The numerical work involved in solving this set of equations is formidable, and the use of a digital computer is recommended. No programming will be necessary at most computer facilities as they will already have a program for linear simultaneous equations in operation. The coefficients in the equations can also be evaluated with the use of a digital computer, if this is desirable.

The nut was separated into a ring and three shells for the structural analysis, Figure 3.6. The deflections, rotations, forces, and moments are shown in Figure 3.6 in a positive sense. The externally applied load, F_n , acts on the nut ring and on the threads. The force on the threads is assumed to be divided equally between two finite locations. Because of the small thread angle there is no radial component of F_n on the threads. The following set of equations will allow the calculations of the deflections, rotations, forces, and moments due to a unit axial force ($F_n = 1$). From these results the spring constant is calculated. The set of equations is written in a condensed form and the coefficients of the variables and constant terms, C_i , are written separately in Section 3.11.1.

3-13

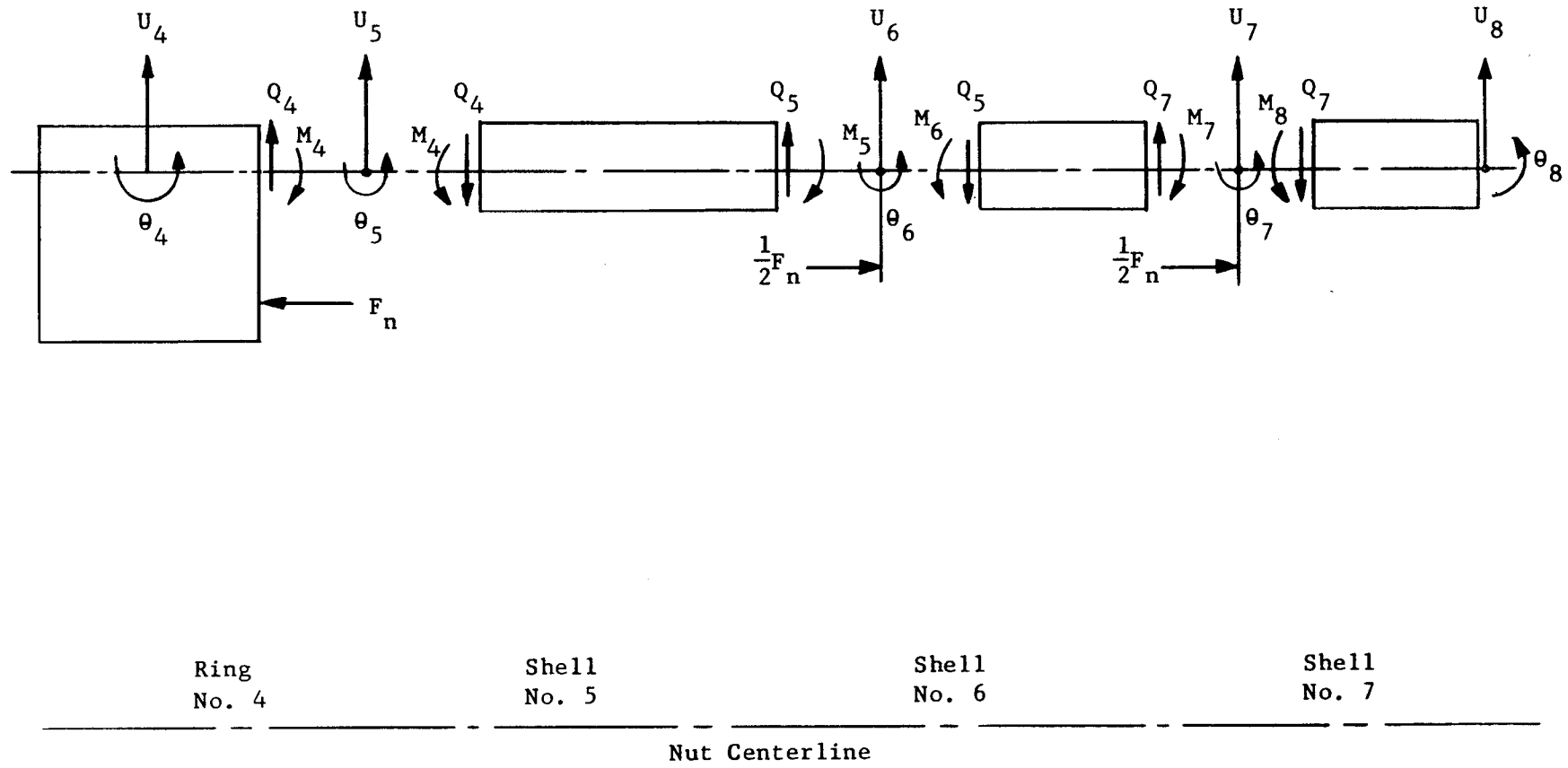


Figure 3.6 Separation of Nut for Structural Analysis

$$u_4 - u_5 + c_1\theta_4 = 0$$

$$u_4 + c_2Q_4 = 0$$

$$c_3u_5 - c_4u_6 + c_5\theta_5 + c_6\theta_6 + c_7Q_4 = c_8$$

$$c_4u_5 - c_3u_6 + c_6\theta_5 + c_5\theta_6 + c_7Q_5 = -c_8$$

$$-c_5u_5 + c_6u_6 - c_9\theta_5 - c_{10}\theta_6 + c_7M_4 = c_{11}$$

$$c_6u_5 - c_5u_6 + c_{10}\theta_5 + c_9\theta_6 + c_7M_5 = c_{11}$$

$$c_{12}u_6 - c_{13}u_7 + c_{14}\theta_6 + c_{15}\theta_7 + c_{16}Q_5 = c_{17}$$

$$c_{13}u_6 - c_{12}u_7 + c_{15}\theta_6 + c_{14}\theta_7 + c_{16}Q_7 = -c_{17}$$

$$-c_{14}u_6 + c_{15}u_7 - c_{18}\theta_6 - c_{19}\theta_7 + c_{16}M_6 = c_{20}$$

$$c_{15}u_6 - c_{14}u_7 + c_{19}\theta_6 + c_{18}\theta_7 + c_{16}M_7 = c_{20}$$

$$c_{21}u_7 - c_{22}u_8 + c_{23}\theta_7 + c_{24}\theta_8 = 0$$

$$c_{25}u_7 - c_{26}u_8 + c_{21}\theta_7 + c_{22}\theta_8 = 0$$

$$c_{26}u_7 - c_{25}u_8 + c_{22}\theta_7 + c_{21}\theta_8 + c_{27}Q_7 = 0$$

$$-c_{22}u_7 + c_{21}u_8 - c_{24}\theta_7 - c_{23}\theta_8 + c_{27}M_8 = 0$$

$$\theta_4 - \theta_5 + c_{28}Q_4 + c_{29}M_4 = 0$$

$$c_{30}\theta_4 + c_{31}Q_4 + c_{32}M_4 = c_{33}$$

$$M_5 - M_6 = c_{34}$$

$$M_7 - M_8 = c_{34}$$

(3.19)

Having solved Eq. 3.19, it is possible to calculate the spring constant for the nut directly.

$$\begin{aligned} \frac{1}{G_n} = & -0.25 (D_n + d_s - 2d_n - 2w) \theta_4 \\ & + 0.125 (D_n + d_s - 2D_b + \frac{1.2}{n}) (\theta_6 + \theta_7) \\ & + \frac{1.273(L_s + L_t) - 0.7417 L_e}{E_n (D_n^2 - d_s^2)} \end{aligned} \quad (3.20)$$

The spring constant is a linear function of the modulus of elasticity, E_n , which is temperature dependent. Therefore, a different value of the spring constant is calculated for each nut temperature. This is easily done by calculating the spring constant at room temperature and then using Eq. 3.21 to calculate the spring constants at various temperatures.

$$G_n(\text{operating temperature}) = G_n(\text{room temperature}) \frac{E_n(\text{operating temperature})}{E_n(\text{room temperature})} \quad (3.21)$$

3.8.2.2 Seal Force Calculation

The use of direct contact between the flange and the union to transmit the major portion of the compressive load means that the force on the seal during operation does not appreciably increase over F_s , the seating force. Therefore, it is more meaningful to calculate the force F_3 , and moment, M_3 , between the flange and the union. The seal force, F_g , is some function of this force and moment, and this functional relationship depends on the seal, flange face, and union face.

$$F_g = \text{function}(F_3, M_3) \quad (3.22)$$

To determine M_3 for any operating condition a thorough structural analysis of the flange and union was made. Because of the complexity of the analysis and the need to determine the forces and moments at various locations for the subsequent stress calculation, the result of the analysis is a set of linear simultaneous equations. Again, it is recommended to use a digital computer for their solution.

The flange was separated into three shells and the union was separated into two shells as shown in Figure 3.7. The deflections, rotations, forces, and moments are shown in a positive sense. The nut force, F_n , acts on the flange and the union. Because of the comparative

rigidity of the union, it was possible to assume the nut force concentrated at one point, with negligible error. The flange and union are also loaded by an axial force F_a , and internal pressure, p . The axial force is a composite of a constant and cyclical axial pressure force, an externally applied axial force, and an externally applied transverse moment. The maximum value of F_a for a particular operating condition is calculated from Eq. 3.23. In this equation some of the forces may be zero for a particular operating condition.

$$F_a = (F_k + F_c) + .7854 D_t^2 (p_k + p_c) + \frac{4}{D_t + t} (m_k + m_c) \quad (3.23)$$

For each critical operating condition F_a may be different and may require a separate calculation. This is also true for G_n , the pressure ($p = p_k + p_c$), and the temperature of the various connector parts. Having determined the nut spring constant, and the loads and temperatures for each critical operating condition the next step is to calculate M_3 for a unit preload ($F_p = 1$) for each operating condition. This requires the solution of the following set of simultaneous equations for each operating condition. The set of equations is written in a condensed form and the coefficients of the variables and constant terms, c_i , are written separately in Section 3.11.2.

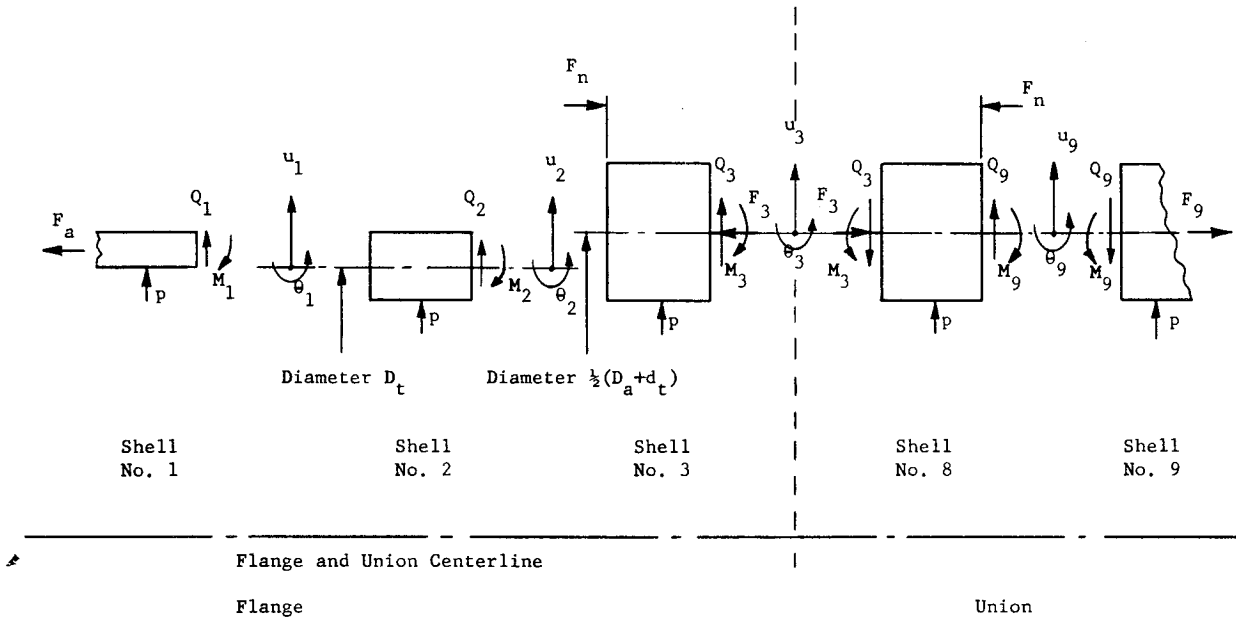


Figure 3.7. Separation of Flange and Union for Structural Analysis

$$C_{35}u_1 - C_{36}u_2 + C_{37}\theta_1 + C_{38}\theta_2 + C_{39}Q_1 + C_{40}Q_2 + C_{41}M_2 = C_{42} \quad (3.24)$$

$$C_{43}u_1 - C_{44}u_2 + C_{45}\theta_1 + C_{46}\theta_2 + C_{47}Q_2 + C_{48}M_1 + C_{49}M_2 = C_{50}$$

$$C_{44}u_1 - C_{43}u_2 + C_{46}\theta_1 + C_{45}\theta_2 + C_{51}Q_2 + C_{52}M_2 = C_{53}$$

$$C_{36}u_1 - C_{35}u_2 + C_{38}\theta_1 + C_{37}\theta_2 + C_{54}Q_2 + C_{55}M_2 = -C_{42}$$

$$u_1 + C_{56}Q_1 + C_{57}M_1 = C_{58}$$

$$C_{60}u_2 - C_{61}u_3 + C_{62}\theta_2 + C_{63}\theta_3 + C_{64}Q_2 + C_{65}F_n = C_{66}$$

$$C_{67}u_2 - C_{59}u_3 + C_{63}\theta_2 + C_{62}\theta_3 + C_{68}Q_3 - C_{65}F_n = C_{69}$$

$$C_{71}u_2 - C_{72}u_3 + C_{73}\theta_2 + C_{74}\theta_3 + C_{75}M_2 + C_{76}F_n = C_{77}$$

$$C_{78}u_2 - C_{70}u_3 + C_{74}\theta_2 + C_{73}\theta_3 + C_{79}M_3 + C_{80}F_n = C_{81}$$

$$C_{82}u_3 - C_{83}u_9 + C_{84}\theta_3 + C_{85}\theta_9 + C_{86}Q_3 + C_{87}F_n = C_{88}$$

$$C_{83}u_3 - C_{82}u_9 + C_{85}\theta_3 + C_{84}\theta_9 + C_{86}Q_9 - C_{87}F_n = -C_{88}$$

$$C_{89}u_3 - C_{90}u_9 + C_{91}\theta_3 + C_{92}\theta_9 + C_{93}M_3 + C_{94}F_n = C_{95}$$

$$C_{90}u_3 - C_{89}u_9 + C_{92}\theta_3 + C_{91}\theta_9 - C_{93}M_9 + C_{96}F_n = C_{97}$$

$$u_9 + C_{98}Q_9 + C_{99}M_9 = C_{100}$$

$$\theta_1 + C_{101}Q_1 + C_{102}M_1 = 0$$

$$\theta_9 - C_{99}Q_9 + C_{103}M_9 = 0$$

$$F_n = C_{104}$$

* Then F_3 is calculated from Eq. 3.25.

$$F_3 = C_{104} - F + \frac{\pi}{4} \left[D_t^2 - d_t^2 - \frac{1}{4} (D_g + d_g - 2d_t) (D_g + d_g + 2d_t) \right] p \quad (3.25)$$

After which, F_g is calculated using Eq. 3.22. The operating condition giving the smallest F_g , that is the smallest compressive force (it may be the largest tensile force), is the most critical operating condition. This is the condition which determines F_p .

M_3 is linearly related to F_p in the following manner.

$$M_3 = A_3 + A_4 F_p \quad (3.26)$$

By repeating the solution of Eqs. 3.24 and 3.25 for the most critical operating condition with $F_p = 0$, the constants A_1 and A_3 are determined.

$$A_1 = (F_3)_{F_p=0} \quad (3.27)$$

$$A_3 = (M_3)_{F_p=0}$$

From the previous calculation of M_3 where $F_p = 1$ the other constants are determined.

$$A_2 = (F_3)_{F_p=1} - A_1 \quad (3.28)$$

$$A_4 = (M_3)_{F_p=1} - A_3$$

Then substituting Eqs. 3.26 in Eq. 3.22 gives F_g as a function of only F_p .

$$F_g = \text{function}(F_p) \quad (3.29)$$

F_g is equal to F_s times a safety factor. Thus, with F_s and the safety factor known, the preload is determined by solving Eq. 3.29 for F_p .

3.8.3 Assembly Torque Calculation

The most common method of setting the preload at assembly is by torquing the nut to a specified torque value using a torque wrench. The accuracy of this method depends on the accuracy of the torque wrench, skill of the mechanic, and accurate knowledge of the friction factors. The torque required to obtain a given preload is calculated from Eq. 3.30 where f_t is the friction factor for the nut and union threads and f_n is the friction factor for the bearing surface between the nut and flange.

$$W = \frac{F_p}{2n} \left\{ .3183 + n f_n (d_n + W) + \frac{n^2 D_b^2 - 1.2n D_b + .4613}{\frac{n D_b - .6}{1.007 f_t} - .3183} \right\} \quad (3.30)$$

3.9 Stress Analysis

The preload was determined without any regard to the stresses in the connector. Therefore, the next step in the design procedure is a calculation of the stresses at the critical operating conditions. There is no assurance that the operating condition determining the preload will also result in the most severe stress condition and it is therefore necessary to consider each operating

condition which is suspected of causing an adverse stress condition. For each operating condition the deflections, rotations, forces and moments of the flange and union are calculated using Eq. 3.24, and the value of F_p previously determined. The calculation also gives the value of F_n for each operating condition. As the deflections, rotations, forces, and moments of the nut were calculated for a unit force F_n , as part of the spring constant calculation, it is possible to use these values in the stress calculations by simply multiplying them by the appropriate value of F_n . This assumes that the spring constant calculation was performed for every operating condition of interest. Otherwise the spring constant calculation is made for those operating conditions not previously considered.

Thus the maximum deflections, rotations, forces, and moments are known throughout the connector for each critical operating condition. It is noted that the maximum loading conditions have been used in the preceding calculations. In the calculation of F_a by Eq. 3.23, the maximum mean (or constant) load and the maximum amplitude of the cyclic load, for a particular operating condition, were added together. This method of calculation results in the determination of the peak stresses and the calculation is necessary for the static load analysis discussed in the next section. However, for the vibration analysis a separate mean value and cyclic amplitude of the total load, F_a , is necessary. Thus, a mean value of F_a and a cyclic value of F_a are calculated for each operating condition using Eq. 3.23. Again the deflections, rotations, forces, moments and F_n are calculated separately for the constant and cyclic load for each operating condition using Eq. 3.24. Then the results of the spring constant calculation are again used to obtain the deflections, rotations, forces, and moments for the nut for the constant and cyclic loadings separately.

In the following sections the static load and vibration analysis of the connector design are discussed. The stress formulas are for the static and cyclic stresses at various connector locations for one particular operating condition. After the stress calculations have been made for each critical operating condition, the operating condition resulting in the largest stresses is chosen. The connector design is then optimized using this operating condition as outlined in Section 3.9.3.

3.9.1 Static Stress Analysis

The static stress analysis is performed to prevent yielding of the connector during any operating condition (including the proof test), to prevent fracture during the burst test, and to reduce the connector weight to a minimum. Two failure criteria are used; one for yielding and one for fracture. For the yielding criteria, the shear distortion energy theory is most appropriate for this design procedure. Further, as the material properties are usually expressed as uniaxial stresses for yielding the effective stress, S , is chosen as the calculated parameter in applying the shear distortion energy theory. This effective stress can be compared directly with the uniaxial test data to determine whether yielding will occur. The effective stress, calculated for a triaxial stress field, is the uniaxial stress which would result in the same amount of shear distortion energy as would the triaxial stress field.

In the following sections of the static stress analysis the stress formulas given are for the effective stress at the critical connector locations.

The effective stresses calculated should be multiplied by a safety factor (equal to or larger than 1.1) before comparing them to the uniaxial yield strengths. It is also important to determine the temperature at the connector location under consideration and to use the proper values of the yield and fracture strength.

The complexity of the fracture strength calculation makes it impractical to carry it out. The nonlinearity of the stress-strain curve in the region between yielding and fracture is contrary to the basic assumption in the preceding analysis. A nonlinear analysis is too complex. Therefore, fracture is prevented by choosing a ductile material whose fracture strength is sufficiently larger than its yield strength to meet the design requirements.

3.9.1.1 Flange

Before proceeding with the stress calculations the deflections and rotations of the various parts of the connector are reviewed to see whether they are consistent with the proper functioning of the connector. After correcting any inconsistencies, the stresses are calculated using the following formulas. The subscript on the effective stress refers to the flange location of the stress. These locations are noted in Figure 3.8.

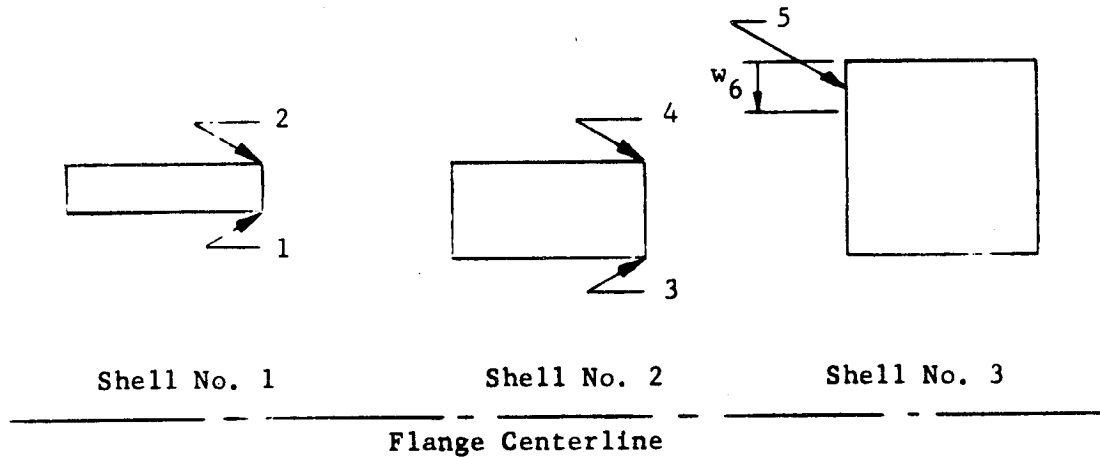


Figure 3.8 Location of Flange Stresses Calculated

The square of the effective stress is calculated because it is more convenient to present the stress formulas this way. The σ_h and σ_r are the hoop and radial thermal stresses respectively. These are only important during thermal transients and are calculated using the methods of Ref. 4.

Location 1

$$\begin{aligned}
 S_1^2 = & \left\{ \frac{1.414E_f}{D_t} u_1 - \frac{0.4502}{t(D_t + t)} F_a + \frac{8.486}{t^2} M_1 - 0.07778p + 0.7071 \sigma_h \right\}^2 \\
 + & \left\{ -\frac{1.273}{t^2} M_1 + \frac{1.414E_f}{D_t} u_1 + \frac{0.06751}{t(D_t + t)} F_a + 0.6293p + 0.7071 (\sigma_h - \sigma_r) \right\}^2 \\
 + & \left\{ \frac{0.5177}{t(D_t + t)} F_a - \frac{9.759}{t^2} M_1 + 0.7071p - 0.7071 \sigma_r \right\}^2 \quad (3.31)
 \end{aligned}$$

Location 2

$$\begin{aligned} S_2^2 = & \left\{ \frac{1.414E_f}{D_t} u_1 - \frac{0.1576}{t(D_t + t)} F_a - \frac{2.97}{t^2} M_1 - 0.07778p + 0.7071\sigma_h \right\}^2 \\ & + \left\{ \frac{1.273}{t^2} M_1 + \frac{1.414E_f}{D_t} u_1 + \frac{0.06751}{t(D_t + t)} F_a - 0.07778p + 0.7071 (\sigma_h - \sigma_r) \right\}^2 \\ & + \left\{ \frac{0.2251}{t(D_t + t)} F_a + \frac{4.243}{t^2} M_1 - 0.7071\sigma_r \right\}^2 \end{aligned} \quad (3.32)$$

Location 3

$$\begin{aligned} S_3^2 = & \left\{ \frac{1.414E_f}{D_t} u_2 - \frac{0.6302}{(D_t + 2t)^2 - d_t^2} F_a + \frac{11.88}{(D_t + 2t - d_t)^2} M_2 \right. \\ & \left. + 0.7071\sigma_h + \left[\frac{0.495(D_t^2 - d_t^2)}{(D_t + 2t)^2 - d_t^2} - 0.07778 \right] p \right\}^2 \\ & + \left\{ \frac{1.414E_f}{D_t} u_2 + \frac{0.2701}{(D_t + 2t)^2 - d_t^2} F_a + 0.7071 (\sigma_h - \sigma_r) - \frac{5.092}{(D_t + 2t - d_t)^2} M_2 \right. \\ & \left. + \left[0.6293 - \frac{0.2121 (D_t^2 - d_t^2)}{(D_t + 2t)^2 - d_t^2} \right] p \right\}^2 \\ & + \left\{ \frac{0.9003}{(D_t + 2t)^2 - d_t^2} F_a - \frac{16.97}{(D_t + 2t - d_t)^2} M_2 - 0.7071\sigma_r \right. \\ & \left. + \frac{2.828 t (D_t + t)}{(D_t + 2t)^2 - d_t^2} p \right\}^2 \end{aligned} \quad (3.33)$$

Location 4

$$\begin{aligned} S_4^2 = & \left\{ \frac{1.414E_f}{D_t} u_2 - \frac{1.224}{(D_t + 2t)^2 - d_t^2} F_a - \frac{23.08}{(D_t + 2t - d_t)^2} M_2 \right. \\ & \left. + 0.7071 \sigma_h + \left[\frac{0.9617(D_t^2 - d_t^2)}{(D_t + 2t)^2 - d_t^2} - 0.07778 \right] p \right\}^2 \\ & + \left\{ \frac{1.414E_f}{D_t} u_2 + \frac{0.2701}{(D_t + 2t)^2 - d_t^2} F_a + 0.7071 (\sigma_h - \sigma_r) \right\}^2 \end{aligned} \quad (3.34)$$

(continued)

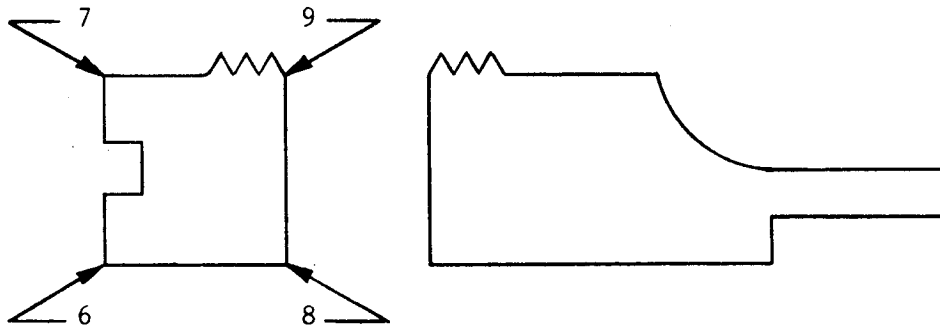
$$\begin{aligned}
& + \frac{5.092}{(D_t + 2t - d_t)^2} M_2 - \left[0.07778 + \frac{0.2121(D_t^2 - d_t^2)}{(D_t + 2t)^2 - d_t^2} \right] p \Bigg\}^2 \\
& + \left\{ \frac{1.494}{(D_t + 2t)^2 - d_t^2} F_a - \frac{1.174 (D_t^2 - d_t^2)}{(D_t + 2t)^2 - d_t^2} p + \frac{28.17}{(D_t + 2t - d_t)^2} M_2 \right. \\
& \quad \left. - 0.7071\sigma_r \right\}^2
\end{aligned} \tag{3.34}$$

Location 5

$$\begin{aligned}
S_5^2 & = \left\{ \frac{1.414E_f}{D_t} u_2 - \frac{0.1576}{w(D_f - w)} F_n - 0.07778 p + 0.7071\sigma_h \right\}^2 \\
& + \left\{ \frac{1.414E_f}{D_t} u_2 + \frac{0.06752}{w(D_f - w)} F_n - 0.07778 p + 0.7071 (\sigma_h - \sigma_r) \right\}^2 \\
& + \left\{ \frac{0.2251}{w (D_f - w)} F_n - 0.7071\sigma_r \right\}^2
\end{aligned} \tag{3.35}$$

3.9.1.2 Union

The locations of stresses calculated in the union are shown in Figure 3.9.



Shell No. 8

Union Centerline

Figure 3.9. Location of Union Stresses Calculated

The stresses at locations 6 and 7 depend on whether there is full contact between the flange face and the union face or whether there is separation of the faces at the inside diameter. The stress formulas assume full face contact. These formulas, when used with an appropriate safety factor, can be used for design calculations even when there is less than full face contact.

Location 6

$$\begin{aligned}
 S_6^2 = & \left\{ \frac{2.828E_u}{D_u + d_t} u_3 - \frac{0.2701}{D_u^2 - d_t^2} (F_n - F_a) + \frac{0.9003}{D_u^2 + d_g^2 - D_g^2 - d_t^2} F_3 \right. \\
 & + \frac{11.88 (D_u - d_t)}{(D_u - d_t)^3 - (D_g - d_g)^3} M_3 + \left. \left[0.6293 - \frac{0.2121(D_t^2 - d_t^2)}{D_u^2 - d_t^2} \right] p + 0.7071\sigma_h \right\}^2 \\
 & + \left\{ \frac{2.828E_u}{D_u + d_t} u_3 - \frac{0.2701}{D_u^2 - d_t^2} (F_n - F_a) + 0.7071 (\sigma_h - \sigma_r) \right. \\
 & - \frac{5.092 (D_u - d_t)}{(D_u - d_t)^3 - (D_g - d_g)^3} M_3 + \left. \left[0.6293 - \frac{0.2121 (D_t^2 - d_t^2)}{D_u^2 - d_t^2} \right] p \right\}^2 \\
 & + \left\{ \frac{0.9003}{D_u^2 + d_g^2 - D_g^2 - d_t^2} F_3 + \frac{16.97 (D_u - d_t)}{(D_u - d_t)^3 - (D_g - d_g)^3} M_3 + 0.7071\sigma_r \right\}^2 \quad (3.36)
 \end{aligned}$$

Location 7

$$\begin{aligned}
 S_7^2 = & \left\{ \frac{2.828E_u}{D_u + d_t} u_3 - \frac{0.2701}{D_u^2 - d_t^2} (F_n - F_a) + \frac{0.9003}{D_u^2 + d_g^2 - D_g^2 - d_t^2} F_3 \right. \\
 & - \frac{11.88 (D_u - d_t)}{(D_u - d_t)^3 - (D_g - d_g)^3} M_3 - \left. \left[0.07778 + \frac{0.2121(D_t^2 - d_t^2)}{D_u^2 - d_t^2} \right] p + 0.7071\sigma_h \right\}^2 \\
 & + \left\{ \frac{2.828E_u}{D_u + d_t} u_3 - \frac{0.2701}{D_u^2 - d_t^2} (F_n - F_a) + 0.7071 (\sigma_h - \sigma_r) \right. \\
 & + \frac{5.092 (D_u - d_t)}{(D_u - d_t)^3 - (D_g - d_g)^3} M_3 - \left. \left[0.07778 + \frac{0.2121 (D_t^2 - d_t^2)}{D_u^2 - d_t^2} \right] p \right\}^2 \\
 & + \left\{ \frac{0.9003}{D_u^2 + d_g^2 - D_g^2 - d_t^2} F_3 - \frac{16.97 (D_u - d_t)}{(D_u - d_t)^3 - (D_g - d_g)^3} M_3 + 0.7071\sigma_r \right\}^2 \quad (3.37)
 \end{aligned}$$

Location 8

$$\begin{aligned}
 S_8^2 = & \left\{ \frac{2.828E_u}{D_u + d_t} u_9 - \frac{0.6302}{(D_u^2 - d_t^2)} F_a + \frac{11.88}{(D_u - d_t)^2} M_9 + 0.7071\sigma_h \right. \\
 & + \frac{2.521 D_u + 1.261 d_t - 3.782D_b + \frac{2.269}{n}}{(D_u + d_t)(D_u - d_t)^2} F_n + \left[\frac{0.495(D_t^2 - d_t^2)}{D_u^2 - d_t^2} - 0.07778 \right] P \left. \right\}^2 \\
 & + \left\{ \frac{2.828E_u}{D_u + d_t} u_9 + \frac{0.2701}{D_u^2 - d_t^2} F_a + 0.7071(\sigma_h - \sigma_r) - \frac{5.092}{(D_u - d_t)^2} M_9 \right. \\
 & + \frac{1.621 D_b - \frac{0.9724}{n} - 1.081 D_u - 0.5403 d_t}{(D_u + d_t)(D_u - d_t)^2} F_n + \left[0.6293 - \frac{0.2121(D_t^2 - d_t^2)}{D_u^2 - d_t^2} \right] P \left. \right\}^2 \\
 & + \left\{ \frac{0.9003}{D_u^2 - d_t^2} F_a - \frac{16.97}{(D_u - d_t)^2} M_9 - 0.7071\sigma_r \right. \\
 & \left. + 0.7071 \frac{D_u^2 - D_t^2}{D_u^2 - d_t^2} P + \frac{5.402D_b - 3.601D_u - 1.801d_t - \frac{3.241}{n}}{(D_u + d_t)(D_u - d_t)^2} F_n \right\}^2 \quad (3.38)
 \end{aligned}$$

Location 9

$$\begin{aligned}
 S_9^2 = & \left\{ \frac{2.828E_u}{D_u + d_t} u_9 - \frac{1.531}{D_u^2 - d_t^2} F_a - \frac{28.85}{(D_u - d_t)^2} M_9 + 0.7071\sigma_h \right. \\
 & + \left[\frac{1.202(D_t^2 - d_t^2)}{D_u^2 - d_t^2} - 0.07778 \right] P \\
 & + \frac{9.183D_b - 3.061D_u - 6.122d_t - \frac{5.51}{n}}{(D_u + d_t)(D_u - d_t)^2} F_n \left. \right\}^2 \quad (3.39) \\
 & \text{(continued)}
 \end{aligned}$$

$$\begin{aligned}
& + \left\{ \frac{2.828E_u}{D_u + d_t} u_9 + \frac{0.2701}{D_u^2 - d_t^2} F_a + 0.7071 (\sigma_h - \sigma_r - \sigma_t) \right. \\
& - \left. \frac{1.621D_b - \frac{0.9724}{n} - 0.5402D_u - 1.08d_t}{(D_u + d_t)(D_u - d_t)^2} F_n - \left[.07778 + \frac{0.2121(D_t^2 - d_t^2)}{D_u^2 - d_t^2} \right] p + \frac{5.092}{(D_u - d_t)^2} M_9 \right\}^2 \\
& + \left\{ \frac{1.801}{(D_u^2 - d_t^2)^2} F_a - \frac{10.8D_b - 3.601D_u - 7.202d_t - \frac{6.482}{n}}{(D_u + d_t)(D_u - d_t)^2} F_n \right. \\
& + \left. \frac{33.94}{(D_u - d_t)^2} M_9 - \frac{1.414(D_t^2 - d_t^2)}{D_u^2 - d_t^2} p - 0.7071 (\sigma_r + \sigma_t) \right\}^2 \quad (3.39)
\end{aligned}$$

where the maximum bending stress in the thread, σ_t , is:

$$\sigma_t = \frac{1.053C_{105}F_n(1 - C_{106} + C_{106} \cosh C_{105})}{L_e(D_b - \frac{6}{n}) \sinh C_{105}} \quad (3.40)$$

and C_{105} and C_{106} are given in Section 3.11.3.

3.9.1.3 Nut

The locations of stresses calculated in the nut are shown in Figure 3.10.

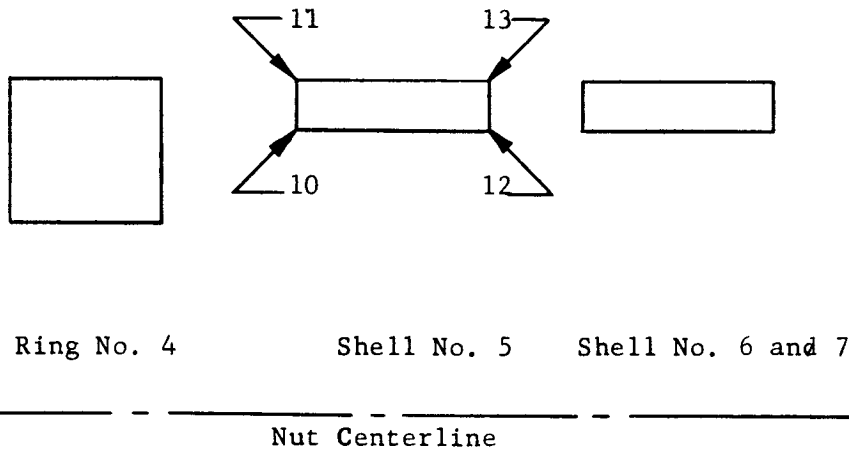


Figure 3.10. Location of Nut Stresses Calculated

Location 10

$$\begin{aligned} S_{10}^2 = & \left\{ \frac{2.828E_n}{D_n + d_s} u_5 - \frac{1.278}{D_n^2 - d_s^2} F_n + \frac{24.1}{(D_n - d_s)^2} M_4 + 0.7071\sigma_h \right\}^2 \\ & + \left\{ -\frac{5.092}{(D_n + d_s)^2} M_4 + \frac{2.828E_n}{D_n + d_s} u_5 + \frac{0.2701}{D_n^2 - d_s^2} F_n + 0.7071(\sigma_h - \sigma_r) \right\}^2 \\ & + \left\{ \frac{1.549}{D_n^2 - d_s^2} F_n - \frac{29.19}{(D_n - d_s)^2} M_4 - 0.7071\sigma_r \right\}^2 \end{aligned} \quad (3.41)$$

Location 11

$$\begin{aligned} S_{11}^2 = & \left\{ \frac{2.828E_n}{D_n + d_s} u_5 - \frac{0.6302}{D_n^2 - d_s^2} F_n - \frac{11.88}{(D_n - d_s)^2} M_4 + 0.7071\sigma_h \right\}^2 \\ & + \left\{ \frac{5.092}{(D_n - d_s)^2} M_4 + \frac{2.828E_n}{D_n + d_s} u_5 + \frac{0.2701}{D_n^2 - d_s^2} F_n + 0.7071(\sigma_h - \sigma_r) \right\}^2 \\ & + \left\{ \frac{0.9003}{D_n^2 - d_s^2} F_n + \frac{16.97}{(D_n - d_s)^2} M_4 - 0.7071\sigma_r \right\}^2 \end{aligned} \quad (3.42)$$

Location 12

$$\begin{aligned} S_{12}^2 = & \left\{ \frac{2.828E_n}{D_n + d_s} u_6 - \frac{1.531}{D_n^2 - d_s^2} F_n + \frac{28.85}{(D_n - d_s)^2} M_5 + 0.7071\sigma_h \right\}^2 \\ & + \left\{ -\frac{5.092}{(D_n - d_s)^2} M_5 + \frac{2.828E_n}{D_n + d_s} u_6 + \frac{0.2701}{D_n^2 - d_s^2} F_n + 0.7071(\sigma_h - \sigma_t - \sigma_r) \right\}^2 \\ & + \left\{ \frac{1.801}{D_n^2 - d_s^2} F_n - \frac{33.94}{(D_n - d_s)^2} M_5 - 0.7071(\sigma_t + \sigma_r) \right\}^2 \end{aligned} \quad (3.43)$$

where σ_t is given by Eq. 3.40.

Location 13

$$\begin{aligned}
 S_{13}^2 = & \left\{ \frac{2.828E_n}{D_n + d_s} u_6 - \frac{0.6302}{D_n^2 - d_s^2} F_n - \frac{11.88}{(D_n - d_s)^2} M_5 + 0.7071\sigma_h \right\}^2 \\
 & + \left\{ \frac{5.092}{(D_n - d_s)^2} M_5 + \frac{2.828E_n}{D_n + d_s} u_6 + \frac{0.2701}{D_n^2 - d_s^2} F_n + 0.7071(\sigma_h - \sigma_r) \right\}^2 \\
 & + \left\{ \frac{0.9003}{D_n^2 - d_s^2} F_n + \frac{16.97}{(D_n - d_s)^2} M_5 - 0.7071\sigma_r \right\}^2
 \end{aligned} \tag{3.44}$$

3.9.1.4 Assembly Stresses

During assembly there are usually only two static loads, the axial preload, F_p , and the torque, W . The connector stresses due to the preload are calculated in the same manner as the stresses for any operating condition. The major differences are that F_a and p are zero.

However, the stresses due to the applied torque on the nut and union are calculated separately. The stress in the length L_f of the union (See Figure 3.4) is:

$$\begin{aligned}
 S_{14} = & \frac{0.2676W(D_a + 20.42d_t)}{L_f D_a (D_a - d_t)^2} \left\{ 1 - e^{-\frac{1.914L_f}{(D_a + d_t)^{3/4}}} \cos \left[\frac{1.914L_f}{(D_a + d_t)^{3/4}} \right] \right\} \\
 & + \frac{24M_g}{(D_a - d_t)^2}
 \end{aligned} \tag{3.45}$$

The effective stresses in the nut due to F_p and W can be calculated using the formulas of Section 3.9.1.3. The required values of σ_n in S_{10} and S_{11} can be gained from Eqs. 3.46 and 3.47. Normally there are no thermal stresses during assembly (σ_h and $\sigma_r = 0$); but even if there are, these can be added to the stresses calculated below.

$$(\sigma_h)_{10} = - \frac{1.635 W (D_n + d_s)}{D_n (L_a - L_n) (D_n - d_s)^2} \frac{1}{1 + \frac{L_n (D_n - d_n)^3 (D_n + d_s)^3}{(L_a - L_n) (D_n - d_s)^3 (D_n + d_n)^3}} \tag{3.46}$$

$$(\sigma_h)_{11} = - (\sigma_h)_{10} \tag{3.47}$$

If S_{14} is too large compared to the yield strength, D_a is increased to the next standard wrench size and S_{14} is again calculated. Likewise, if the nut stresses are too large, D_n is increased to the next standard wrench size and the stresses are calculated again.

3.9.2 Fatigue Analysis

The fatigue analysis also depends on the use of the effective stress in order to use the fatigue data from uniaxially loaded specimens as a criterion for the triaxially loaded connector. However, the effective stress calculations are done in two parts. First the effective stress due to the constant (or mean) axial force and pressure, S_k , is calculated. Then the effective stress due to the amplitude of the cyclical axial force and pressure, S_c , is calculated. These calculations are readily done using the formulas of the preceding section.

Thus, for each stress location, an equivalent fatigue stress is calculated using Eq. 3.48. All of the stresses refer to only

$$S_f = \frac{S_c}{1 - \frac{S_k}{S_u}} \quad (3.48)$$

one stress location and S_c and S_k were both calculated using the same formula from the preceding section. The equivalent fatigue stress is then compared to the fatigue strength, S_n , for the number of fatigue cycles, N , desired. A factor of safety of 1.1 or larger is applied to S_f .

$$H_f S_f \leq S_n \quad (3.49)$$

S_f must satisfy Eq. 3.49

3.9.3 Connector Modifications

In order to choose the most severe operating condition the stresses calculated in the previous sections are tabulated in the manner shown below for each operating condition.

Table 3.2

FORMAT FOR COMPILATION OF STRESS CALCULATIONS

Operating Condition _____								
(1) Stress Location	(2) S_m	(3) S_f	(4) H_m	(5) H_f	(6) S_y	(7) S_n	(8) $\frac{H S_m}{m m y}$	(9) $\frac{H S_f}{f f n}$
1								
2								
3								
4								
.								
.								
.								

Table 3.3. Format for Optimization of Connector Design for Most Severe Operating Condition

(1) <u>Stress Location</u>	(2) <u>S_m</u>	(3) <u>S_f</u>	(4) <u>H_m</u>	(5) <u>H_f</u>	(6) <u>S_y</u>	(7) <u>S_n</u>	(8) <u>H_mS_m/S_y</u>	(9) <u>H_fS_f/S_n</u>	<u>Recommended Changes in Parameters to Change Stresses. Prime Denotes New Dimension.</u>
1									$t' = [(8) \text{ or } (9)]^{2/3} t \text{ or } L'_h = [(8) \text{ or } (9)] L_h$
2									$t' = [(8) \text{ or } (9)]^{2/3} t \text{ or } L'_h = [(8) \text{ or } (9)] L_h$
3									$(D'_t - d_t + 2t') = [(8) \text{ or } (9)]^{2/3} (D_t - d_t + 2t) \text{ or } L'_h = [(8) \text{ or } (9)] L_h$
4									$(D'_t - d_t + 2t') = [(8) \text{ or } (9)]^{2/3} (D_t - d_t + 2t) \text{ or } L'_h = [(8) \text{ or } (9)] L_h$
5									$w' = [(8) \text{ or } (9)] w$
6									$(D'_u - d_t) = [(8) \text{ or } (9)]^{2/3} (D_u - d_t) \text{ or } L'_u = [(8) \text{ or } (9)] L_u$
7									$(D'_u - d_t) = [(8) \text{ or } (9)]^{2/3} (D_u - d_t) \text{ or } L'_u = [(8) \text{ or } (9)] L_u$
8									$(D'_u - d_t) = [(8) \text{ or } (9)]^{2/3} (D_u - d_t)$
9									$(D'_u - d_t) = [(8) \text{ or } (9)]^{2/3} (D_u - d_t)$
10									$(D'_n - d_s) = [(8) \text{ or } (9)]^{2/3} (D_n - d_s) \text{ or } L'_n = [(8) \text{ or } (9)]^{1/2} L_n$
11									$(D'_n - d_s) = [(8) \text{ or } (9)]^{2/3} (D_n - d_s) \text{ or } L'_n = [(8) \text{ or } (9)]^{1/2} L_n$
12									$(D'_n - d_s) = [(8) \text{ or } (9)]^{2/3} (D_n - d_s)$
13									$(D'_n - d_s) = [(8) \text{ or } (9)]^{2/3} (D_n - d_s)$

From this tabulation the most severe operating condition is chosen by choosing the condition which has the largest value in Column 8 or 9 of Table 3.3. The connector design is then optimized for this operating condition as discussed in the remainder of this Section. Once this optimization is complete, another check is made (by a table such as Table 3.2, if necessary) to make sure that the chosen operating condition is still the most severe. If another operating condition is the most severe, the optimizing procedure is repeated.

The table is expanded for the most severe condition to include the calculation of the dimensional parameters to be changed in order to optimize the design, see Table 3.3. In Table 3.3 the largest value in Column 8 or 9 is checked in the following inequality.

$$0.9 \leq [(8) \text{ or } (9)] \leq 1.0 \quad (3.50)$$

If the inequality is not satisfied, the parameter recommended in the table is changed. Then the second largest value in Column 8 or 9 is checked in Eq. 3.50. If this does not satisfy the inequality, the parameter recommended in the table is changed, but only if it was not changed in the previous step. The procedure is continued with the third largest value of Column 8 or 9, the fourth largest and on till all values have been considered. Then the preload and stress calculations are repeated, the most severe operating condition is selected and the changes in parameters are again calculated. This procedure is continued until the largest algebraic stresses of the most severe operating condition satisfy Eq. 3.50.

3.10 Testing

Each new connector design is tested. The extent of the testing is determined by the design requirements and past experience with similar designs. The testing serves a twofold purpose: prove the new design meets all the specifications and gain experience for future designs. The type of tests depends upon the design, and care is necessary to be certain that the operating conditions are duplicated and accurate measurements are taken.

3.11 Appendix

3.11.1 Coefficients for the nut spring constant calculation

The values for the K_s are given in Section 3.11.4.

$$C_1 = L_n / 2$$

$$C_2 = - \frac{D_n \left[.0875(D_n + d_s)^2 + .65 d_n^2 \right]}{L_n E_n (D_n^2 - d_n^2)}$$

$$C_3 = K_5 \text{ where } \begin{aligned} h &= 1/2 (D_n - d_s) \\ \ell &= L_s + L_t - .72 L_e \\ r &= 1/4 (D_n + d_s) \end{aligned}$$

$$C_4 = K_6 \text{ where } (h, \ell, r)_4 = (h, \ell, r)_3$$

$$C_5 = K_1 (L_s + L_t - 0.72L_e) \text{ where } (h, l, r)_5 = (h, l, r)_3$$

$$C_6 = K_2 (L_s + L_t - 0.72L_e) \text{ where } (h, l, r)_6 = (h, l, r)_3$$

$$C_7 = \frac{87.36 (L_s + L_t - 0.72L_e)^3}{E_n (D_n - d_s)^3}$$

$$C_8 = \frac{0.09549 (C_4 - C_3)}{E_n (D_n - d_s)}$$

$$C_9 = K_3 (L_s + L_t - 0.72L_e)^2 \text{ where } (h, l, r)_9 = (h, l, r)_3$$

$$C_{10} = K_4 (L_s + L_t - 0.72L_e)^2 \text{ where } (h, l, r)_{10} = (h, l, r)_3$$

$$C_{11} = \frac{0.09549 (C_5 - C_6)}{E_n (D_n - d_s)}$$

$$C_{12} = K_5 \text{ where } h = 1/2 (D_n - d_s)$$

$$l = 0.55 L_e$$

$$r = 1/4 (D_n + d_s)$$

$$C_{13} = K_6 \text{ where } (h, l, r)_{13} = (h, l, r)_{12}$$

$$C_{14} = 0.55L_e K_1 \text{ where } (h, l, r)_{14} = (h, l, r)_{12}$$

$$C_{15} = 0.55L_e K_2 \text{ where } (h, l, r)_{15} = (h, l, r)_{12}$$

$$C_{16} = \frac{14.53L_e^3}{E_n (D_n - d_s)^3}$$

$$C_{17} = \frac{0.04775 (C_{13} - C_{12})}{E_n (D_n - d_s)}$$

$$C_{18} = 0.3025 L_e^2 K_3 \text{ where } (h, l, r)_{18} = (h, l, r)_{12}$$

$$C_{19} = 0.3025 L_e^2 K_4 \text{ where } (h, l, r)_{19} = (h, l, r)_{12}$$

$$C_{20} = \frac{0.04775 (C_{14} - C_{15})}{E_n (D_n - d_s)}$$

$$C_{21} = 0.17 L_e K_2 \quad \text{where } h = 1/2 (D_n - d_s)$$

$$\ell = 0.17 L_e$$

$$r = 1/4 (D_n + d_s)$$

$$C_{22} = 0.17 L_e K_1 \quad \text{where } (h, \ell, r)_{22} = (h, \ell, r)_{21}$$

$$C_{23} = 0.0289 L_e^2 K_4 \quad \text{where } (h, \ell, r)_{23} = (h, \ell, r)_{21}$$

$$C_{24} = 0.0289 L_e^2 K_3 \quad \text{where } (h, \ell, r)_{24} = (h, \ell, r)_{21}$$

$$C_{25} = K_6 \quad \text{where } (h, \ell, r)_{25} = (h, \ell, r)_{21}$$

$$C_{26} = K_5 \quad \text{where } (h, \ell, r)_{26} = (h, \ell, r)_{21}$$

$$C_{27} = \frac{0.4292 L_e^3}{E_n (D_n - d_s)^3}$$

$$C_{28} = \frac{2.08}{E_n (2D_n - 2d_s + 3R_n)}$$

$$C_{29} = - \frac{77.26}{E_n (2D_n - 2d_s + 3R_n)^2}$$

$$C_{30} = - \frac{2}{3} \frac{E_n L_n^3 (D_n - d_n)}{(D_n + d_n)}$$

$$C_{31} = 1/2 L_n (D_n + d_s)$$

$$C_{32} = - (D_n + d_s)$$

$$C_{33} = 0.15915 (d_s + D_n - 2d_n - 2w)$$

$$C_{34} = - \frac{0.07958}{D_n + d_s} (D_n + d_s - 2D_b + \frac{1.2}{n})$$

3.11.2 Coefficients for F₃ and M₃ Calculation

$$C_{35} = K_5 \frac{(D_t + d_t + 2t)}{2D_t} \quad \text{where } h = 1/2 (D_t - d_t + 2t)$$

$$l = L_h$$

$$r = 1/4 (D_t + d_t + 2t)$$

$$C_{36} = K_6 \frac{(D_t + d_t + 2t)}{2D_t} \quad \text{where } (h, l, r)_{36} = (h, l, r)_{35}$$

$$C_{37} = K_1 L_h \quad \text{where } (h, l, r)_{37} = (h, l, r)_{35}$$

$$C_{38} = K_2 L_h \quad \text{where } (h, l, r)_{38} = (h, l, r)_{35}$$

$$C_{39} = \frac{174.7 L_h^3 (D_t + t)}{E_f (D_t - d_t + 2t)^3 (D_t + d_t + 2t)}$$

$$C_{40} = \frac{1.04 C_{38}}{E_f (D_t - d_t + 3.5t)}$$

$$C_{41} = \frac{19.31 C_{38}}{E_f (D_t - d_t + 3.5t)^2}$$

$$C_{42} = \frac{d_t^2 (C_{35} - C_{36}) (D_t^2 + 2.6tD_t + 2.6t^2)}{D_t E_f [(D_t + 2t)^2 - d_t^2]} P$$

$$- \frac{0.191 (C_{35} - C_{36}) D_t}{E_f [(D_t + 2t)^2 - d_t^2]} [F_a - .7854p (D_t^2 - d_t^2)]$$

$$C_{43} = K_1 \frac{(D_t + d_t + 2t)}{2D_t} \quad \text{where } (h, l, r)_{43} = (h, l, r)_{35}$$

$$C_{44} = K_2 \frac{(D_t + d_t + 2t)}{2D_t} \quad \text{where } (h, l, r)_{44} = (h, l, r)_{35}$$

$$C_{45} = K_3 L_h \quad \text{where } (h, l, r)_{45} = (h, l, r)_{35}$$

$$C_{46} = K_4 L_h \text{ where } (h, l, r)_{46} = (h, l, r)_{35}$$

$$C_{47} = \frac{1.04 C_{46}}{E_f (D_t - d_t + 3.5t)}$$

$$C_{48} = - \frac{174.7 L_h^2 (D_t + t)}{E_f (D_t - d_t + 2t)^3 (D_t + d_t + 2t)}$$

$$C_{49} = \frac{19.31 C_{46}}{E_f (D_t - d_t + 3.5t)^2}$$

$$C_{50} = \frac{13.9 L_h^2 (D_t - d_t)}{E_f (D_t - d_t + 2t)^3 (D_t + d_t + 2t)} F_a$$

$$+ \frac{p}{E_f [(D_t + 2t)^2 - d_t^2]} \left[\frac{21.84t L_h^2 (D_t^2 - d_t^2)}{(D_t - d_t + 2t)^2} + \frac{d_t^2}{D_t} (D_t^2 + 2.6tD_t + 2.6t^2) (C_{43} - C_{44}) \right]$$

$$- \frac{0.191 D_t (C_{43} - C_{44})}{E_f [(D_t + 2t)^2 - d_t^2]} \left[F_a - .7854p (D_t^2 - d_t^2) \right]$$

$$C_{51} = \frac{1.04 C_{45}}{E_f (D_t - d_t + 3.5t)}$$

$$C_{52} = \frac{1}{E_f} \left[\frac{87.36 L_h^2}{(D_t - d_t + 2t)^3} + \frac{19.31 C_{45}}{(D_t - d_t + 3.5t)^2} \right]$$

$$C_{53} = \frac{d_t^2 (C_{44} - C_{43}) (D_t^2 + 2.6tD_t + 2.6t^2)}{D_t E_f [(D_t + 2t)^2 - d_t^2]} p$$

$$- \frac{0.191 (C_{44} - C_{43}) D_t}{E_f [(D_t + 2t)^2 - d_t^2]} \left[F_a - .7854p (D_t^2 - d_t^2) \right]$$

$$C_{54} = \frac{1}{E_f} \left[\frac{87.36 L_h^3}{(D_t - d_t + 2t)^3} + \frac{1.04 C_{37}}{(D_t - d_t + 3.5t)} \right]$$

$$C_{55} = \frac{19.31 C_{37}}{E_f (D_t - d_t + 3.5t)^2}$$

$$C_{56} = - \frac{0.0988 D_t}{E_f t} \sqrt{\frac{D_t + 2.18t}{t}}$$

$$C_{57} = \frac{1.652 D_t}{E_f t^2}$$

$$C_{58} = - \frac{0.04775 D_t}{t E_f (D_t + t)} F_a + \frac{D_t (D_t^2 + 2.6t D_t + 2.6t^2)}{4t E_f (D_t + t)} P$$

$$C_{59} = K_5 \text{ where } h = 1/2 (D_u - d_t)$$

$$l = L_r$$

$$r = 1/4 (D_u + d_t)$$

$$C_{60} = \frac{D_u + d_t}{2D_t} C_{59}$$

$$C_{61} = K_6 \text{ where } (h, l, r)_{61} = (h, l, r)_{59}$$

$$C_{62} = K_1 L_r \text{ where } (h, l, r)_{62} = (h, l, r)_{59}$$

$$C_{63} = K_2 L_r \text{ where } (h, l, r)_{63} = (h, l, r)_{59}$$

$$C_{64} = \frac{87.36 L_r^3 (D_t + d_t + 2t)}{E_f (D_u - d_t)^3 (D_u + d_t)}$$

$$C_{65} = \frac{0.09549 (C_{61} - C_{59})}{E_f (D_u - d_t)}$$

$$C_{66} = C_{65} \left[F_a - .7854p (D_t^2 - d_t^2) \right] + \frac{d_t^2 p}{E_f (D_u - d_t)} \left\{ C_{59} \left(0.175 + 0.325 \frac{D_u^2}{D_t^2} \right) - C_{61} \left[0.175 + \frac{1.3 D_u^2}{(D_u + d_t)^2} \right] \right\}$$

$$C_{67} = \frac{D_u + d_t}{2D_t} C_{61}$$

$$C_{68} = \frac{87.36 L_r^3}{E_f (D_u - d_t)^3}$$

$$C_{69} = - C_{65} \left[F_a - 0.7854p (D_t^2 - d_t^2) \right] + \frac{d_t^2 p}{E_f (D_u - d_t)} \left\{ C_{61} \left(0.175 + 0.325 \frac{D_u^2}{D_t^2} \right) - C_{59} \left[0.175 + \frac{1.3 D_u^2}{(D_u + d_t)^2} \right] \right\}$$

$$C_{70} = K_1 \text{ where } (h, \ell, r)_{70} = (h, \ell, r)_{59}$$

$$C_{71} = \frac{D_u + d_t}{2D_t} C_{70}$$

$$C_{72} = K_2 \text{ where } (h, \ell, r)_{72} = (h, \ell, r)_{59}$$

$$C_{73} = K_3 L_r \text{ where } (h, \ell, r)_{73} = (h, \ell, r)_{59}$$

$$C_{74} = K_4 L_r \text{ where } (h, \ell, r)_{74} = (h, \ell, r)_{59}$$

$$C_{75} = - \frac{1}{L_r} C_{64}$$

$$C_{76} = - \frac{1}{E_f (D_u - d_t)} \left\{ 0.09549 (C_{70} - C_{72}) - \frac{13.9 L_r^2 (2D_f - 2w - D_u - d_t)}{(D_u - d_t)^2 (D_u + d_t)} \right\}$$

$$C_{77} = - \left\{ 0.09549 (C_{70} - C_{72}) + \frac{13.9 L_r^2 (D_u - D_t - 2t)}{(D_u - d_t)^2 (D_u + d_t)} \right\} \frac{[F_a - 0.7854p(D_t^2 - d_t^2)]}{E_f (D_u - d_t)} - \frac{d_t^2 p}{E_f (D_u - d_t)} \left\{ C_{72} \left[0.175 + \frac{1.3 D_u^2}{(D_u + d_t)^2} \right] - C_{70} \left[0.175 + 0.325 \frac{D_u^2}{D_t^2} \right] \right\}$$

$$C_{78} = \frac{D_u + d_t}{2 D_t} C_{72}$$

$$C_{79} = \frac{C_{68}}{L_r}$$

$$C_{80} = \frac{0.09549 (C_{70} - C_{72})}{E_f (D_u - d_t)}$$

$$C_{81} = C_{80} \left[F_a - 0.7854p (D_t^2 - d_t^2) \right] + \frac{d_t^2 p}{E_f (D_u - d_t)} \left\{ C_{72} \left(0.175 + .325 \frac{D_u^2}{D_t^2} \right) - C_{70} \left[0.175 + \frac{1.3 D_u^2}{(D_u + d_t)^2} \right] \right\} + \frac{1.365 L_r^2 p}{E_f (D_u - d_t)^3 (D_u + d_t)} (D_g + d_g + 2d_t) (D_g + d_g - 2d_t) (D_g + d_g - 2D_u)$$

$$C_{82} = K_5 \text{ where } h = 1/2 (D_u - d_t) \\ l = L_u + .56 L_e \\ r = 1/4 (D_u + d_t)$$

$$C_{83} = K_6 \text{ where } (h, l, r)_{83} = (h, l, r)_{82}$$

$$C_{84} = K_1 (L_u + 0.56 L_e) \text{ where } (h, l, r)_{84} = (h, l, r)_{82}$$

$$C_{85} = K_2 (L_u + 0.56 L_e) \text{ where } (h, l, r)_{85} = (h, l, r)_{82}$$

$$C_{86} = \frac{87.36 (L_u + 0.56 L_e)^3}{E_u (D_u - d_t)^3}$$

$$C_{87} = \frac{0.09549 (C_{82} - C_{83})}{E_u (D_u - d_t)}$$

$$C_{88} = C_{87} \left[F_a - 0.7854p (D_t^2 - d_t^2) \right] + \frac{(C_{82} - C_{83}) d_t^2}{E_u (D_u - d_t)} \left[0.175 + \frac{1.3 D_u^2}{(D_u + d_t)^2} \right] p$$

$$C_{89} = K_1 \text{ where } (h, l, r)_{89} = (h, l, r)_{82}$$

$$C_{90} = K_2 \text{ where } (h, l, r)_{90} = (h, l, r)_{82}$$

$$C_{91} = K_3 (L_u + 0.56 L_e) \text{ where } (h, l, r)_{91} = (h, l, r)_{82}$$

$$C_{92} = K_4 (L_u + 0.56 L_e) \text{ where } (h, l, r)_{92} = (h, l, r)_{82}$$

$$C_{93} = - \frac{C_{86}}{L_u + 0.56 L_e}$$

$$C_{94} = - \frac{0.09549 (C_{89} - C_{90})}{E_u (D_u - d_t)}$$

$$C_{95} = C_{94} \left[F_a - 0.7854p (D_t^2 - d_t^2) \right] - \left\{ \frac{1.365 (L_u + 0.56 L_e)^2}{(D_u + d_t) (D_u - d_t)^2} (D_g + d_g - 2d_t) (D_g + d_g + 2d_t) (D_g + d_g - 2D_u) - (C_{89} - C_{90}) d_t^2 \left[0.175 + \frac{1.3 D_u^2}{(D_u + d_t)^2} \right] \right\} \frac{p}{E_u (D_u - d_t)}$$

$$C_{96} = \frac{1}{E_u (D_u - d_t)} \left[0.09549 (C_{89} - C_{90}) - \frac{13.9 (L_u + 0.56 L_e)^2 (2D_b - \frac{1.2}{n} - D_u - d_t)}{(D_u - d_t)^2 (D_u + d_t)} \right]$$

$$C_{97} = - C_{94} \left[F_a - 0.7854p (D_t^2 - d_t^2) \right] - \frac{(C_{89} - C_{90}) d_t^2}{E_u (D_u - d_t)} \left[0.175 + \frac{1.3 D_u^2}{(D_u + d_t)^2} \right] p$$

$$C_{98} = \frac{0.909 (D_u + d_t)}{E_u (D_u - d_t)} \sqrt{\frac{2.18 D_u - 0.18d_t}{D_u - d_t}}$$

$$C_{99} = \frac{3.305 (D_u + d_t)}{E_u (D_u - d_t)^2}$$

$$C_{100} = - \frac{0.09549}{E_u (D_u - d_t)} \left[F_a - 0.7854p (D_t^2 - d_t^2) \right] \\ + \frac{d_t^2}{E_u (D_u - d_t)} \left[0.175 + \frac{1.3 D_u^2}{(D_u + d_t)^2} \right] p$$

$$C_{101} = - \frac{1.652 (D_t + t)}{E_f t^2}$$

$$C_{102} = \frac{6.006}{E_f t^2} \sqrt{\frac{D_t + 2.18t}{t}}$$

$$C_{103} = - \frac{24.03}{E_u (D_u - d_t)^2} \sqrt{\frac{2.18 D_u - 0.18 d_t}{D_u - d_t}}$$

$$C_{104} = F_p + \frac{G_n G_u}{G_n + G_u} \left[a_f L_r (T_f - T_r) \right.$$

$$\left. + a_u (L_u + 0.56 L_e) (T_u - T_r) - a_n (L_r + L_u + 0.56 L_e) (T_n - T_r) \right]$$

$$+ \frac{G_n}{G_n + G_u} \left[F_a - 0.7854 (D_t^2 - d_t^2) p \right]$$

$$- \frac{G_n G_u}{G_n + G_u} \left[\frac{0.6 d_t^2}{D_u^2 - d_t^2} \left(\frac{L_r}{E_f} + \frac{L_u + 0.56 L_e}{E_u} \right) \right] p$$

where

$$\frac{1}{G_u} = \frac{1.2732 L_g}{E_u (D_u^2 - d_t^2 + d_g^2 - D_g^2)} + \frac{1.2732 L_r}{E_f (D_u^2 - d_t^2)} \\ + \frac{1.2732 (L_u + 0.56 L_e - L_g)}{E_u (D_u^2 - d_t^2)}$$

3.11.3 Miscellaneous Coefficients

$$C_{105} = \frac{1.079 L_e}{\sqrt{\left(\frac{D_b - 0.6}{n}\right) \left\{ \frac{\left[D_n^2 - \left(D_b - \frac{0.6}{n} \right)^2 \right] \left[\left(D_b - \frac{0.6}{n} \right)^2 - d_t^2 \right]}{\left[D_b - \frac{0.6}{n} \right]^2 \left[D_n^2 - d_t^2 \right]} - .02145 \right\}}}$$

$$C_{106} = \frac{\left(D_b - \frac{1.3}{n} \right)^2 - d_t^2}{D_n^2 - d_t^2 - \frac{2.94 D_b}{n} + \frac{1.661}{n^2}}$$

3.11.4 Constants (K_1) for Shell Equations

The constants are used for a number of shells in the analysis. Therefore the nomenclature in this section is kept general.

let

- l = Axial length of shell
- r = Radius of midplane of shell
- h = Thickness of shell
- β = Shell constant
- g = Groupings of terms

$$g_1 = 0.59 \frac{h}{r}$$

$$\beta = \sqrt{\frac{1.65227}{rh}}$$

$$g_2 = \beta \sqrt{1 + g_1}$$

$$g_3 = \beta \sqrt{1 - g_1}$$

$$g_4 = \sinh g_2 l$$

$$g_5 = \cosh g_2 l$$

$$g_6 = \sin g_3 l$$

$$g_7 = \cos g_3 l$$

$$g_8 = g_4^2 g_3^2 (1 + 2g_1)^2 - g_6^2 g_2^2 (1 - 2g_1)^2$$

$$K_1 = \frac{5.6 g_1 l^2}{g_8 h^2} \left[g_4^2 g_3^2 (1 + 2g_1) + g_6^2 g_2^2 (1 - 2g_1) \right]$$

$$K_2 = \frac{11.2 g_1 g_2 g_3 g_4 g_6 \ell^2}{h^2 g_8}$$

$$K_3 = \frac{2g_2 \ell}{g_4 g_8 (1 + 2g_1)} \left\{ g_5 g_8 - g_6 g_2 (1 - 2g_1) [g_4 g_7 g_3 (1 + 2g_1) - g_5 g_6 g_2 (1 - 2g_1)] \right\}$$

$$K_4 = \frac{2g_2 g_3 \ell}{g_8} [g_5 g_6 g_2 (1 - 2g_1) - g_4 g_7 g_3 (1 + 2g_1)]$$

$$K_5 = \frac{11.2 g_1 g_2 g_3 \ell^3}{g_8 h^2} [g_4 g_5 g_3 (1 + 2g_1) + g_6 g_7 g_2 (1 - 2g_1)]$$

$$K_6 = \frac{11.2 g_1 g_2 g_3 \ell^3}{g_8 h^2} [g_4 g_7 g_3 (1 + 2g_1) + g_5 g_6 g_2 (1 - 2g_1)]$$

The K_i can be calculated from the above equations or taken from the following curves (Figures 3.11 through 3.16). In most cases the K_i are calculated to a number of significant digits in order to maintain a reasonable amount of accuracy in the calculations.

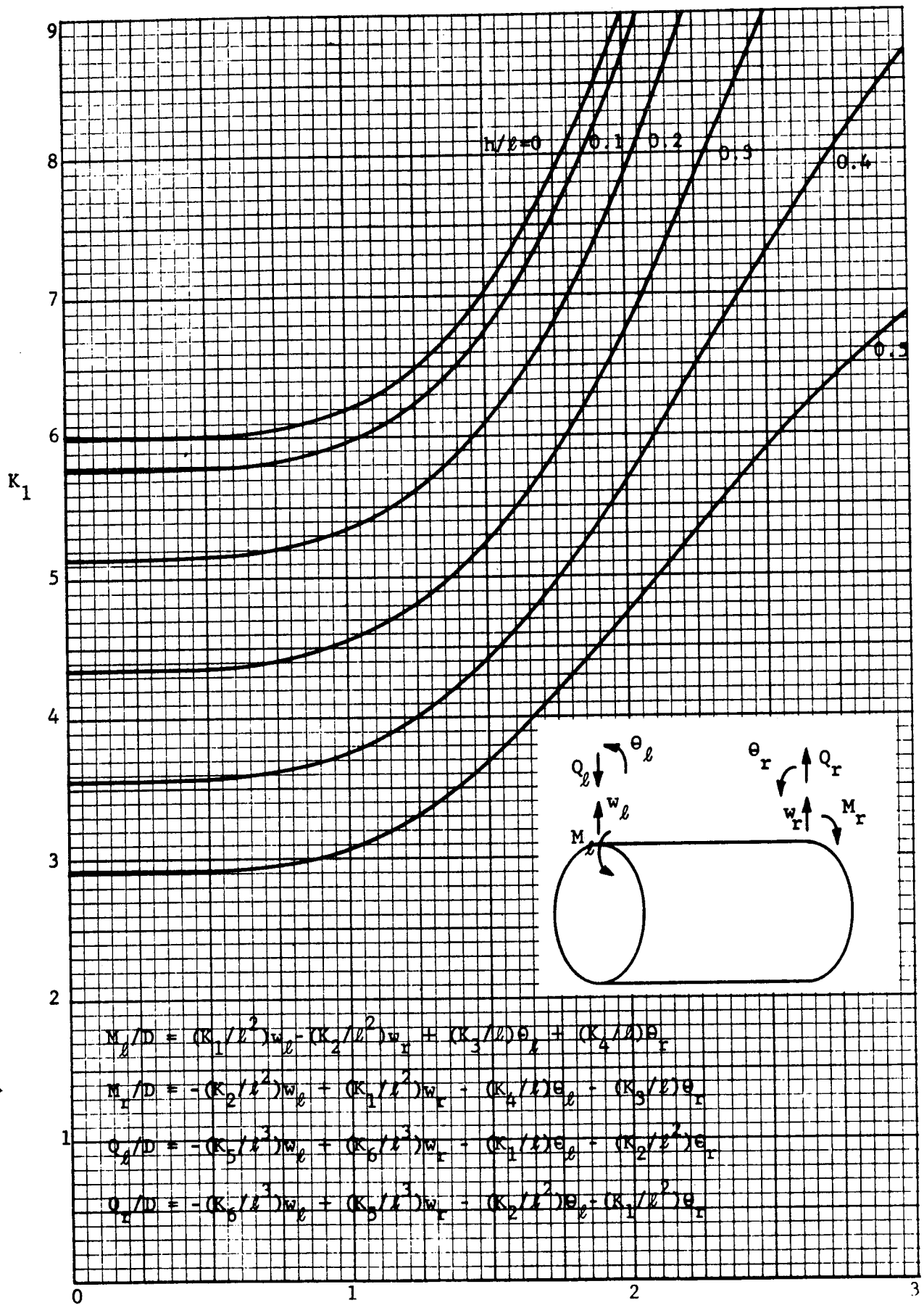


Figure 3.11. Values of K_1

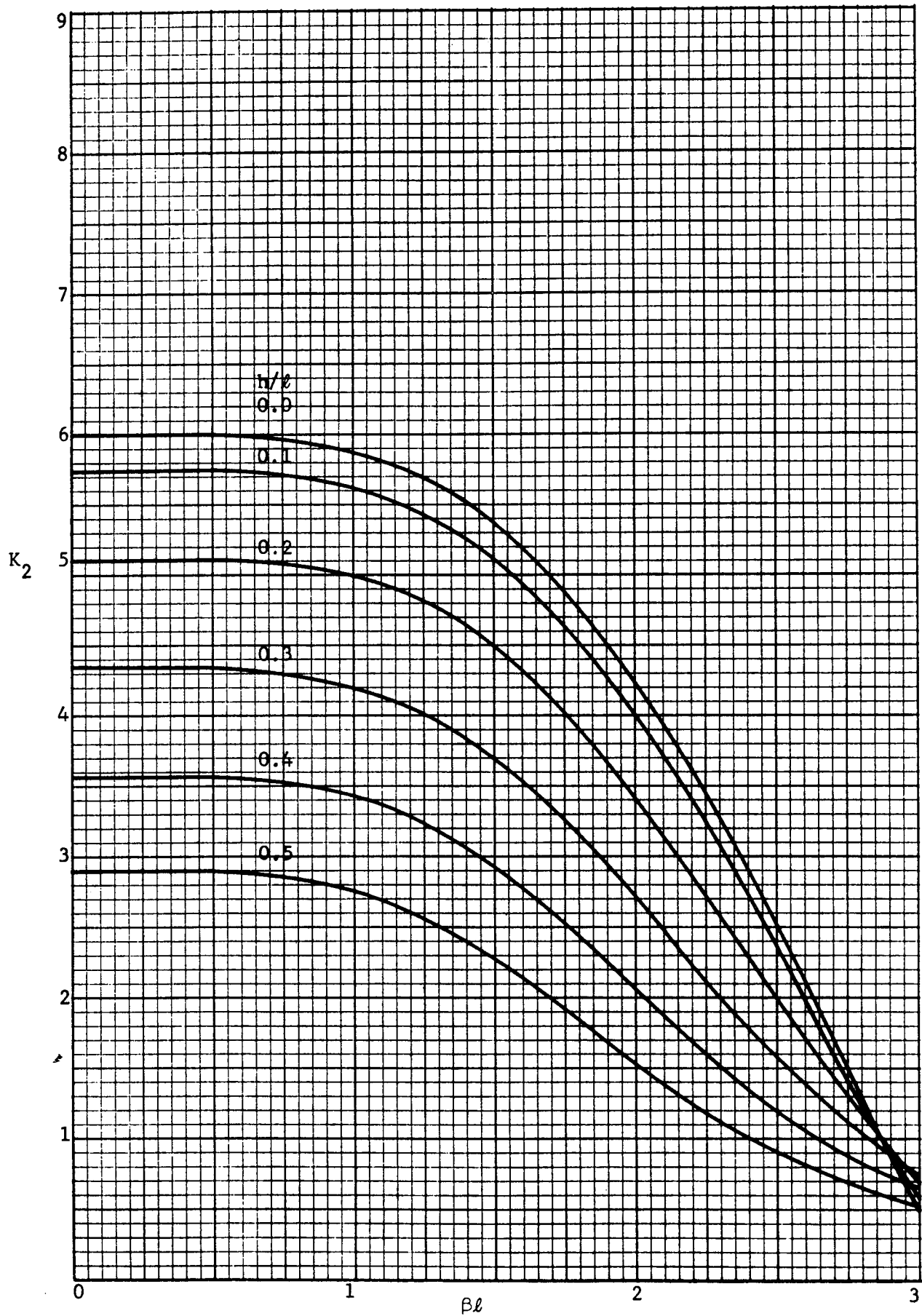


Figure 3.12. Values of K_2

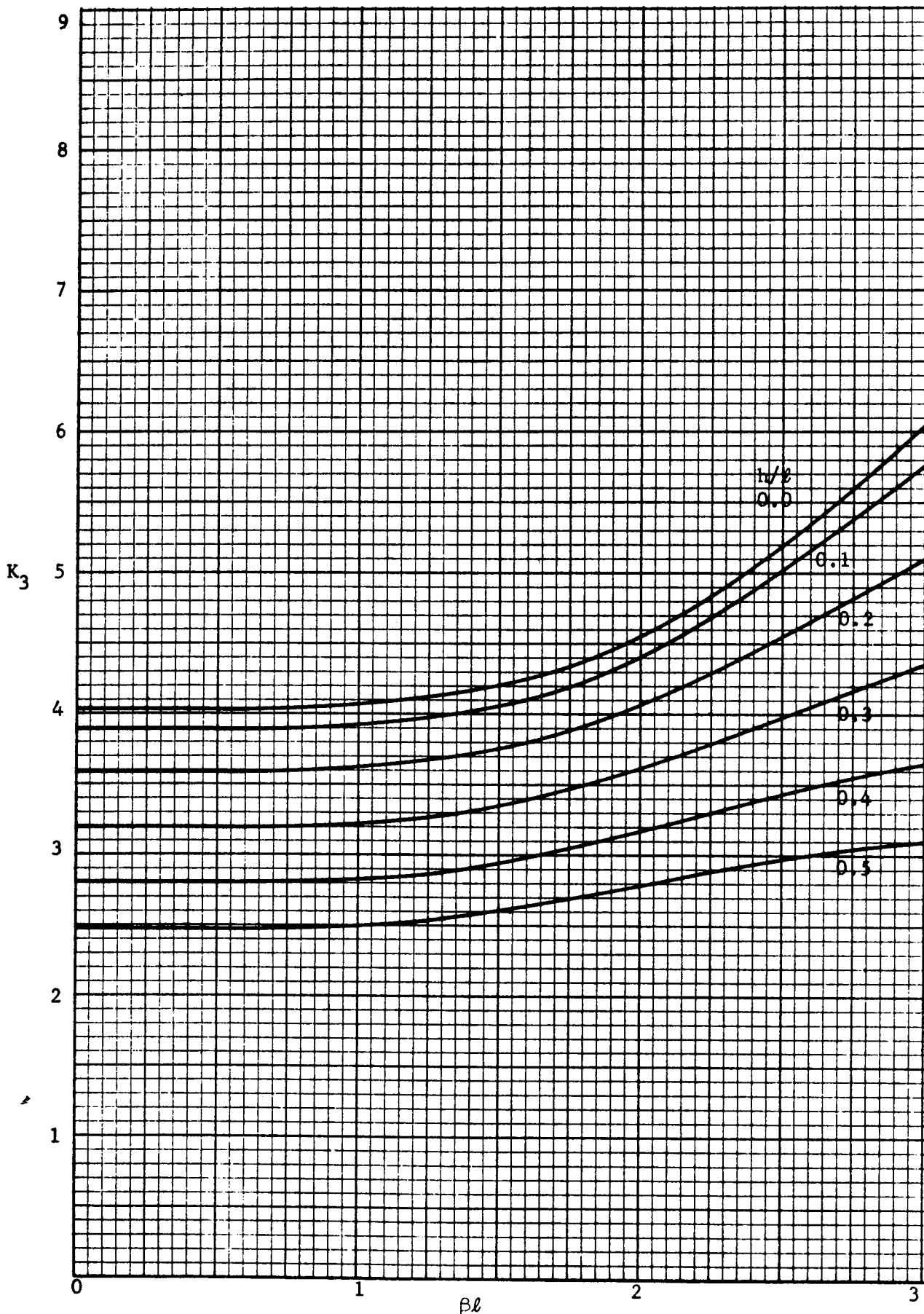


Figure 3.13. Values of K_3

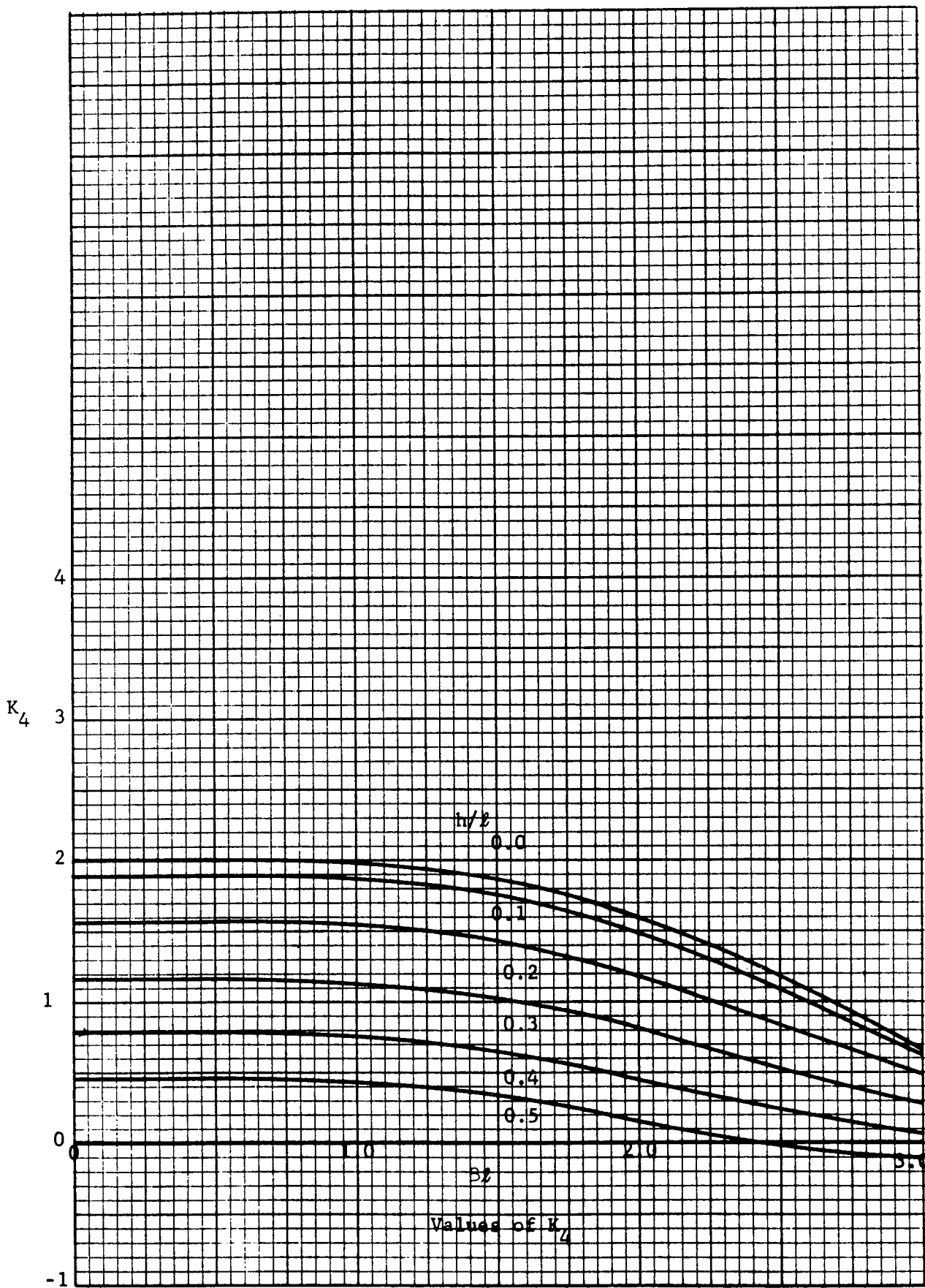


Figure 3.14. Values of K_4

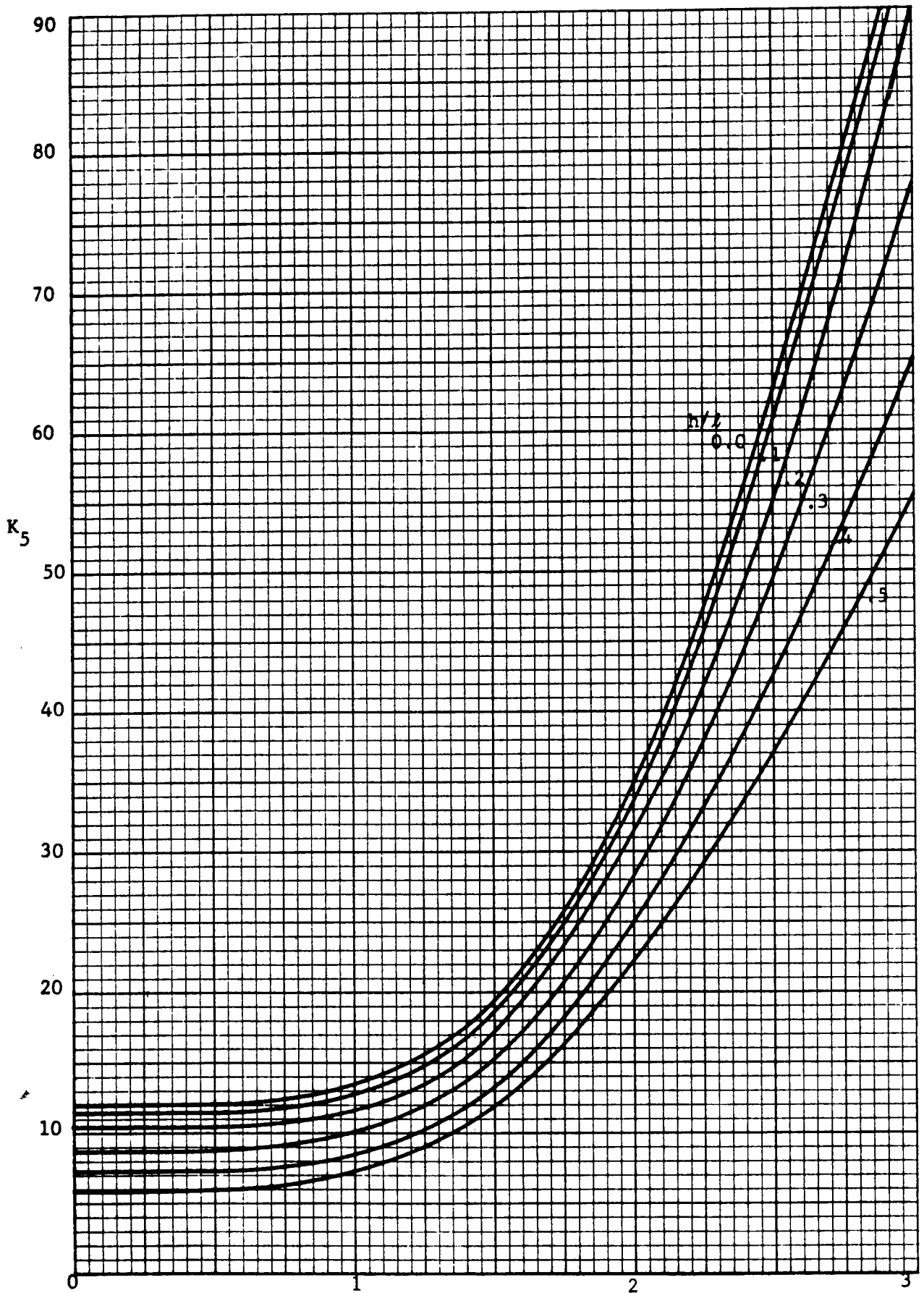


Figure 3.15. Values of K_5

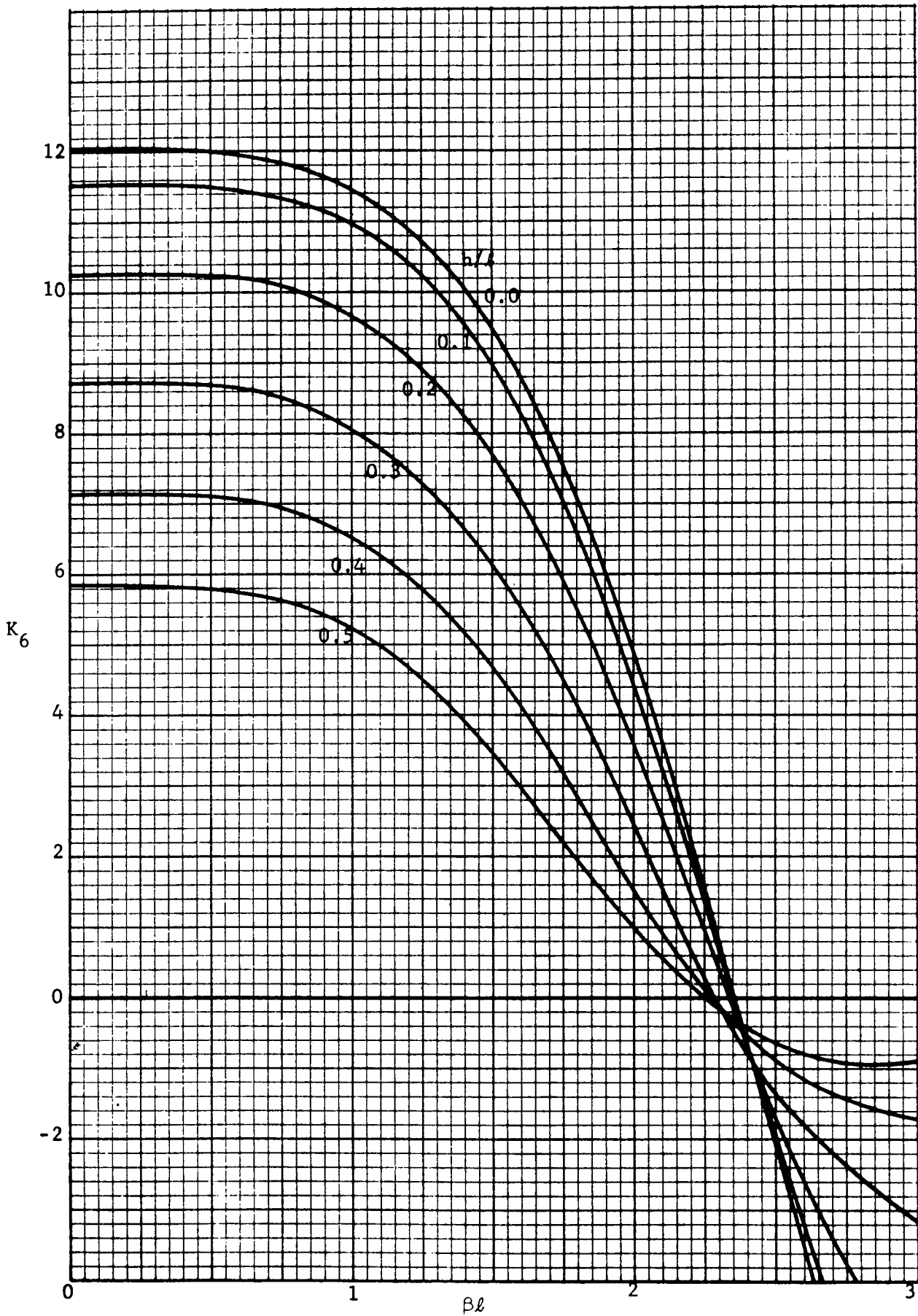


Figure 3.16. Values of K_6

3.11.5 Sample Calculation

The design procedure was used to design a high-temperature separable connector. This connector was designed to meet the operating requirements of Table 3.4. The connector geometry, seal, and final dimensions are shown in Figures 3.17, 3.18, 3.19, 3.20, and 3.21.

Table 3.4

<u>Test Description</u>	<u>Temperature OF</u>	<u>Pressure psi</u>	<u>OPERATING CONDITIONS FOR HIGH-TEMPERATURE CONNECTOR</u>	
			<u>Transverse Moment in -lb.</u>	<u>Leakage Level</u>
High-temperature	1440	4700 ⁽¹⁾	0	"zero"
Proof	70	9400 ⁽¹⁾	0	no requirement
Vibration (10 ⁶ cycles)	70	4700 ⁽¹⁾	221 ⁽²⁾	"zero"
Impulse (2000 cycles)	70	6000 ⁽²⁾	0	"zero"

(1) static

(2) cyclic

3.11.5.1 Design Requirements

The detailed design requirements are:

a. Tubing

Inconel - X

$D_t = 0.75$

$d_t = 0.62$

b. Fluid

Hot gas

Temperatures and pressures as prescribed in Table 3.4.

c. Environmental Conditions

Air at room temperature and pressure

d. External Loads

As prescribed in Table 3.4

e. Allowable leakage level

"zero"

Four critical operating conditions are given in Table 3.4. The high-temperature, vibration, and impulse condition all require "zero" leakage and, therefore, had to be considered in the preload determination. The high-temperature, vibration, and proof condition had to be considered to determine which one resulted in highest static stresses and to make sure that these stresses did not exceed the yield stress at the operating temperature. The vibration and impulse condition had to be considered for determining which one resulted in the most severe fatigue stress condition and to make sure that there was no chance of a fatigue failure.

A complete set of calculations were made for each of the four operating conditions. It turned out that: the vibration condition determined the preload; the high-temperature condition resulted in the highest static stresses; and the impulse condition resulted in the most severe fatigue stress condition. Each of the calculations is identical except for a few numbers. Therefore, only the calculations for the vibration condition are included here. Inclusion of the other conditions would only add to the length and confusion of this sample calculation.

3.11.5.2 Connector Configuration

The connector configuration chosen, Figure 3.17, is like that shown in the design procedure, Figure 3.1. Rene' 41 was chosen as the connector material because of its good high temperature properties. The heat treatment designed to give the Rene' 41 its optimum creep properties was chosen. However, for the flange and the union, this heat treatment was modified to take into consideration the Inconel-X tubing which is welded to the flange and the union prior to heat treating. The last step of the three-step heat treatment for Inconel-X was added to the Rene' 41 heat treatment. The heat treatment used is:

- a. 2150°F for 2 hours, air cool to room temperature
- b. 1650°F for 4 hours, air cool to room temperature
- c. 1300°F for 20 hours, air cool to room temperature

3.11.5.3 Seal

The "triangle" seal was chosen because of the high temperature requirements. The seal consists of a soft nickel gasket and knife-edges cut on the union and the flange. The triangle seal had been previously tested and found satisfactory. The gasket, shown in Figure 3.21, is not triangular in cross-section, because the apices were cut-off to facilitate manufacture of the sealing faces on the union and flange. The knife-edges still cut into the slanted surfaces of the gasket.

The seal determined the following connector dimensions:

$$D_g = 0.89$$

$$d_g = 0.75$$

$$L_g = 0.08$$

To facilitate manufacture of the flange and the union, L_g was later reduced, but the above value was used in the calculations.

3.11.5.4 Attachment to Tubing

The weld configuration shown in Figure 3.2 of the design procedure was chosen because of the high pressures and temperatures involved. In order to establish a welding schedule and to evaluate the weld a number of pieces of Inconel-X tubing were welded to pieces of Rene 41 in the manner indicated in Figure 3.2. One sample was heat treated and tested. It was determined that the yield strength, B_y , is greater than 5,900 lbs/inch. No fatigue properties were determined.

The adequacy of the weld is determined from Eq. 3.1 which states that for the vibration condition $B_y \geq 1320$ lbs/in. This requirement is obviously met. The numerical values used in this calculation, that are not previously defined in this section, are:

$$H_m = 1.2$$

$$F_k = F_c = P_c = m_k = 0$$

$$P_k = 4700$$

$$m_c = 221$$

3.11.5.5 Approximate Connector Dimensions

In order to begin the iterative procedure of calculating the stresses in the connector, modifying the dimensions, and again calculating the stresses, an initial set of dimensions must be determined. The initial dimensions, as determined by the procedures of Sections 3.5.2, 3.6.2, and 3.7.2 are given in Table 3.5.

3.11.5.6 Preload

The dimensions of Table 3.5 were used to calculate a preload and the stresses in the connector. An examination of the stresses showed that certain dimensions should be increased and others decreased. The dimensions were changed and the stresses calculated. Again it was necessary to change certain dimensions. The results of the third stress calculation were satisfactory and no further calculations were made.

Rather than present all of the calculations, only the final set is included here. The dimensions, physical constants, and loads used in these calculations are given in Table 3.6.

Table 3.5

APPROXIMATE DIMENSIONS USED TO INITIALIZE THE ITERATIVE DESIGN PROCEDURE

<u>Symbol</u>	<u>Number</u>	<u>Equation Used</u>
D_a	1.0	3.11, Ref. 5 (page 1046)
D_b	1.375	3.10, Table 3.1, Ref. 5 (Table 5, page 1183)
D_f	1.14	3.5
D_g	0.89	from seal
D_n	1.875	3.17, Ref. 5 (page 1045)
D_t	0.75	from tube
D_u	1.078	3.8
d_g	0.75	from seal
d_n	1.01	3.15
d_s	1.415	3.13
d_t	0.62	from tube
L_a	0.69	Ref. 5 (page 1046)
L_e	0.562	Table 3.1
L_f	0.5	Ref. 5 (page 1046)
L_g	0.08	from seal
L_h	0.39	3.4
L_n	0.432	3.18
L_r	0.26	3.6
L_s	0.277	3.14
L_t	0.625	Table 3.1
L_u	0.08	3.9
L_w	0.75	from weld
n	8.0	Table 3.1
R_n	0.137	3.16
R_u	0.06	3.12
t	0.065	from weld
w	0.065	3.7

Table 3.6

DIMENSIONS, PHYSICAL CONSTANTS, AND LOADS USED IN THE FINAL SET OF
CALCULATIONS FOR THE VIBRATION CONDITION

<u>Symbol</u>	<u>Number</u>	<u>Symbol</u>	<u>Number</u>
D _a	1.0	R _u	0.014
D _b	1.25	t	0.08
D _f	1.11	w	0.05
D _g	0.89		
D _n	1.687	F _k	0
D _t	0.75	F _c	0
D _u	1.048	m _k	0
d _g	0.75	m _c	221.0
d _n	1.01	P _k	4700.0
d _s	1.285	P _c	0
d _t	0.62	T _f	70.0
L _a	0.69	T _n	70.0
L _e	0.438	T _r	70.0
L _f	0.5	T _u	70.0
L _g	0.08		
L _h	0.5	E _f	3.16 x 10 ⁷
L _n	0.3	E _n	3.16 x 10 ⁷
L _r	0.24	E _u	3.16 x 10 ⁷
L _s	0.258		
L _t	0.5	H _f	1.2
L _u	0.08	H _m	1.2
L _w	0.75	S _n	4.8 x 10 ⁴
n	10.0	S _u	1.52 x 10 ⁵
R _n	0.087	S _y	1.0 x 10 ⁵

First the spring constant for the nut is calculated. This is done in four steps: the constants (K_1) for the shells are calculated; the coefficients for the set of simultaneous equations are calculated; the simultaneous equations are solved, and the spring constant is calculated. For convenience the K_1 for all of the connector shells are calculated at one time and tabulated in Table 3.7. The K_1 are referenced to the coefficients (C_1) in which they are first used. A Poisson's ratio of 0.3 is used throughout. The formulas for the K_1 are in Section 3.11.4 and the formulas for the l , r , and h used in calculating the K_1 are given with the respective coefficient in Sections 3.11.1 and 3.11.2.

Table 3.7

SHELL EQUATION CONSTANTS FOR USE IN COEFFICIENT CALCULATIONS

Coefficients where K_1 are first used

K	3	12	21	35	59	82
1	3.951	1.577	0.1846	10.32	1.537	2.65
2	2.609	1.445	0.1833	1.18	1.203	1.641
3	2.733	1.767	1.092	4.204	1.714	2.152
4	0.4663	-0.2595	-0.9082	0.4361	-0.3523	-.04876
5	12.4	3.564	0.3728	62.25	4.151	8.76
6	4.105	2.767	0.3655	-2.531	2.104	2.433

The coefficients for the simultaneous equations used in the nut spring constant calculation are in Section 3.11.1. The results of the calculation are in Table 3.8.

Table 3.8

COEFFICIENTS FOR NUT SPRING CONSTANT CALCULATION

<u>Coefficient</u>	<u>Number</u>	<u>Coefficient</u>	<u>Number</u>	<u>Coefficient</u>	<u>Number</u>
1	1.5×10^{-1}	13	2.767	24	6.055×10^{-3}
2	-1.399×10^{-7}	14	3.798×10^{-1}	25	3.655×10^{-1}
3	1.24×10^1	15	3.481×10^{-1}	26	3.728×10^{-1}
4	4.105	16	5.947×10^{-7}	27	1.757×10^{-8}
5	1.749	17	-2.996×10^{-9}	28	6.181×10^{-8}
6	1.155	18	1.025×10^{-1}	29	-2.156×10^{-6}
7	3.691×10^{-6}	19	-1.506×10^{-2}	30	-1.428×10^5
8	-6.232×10^{-8}	20	1.194×10^{-10}	31	4.458×10^{-1}
9	5.356×10^{-1}	21	1.365×10^{-2}	32	-2.972
10	9.136×10^{-2}	22	1.374×10^{-2}	33	1.356×10^{-1}
11	4.463×10^{-9}	23	-5.035×10^{-3}	34	-1.585×10^{-2}
12	3.564				

The solution of the simultaneous Eqs. 3.19 are given in Table 3.9. Note that these are for a unit force ($F_n = 1$ lb) acting on the nut and these values must be multiplied by the appropriate value of F_n in order to calculate the nut stresses.

Table 3.9

DEFLECTION, ROTATIONS, FORCES, AND MOMENTS IN NUT DUE TO A UNIT FORCE

<u>Symbol</u>	<u>Number</u>	<u>Symbol</u>	<u>Number</u>	<u>Symbol</u>	<u>Number</u>
u_4	9.77×10^{-9}	Θ_5	-1.659×10^{-7}	Q_7	-2.845×10^{-2}
u_5	-2.367×10^{-8}	Θ_6	1.651×10^{-7}	M_4	-2.444×10^{-2}
u_6	-1.774×10^{-8}	Θ_7	2.626×10^{-7}	M_5	-1.965×10^{-2}
u_7	2.476×10^{-8}	Θ_8	2.613×10^{-7}	M_6	-3.798×10^{-3}
u_8	4.352×10^{-8}	Q_4	6.981×10^{-2}	M_7	-1.47×10^{-2}
Θ_4	-2.229×10^{-7}	Q_5	-4.271×10^{-2}	M_8	1.156×10^{-3}

The spring constant for the nut is calculated using Eq. 3.20.

$$G_n = 1.041 \times 10^7$$

Next the functional relationship of F_g to F_3 and M_3 should be determined, Eq. 3.22. However, for the seal used in this example it will suffice to consider only F_3 . F_3 is determined by the geometry and loading, which have already been established, and the preload, which is to be determined. First, F_a is calculated using Eq. 3.23.

$$F_a = 3141.0$$

Then C_{104} (Section 3.11.2) is calculated with F_p undetermined.

$$C_{104} = 441.0 + F_p$$

Finally, F_3 is calculated using Eq. 3.23.

$$F_3 = -3106.0 + F_p$$

In order to have a compressive force of 1200 lbs. (i.e., $F_3 = 1200$) between the flange and the union during the vibration test condition, F_p is chosen equal to 4300 lbs.

$$F_p = 4300.0$$

Before accepting this as the value to use in the subsequent stress calculations, the assembly torque necessary to achieve this preload is calculated. This is important, because the assembly torque may be larger than the torque which a man can apply to the connector with a set of ordinary wrenches. Using friction factors of 0.3 in Eq. 3.30, the calculated assembly torque is 1550 inch lb.

$$W = 1550.$$

3.11.5.7 Stress Calculation

Having determined the preload, the stress calculation can begin. In order to investigate the possibility of localized yielding or fatigue failure occurring in the connector, three sets of stresses must be calculated. The stress equations in the design procedure are for the equivalent stresses, and these cannot be added algebraically. Therefore, to investigate the possibility of yielding the effective stresses due to the total load (constant and cyclic) must be calculated. And to investigate the possibility of a fatigue failure the effective stresses due to the constant load and the cyclic load must be calculated separately. The latter two stresses cannot be added to get the total effective stress.

The first step in the stress calculation is the calculation of the coefficients (C₃₅ through C₁₀₄) for the simultaneous equations for the flange and the union. The procedure for calculating the coefficients for each of the three stress cases are identical. Therefore, the intermediate results of the stress calculation are given only for the calculation of the stresses due to the total load. For the other two cases only the constant in each equation is different. The important thing is to separate the constant forces from the cyclic forces. Note that F_p is a constant force and does not enter into the calculation of the cyclic stresses.

The coefficients for the simultaneous equations for the flange and the union for the total stress calculation are given in Table 3.10.

Table 3.10

COEFFICIENTS FOR FLANGE AND UNION SIMULTANEOUS EQUATIONS

<u>Coefficient</u>	<u>Number</u>	<u>Coefficient</u>	<u>Number</u>	<u>Coefficient</u>	<u>Number</u>
35	6.349×10^1	44	1.203	53	-9.408×10^{-4}
36	-2.582	45	2.102	54	1.458×10^{-5}
37	5.16	46	2.18×10^{-1}	55	1.876×10^{-5}
38	5.899×10^{-1}	47	1.75×10^{-8}	56	-9.165×10^{-7}
39	1.537×10^{-5}	48	-3.074×10^{-5}	57	6.126×10^{-6}
40	4.735×10^{-8}	49	7.926×10^{-7}	58	2.551×10^{-4}
41	2.144×10^{-6}	50	2.454×10^{-3}	59	4.151
42	6.669×10^{-3}	51	1.687×10^{-7}	60	4.616
43	1.053×10^1	52	3.598×10^{-5}	61	2.104

Table 3.10(continued)

<u>Coefficient</u>	<u>Number</u>	<u>Coefficient</u>	<u>Number</u>	<u>Coefficient</u>	<u>Number</u>
		76	8.522×10^{-8}	91	7.001×10^{-1}
62	3.689×10^{-1}	77	-1.669×10^{-5}	92	-1.586×10^{-2}
63	2.888×10^{-1}	78	1.338	93	-3.731×10^{-6}
64	4.471×10^{-7}	79	2.031×10^{-6}	94	-7.127×10^{-9}
65	-1.445×10^{-8}	80	2.354×10^{-9}	95	1.614×10^{-4}
66	2.196×10^{-4}	81	-5.226×10^{-5}	96	-2.463×10^{-7}
67	2.34	82	8.76	97	-7.51×10^{-5}
68	4.874×10^{-7}	83	2.433	98	2.526×10^{-7}
69	-1.181×10^{-4}	84	8.62×10^{-1}	99	9.523×10^{-7}
70	1.537	85	5.337×10^{-1}	100	7.439×10^{-5}
71	1.709	86	1.214×10^{-6}	101	-6.78×10^{-6}
72	1.203	87	-4.467×10^{-8}	102	1.009×10^{-4}
73	4.114×10^{-1}	88	4.707×10^{-4}	103	-9.354×10^{-6}
74	-8.456×10^{-2}	89	2.65	104	4.741×10^3
75	-1.863×10^{-6}	90	1.641		

The solutions to the simultaneous equations for the total stress calculation are given in Table 3.11.

Table 3.11

DEFLECTIONS, ROTATIONS, FORCES, AND MOMENTS
FOR THE FLANGE AND THE UNION FOR TOTAL STRESS CALCULATION

<u>Symbol</u>	<u>Number</u>	<u>Symbol</u>	<u>Number</u>	<u>Symbol</u>	<u>Number</u>
u_1	1.44×10^{-4}	Θ_3	-2.074×10^{-4}	M_1	-2.05×10^1
u_2	1.418×10^{-4}	Θ_9	9.032×10^{-4}	M_2	7.561×10^1
u_3	4.294×10^{-5}	Q_1	-2.583×10^2	M_3	-9.958×10^1
u_9	7.96×10^{-5}	Q_2	4.955×10^2	M_9	1.601×10^2
Θ_1	3.184×10^{-4}	Q_3	1.622×10^2	F_n	4.741×10^3
Θ_2	-1.187×10^{-3}	Q_9	-6.243×10^2		

The stresses are calculated using Eqs. 3.31 through 3.44. The results are compiled in Table 3.12. The stresses are the stresses due to the combined constant and cyclical load. As there is no thermal transient, σ_h and σ_r are zero at each stress location.

Table 3.12

COMPILATION OF STRESS CALCULATIONS FOR VIBRATION TEST CONDITION--TOTAL STRESSES

Stress Location	Stress Calculated S_m psi	Factor of Safety H_m	Yield Strength S_y psi	Ratio $H_m S_m / S_y$
1	51,870	1.2	100,000	0.62
2	12,960	1.2	100,000	0.16
3	18,690	1.2	100,000	0.22
4	41,440	1.2	100,000	0.50
5	25,320	1.2	100,000	0.30
6	10,330	1.2	100,000	0.12
7	15,550	1.2	100,000	0.19
8	19,480	1.2	100,000	0.23
9	56,470	1.2	100,000	0.68
10	37,380	1.2	100,000	0.45
11	10,790	1.2	100,000	0.13
12	14,590	1.2	100,000	0.18
13	7,820	1.2	100,000	0.09

The constant and cyclical stresses were also calculated using equations 3.31 through 3.44. These are compiled in Table 3.13. Each set of stresses was calculated separately and then combined using equation 3.48.

Table 3.13

COMPILATION OF STRESS CALCULATIONS FOR VIBRATION TEST CONDITION--FATIGUE ANALYSIS

Stress Location	Calculated Constant S_k psi	Stress Cyclical S_c psi	Factor of Safety H_f	Ultimate Strength S_u psi	Fatigue Strength S_n psi	Ratio $H_f^* S_f / S_m$
1	37,290	15,270	1.2	152,000	48,000	0.51
2	15,260	2,400	1.2	152,000	48,000	0.07
3	19,240	650	1.2	152,000	48,000	0.02
4	33,420	8,440	1.2	152,000	48,000	0.27

Table 3.13 (continued)

Stress Location	Calculated Constant S_k psi	Stress Cyclical S_c psi	Factor of Safety H_f	Ultimate Strength H_f	Fatigue Strength S_n psi	Ratio $H_f^* S_f/S_n$
5	24,040	1,550	1.2	152,000	48,000	0.05
6	9,280	3,100	1.2	152,000	48,000	0.08
7	16,940	1,590	1.2	152,000	48,000	0.04
8	17,570	2,550	1.2	152,000	48,000	0.07
9	56,500	1,090	1.2	152,000	48,000	0.04
10	35,190	2,200	1.2	152,000	48,000	0.07
11	10,150	630	1.2	152,000	48,000	0.02
12	13,730	860	1.2	152,000	48,000	0.02
13	7,360	460	1.2	152,000	48,000	0.01

* H_f was calculated using equation 3.48.

The stresses for the other operating conditions are calculated in a similar manner using the same equations. However, there is a slight difference in calculating the assembly stresses. These stresses are calculated in the same manner as the stresses for an operating condition and using the same equations, except that the only force is the constant preload, F_p , and the σ_h and σ_r are everywhere zero except at stress locations 10 and 11 where σ_h is calculated using Eqs. 3.46 and 3.47 respectively. Also, a stress is calculated in an additional location using Eq. 3.45. For this sample calculation, using the dimensions of Table 3.6, the assembly stresses are:

$$\begin{aligned}
 (\sigma_h)_{10} &= -14,900 && \text{using equation 3.46} \\
 (\sigma_n)_{11} &= 14,900 && \text{using equation 3.47} \\
 S_{14} &= 82,500 && \text{using equation 3.45}
 \end{aligned}$$

3.11.5.8 Final Connector Configuration

The final connector configuration is based on the dimensions of Table 3.6 with a number of minor modifications. The dimensions established by use of the design procedure should be subjected to sound design judgment. Some of the modifications are:

1. L_g was reduced to facilitate manufacture.
2. The socket thickness on the flange and the union was reduced in the weld area to facilitate welding.
3. The length L_h of the union was reduced to decrease the weight.

4. The radius between the flange ring and the hub was reduced to decrease the connector weight.

Note that none of these modifications resulted in an adverse stress condition.

3-60

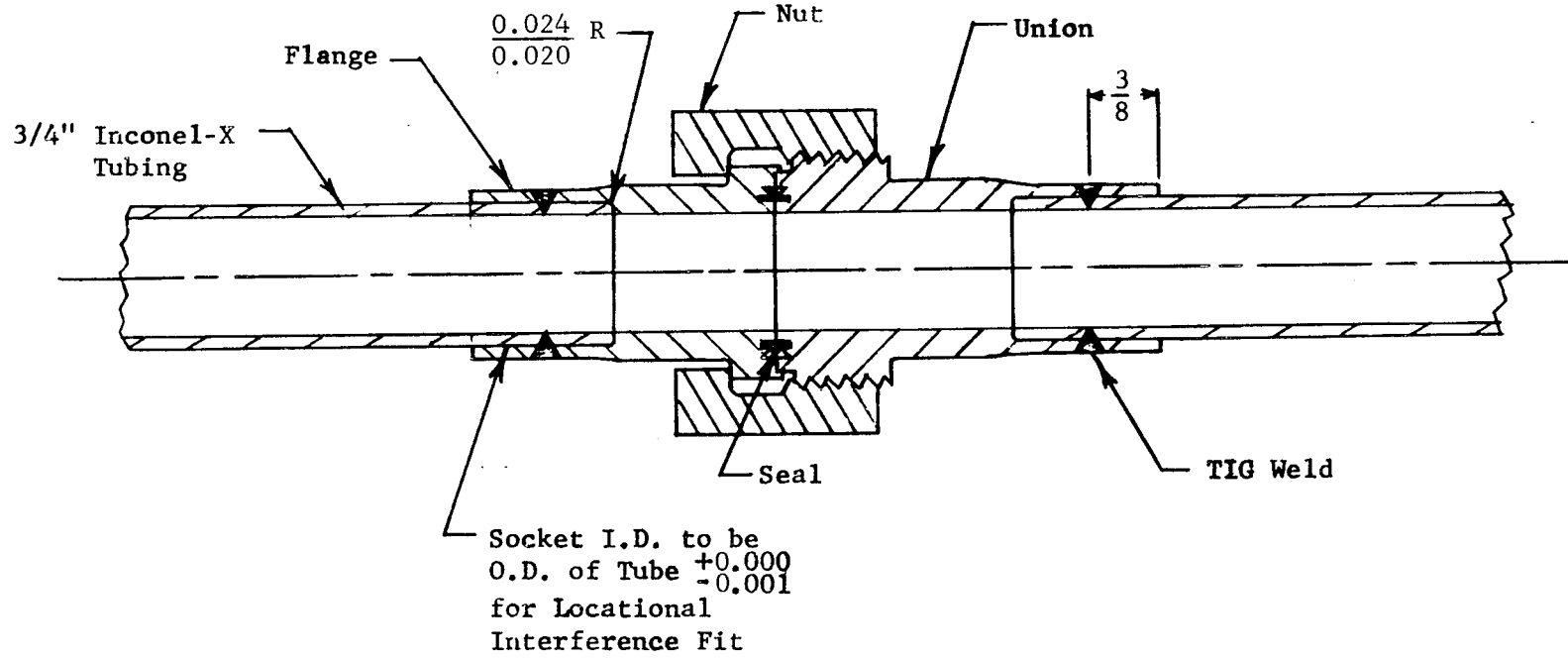


Figure 3.17. High Temperature Tube Connector

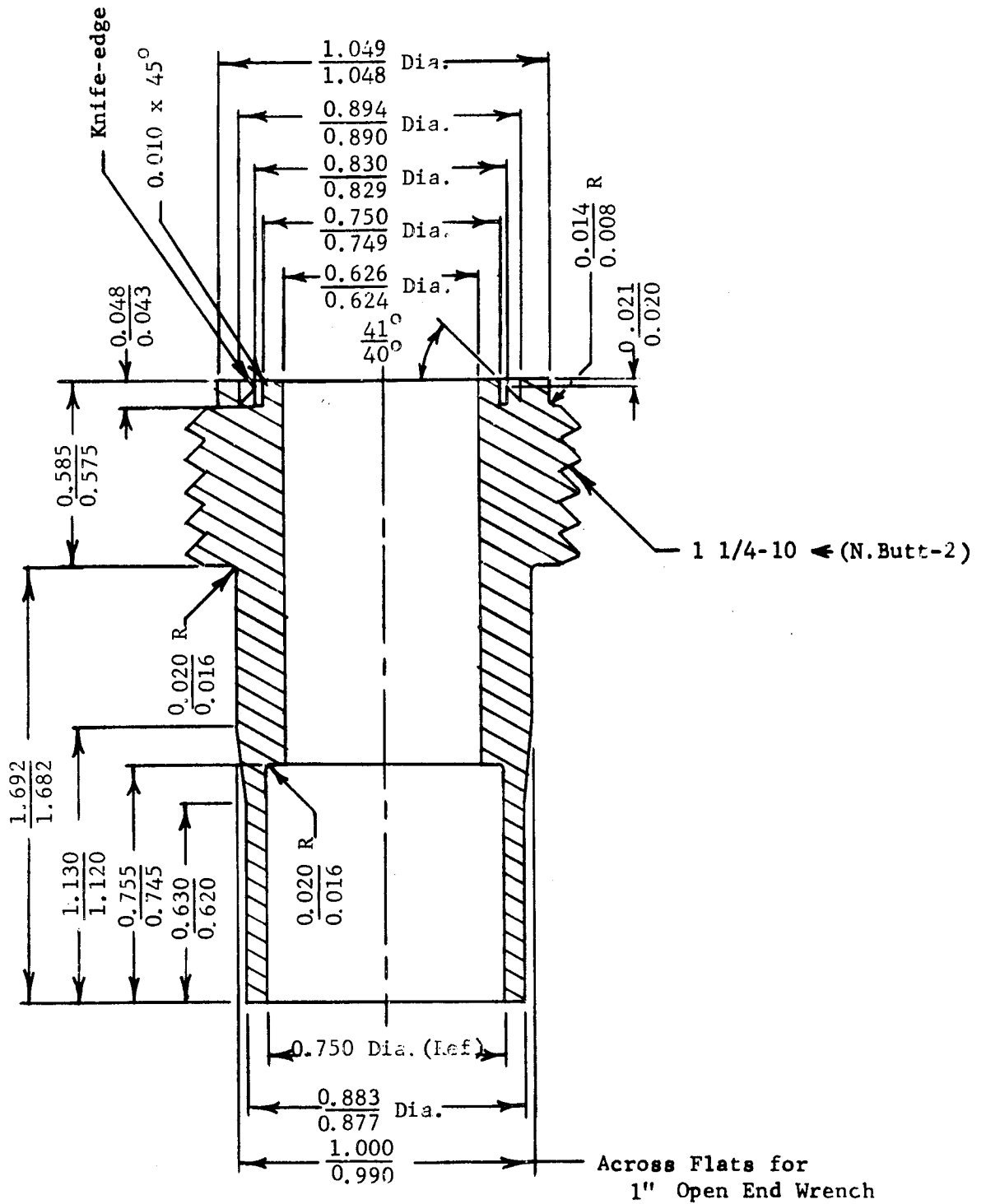


Figure 3.18. Union (Material Rene' 41)

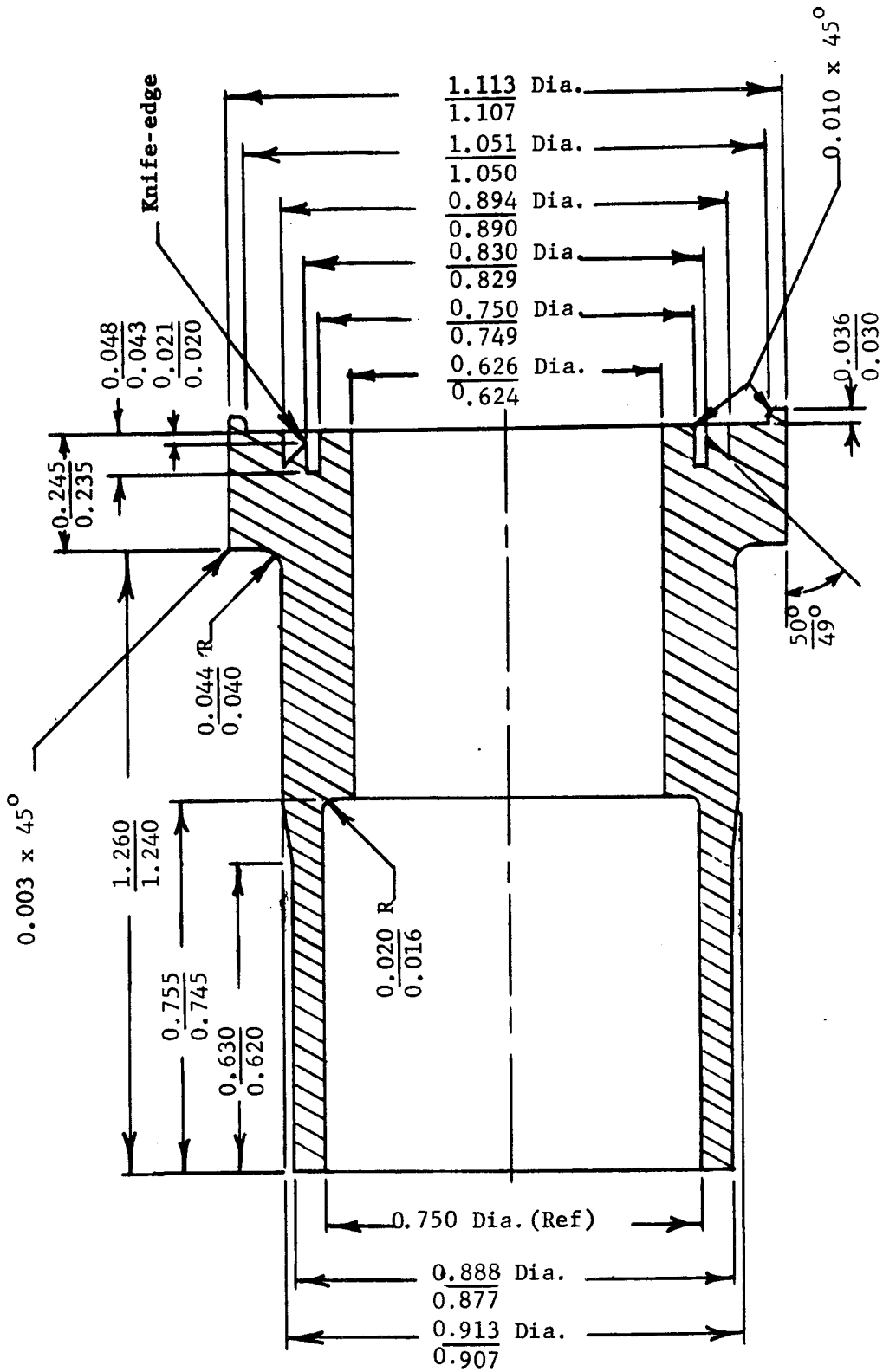


Figure 3.19. Flange (Material Rene' 41)

Minimum Length
of Flats for
1 11/16 Open End Wrench,
 $\frac{1.690}{1.685}$ Across Flats

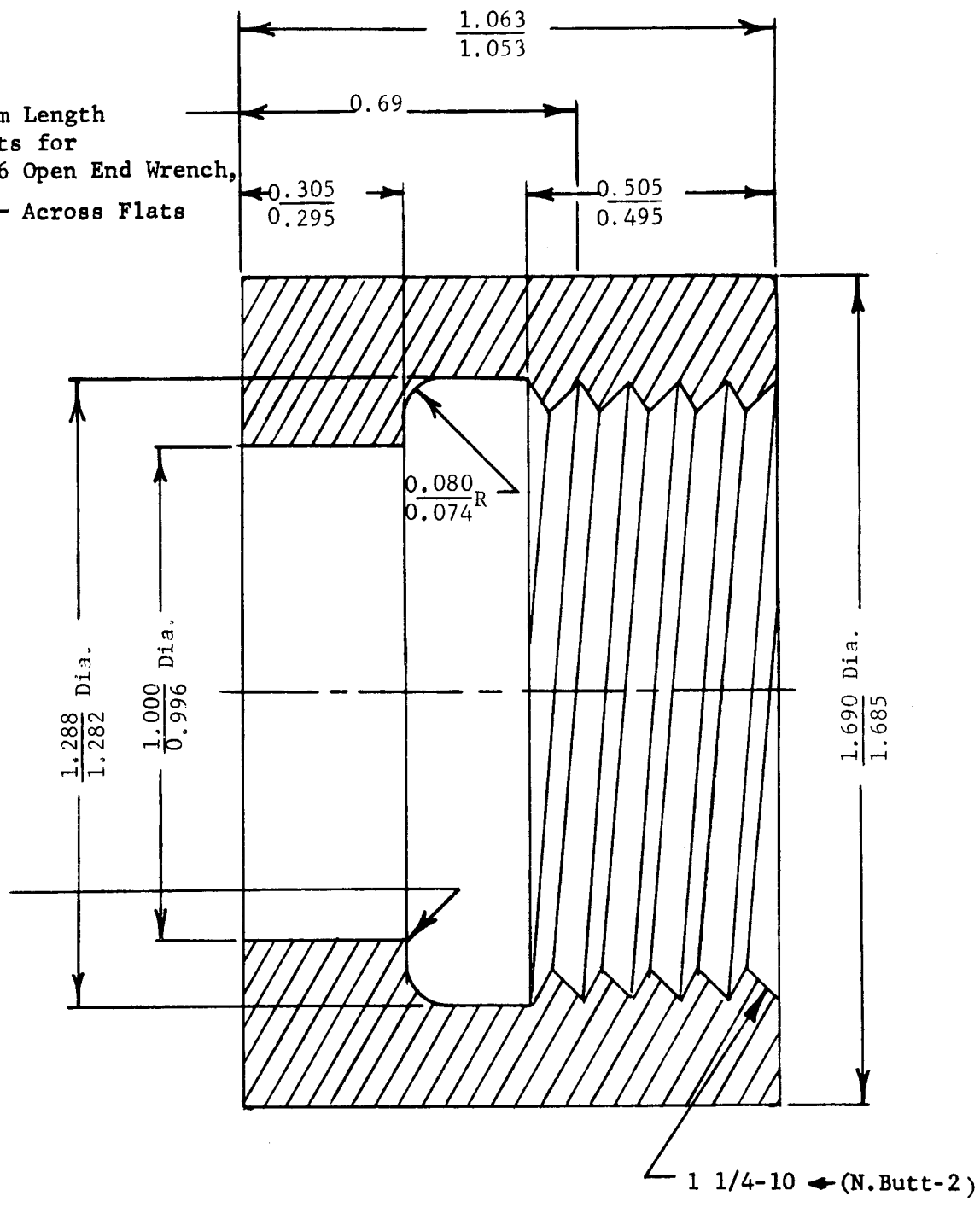


Figure 3.20. Nut (Material Rene' 41).

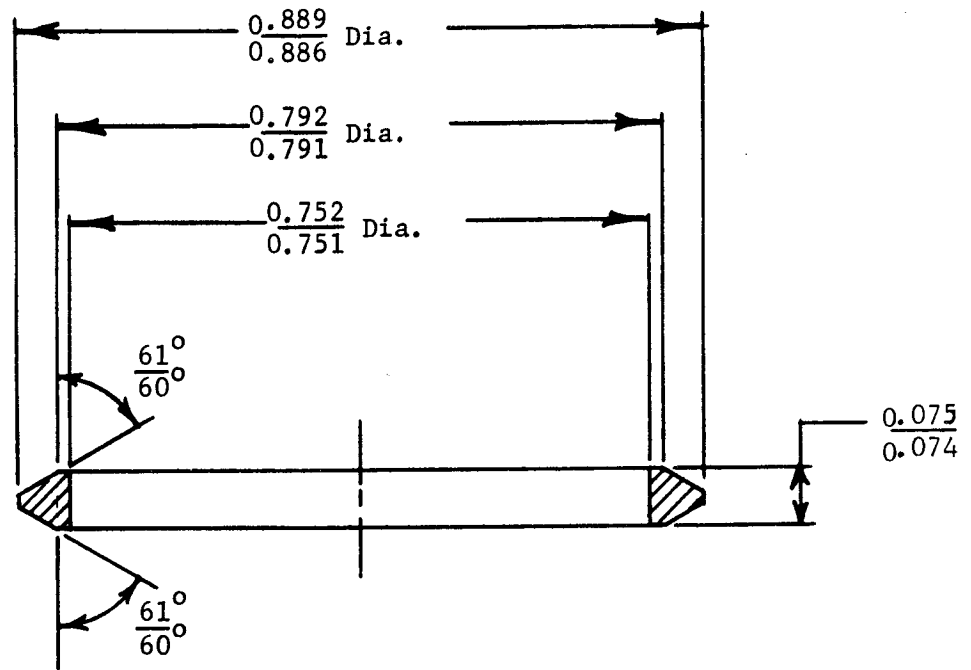


Figure 3.21. Triangle Seal (Material Nickel 200).

3.12 References

1. Barton, G.R., "Tubular Joining by Induction Brazing and Fusion Welding Methods," (paper presented at the 25th SAE National Aeronautic and Space Engineering and Manufacturing Meeting and Engineering Display, Los Angeles, October 1962)
2. Weisman, M.H., Applied Research and Development Work on Families of Brazed and Welded Fittings for Rocket Propulsion Fluid Systems, Technical Documentary Report No. RTD-TDR-63-1027, November 1962
3. Sopwith, D.G., Bending Stresses and Load Distribution in Screw Threads, Paper No. P.M. 15, Dept. of Scientific and Industrial Research, National Engineering Laboratory, Glasgow, Scotland, March 1948
4. Levy, S., "Design of Connectors," Design Criteria for Zero-Leakage Connectors for Launch Vehicles, Vol. 4, N 63-18494, NASA-CR-50560
5. Oberg, E., and Jones, F.D., Machinery's Handbook, Sixteenth Edition, The Industrial Press, 1959

.13 Nomenclature

<u>Symbol</u>	<u>Subscript</u>		<u>Units</u>
A		Constant	
a		Coefficient of thermal expansion	in/in ^o F
	f	flange	
	n	nut	
	u	union	
B		Strength of weld per linear inch of circumference	lb/in
	n	fatigue	
	u	fracture	
	y	yield	
b		Width of weld	in
C _i		Coefficients of variables and constant terms in the sets of simultaneous equations	
D		Outside diameter	in
d		Inside diameter	in
	a	across wrenching flats of the union	
	b	thread	
	f	flange	
	g	seal	
	n	nut ring	
	s	nut shell	
	t	tube	
	u	union	
	w	weld	
E		Modulus of elasticity	lb/in ²
	f	flange	
	n	nut	
	u	union	

<u>Symbol</u>	<u>Subscript</u>		<u>Units</u>
F		Axial force	lb
	a	on connector	
	c	cyclical (exclusive of pressure)	
	g	seal	
	k	constant (exclusive of pressure)	
	n	nut	
	p	preload	
s	seating		
f		Friction factor	
	n	nut to flange	
t	threads		
G		Spring constant	lb/in
	n	nut	
u	union and flange		
H		Safety factor	
	m	static stresses	
f	fatigue stresses		
K_i		Shell constants in Section 3.11.3	
L		Axial length	in
	a	wrenching flat on nut	
	e	engagement of thread	
	f	wrenching flat on union	
	g	seal	
	h	flange hub	
	n	nut ring	
	r	flange ring	
	s	nut shell	
	t	thread	
	u	union	
	w	weld socket	
	M_i		
m		Moment externally applied	in lb
	c	cyclical	
k	constant		

<u>Symbol</u>	<u>Subscript</u>		<u>Units</u>
N		Number of cycles	
	f	force	
	m	moment	
	p	pressure	
n		Number of threads per inch	in ⁻¹
P		Pressure	lb/in ²
	a	ambient	
	c	cyclical	
	k	constant	
	o	operating	
Q _i		Edge shear force at location i = 1, 2, 3 . . .	lb/in
R		Radius	in
	n	nut	
	u	union	
S		Effective Stress	lb/in ²
	i	at a particular location (i = 1, 2, 3, . . .)	
	n	fatigue strength for N cycles	
	u	ultimate strength	
	y	yield strength	
	f	equivalent fatigue stress	
	c	cyclical stress	
	k	constant (or mean) stress	
	m	maximum static stress	
T		Temperature	°F
	a	ambient temperature during operation	
	f	flange	
	g	fluid contained	
	n	nut	
	r	ambient temperature during assembly	
	u	union	
t		Wall thickness of tube socket	in
u _i		Radial displacement	in
W		Wrenching torque for assembly	in lb



<u>Symbol</u>	<u>Subscript</u>		<u>Units</u>
w		Radial width of bearing surface between nut and flange	in
σ		Stress	lb/in ²
	h	thermal hoop stress	
	r	thermal radial stress	
	t	bending stress in threads	
θ_i		Angular rotation	radians

Section 4

PRESSURE-ENERGIZED CANTILEVER SEALS AND HOLLOW METALLIC O-RINGS

by

J. Wallach, B. T. Fang and G. L. Harrison

4.0 Introduction

Conventional "passive" types of seals are maintained leak-tight by designing the flange system to be quite rigid. This is necessary so that the deflections caused by internal fluid pressure and pipe loads will not cause the load at the seal interfaces to drop off too far, thus resulting in a leak. The pressure-energized seal has a flexible light cross-section, which tends to expand with application of internal fluid pressure and generate a seal. It can follow deflections of the sealing face which are large compared to the deflections permissible in a "passive" type seal. Thus, the flange system for pressure-energized seals need not be as rigid and can be made lighter.

The primary function of a pressure-energized seal is to provide leak-tightness, and not to transmit structural loads from one tube to the other. Therefore, a recessed flange is often used in which to seat the seal (or a spacer may be used between the flanges). The depth of the recess or the height of the spacer determines the preload on the seal that is the sealing force at zero pressure. The area of contact between the seal and the sealing surface is generally small. A smooth surface finish is required. For structural strength, pressure-energized seals are usually made of high strength material. To facilitate plastic flow of sealing material into the asperities of the sealing surfaces, a coating of soft material such as Teflon or a soft metal plated on to the contact area is often desirable.

To summarize, the advantages of the light cross-section cantilever-type, pressure-energized seals and hollow metallic O-rings are as follows:

1. High resiliency in seal and lower clamping pressures permit less rigid light weight flanges.
2. High localized sealing stress.
3. External load is taken by other components of the connector.
4. Utilization of available pressure to enhance sealing.
5. Reduction in negative effects of extreme temperatures due to the ability of the seal to "follow through".

Some of the disadvantages are:

1. Requires a smooth surface finish
2. Comparatively complex

4.1 Types of Seals Considered

4.1.1 Cantilever-type, Pressure-energized Seals

A typical configuration of a cantilever seal in a sealing recess is shown in the following sketch:

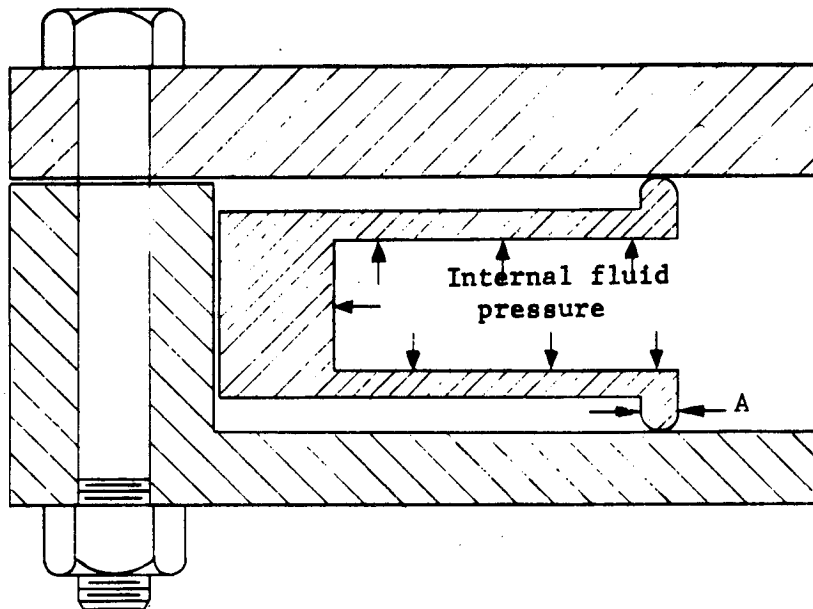


Figure 4.1. Cantilever Seal Configuration.

The seal cross-section consists of a web and two legs with a small lip on the end of each leg. The seal, which is a ring, is supported at the lip and at the outer face of the web. Internal pressure tends to push the tip toward the flange surface and provides the pressure-energizing effect. The cross-sectional dimensions of the seal are usually much smaller than the inside radius of the seal, and the seal legs are much more flexible than the web. The following three types of cantilever seals are considered; drawings for them are given in Section 4.2:

1. Seal with straight leg of constant width with lip.
2. Seal with straight leg of linearly varying thickness with lip.
3. Seal with straight leg of constant width without lip.

4.1.2 Hollow Metallic O-Rings

The following three types of O-rings are considered; drawings for them are given in Section 4.2:

1. Standard O-ring.
2. Pressure-filled O-ring.
3. Pressure-energized O-ring.

4.1.3 Choice of Seal

The O-ring and cantilever seals can be used in many applications, and there is no sharp distinction between the applications for one or the other.

Both types are available in a number of structural materials and can be coated with a number of sealing materials. Therefore, they can be made compatible with most fluids and will operate effectively over a wide range of temperatures. It is in the response of the seal to the axial clamping force and fluid pressure that the two types of seals differ. The O-ring seal has a sturdier cross-section, and a larger sealing pressure can be realized at assembly. It should be used for low internal pressure applications. The cantilever seal is more flexible and can be used to obtain a larger sealing pressure because of the greater pressure multiplication possible. It should be used at higher pressures. However, at very high internal pressures the O-ring is recommended for its greater structural strength. The cantilever seal can be used for internal or external pressures, but the O-ring can be used only for internal pressures unless a back-up ring is used. The pressure-energized O-rings (vented or pressurized) have no particular advantage over the plain O-rings.

4.2 Details of Design

4.2.1 Material Selection

For the user of available pressure-energized seals, consideration must be given to:

1. Resiliency
2. Permissible deflections
3. Strength
4. Compatibility of materials in the seal with fluid handled
5. Temperature range
6. Differential thermal expansion
7. Weight
8. Pressure limitations
9. Cost

The seal designer must also give consideration to ease of fabrication and those basic properties of the material which affect the above items.

4.2.2 Determination of Sealing Force

Presumably, for the user of commercially available pressure-energized seals, information on sealing force will be available from the vendor.

One who designs seals will have to determine from fundamental considerations, the sealing force required; but because of the many variations possible in design there is no one solution. A guide to the stress required in the seal area and leakage prediction is given in Section 1 of this handbook for various materials for seals about one-eighth-inch wide. Thus, for a seal with a flat-faced lip one-eighth-inch wide seating squarely against the flange face, these values of stress can be used to calculate the force needed per inch of seal. However, the applicability of these values decreases as one departs radically from a one-eighth-inch width. Thus, for a very narrow line seal, likely in some self-energized seals, the appropriate stress level would be somewhat higher. If the contact lip had a semicircular contact section (as shown in Figure 4.1) and the materials were homogeneous and remained elastic, then the equation for maximum contact stress σ_c between

a cylinder and plane, for a given force per inch of length g , could be used. It is:

$$\sigma_c = 0.798 \sqrt{A \frac{g}{\left[\frac{1-\nu_1^2}{E_1} + \frac{1-\nu_2^2}{E_2} \right]}} \quad (4.1)$$

where the subscripts 1 and 2 refer to the two materials in contact.

Usually the required conditions noted will not be met and the calculations are at best a rough guide. If the seal is a homogeneous metal, the condition of remaining entirely elastic in the contact region must be violated to effect a seal. If it is coated with a softer material, such as an elastomer or a plastic, the assumption of homogeneity will be violated.

The recommended approach to making such designs is to utilize, with discretion and judgment, data that is available in Section 1 of this handbook and the vendor's catalogs, approximate calculations one can make, and then check the resulting design experimentally to make certain that it is satisfactory. Such an experiment will be a check against errors made in determining proper seal force per inch of seal length, as well as a check against errors resulting from approximations made elsewhere in the design, and is most important.

4.2.3 Detailed Design Procedure for Specific Seals

4.2.3.1 Accuracy of Seal Design Using Nomographs

The detailed design of specific seals has been based on the use of nomographs. These nomographs are recognized for the ease of operation and for the time saved in the solution of the design formulas of Ref. 4.1. It should also be recognized that the use of nomographs can produce small inaccuracies due to the graphical presentation of the design formulas. Various scales, scale ranges, and scale arrangements have been used to minimize this loss in accuracy. Since the detailed design procedure can involve iterative calculations, it is recommended that the nomographs be used until a satisfactory design is obtained at which time the design formulas of Ref. 4.1 should be used as a check.

The design formulas are based on an elastic analysis of somewhat idealized mathematical models. Therefore, the nomographs and design formulas must be applied with care. The geometry of the seal must be well approximated by the mathematical model. A proper application of the formulas will result in very adequate design calculations, even if the seal is slightly deformed plastically. Once plastic deformation has occurred, the recovery is elastic and the nomographs and formulas can be used to calculate the elastic recovery.

4.2.3.1.1 Cantilever-type, Pressure-energized Seals

For a seal with straight leg of constant width:

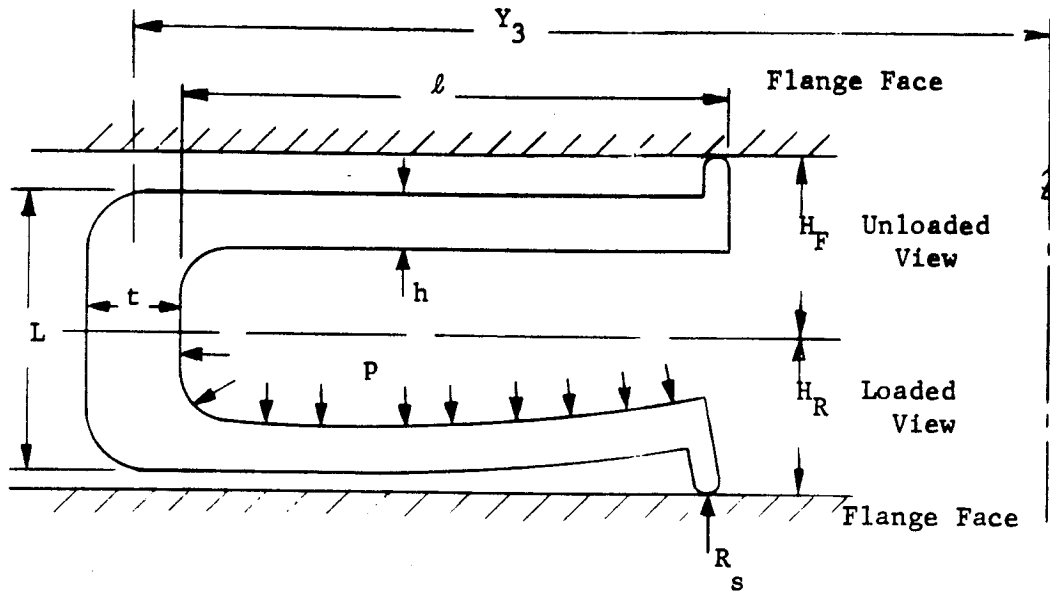


Figure 4.2. Cantilever Seal - Loaded.

- a) Assume a value of the leg length to thickness ratio l/h . This parameter defines the proportions of the seal leg.
- b) From the required sealing force R_s^* determine the initial deflection parameter $\frac{YlE^*}{1-\nu^2}$ at the tip of the seal from Figure 4.6.
- c) Determine the minimum seal leg length l_{min} from Figure 4.7. l_{min} is the minimum length the seal leg can be and have the stress within the maximum allowable stress σ_b at $p=0$.
- d) Determine the critical seal leg length l_{crit} from Figure 4.8. l_{crit} is the length of seal leg required for the stress to be zero at $p=p$.
- e) If $l_{crit} \geq l_{min}$: choose a length l equal to l_{min} , omit steps (f, g, and h) and proceed with step (i).
- f) If $l_{crit} < l_{min}$: determine the maximum length l_{max} from Figure 4.9. l_{max} is the maximum length the seal leg can be and have the stress within the maximum allowable stress at $p=p$.
- g) If $l_{max} \geq l_{min}$: choose a length l equal to l_{min} , omit step

(h) and proceed with step (i).

- h) If $l_{max} < l_{min}$: choose a new, lower value of l/h and return to step (b).
- i) Based on the length l and the value of l/h selected, calculate h .
- j) Choose a web length L as short as possible consistent with the overall structural requirement and deflection of the seal.
- k) Calculate the depth of the flange recess, $2H_r$, from

$$2H_r = 2H_f - 2Y_{\ell}^* \quad (4.2)$$

- l) Determine the web thickness t from the dual requirements

$$t \geq h \quad (4.3)$$

and

$$t \geq \frac{pr_3}{\sigma_m} \quad (4.4)$$

- m) Note that the calculation of deflection neglects deflection of the web. Check to see that $t \geq 2h$ and that $L/t < 1$. If these conditions are not met, it is advisable to recheck the deflection Y_{ℓ}^* including web deflection, or to increase t .

If the seal leg is at an angle ϕ to the flange face as shown in the following drawing:

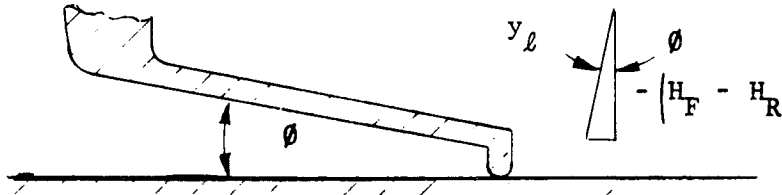


Figure 4.3. Cantilever Seal - Angled.

Design procedure for this case is as follows:

- a) Assume a value of the leg length to thickness ratio l/h . This parameter defines the proportions of the seal leg.
- b) From the required sealing force R_s^* and the angle θ determine the initial deflection parameter $\frac{YlE}{1-\nu^2}$ at the tip of the seal from Figure 4.10.
- c) Determine the minimum seal leg length l_{min} from Figure 4.7. l_{min} is the minimum length the seal leg can be and have the stress within the maximum allowable stress σ_b at $p=0$.
- d) Determine the critical seal leg length l_{crit} from Figure 4.8. l_{crit} is the length of seal leg required for the stress to be zero at $p=p$.
- e) If $l_{crit} \geq l_{min}$: choose a length l equal to l_{min} , omit steps (f, g, and h) and proceed with step (i).
- f) If $l_{crit} < l_{min}$: determine the maximum length l_{max} from Figure 4.9. l_{max} is the maximum length the seal leg can be and have the stress within the maximum allowable stress at $p=p$.
- g) If $l_{max} \geq l_{min}$: choose a length l equal to l_{min} , omit step (h) and proceed with step (i).
- h) If $l_{max} < l_{min}$: choose a new lower value of l/h and return to step (b).
- i) Based on the length l and the value of l/h selected, calculate h .
- j) Choose a web length L as short as possible consistent with the overall structural requirement and deflection of the seal.
- k) Calculate the depth of the flange recess, $2H_r$, from

$$2H_r = 2H_f - 2Y_l^* \cos\theta$$

- l) Determine the web thickness t from the dual requirements

$$t \geq h \quad (4.5)$$

$$t \geq \frac{pr_3}{\sigma_m} \quad (4.6)$$

- m) Note that the calculation of deflection neglects deflection of the web. Check to see that $t \geq 2h$ and that $\frac{L}{t} < 1$. If

these conditions are not met, it is advisable to recheck the deflection Y_{ℓ}^* including web deflection, or to increase t .

For a seal with straight leg of linearly varying thickness:

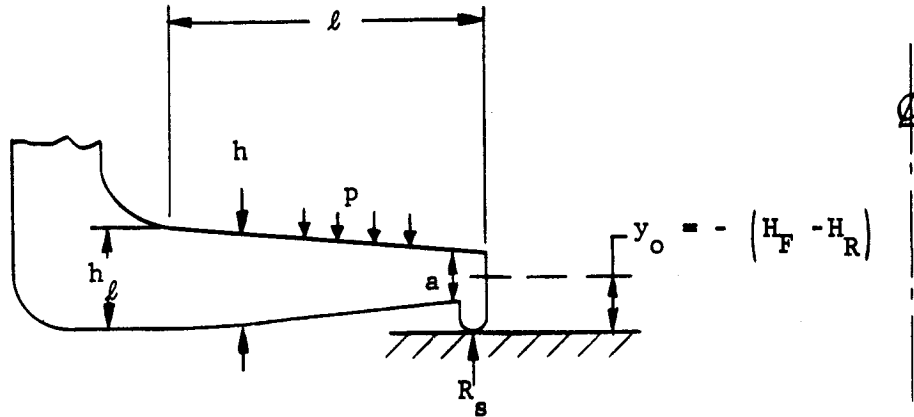


Figure 4.4. Tapered Cantilever Seals

- Assume values for the ratios l/h_{ℓ} and l/a , which specifies the ratio $h_{\ell}/a = \frac{1}{l/h_{\ell}} \times l/a$.
- From the required sealing force R_s^* determine the minimum seal leg length l_{min} from Figure 4.11. l_{min} is the minimum length the seal leg can be and have the stress within the maximum allowable stress σ_b at $p=0$.
- Determine the critical seal leg length l_{crit} from Figure 4.12. l_{crit} is the length of seal leg required for the stress to be zero at $p=p$.
- If $l_{crit} \geq l_{min}$: choose a length l equal to l_{min} , omit steps (e, f, and g) and proceed with step (h).
- If $l_{crit} < l_{min}$: determine the maximum length l_{max} from Figure 4.13. l_{max} is the maximum length the seal leg can be and have the stress within the maximum allowable stress at $p=p$.
- If $l_{max} \geq l_{min}$: choose a length l equal to l_{min} , omit step (g) and proceed with step (h).
- If $l_{max} < l_{min}$: choose a new, lower value of l/h_{ℓ} and return to step (a).
- Determine the initial deflection Y_0 at the sealing end from Figure 4.14.

- i) Calculate (h_ℓ) and (a) from the assumed ratios of ℓ/h_ℓ and ℓ/a , based on the ℓ length ℓ .
- j) If the values (Y_o) , (h_ℓ) , (a) and (ℓ) are not a reasonable design, return to step (a) and assume new ratios ℓ/h_ℓ and a/ℓ .
- k) Choose a web length L as short as possible consistent with the overall structural requirement and deflection of the seal.
- l) Calculate the depth of the flange recess, $2H_r$, from

$$2H_r = 2H_f - 2Y_o \quad (4.7)$$

- m) Determine the web thickness t from the dual requirements.

$$t \geq h_\ell \quad (4.8)$$

$$t \geq \frac{pr_3}{\sigma_m} \quad (4.9)$$

- n) Note that the calculation of deflection neglects deflection of the web. Check to see that $t \geq 2h$ and that $L/t < 1$. If these conditions are not met, it is advisable to recheck the deflection Y_o including web thickness, or to increase t .

A seal with straight leg of constant width without tip (Figure 4.5)

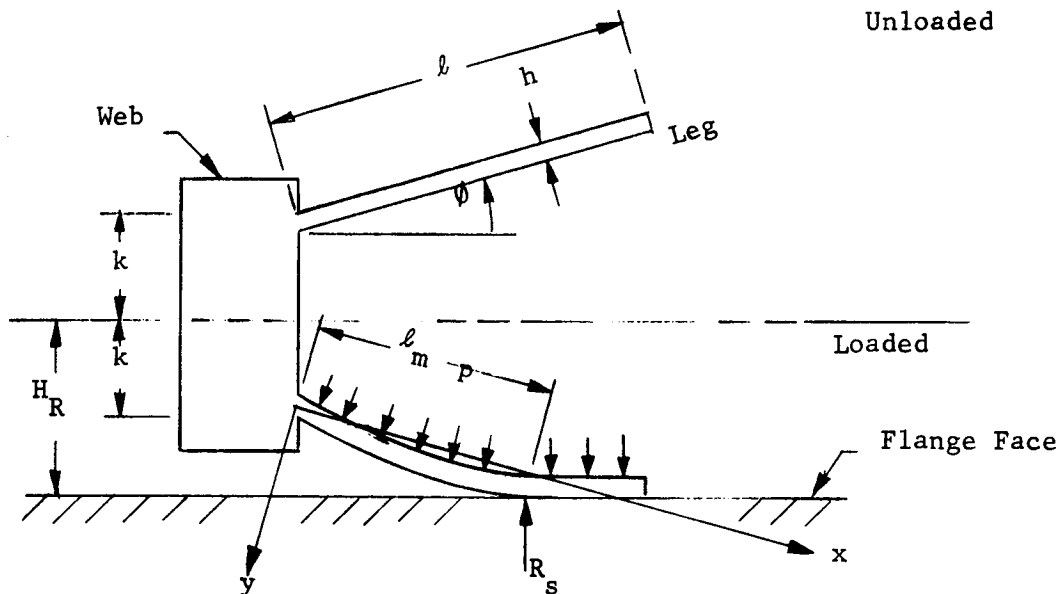
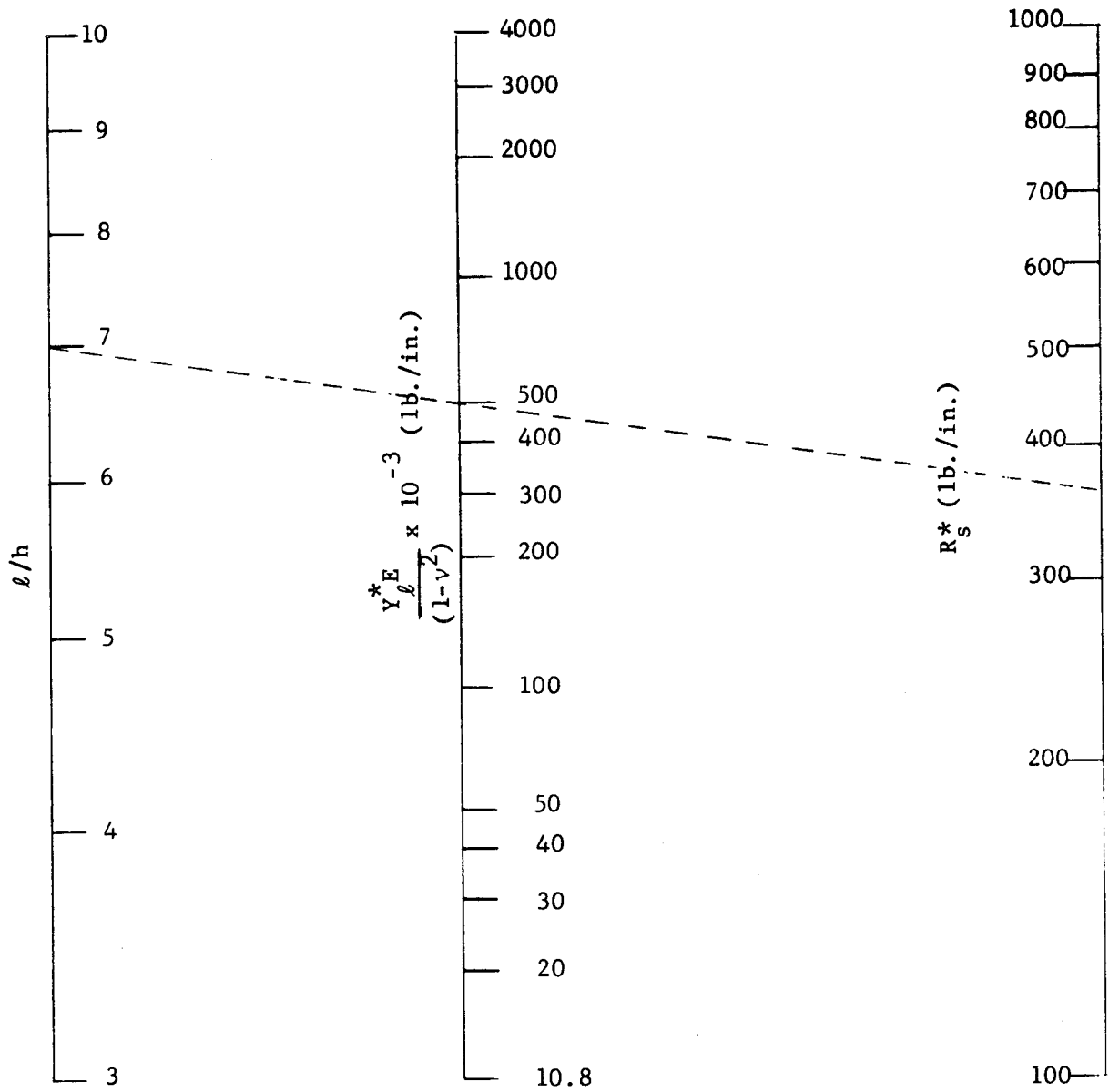
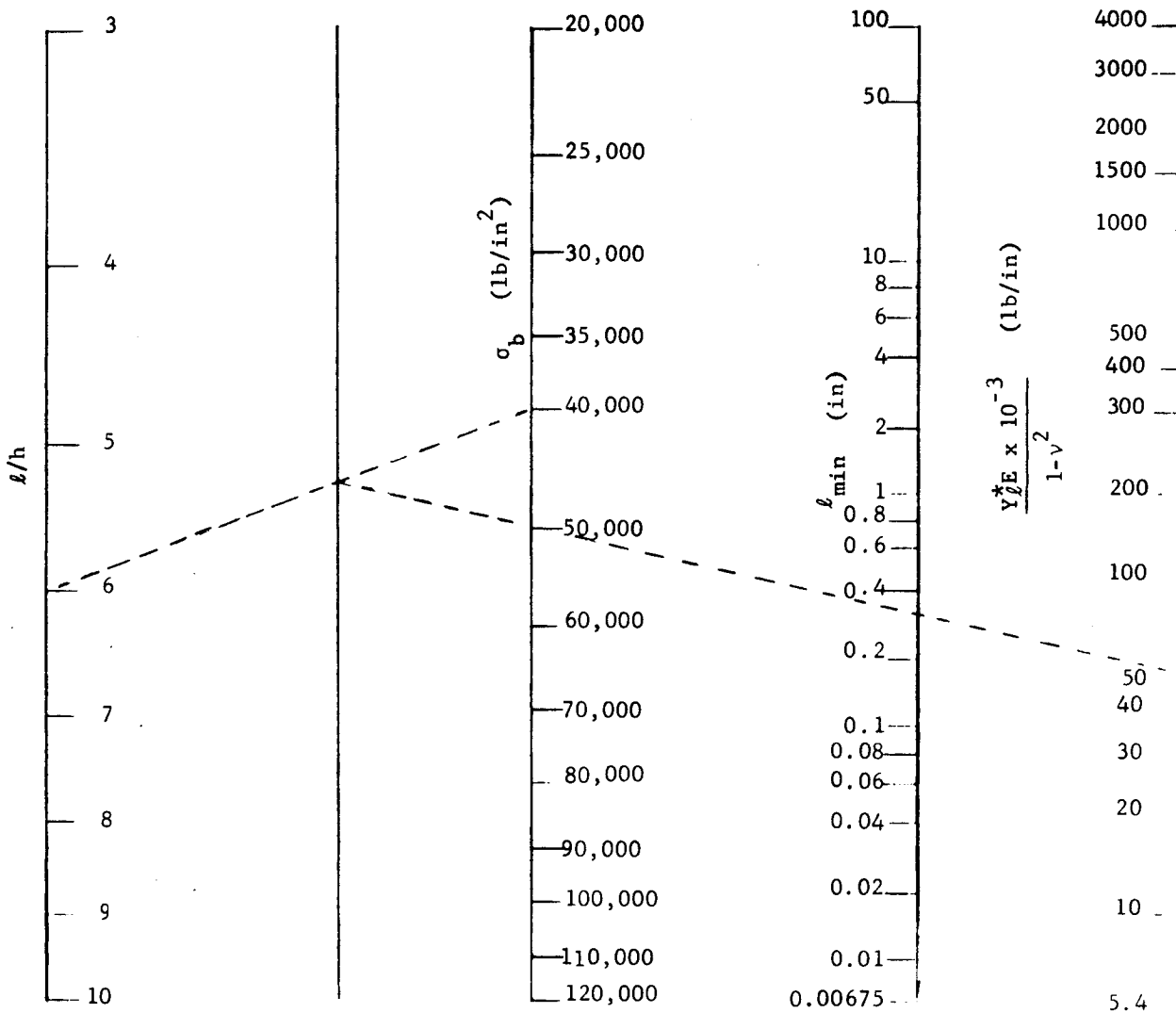


Figure 4.5. Angled Cantilever Seal Without Tip.



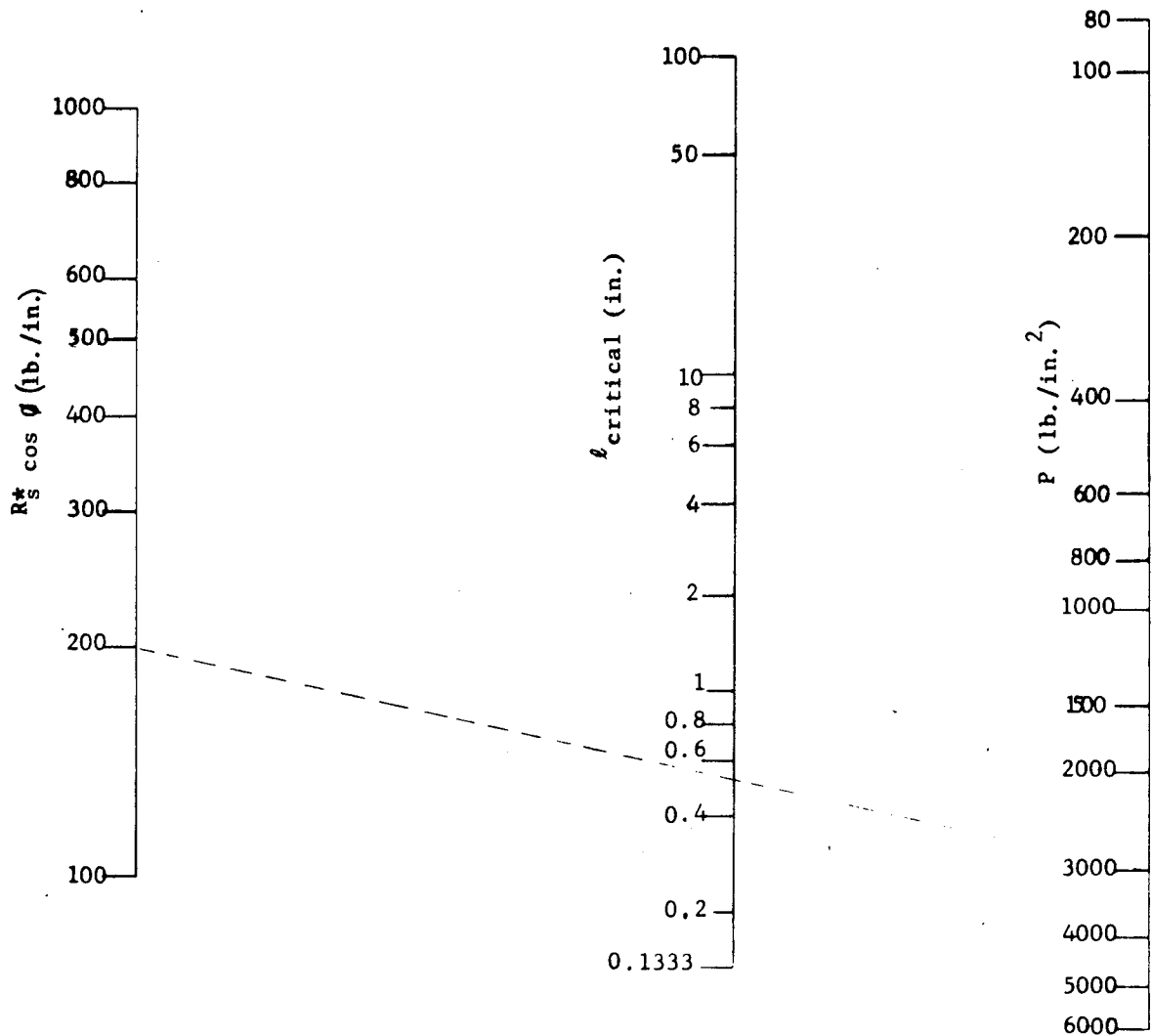
$$Y_l^* = \frac{4R_s^*}{E} (1 - \nu^2) (l/h) \quad (\text{Ref. 4.1, Eq. 5})$$

Figure 4.6. Nomograph - Straight Contilever Seal Design - $\phi = 0$



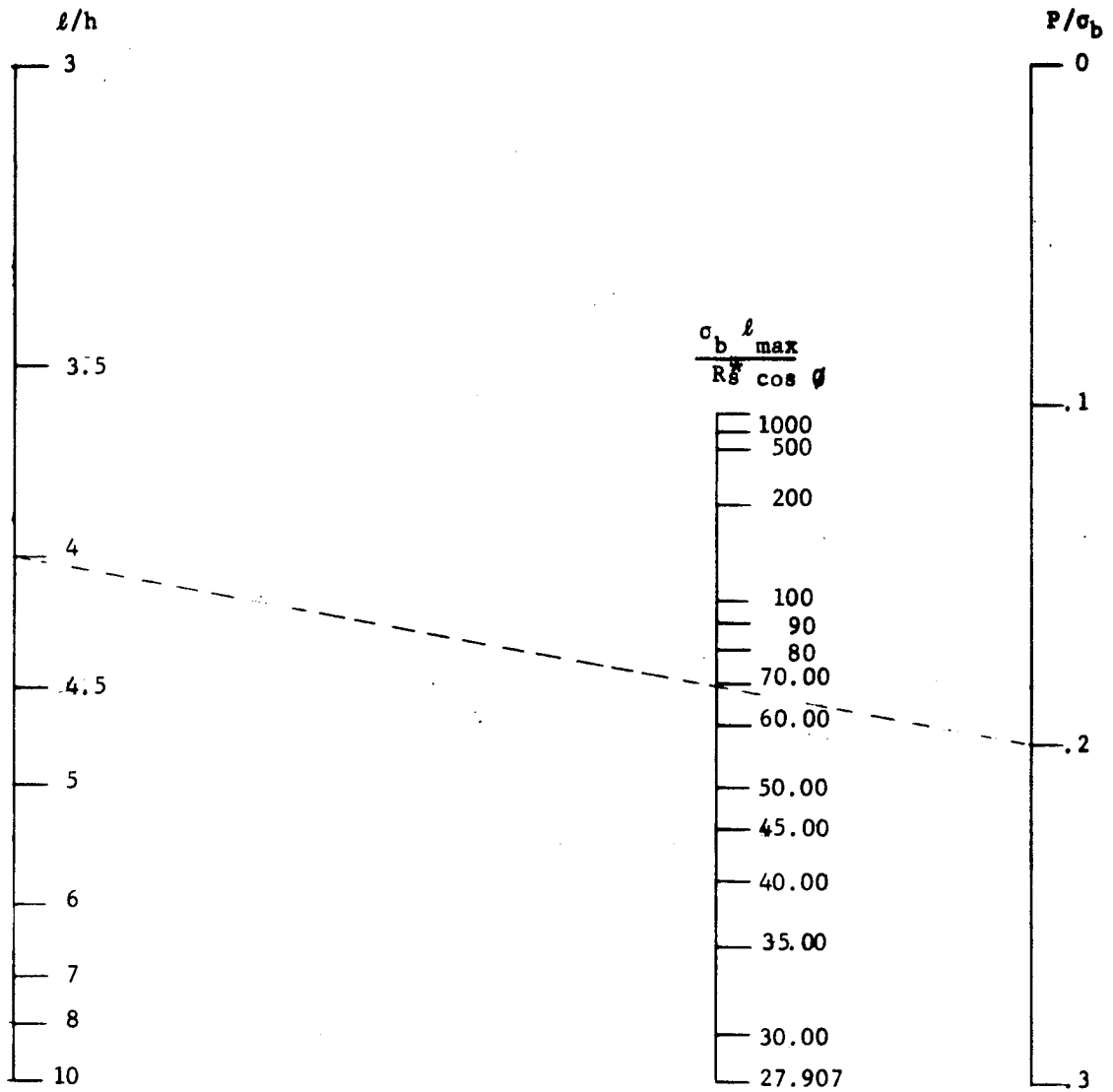
$$l_{min} = \frac{3/2 Y^*E}{(1-\nu^2) (l/h) \sigma_b} \quad (\text{Ref. 4.1, Eq. 6, } p = 0)$$

Figure 4.7. Nomograph - Straight Cantilever Seal Design - $\phi = \phi$.



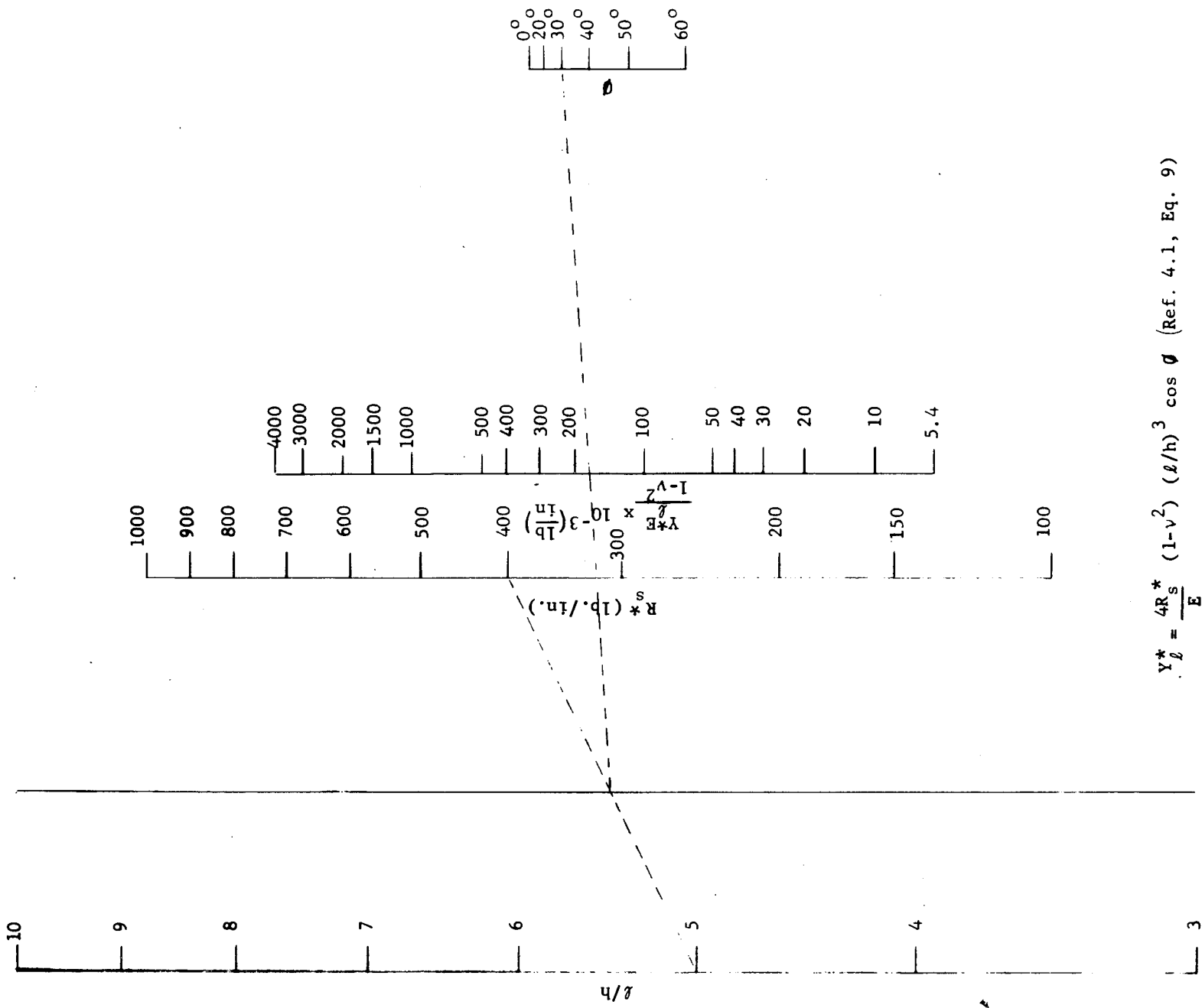
$$l_{\text{crit}} = \frac{8R_s^*}{P} \cos \phi \quad (\text{Ref. 4.1, Eqs. 5, 6, and 9, } \sigma_b = 0)$$

Figure 4.8. Nomograph - Straight Cantilever Seal Design - $\phi = \phi$.



$$\frac{1}{\frac{\sigma_b l_{\max}}{R_s}} = \frac{1}{8} P/\sigma_b - \frac{1}{6} (\ell/h)^2 \quad (\text{Ref. 4.1, Eqs. 5, and 6, } P > P_{\text{crit}})$$

Figure 4.9. Nomograph - Straight Cantilever Seal Design - $\phi = \phi$.



$$Y_l^* = \frac{4R_s^*}{E} (1-\nu^2) \left(\frac{l}{h} \right)^3 \cos \phi \quad (\text{Ref. 4.1, Eq. 9})$$

Figure 4.10. Nomograph - Straight Cantilever Seal Design - $\phi = \phi$.

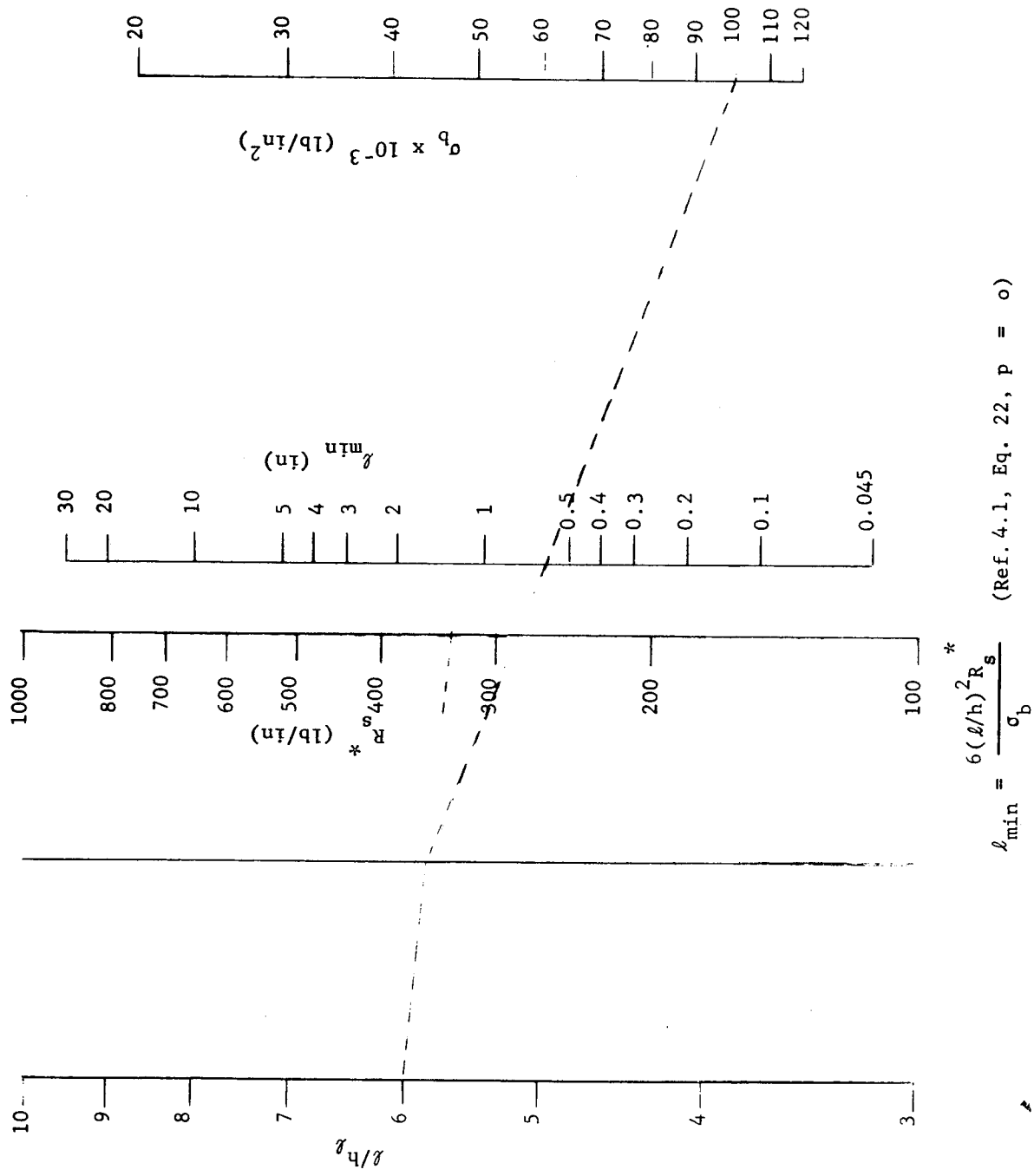
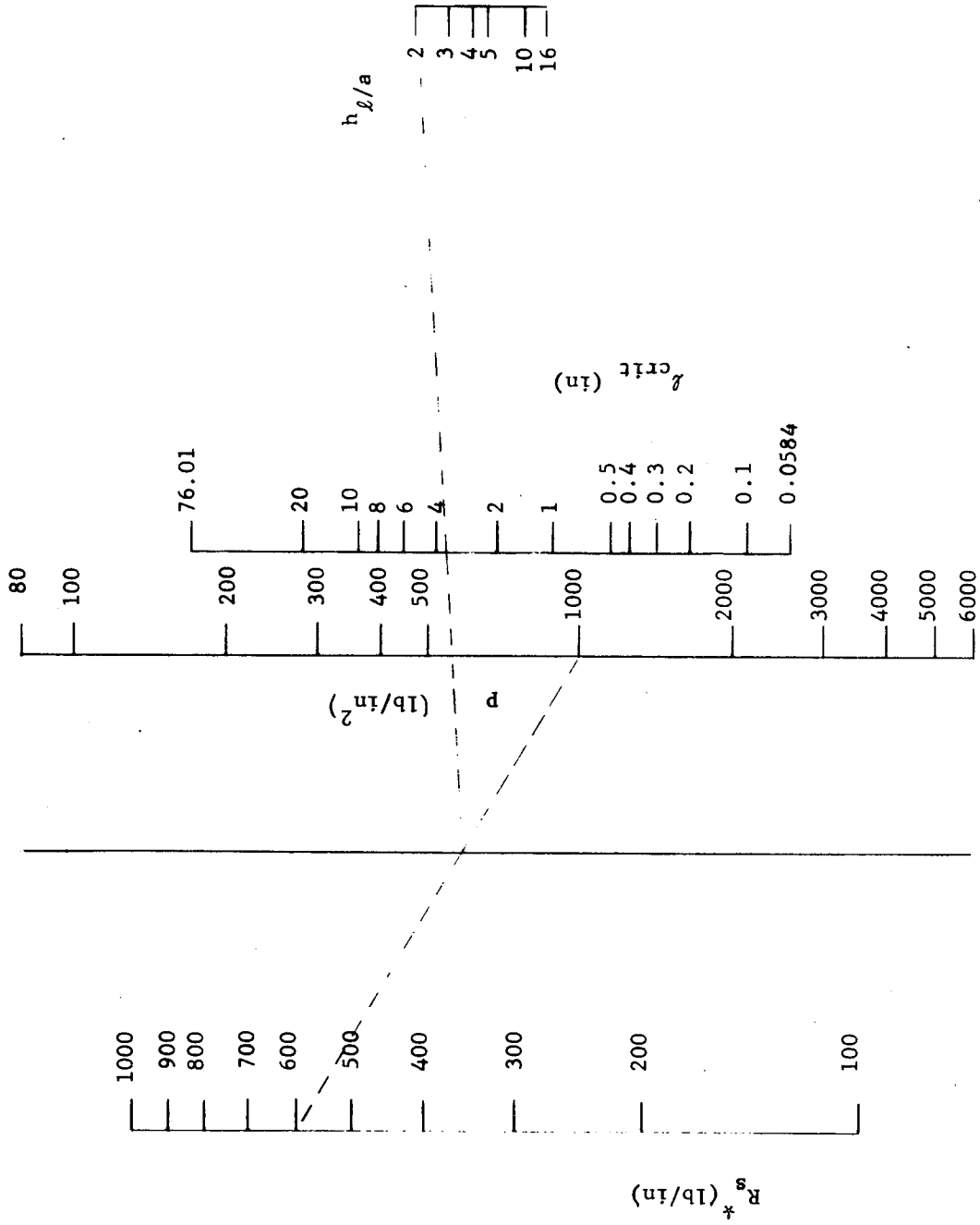


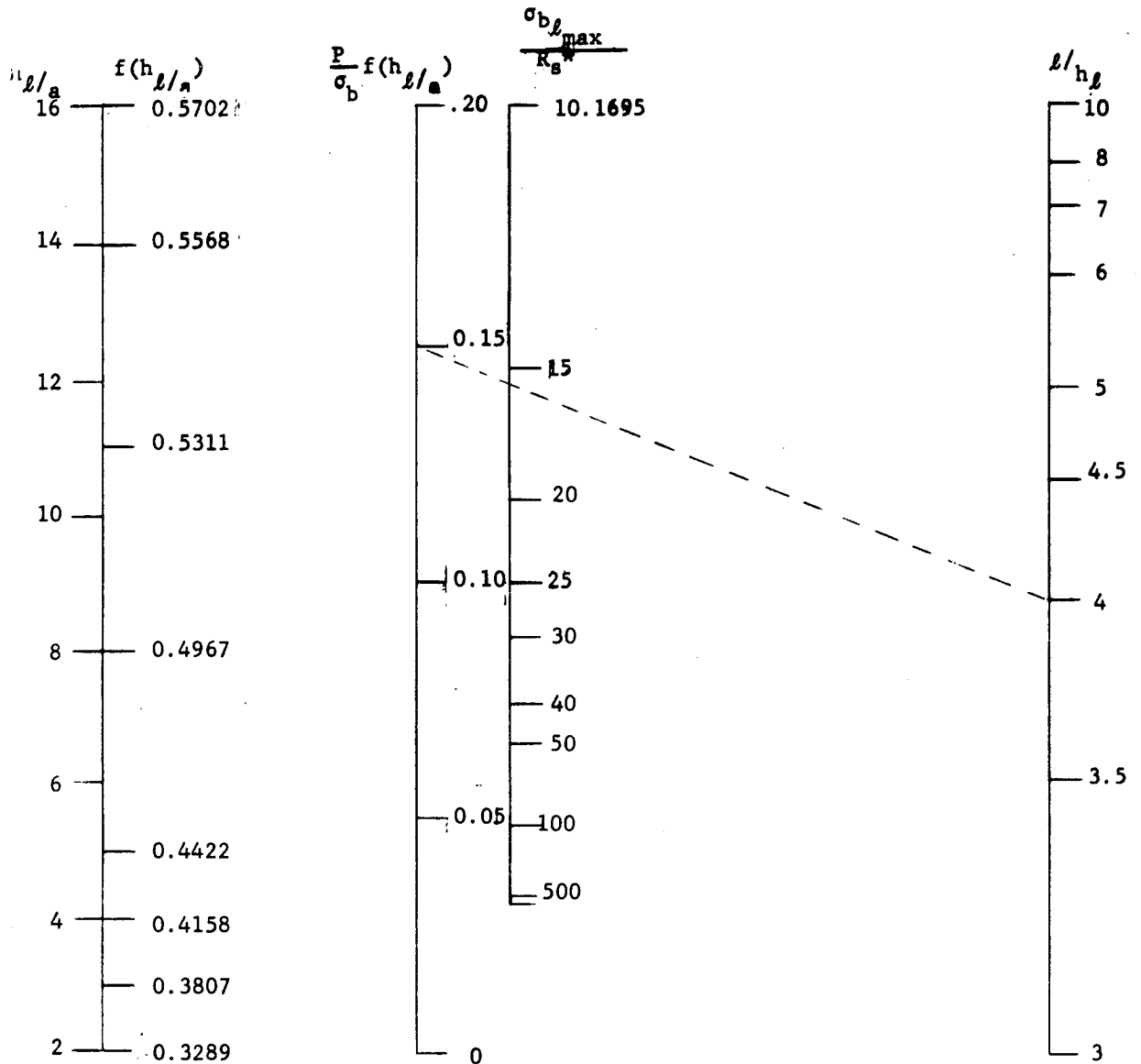
Figure 4.11. Nomograph - Cantilever Seal Design - Varying Thickness.



$$l_{crit} = \frac{2R_g^*}{P \left(1 + \frac{6(h_{l/a}^{-1}) + 9(h_{l/a}^{-1})^2 + 2(h_{l/a}^{-1})^3 - 6(h_{l/a}^{-1})^2 \log h_{l/a}}{(h_{l/a}^{-1})(3h_{l/a}^{-1} - 2(h_{l/a}^{-1})^2 \log h_{l/a})} \right)}$$

(Ref. 4.1, Eq. 22, $\sigma_b = 0$)

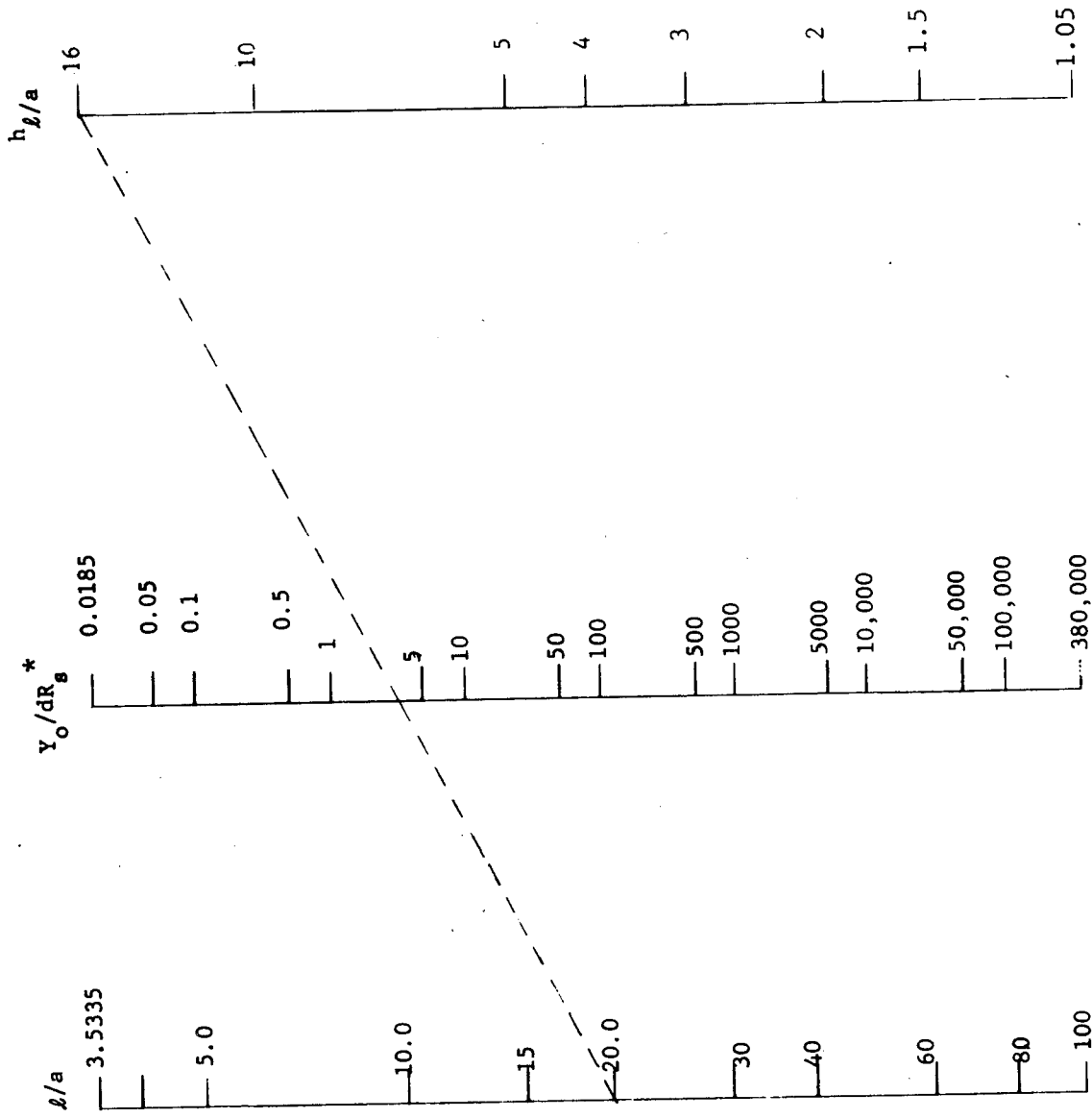
Figure 4.12. Nomograph - Cantilever Seal Design - Varying Thickness.



$$\frac{6R_s^*}{\sigma_b l_{max}} = \frac{3P}{\sigma_b} f(h_l/a) - (h_l/l)^2 = \frac{3P}{\sigma_b} \left\{ 1 + \frac{[6(h_l/a - 1) + 9(h_l/a - 1)^2 - 6(h_l/a)^2 \log h_l/a + 2(h_l/a - 1)^3]}{(h_l/a - 1) [(h_l/a - 1)(3h_l/a - 1) - 2(h_l/a)^2 \log h_l/a]} \right\} (h_l/l)^2$$

(Ref. 4.1, Eq. 22, $P > P_{crit}$)

Figure 4.13. Nomograph - Cantilever Seal Design - Varying Thickness.



$$(a/l)^3 \frac{Y_o}{dR_s} = \frac{1}{2} (a/h_l)^2 \frac{(3h_l/a-1)}{(h_l/a-1)^2} - \frac{\log h_l/a}{(h_l/a-1)^3} \quad (\text{Ref. 4.1, Eq. 21})$$

Figure 4.14. Nomograph - Cantilever Seal Design - Varying Thickness.

behaves differently from the two seals discussed above in that the point of sealing and the active seal-leg length change with the internal pressure. This makes the design calculations more complicated and the optimization of design difficult. Because of this complication and because of no particular advantage to this configuration, design procedures are not given here. For those who prefer to use this configuration, see Ref. 4.1 for detailed design procedures.

Examples

To illustrate the characteristics of the first three seals and the use of the nomographs, an example design for each seal is given below. The following steps agree exactly with the steps outlined in the procedure sections.

Example #1 - Seal with straight leg of constant width

Let $R_s^* = 200$ lb, required load
 $P = 5000$ lb/in², design pressure
 $\sigma_b = 40,000$, allowable bending stress
 $l/h = 6$, arbitrarily selected
 $\theta = 0$, $\cos\theta = 1$, design requirement

a) $l/h = 6$

b) From Figure 4.6, $\frac{Y_l^* E}{1-\nu^2} = (175)(10^3)$ lb/in

c) From Figure 4.7, $l_{min} = 0.95$

d) From Figure 4.8, $l_{crit} = 0.35$

e) N/A

f) $l_{crit} < l_{min}$ From Figure 4.9 $l_{max} = 0.4$

g) N/A

h) $l_{max} < l_{min}$ - choose $l/h = 4$

b) From Figure 4.6, $\frac{Y_l^* E}{1-\nu^2} = (50)(10^3)$

c) From Figure 4.7, $l_{min} = 0.45$

d) From Figure 4.8, $l_{crit} = 0.35$

e) N/A

f) $l_{crit} < l_{min}$ From Figure 4.9 $l_{max} = 1.00$

g) $l_{max} \geq l_{min}$ Choose $l = l_{min} = 0.45$

h) N/A

i) $l/h = 4, l = 0.45: h = \frac{0.45}{4} = 0.1125$

Example #2 - Seal with straight leg of constant width at an angle ϕ .

Let $R_s^* = 400$, required load

$p = 3000$, design pressure

$\sigma_B = 80,000$, allowable bending stress

$l/h = 5$, arbitrarily chosen

$\phi = 40^\circ$, $\cos\phi = 0.766$, selected or design requirement

a) $l/h = 5$

b) From Figure 4.10 $\frac{Y^* E}{l(1-\nu^2)} = (170)(10^3)$

c) From Figure 4.7 $l_{min} = 0.5''$

d) From Figure 4.8 $l_{crit} = 0.8''$

e) $l_{crit} > l_{min}: l = l_{min} = 0.5''$

f) N/A

g) N/A

h) N/A

i) $l = 0.5, l/h = 5.0: h = 0.1$

Example #3 - Seal with straight leg of linearly varying thickness

Let $R_s^* = 400$, Required load,

$p = 4000$, Design pressure

$\sigma_B = 100,000$, Allowable bending stress

$\nu = 0.3$ Material property

$E = (30)(10^6)$ Material property

- a) Assume $l/h_\ell = 5$ and $l/a = 10$: hence $h_{\ell/a} = 2$
- b) From Figure 4.11 $l_{min} = 0.45$
- c) From Figure 4.12 $l_{crit} = 0.50$
- d) $l_{crit} \geq l_{min}$: $l = l_{min} = 0.45$
- e) N/A
- f) N/A
- g) N/A
- h) From Figure 4.14 $Y_o = 0.0124$
- i) $l/h_\ell = 5$, $l/a = 10$, $l = 0.45$: $h_\ell = 0.09$ and $a = 0.045$

4.2.3.1.2 Hollow Metallic O-Rings

The following drawings show the differences of the three different O-rings considered here:

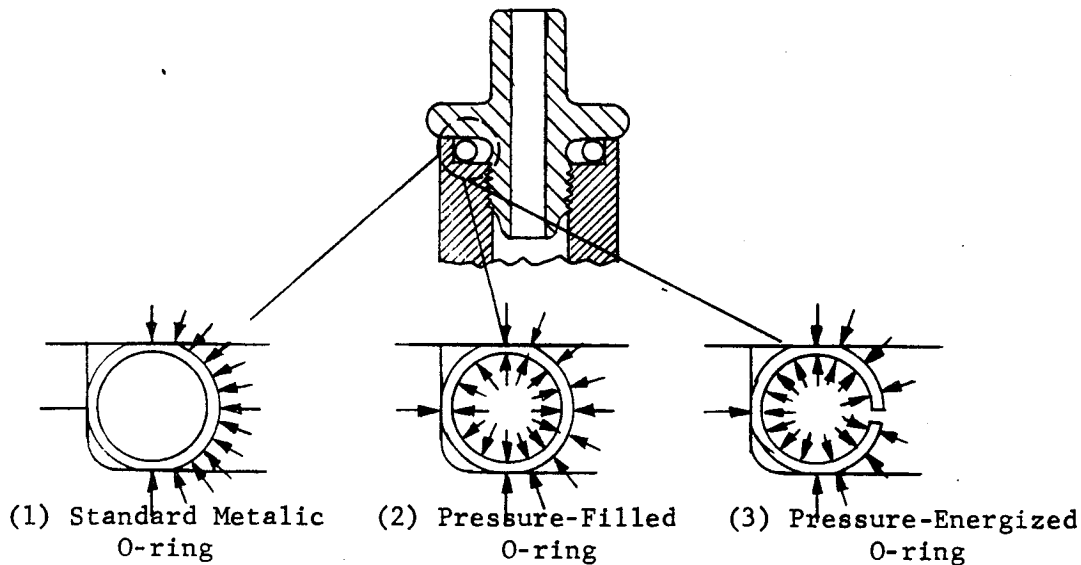


Figure 4.15. O-Ring Designs.

Except in very specialized applications, the pressure-filled O ring does not seem to offer any particular advantage. On the other hand, they are more difficult to make and have lower reliability. Because the O-rings are usually compressed to such an extent, their structural behavior are in the elasto-plastic range, rational design becomes difficult and experimental design data furnished by manufacturers have to be resorted to. In the absence of such data, the initial sealing force between the O-ring and the flanges can be estimated from the formula

$$R_s = \pi h^2 \sigma_y / 4b \quad (4.10)$$

This sealing force should be greater than the minimum required sealing force as established by tests or by the considerations of Section 1.

The formula assumes a perfectly flat flange, but is also applicable if there is a small amount of flange warpage. However, the seal cannot compensate for a large flange warpage over a short circumferential length of the flange.

The decrease of the sealing force with the separation of the flanges can be estimated from the formula,

$$\begin{aligned} \text{(Decrease of sealing force)} &= \text{(Elastic spring constant of O-ring)} \\ &\times \text{(amount of flange separation)} \end{aligned} \quad (4.11)$$

where the elastic spring constant of an O-ring is

$$K = \frac{D}{b^3} \left[0.149 - \frac{0.141}{1 + 14.4/\mu^2} \right] \quad (4.12)$$

The amount of compression at which the O-ring material starts to yield is given approximately by

$$\delta = \frac{2}{3} R_s / K \quad (4.13)$$

Theoretically, with an O-ring having soft-coating material, there does not seem to be any advantage to compress the O-ring initially much beyond the amount 3δ . In other words, the difference between the O-ring outside diameter and the flange groove depth might be taken as

$$3\delta = 2R_s / K \quad (4.14)$$

Manufacturing tolerances, however, may make it necessary to increase this amount considerably. The 3δ is a minimum value to which the manufacturing tolerance on the O-ring cross-sectional diameter and the flange groove depth are added to obtain the maximum value. In order to retain reasonable manufacturing costs, the tolerances cannot be too tight. As the 3δ is small compared to the tolerances, the maximum value is considerably larger than the minimum value. This is perhaps one of the reasons why most O-rings presently in use are compressed far beyond the 3δ value.

In the installation of O-rings it is important that some kind of mechanical back-up, such as back-up rings, should be provided. This not only prevents excessive hoop expansion of the O-ring but also tends to increase the sealing force.

4.3 Reference

Fang, B. T., (Editor), "Pressure-energized Seals", Design Criteria for Zero-Leakage Connectors for Launch Vehicles, Vol. 5, General Electric Company Technical Information Report No. 63GL45, March 15, 1963, (NASA Contract No. NAS 8-4012).

4.4 Nomenclature

A	Cylinder radius	in.
a	Seal leg thickness at small end - tapered seal leg, or O-ring tube radius	in.
b	O-ring radius	in.
d	$\frac{12(1-\nu^2)}{E}$	in ² /lb
D	$\frac{Eh^3}{12(1-\nu^2)}$ Bending rigidity	in - lb
E	Modulus of elasticity	lb/in. ²
h	Thickness of seal leg - constant thickness seal leg or O-ring wall thickness	in.
h_ℓ	Seal leg thickness at large end - tapered seal leg	in.
H_f	Free height of seal	in.
H_r	Restrained height of seal	in.
K	O-ring elastic spring constant	lb/in.
k	Axial distance from seal centerline to outside surface of sea leg	in.
l	Length of seal leg	in.
l_{crit}	Length of seal leg to yield zero stress at $p=p$	in.
l_{max}	Maximum length seal leg can be and have the stress equal to maximum allowable σ_b at $p=p$	in.
* l_{min}	Minimum length seal leg can be and have the stress equal to maximum allowable σ_b at $p=0$	in.
L	Axial length	in.
p	Pressure	lb/in. ²
g	Bearing load	lb/in.
r	Radius of seal	in.
R_s^*	Sealing force to produce Y_ℓ^*	lb/in.



R_s	Sealing force, general	lb/in.
t	Web thickness	in.
Y_ℓ^*	Initial deflection at tip of seal leg	in.
Y_o	Initial deflection at tip of seal leg	in.
δ	Amount of compression, % /100	
ν	Poisson's ratio	
σ	Stress with subscripts	lb/in. ²
	c - contact stress	
	b - maximum allowable bending stress, $\sigma_b = 0.9\sigma_y$ *	
	m - maximum allowable membrane stress, $\sigma_m = 2/3 \sigma_y$ *	
	y - yield stress	
μ^2	$\frac{12(1-\nu^2)b^4}{a^2h^2}$	
θ	Angle	radians

* See Section 6, "Material Properties and Compatibility," for values of several materials.



Section 5

LEAKAGE MEASUREMENT TECHNIQUES

By

F. O. Rathbun, Jr.

5.0 Introduction

Following is a technique recommended for laboratory or development shop use for the measurement of leakage from separable fluid connectors. The same technique may be used for both tube connectors (diameters less than one inch) and duct connectors (diameters larger than one inch). Details for the construction of the necessary apparatus for tube leak testing are given. Similar equipment must be designed for larger sized ducts. While the general technique is applicable for both connector development use and the leak checking of production connectors, the apparatus described herein for tube connector evaluation is suitable for development work only.

The technique outlined will yield the magnitude of leakage for a given connector under a given assembly procedure for variable pressure differences across the seal; leakage rates from 10^{-3} atm cc/sec to less than 10^{-9} atm cc/sec can be measured. Internal pressures up to 2000 psi are attainable in the system described. The method outlined is applicable for static conditions at room temperature only. A discussion of tests suitable for other environments is given. A simpler technique for leak detection only is described.

It is recommended that when a leak measurement facility is initially established, a qualified vacuum technology technician be consulted on component assembly and check out.

5.1 Leakage Measurement Requirements

The use of a common gas (helium) in all connectors allows a single leakage rate measurement instrument to be used in all tests. Briefly, the technique consists of:

1. Providing a means of supplying high-pressure helium to the interior of the connector.
2. Constructing a vacuum chamber exterior to the connector.
3. Providing a means of evacuating the vacuum chamber.
4. Attaching a calibrated helium mass spectrometer leak detector to the vacuum chamber for measurement of the actual connector leak.

5.2 Test Apparatus

5.2.1 Test Chamber for Tube Connectors

A test vacuum chamber capable of being used with a commercial leak

detector and a helium high-pressure tank is shown in detail in Figure 5.1 (parts list is included). The same basic vacuum chamber can be used for all tube connectors with a maximum diametral dimension of 2.5 inches and a maximum length of 4.5 inches by utilizing end plates with different sized tubing holes. Provision in the design is made for standard outside diameter tube sizes from one-eighth-inch to one inch. Also shown in Figure 5.1 is the means of attaching end fittings to the test tubing.

5.2.2 High-pressure System

High-pressure helium can be introduced into the tubing by the use of a commercial high-pressure tank. Associated equipment for the high-pressure system includes:

- a. A pressure regulator (example: Hoke helium regulator #521B10 model) to enable the connector to be pressurized at a programmed rate.
- b. A particle filter (example: Micro Metallic Division, Pall Corporation, Part #ABH-706-2 Inline Filter, Grade H, 1 Micron Filtration) to insure a low level of particle size inside the connector.
- c. A pressure gage (example: Acco Helicoid Gage) to determine the pressure within the test length of tubing.
- d. A cold trap, consisting of a U-section of high-pressure tubing immersed in a dewar filled with liquid nitrogen to remove most of the moisture content in the helium.
- e. A high-pressure line restriction (example: Pneu-trol 1/8 inch NV 1000 S.S. needle valve) to reduce high-pressure helium flow in event of a catastrophic connector failure.

The tubing system for the high-pressure system is shown in Figure 5.2. One-quarter-inch 304 stainless steel tubing (wall thickness-0.049 inch) is adequate for the high-pressure lines. Swagelok stainless steel fittings may be used throughout.

5.2.3 Mass Spectrometer - Vacuum System

Necessary components for the vacuum system are the leak detector, a thermocouple vacuum gauge, a rotary roughing pump, a set of calibrated standard leaks, and a manifold with provisions for appropriate valving and component attachment. Figure 5.3 shows a typical layout for the system.

Several mass spectrometer leak detectors are commercially available, all being able to detect leakage rates to below 10^{-8} atm cc/sec. A partial list of American made leak detectors is given below for convenience.

1. General Electric M-60 Mass Spectrometer Leak Detector.
2. Consolidated Electrodynamics Type 24-120A Leak Detector.
3. Veeco MS-9A Leak Test Station.

4. Elion DLD 1101 Mass Spectrometer Leak Detector.

5. Vacuum Instrument Corporation Model MD-140 Mass Spectrometer Leak Detector.

Each of the above leak detectors has incorporated into it the necessary pumps to evacuate its own vacuum components; however, an external pump is required to evacuate the test chamber. Each leak detector manufacturer can provide such a pump.

A thermocouple vacuum gauge cell (and the associated electronic equipment) is required in order that the vacuum level in the test chamber can be determined. Typical cells are affixed with one-eighth-inch male pipe threads which can be threaded into a manifold (and then sealed with a vacuum sealant).

A series of standard calibrated leaks are required to calibrate the leak detector (see Section 5.3). Provision must be made in the manifold for insertion of the leak into the system. A compression fitting on the manifold is suitable; however, the type and size of the standard leak to be used must be determined prior to establishing fitting dimensions.

A partial list of calibrated helium leak manufacturers is given below. Listed are the range of leaks, along with the type construction, and means of gas supply.

<u>Manufacturer</u>	<u>Type</u>	<u>Gas Supply*</u>	<u>Leakage Range atm cc/sec</u>
Consolidated Electrodynamics Corp. Pasadena, California	Permeation	S.C.	10^{-6} - 10^{-10}
Elion Instruments, Inc. Burlington, New Jersey	Permeation	S.C.	10^{-8} - 10^{-9}
General Electric Co. (Instrument Dept.) West Lynn, Mass.	Capillary-glass	S.C. or Ind.	10^{-2} - 10^{-7}
Heraeus-Engelhard Vacuum, Inc. Monroeville, Pa.	Capillary Permeation	S.C. S.C.	10^{-6} - 10^{-8} 10^{-8}
Vacuum Electronics Corp. (Veeco) Plainview, L.I., N.Y.	Permeation	S.C.	10^{-9}
Vacuum Instruments Corp. Huntington Station, N.Y.	Permeation	S.C.	10^{-9}
R.H. Work Co. Paulsboro, N.J.	Permeation Capillary-glass	S.C. S.C.	10^{-6} - 10^{-10} 10^{-2} - 10^{-7}

*S.C. - Self-contained

Ind - Independently supplied.

The required manifold can be fabricated to be compatible with the other components used, or may be purchased from a leak detector vendor.

5.3 Calibration of Mass Spectrometer Leak Detector

The mass spectrometer operates by ionizing the helium molecules entering it; a current proportional to the rate of flow of helium molecules is then produced. However, the electronic circuitry involved in the instrument may be such that the relationship between output current and helium flow is not linear over the entire range of flow rates of interest. Hence, a known relationship between helium flow and output current for the particular leak detector being used must be gained for reliable leakage measurements.

A method for establishing such a relationship is that of plotting (on log-log paper) the output current of the leak detector for a series of known calibrated leaks. A curve fit of these data points yields a satisfactory relationship. A minimum of one standard leak per decade of leakage rate is sufficient.

With the vacuum system as shown in Figure 5.3, the leak detector must be calibrated with valve 3 open, valve 1 closed, and valve 2 in the same setting as when the system will be used for connector leak checks. The distribution of helium flow during both calibration and leak check operations must be the same.

Should standard leaks with self-contained helium sources be used, the leak is merely fitting properly into the system; should leaks requiring independent helium sources be used, an inverted container with helium at one atmosphere pressure placed over the standard leak will be satisfactory.

The leak detector system should be recalibrated frequently, since mass spectrometer characteristics may gradually change.

The resultant leakage rate amperage graph is used as a calibration curve for all current readings taken during a connector leak measuring experiment.

5.4 Procedure

5.4.1 General

The fluid connector is assembled and placed inside the vacuum chamber. The vacuum chamber is then leak checked by the following method:

1. The test connector is closed off from the helium source, thus allowing no helium to be present in the high-pressure system.
2. The vacuum chamber is evacuated by use of the rotary rough pump. (Valves 1 and 2 open, Valve 3 closed, Figure 5.3).
3. With the leak detector then opened to the vacuum chamber, all seals on the chamber are probed externally with a helium source. Caution should be taken that Valve 2 (Figure 5.3) is not

opened until the vacuum chamber level is sufficiently low (level depends on the detector used).

4. The leak tightness of the vacuum chamber is evaluated. Should the helium flow rate be as high as the order of magnitude of the lowest connector leak rate under consideration, the chamber must be resealed. Vacuum grease may be used on vacuum chamber fittings.

5.4.2 Tube Connector Procedure

The general procedure above applies completely. However, in addition, in assembly of the connector, the vacuum chamber end flanges are placed over the tube pieces prior to the flaring of the tube ends. (Figure 5.1) Flaring can be done with a hand flaring tool. The connector tubing is cut in order to remove the chamber flanges at the conclusion of the test.

5.5 Safety Precautions

A restriction in the high-pressure system (Figure 5.2) will prevent large flow rates into the vacuum chamber in case of a catastrophic connector failure. However, the vacuum chamber should be covered by a lead or thick wood shield to reduce the energy of the projectile fragments in case of a failure. Exacting caution in following the leak detector operating instructions is necessary for proper care of the detector.

5.6 Other Environments

Either high-temperature or low-temperature static leakage rate tests can be accomplished, if heating elements are provided internal to the vacuum chamber or a cold bath is provided external to the chamber. In both cases, additional engineering is required for the arrangement of components and instrumentation. Thermocouples on the connector should be required since some time will be required for the connector to reach a desired temperature.

5.7 Leakage Detection Testing

Should only the detection of a leak be required, then the connector can be attached directly to the leak detector system and then evacuated. A helium probe applied external to the connector while the leak detector is operating will detect most connector leaks. It must be noted, however, that only one atmosphere pressure differential exists across the seal at this time; hence, small leak rates which are present at high system pressures may not be detected. Also, since, the exterior pressure is higher than the internal pressure, the direction of leakage flow is inward. With such a condition of pressure, it is possible for some connector designs to tend to seal.

Hence, for final connector appraisal, a leak measurement test should always be accomplished.

5.8 Other Leak Detection Techniques

Other techniques, not generally as accurate nor as sensitive, but often satisfactory for development and field testing use are:

1. Soap solution bubble testing.
2. Immersion bubble testing.
3. Sonic leak detection.
4. Halide torch leak detection.
5. Constant volume pressure drop technique.

5.8.1 Soap Solution Bubble Testing

A container to be tested is pressurized and painted with a soap solution. Any leak can be seen by the growth of bubbles. The efficiency of this method depends upon: the observation abilities of the operator, the ability to completely wet the tested area, the surface tension of the soap solution, and the complexity of the part. It has been estimated that under proper conditions the sensitivity of this method is 10^{-4} atm cc/sec.

5.8.2 Immersion Bubble Testing

A pressurized vessel may be immersed in a liquid; the bubbles rising to the surface will indicate a leak. This method is dependent on the pressure capability of the vessel, surface tension of the liquid and the size of the testing area. This method is obviously not suitable to large vessels. However, modifications can be made to cover one area by a liquid. This technique is simpler than soap solution testing because the observation abilities of the operator are not as important. The sensitivity of this method is about 10^{-5} atm. cc/sec.

5.8.3 Sonic Leak Detection

Leak detectors are available to physically detect the sound made by the outflow of a gas, presumably choked flow. Manufacturers stated sensitivity of these instruments is approximately 10^{-1} atm. cc/sec.

5.8.4 Halide Torch Leak Detection

The halide leak detector consists of a propane gas torch with a copper plate in the flame with air. The system to be tested is pressurized with Freon gas and the end of the rubber tube which supplies air to the flame is passed over the suspected area. A leak is detected when the flame turns bright green, since a piece of copper in a flame containing halogen atoms gives off a characteristic green flame. This equipment is often used by household refrigerator repairmen because the refrigerant (Freon) acts as the tracer gas and the equipment is inexpensive. The sensitivity of this method is reported to be approximately 10^{-5} atm. cc/sec.

5.8.5 Container Volume Pressure Drop Technique

A container may be pressurized with a gauge attached to it which will show the pressure drop. This essentially is a method of measuring the leakage

rate. The sensitivity of this method is defined by the equation:

$$Q = \frac{V\Delta P}{\theta}$$

where Q = leakage rate sensitivity (cm/sec)

V = container volume (cm³)

ΔP = pressure differences, which may be measured (atm)

θ = time increment between readings (seconds)

The ultimate sensitivity of this method is controlled not only by the length of the time increment and the sensitivity of the gauge, but also because temperature changes in the environment will produce independent pressure changes.

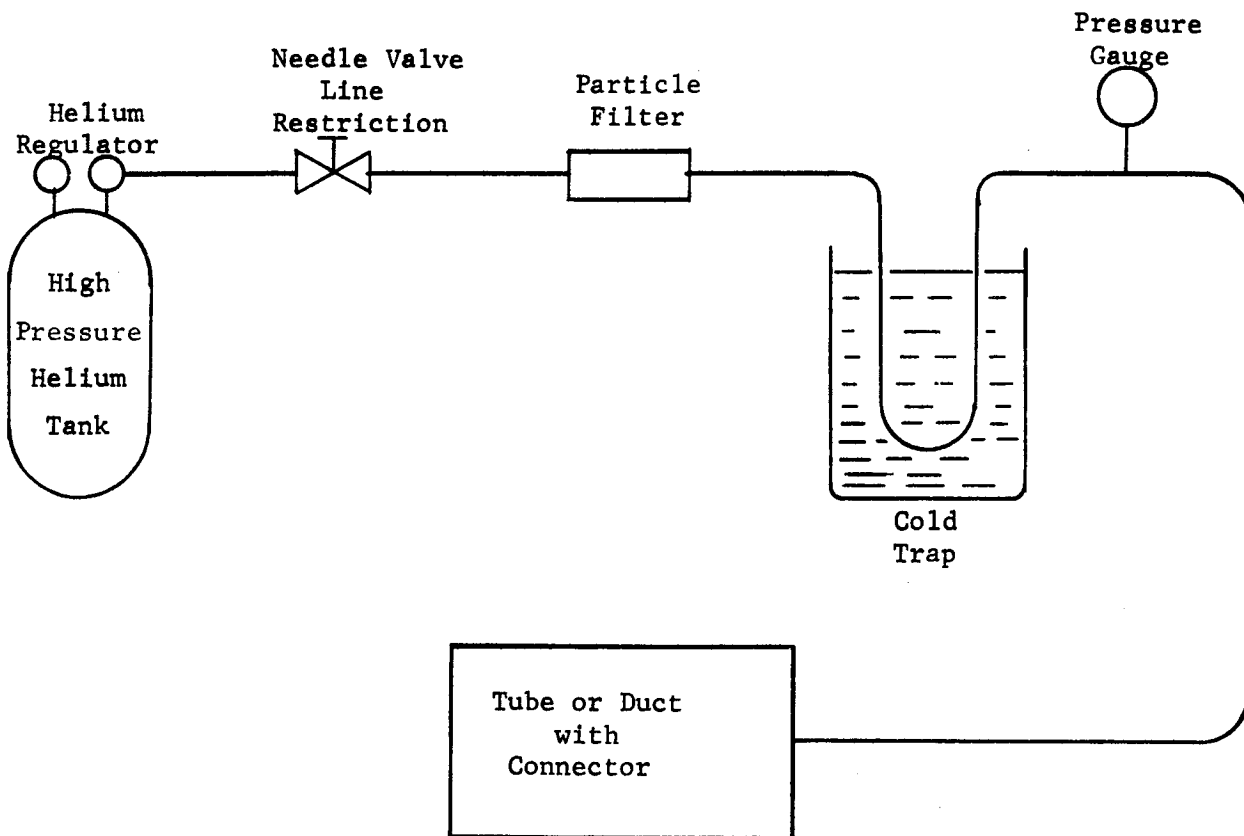


Figure 5.2. High-pressure System.

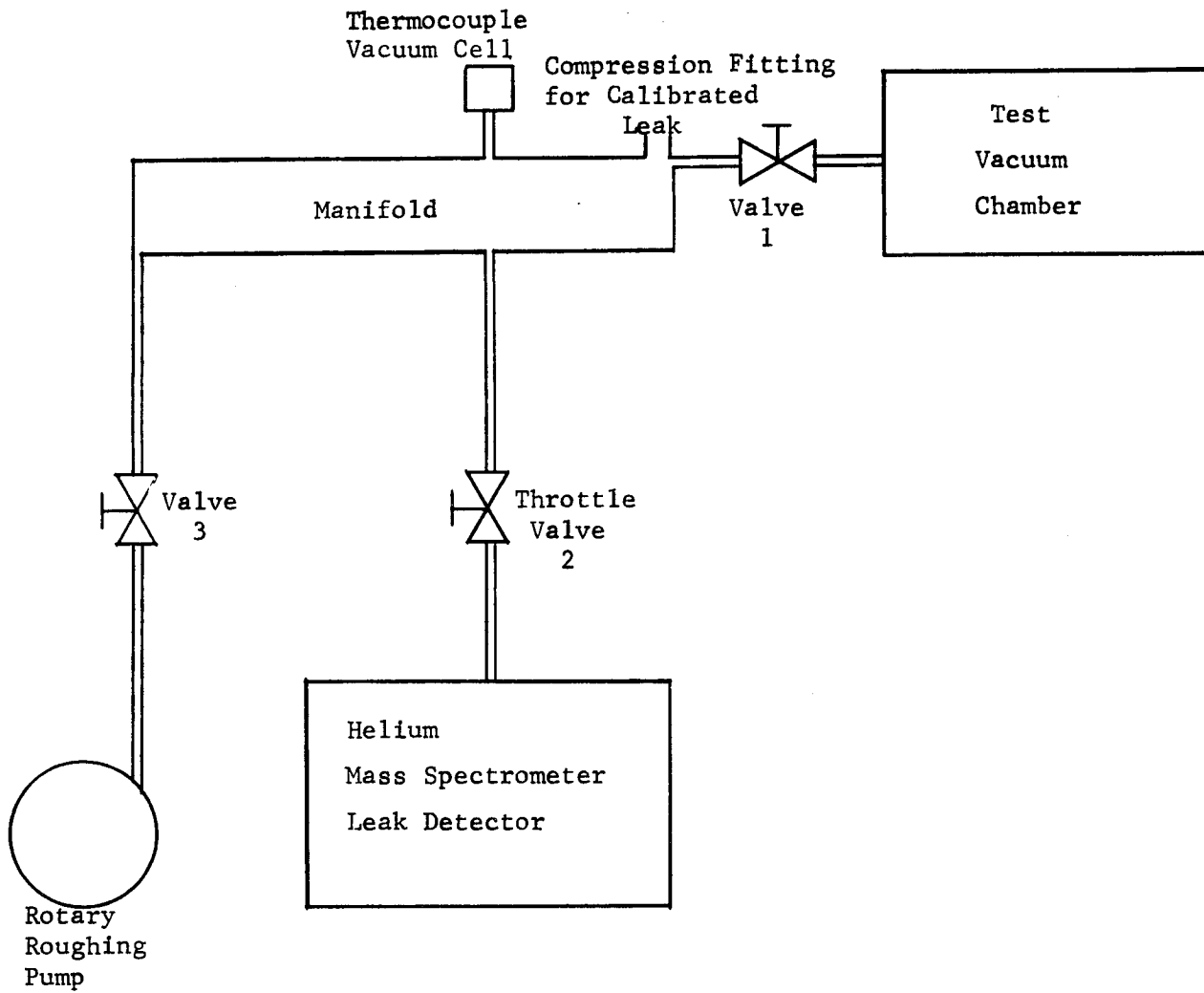


Figure 5.3. Leak Detector - Vacuum System.

REV. NO.							TITLE	
PARTS LIST FOR							TEST CHAMBER	
454C429-SECT. A							FIRST MADE FOR SEAL TEST	
CONT ON SHEET 2 SH NO. 1								
GROUP NO. AND QUANTITY							PART NO.	DRAWING NO., DESCRIPTION, MATERIAL, WEIGHT
1	1	1	1	1	1	1	1	SHELL SEE DETAIL
						1	2	END PLATE
							3	
							4	
							5	
							6	
1							7	END PLATE SEE DETAIL
							8	
							9	
						1	10	PLATE SEE DETAIL
							11	
							12	
							13	
							14	
1							15	PLATE SEE DETAIL
							16	
							17	
						2	18	"O" RING #2-22 COMPOUND #C147-7 PARKER OR EQ.
						2	19	#2-20
						2	20	#2-18
						2	21	#2-16
						2	22	#2-14
2							23	"O" RING #2-12 COMPOUND #C147-7 PARKER OR EQ.
							24	
							25	
1	1	1	1	1	1		26	"O" RING #2-39 COMPOUND #C147-7 PARKER OR EQ.
1	1	1	1	1	1		27	"O" RING #2-36 COMPOUND #C147-7 PARKER OR EQ.

DESCRIPTION OF GROUPS	REVISIONS	PRINTS TO
FOR CONTINUATION OF GROUPS - SECTION B ISSUED		

MADE BY <i>[Signature]</i> JAN 29, 64	APPROVALS	ADV. TECH. LAB. DIV OR DEPT	PARTS LIST FOR
ISSUED <i>[Signature]</i> Feb 3 '64		SCHENECTADY LOCATION	454C429-SECT. A
			CONT ON SHEET 2 SH NO. 1

REV NO.	TITLE
PARTS LIST FOR 454C429-SECT. B	TEST CHAMBER
CONT ON SHEET 2 SH NO. 1	FIRST MADE FOR SEAL TEST

GROUP NO. AND QUANTITY	PART NO.	NAME	DRAWING NO., DESCRIPTION, MATERIAL, WEIGHT
6867	1	SHELL	SEE DETAIL
	2		
	3		
	4		
	5		
	6		
	7		
1	8	END PLATE	SEE DETAIL
1	9	END PLATE	SEE DETAIL
	10		
	11		
	12		
	13		
	14		
	15		
1	16	PLATE	SEE DETAIL
1	17	PLATE	SEE DETAIL
	18		
	19		
	20		
	21		
	22		
	23		
2	24	"O" RING	# 2-10 COMPOUND #G147-7 PARKER OR EQ
2	25		# 2-6
1	26		# 2-39
1	27	"O" RING	# 2-36 COMPOUND #G147-7 PARKER OR EQ

DESCRIPTION OF GROUPS	REVISIONS	PRINTS TO

MADE BY ISSUED JAN 29 '64 FEB 3 '64	APPROVALS	ADV. TECH. LAB. DIV OR DEPT SCHEMECTADY LOCATION	PARTS LIST FOR 454C429-SECT. B CONT ON SHEET 2 SH NO. 1
--	-----------	---	---

REV. NO.						TITLE	
PARTS LIST FOR						TEST CHAMBER	
454C429-SECT. A						FIRST MADE FOR SEAL TEST	
CONT ON SHEET 3 SH NO. 2							
GROUP NO. AND QUANTITY						DRAWING NO., DESCRIPTION, MATERIAL, WEIGHT	
66	65	64	63	62	61	PART NO.	NAME
					2	28	TUBE 1" DIA. X WALL THK. X LENGTH
				2		29	↑ 7/8 DIA. X
		2				30	↑ 3/4 DIA. X
			2			31	↑ 5/8 DIA. X
	2					32	↓ 1/2 DIA. X
2						33	TUBE 3/8 DIA. X WALL THK. X LENGTH
						34	
						35	
				2		36	SLEEVE - FLARED TUBE #16TX-S (1") PARKER OR EQ.
				2		37	↑ #14TX-S (7/8)
		2				38	↑ #12TX-S (3/4)
			2			39	↑ #10TX-S (5/8)
	2					40	↓ #8TX-S (1/2)
2						41	SLEEVE - FLARED TUBE #6TX-S (3/8) PARKER OR EQ.
						42	
						43	
				2		44	NUT, COUPLING #16BTX-S (1") PARKER OR EQ.
				2		45	↑ #14BTX-S (7/8)
		2				46	↑ #12BTX-S (3/4)
			2			47	↑ #10BTX-S (5/8)
	2					48	↓ #8BTX-S (1/2)
2						49	NUT, COUPLING #6BTX-S (3/8) PARKER OR EQ.
						50	
						51	
				1		52	PLUG (DRILLED) #16PNTX-S (1") PARKER OR EQ.
				1		53	PLUG (DRILLED) #14PNTX-S (7/8) PARKER OR EQ.
				1		54	PLUG (DRILLED) #12PNTX-S (3/4) PARKER OR EQ.
DESCRIPTION OF GROUPS						REVISIONS	
FOR CONTINUATION OF GROUPS - SECT. B ISSUED						PRINTS TO	
MADE BY						APPROVALS	
ISSUED						ADV. TECH. LABS. DIV OR DEPT	
SCHEENECTADY LOCATION						PARTS LIST FOR	
454C429-SECT. A						CONT ON SHEET 3 SH NO. 2	

REV. NO.
 PARTS LIST FOR
454C429 - SECT. B
 CONT ON SHEET **3** SH NO. **2**

TITLE
TEST CHAMBER
 FIRST MADE FOR **SEAL TEST**

GROUP NO. AND QUANTITY		PART NO.	NAME	DRAWING NO., DESCRIPTION, MATERIAL, WEIGHT	
		28			
		29			
		30			
		31			
		32			
		33			
	2	34	TUBE	1/4 DIA. X WALL THK. X LENGTH	
	2	35	TUBE	1/8 DIA. X WALL THK. X LENGTH	
		36			
		37			
		38			
		39			
		40			
		41			
	2	42	SLEEVE-FLARED TUBE	#4TX-S (1/4)	PARKER OR EQ.
	2	43	SLEEVE-FLARED TUBE	#2TX-S (1/8)	PARKER OR EQ.
		44			
		45			
		46			
		47			
		48			
		49			
	2	50	NUT, COUPLING	#4BTX-S (1/4)	PARKER OR EQ.
	2	51	NUT, COUPLING	#2BTX-S (1/8)	PARKER OR EQ.
		52			
		53			
		54			

DESCRIPTION OF GROUPS	REVISIONS	PRINTS TO

MADE BY
 [Signature] **JAN 29, 64**
 CHECKED
 [Signature] **FEB 3 64**

APPROVALS
 ADV. TECH. LABS. DIV OR DEPT
 SCHEENECTADY LOCATION

PARTS LIST FOR
454C429 - SECT. B
 CONT ON SHEET **3** SH NO. **2**

FP 401-F (9-53)
 PRINTED IN U.S.A.

REV. NO.	TITLE
PARTS LIST FOR 454C429-SECT. A	TEST CHAMBER
CONT ON SHEET 4 SH NO. 3	FIRST MADE FOR SEAL TEST

GROUP NO. AND QUANTITY						PART NO.	NAME	DRAWING NO., DESCRIPTION, MATERIAL, WEIGHT
66	65	64	63	62	61			
	1					55	PLUG, (DRILLED) # 10 PNTX-S	PARKER OR EQ.
	1					56	PLUG, (DRILLED) # 8 PNTX-S	PARKER OR EQ.
	1					57	PLUG, (DRILLED) # 6 PNTX-S	PARKER OR EQ.
						58		
						59		
				1		60	PLUG	# 16 PNTX-S (1") PARKER OR EQ.
				1		61	↑	# 14 PNTX-S (7/8) ↑
		1				62	↑	# 12 PNTX-S (3/4) ↑
		1				63	↑	# 10 PNTX-S (5/8) ↑
	1					64	↓	# 8 PNTX-S (1/2) ↓
	1					65	PLUG	# 6 PNTX-S (3/8) PARKER OR EQ.
						66		
						67		
						68		
				2		69	NUT, COUPLING	TO BE TESTED
				2		70	↑	↑
		2				71	↑	↑
		2				72	↓	↓
	2					73	↓	↓
	2					74	NUT, COUPLING	TO BE TESTED
						75		
						76		
					1	77	UNION	TO BE TESTED
					1	78	↑	↑
					1	79	↑	↑
					1	80	↓	↓
	1					81	UNION	TO BE TESTED

DESCRIPTION OF GROUPS	REVISIONS	PRINTS TO
FOR CONTINUATION OF GROUPS - SECT. B ISSUED		

MADE BY <i>JAC</i> JAN 29 '64	APPROVALS	ADV. TECH. LABS. DIV OR DEPT SCHEENECTADY LOCATION	PARTS LIST FOR 454C429-SECT. A CONT ON SHEET 4 SH NO. 3
---	-----------	--	--

REV. NO. PARTS LIST FOR 454C429-SECT. B CONT ON SHEET 4 SH NO. 3	TITLE <h2 style="text-align: center;">TEST CHAMBER</h2> FIRST MADE FOR SEAL TEST
--	--

GROUP NO.	AND QUANTITY	PART NO.	NAME	DRAWING NO., DESCRIPTION, MATERIAL, WEIGHT
		55		
		56		
		57		
	1	58	PLUG (DRILLED) #4 PNTX-S (1/4)	PARKER OR EQ.
	1	59	PLUG (DRILLED) #2 PNTX-S (1/8)	PARKER OR EQ.
		60		
		61		
		62		
		63		
		64		
		65		
	1	66	PLUG	#4 PNTX-S (1/4) PARKER OR EQ.
	1	67	PLUG	#2 PNTX-S (1/8) PARKER OR EQ.
		68		
		69		
		70		
		71		
		72		
		73		
		74		
	2	75	NUT, COUPLING	TO BE TESTED
	2	76	NUT, COUPLING	TO BE TESTED
		77		
		78		
		79		
		80		
		81		

DESCRIPTION OF GROUPS	REVISIONS	PRINTS TO

MADE BY <i>[Signature]</i> JAN. 29 '64 ISSUED <i>[Signature]</i> FEB. 3 '64	APPROVALS	ADV. TECH. LABS. DIV OR SCHEENECTADY LOCATION	PARTS LIST FOR 454C429-SECT. B CONT ON SHEET 4 SH NO. 3
--	-----------	--	--

REV NO.	PARTS LIST FOR		TITLE	
	454C429-SECT. B		TEST CHAMBER	
	CONT ON SHEET FINAL SH NO. 4		FIRST MADE FOR SEAL TEST	
GROUP NO.	QTY	PART NO.	NAME	DRAWING NO., DESCRIPTION, MATERIAL, WEIGHT
		82		
	1	83	UNION	TO BE TESTED
	1	84	UNION	TO BE TESTED
	1	85	TUBE	1/2" DIA. X WALL THK. X LENGTH
	6	86	HEX. SOC. HD. CAPSCREW	#8-32 X 1/2 LG. STL.
	6	87	HEX. SOC. HD. CAPSCREW	#8-32 X 3/8 LG. STL.
	12	88	SPRING LOCK WASHER	#8 STL.

DESCRIPTION OF GROUPS	REVISIONS	PRINTS TO

MADE BY <i>J. J. ...</i> JAN. 29 '64 ISSUED <i>JAC</i> FEB 3 '64	APPROVALS _____ _____	ADV. TECH. LABS. DIV OR DEPT SCHEENECTADY LOCATION	PARTS LIST FOR 454C429-SECT. B CONT ON SHEET FINAL SH NO. 4
---	-----------------------------	---	---

***001-P (9-63)

Section 6

MATERIAL PROPERTIES AND COMPATIBILITY

By

R. L. George

Material properties and compatibility data for candidate tube, duct, flange, and gasket materials in launch vehicles are presented in Tables 6.1, 6.2, 6.3, 6.4, and 6.5 to aid in design computations. Candidate materials include aluminum alloys, stainless steels, nickel base alloys, and 4340 steel for ducts, tubes, and flanges, indium, lead, aluminum, copper, and nickel for metallic gaskets, and Teflon, Kel-F, Neoprene, Silicone Rubber, Viton, and Hypalon for organic gaskets.

Table 6.1 presents properties of metallic materials and Table 6.2 those of organic materials. Data has been obtained exclusively from the literature. Since materials exhibit variations in properties, each investigator selects property values for design computations below which there were no failures. Variation in values of material properties are influenced by heat treatment, degree of cold working, method of fabrication, alloy composition, and rate of loading. The range of property values given in Tables 6.1 and 6.2 encompasses variations reported in the literature for the same annealed or hardened alloy. Material properties are also influenced by the environment and, in particular, the temperature and surrounding media. The effect of temperature upon the ultimate tensile stress is shown in Table 6.3. All properties given are for materials in a noncorrosive environment. However, the surrounding atmosphere may cause intergranular corrosion, pitting, erosion, or stress cracking which will have an adverse effect on the material properties.

Compatibility of a material with a propellant indicates that the properties of the duct material are not adversely affected and essentially no contamination to the propellant occurs. Table 6.5 presents chemical compatibility data of candidate materials with propellants. Materials obtain their passivity to a corrosive medium by forming a protective film (similar to the oxide film formed on aluminum) when exposed to air. Passivity will remain as long as the film is not damaged, either by scratching, flaking, or separating from the base metal. If damaged, the exposed base metal or film particle can ignite the propellant, plug the valves or pumps, or chemically contaminate the propellant. The behavior of this film under flow, shock, vibration, or high stress environments must be evaluated if this type of environment is encountered. The data presented in Table 6.5 refers to static environments and may serve as an indication of materials that have the best probability of being compatible in both a severe chemical and mechanical environments.

Table 6.4 presents the nominal chemical composition of the candidate materials.

Table 6.1

METALLIC MATERIAL PROPERTIES*

	Modulus of Elasticity ⁶ psi x 10 ⁶	Ultimate Tensile Strength ³ psi x 10 ³	Yield Strength psi x 10 ³	Coefficient Linear Expansion ⁸ in/in F x 10 ⁻⁶	Annealing Temp. °F	Welda- bility
ALUMINUM						
2024-T3	10.6	64-70	42-50	12.9	775	(A-1)
3003-H18	10	29	27	12.9	775	(A-2)
5052-H38	10.2	39-42	33-37	13.2	650	(A-2)
6061-T6	10	42-45	35-40	13	775	(A-2)
ALLOY STEEL						
4340	30	284-142	228-130	6.5	1475-1700	(S-1)
STAINLESS STEEL						
304L	28	65-85	25-35	9.6	1900-2050	(SS)
316	28	75-85	30-35	9.0	1850-2050	(SS)
321	28	70-87	30-35	9.5	2100-2250	(SS)
347	28	70-92	30-35	9.5	1950	(SS)
17-14 Cu Mo		86	42	8.2	2200 ^(W)	(S2)
A-286	29	130-150	85-100	10.3	1700-2150 ^(W)	
NICKEL ALLOYS						
Inconel-X	31	155-162	92-100	9.2	1900-2225 ^(W)	(N-1)
Hastelloy-X	28.6	114	52.2	9	1800-2220 ^(W)	(SS)
Rene' 41	31.8	206	154	8.7	2150-1850 ^(W)	(N-1)
METALLIC GASKETS						
Indium	1.57	0.380	-	18.3	353 ^{Melting} Point	-
Lead	2	2.15-3	1.18-1.38	16.3	618 ^{Melting} Point	-
Aluminum 1060-0	10	10	4	13.1	650	-
Aluminum 1060-18	10	19	18	13.1	650	-
Copper	17	32-65	10-50	9.35	700-1200	-
Nickel	30	50-80	10-30	7.4	1500	-

- (A-1) Fair relative to aluminum alloys
(A-2) Good relative to aluminum alloys
(S-1) Oxyacetylene, inert arc, electric resistance welding
(SS) Excellent
(S2) Arc and resistant welded
(N1) Satisfactory to good
(W) Hot working temperature °F

*Poisson's Ratio can be assumed to be 0.3 for aluminum alloys, steels, and nickel alloys.

Table 6.2

ORGANIC MATERIAL PROPERTIES

	Modulus of Elasticity psi x 10 ⁵	Ultimate Tensile Strength psi 10 ³	Impact Strength $\frac{\text{ft. Lb}}{\text{in}}$ (IZOD)	Coefficient of Linear Expansion in/in °F x 10 ⁻⁵	Useful Temperature Range
<u>PLASTICS</u>					
KEL-F (PTFCE)	1.8	4.6-5.7	3.5-3.6	3.88	-400 to 400°F
Teflon (PTFE)	0.38-0.65	2.5-3.5	2.5-4.0	5.5	-450 to 500°F
Teflon (FEP)	0.5-0.7	2.5-3.5	No break	8.3-10.5	-450 to 400°F

(PTFCE) Polytrifluorochloroethylene
 (PTFE) Polytetrafluoroethylene
 (FEP) Fluorinated Ethylene Propylene

RUBBERS

	Tensile Strength (Pure gum) psi	Elongation (Pure gum) Percent	Coefficient of Thermal Expansion (Cubical) x 10 ⁻¹⁵ per °F	Recommended Service Temperature	
				Maximum °F	Minimum °F
Neoprene	3000-4000	800-900	34	240	-40
Silicone	600-1300	100-500	45	550	-120
Viton	72000	7350	-	450	-50
Hypalon	4000	600	27	300	-40

Table 6.3

EFFECT OF TEMPERATURE ON ULTIMATE TENSILE STRENGTH*
(Temperature °F)

	-400	-300	-200	0	RT	200	400	600	800	1000	1500	2000
ALUMINUM												
2024-T3	150	118	108	100	100	97	82(S) 24(L)	22(S) 10(L)	-	-	-	-
3003-H18	-	138	120	102	100							
5052-H38	178	138	116	100	100	97	65(S) 42(L)	20(S) 16(L)	8	-	-	-
6061-T6	145	122	114	102	100	91	64(S) 42(L)	22(S) 8(L)	-	-	-	-
ALLOY STEEL												
4340		123	117	100	100	97	93	86	75	51	-	-
STAINLESS STEEL												
304L	264	240	200	110	100	85	79	75	72	64	25	-
316	235	204	170	106	100	95	87	80	72	65	31	-
321	265	230	205	111	100	95	89	81	74	66	24	-
347	235	206	180	108	100	87	76	73	70	65	26	-
17-14 Cu.Mo					100					85(900°F)	39	-
A-286	-	137	128	103	100	98	96	92	88	82	22	-
NICKEL ALLOYS												
Inconel-X	-	172	160	102	100	99	98	96	91	83	34	-
Hastelloy-X					100	100	98	95	91	82	45	20(1800°F)
Rene' 41					100					99	61	27(1700°F)
METALLIC GASKET												
Lead	300	183	167	100	100							
Indium												
Aluminum 1060-0												
Aluminum 1060-18												
Copper	194	155	134	103	100							
Nickel	157	140	126	102	100							
PLASTICS												
KEL-F		260	260	115	100							
Teflon(PTFE)		400	350	100								
Teflon(FEP)												

*Percentage of ultimate tensile strength at room temperature.

Table 6.4

NOMINAL CHEMICAL COMPOSITION

	Fe	C	AL	Ni	Cr	Mn	Mg	Si	Cu	Zn	Co	Mo	V	Ti	Cb
ALUMINUM															
2024-T3	0.5	-	BAL	-	0.1	0.6	1.6	0.5	4.5	0.25	-	-	-	-	-
3003-H18	0.7	-	BAL	-	-	2.5	-	0.6	0.2	0.1	-	-	-	-	-
5052-H38	0.1	-	BAL	-	0.25	-	2.5	0.45	0.1	-	-	-	-	-	-
6061-T6	0.7	-	BAL	-	0.25	-	1.0	0.6	0.28	-	-	-	-	-	-
ALLOY STEEL															
4340	BAL	0.4	-	1.8	0.8	0.7	-	-	-	-	0.1	-	-	-	-
STAINLESS STEEL															
304L	BAL	0.08	-	10.0	19.0	2.0	-	1.0	-	-	-	-	-	-	-
316	BAL	0.08	-	12.0	17.0	2.0	-	1.0	-	-	-	2.0	-	-	-
321	BAL	0.08	-	10.0	18.0	2.0	-	1.0	-	-	-	-	-	0.4	-
347	BAL	0.08	-	11.0	18.0	2.0	-	1.0	-	-	-	-	-	-	0.8Cb-Ta
17-14 Cu Mo	BAL	0.12	-	14.1	15.9	0.75	-	0.5	3.0	-	-	2.0	-	0.25	0.45
A-286	BAL	0.08	0.2	26.0	15.0	1.35	-	0.95	-	-	-	1.25	3	2.15	-
NICKEL ALLOYS															
Inconel-X	7.0	0.05	0.75	BAL	15.0	0.5	-	0.4	0.05	-	-	-	-	2.5	0.9
Hastelloy-X	18.0	0.1	-	BAL	21.0	1.0	-	0.1	-	-	2.0	9.0	-	-	0.15W
Rene' 41	5.0	0.1	1.4	BAL	18-20	0.1	-	0.5	-	-	10	9-10	-	3.1	-
METALLIC GASKETS															
Indium	(99.97% pure)														
Lead	(99.97% pure)														
Aluminum 1060-0			99.6												
Aluminum 1060-18			99.6												
Copper									99.95						
Nickel				99.4											



6.1 References

6.1.1 Material Properties

1. Physical and Mechanical Properties of Pressure Vessel Materials for Application in a Cryogenic Environment, by J. L. Christian, Technical Documentary Report No. AST-TDR-62-258, Contract No. AF 33 (616)-7719.
2. Lyman, Taylor, ed., Metals Handbook 1948 Edition. American Society for Metals, Cleveland, Ohio.
3. National Bureau of Standards, Mechanical Properties of Structural Materials at Low Temperatures, by R. M. McClintock and H. P. Gibbons, Monograph 13, June 1, 1960.
4. General Electric Technical Information Series Report No. R60SD314, Short Time Properties of Materials as a Function of Temperature, by J. R. Vinson, Schenectady, New York, February 8, 1960.
5. "Materials Selector Issue 1963", Materials in Design Engineering, Reinhold Publishing Corp.
6. "Modern Flange Design", Taylor Forge Bulletin 502, Fourth Edition, 1961.
7. Armed Forces Supply Center, Strength of Metal Aircraft Elements, MIL-HDBK-5, Washington, D.C., March 1959.

6.1.2 Compatibility with Liquid Propellants

8. Batelle Memorial Institute, Defense Metals Information Center, Compatibility of Rocket Propellants with Materials of Construction, by W. K. Boyd and E. L. White, Columbus 1, Ohio, September 15, 1960.
9. George C. Marshall Space Flight Center, Compatibility of Engineering Materials with Liquid Oxygen, by J. E. Curry and W. A. Ruhl, Report No. MTP-M-S&M-M-61-7, March 21, 1961.
10. Office of The Director of Defense Research and Engineering, The Handling and Storage of Liquid Propellants, Washington 25, D.C., January 1963.
11. Technical Documentary Report, Material Selection, Process Development, and Preliminary Design, Report No. RTD-TDR-63-1027, Contract No. AF 04(611)-8177, November 1962.



Section 7

CATALOG OF SEALS

By

F. O. Rathbun, Jr.
G. W. Sarney, and J. Wallach

7.0 Introduction

At present, a single seal configuration or material does not exist for optimum utilization in all of the possible operating conditions and environments to which a separable fluid connector can be subjected. Rather, several possibilities present themselves to the designer. He must choose one based on several factors, including compatibility of the material to the fluid to be contained, the temperature to which the connector is to be subjected, the internal pressure, the radius of the piping system in which the fluid connector is to be used, and the available space envelope about the periphery of the connector.

In Section 1, "Fundamental Considerations of Separable Connector Design," of this handbook, several of the problems confronting the seal designer are cited, along with some guide rules as to required sealing stresses for various surface finishes in terms of material properties. To supplement those general rules, this Section has been included to give the connector designer a listing of types of seals which may aid him in making a final seal selection.

Included in this catalog are several seal configurations and materials which have been subjected to tests. Based on these tests, certain characteristics can be cited. The materials and configurations have been included and, where applicable, temperature limitations, load deflection characteristics, sealing characteristics, and advantages and disadvantages of their use. It is not intended that this listing be complete, but merely to present data which is currently available. As new data is obtained, individual entries may be updated and new ones made.

In cases where the design guide rules of Section 1 are not directly applicable nor the seals listed in the catalog useful, and another seal either manufactured or purchased from a vendor is to be used, it is recommended that sufficient testing be accomplished on that seal to insure the intended response.

7.1 Seal Classification and Data

The sealing systems are presented in six groups:

Metal-to-Metal	Section 7.1.1
Metal Flat Gaskets	Section 7.1.2

Shaped Metal Gaskets and Sealing Surfaces	Section 7.1.3
Plastic Gaskets	Section 7.1.4
Elastomeric Gaskets	Section 7.1.5
Miscellaneous	Section 7.1.6

The variable among the metal-to-metal seals is that of surface finish; the variables in the metal flat gaskets are both material and surface finishes. Material is the main variable in both the plastic gasket section and the elastomeric gasket section. The miscellaneous group includes commercially available gaskets and materials.

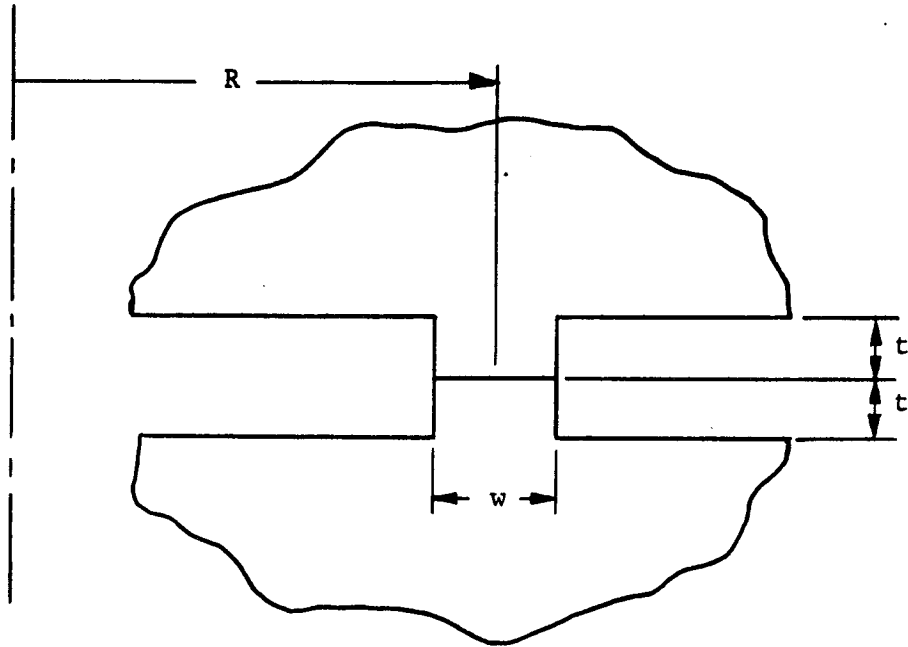
7.1.1 Metal-to-Metal Seals

7.1.1.1

CLASSIFICATION: Superfinished Sealing Surface

MATERIAL: Any structural connector material. Information based on tests with 347 stainless steel and 2024 T4 aluminum.

CONFIGURATION:



TEMPERATURE LIMITATIONS: No inherent seal limitation, limitations dependent on material used. Limitations will be the same as those on the structural members.

SURFACE SPECIFICATIONS: Both surfaces have no low relief asperities greater than one half microinch. Surfaces flat to within one helium light band.

SEALING CHARACTERISTICS: At an internal pressure of 2000 psi, system seals to less than 10^{-6} atm cc/sec with an applied stress less than the yield strength of the materials used. System will reseal satisfactorily up to eight times. Damage due to repeated mating is localized and does not severely diminish the sealing capabilities. System will seal at much less than the yield strength in the initial use; thereafter, more stress is required. Because deformation is generally elastic in nature, the system is sensitive to load removal. (Figure 7.1).

ADVANTAGES:

1. Reusable with planned applied stress levels.
2. No separate gasket required.
3. Seal has same temperature limitations as connector structural components.

DISADVANTAGES:

1. Difficult to manufacture.
2. Sealing surface must be protected from damage during assembly.
3. Sealing surfaces must be brought together normally without relative tangential motion.
4. Structural components must be designed to allow very little radial rotation between mating surfaces.

COMMENTS:

Leakage rates proportional to the major radius, R. Data based on width, w, of 1/8 inch. No data available as to minimum width which can be used for this seal. Data given for height, t, ranging from 0.030 to 0.120 inch. Increase in t (increased flexibility) advantageously affects sealing characteristics.

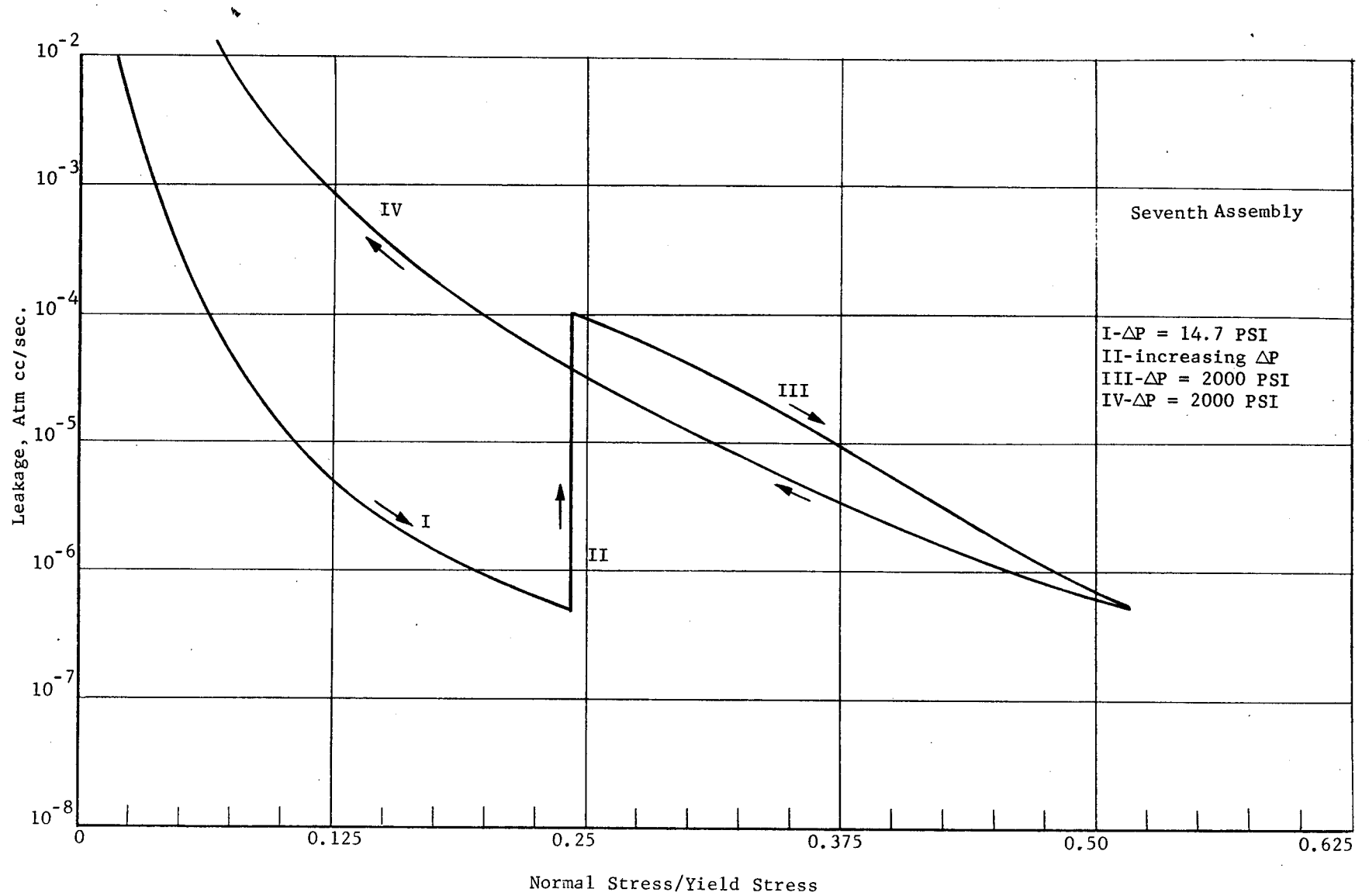


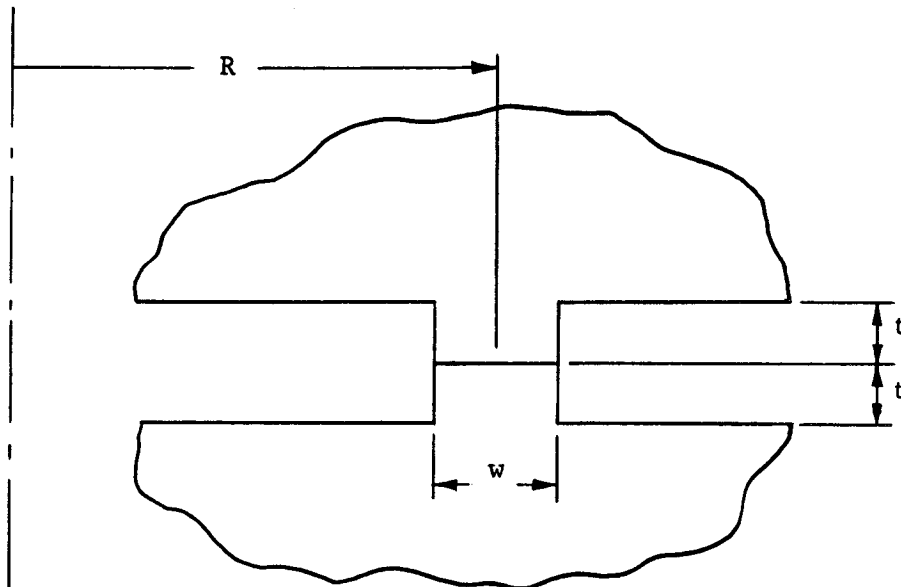
Figure 7.1. Typical Leakage - Normal Stress Response for Superfinished 347 Stainless Steel Seal

7.1.1.2

CLASSIFICATION: Lapped Surfaces

MATERIAL: Any structural connector materials. Information based on 347 stainless steel and 2024 T4 aluminum.

CONFIGURATION:



TEMPERATURE LIMITATIONS: No inherent seal limitation, limitations dependent on material used. Limitations will be the same as those on the structural members.

SURFACE SPECIFICATIONS: Surfaces lapped with randomly oriented asperities; approximately eight microinch rms finish.

SEALING CHARACTERISTICS: With 1000 psi internal pressure, system seals to less than 10^{-6} atm cc/sec at a stress level of approximately 2.9 times the yield strength of the material. Severe surface deformations result. No assurance of reusability at similar stress levels. System is insensitive to load removal down to stress levels of approximately twice the yield strength.

ADVANTAGES:

1. No separate gasket required.
2. Same temperature limitation as connector structural parts.
3. Since mating is caused by plastic material flow, somewhat insensitive to load removal.

DISADVANTAGES:

1. Not reusable at planned stress levels.
2. Gross surface deformations necessary to effect sealing result in changes to connector dimensions. Must be used in systems with single load path only.

COMMENTS:

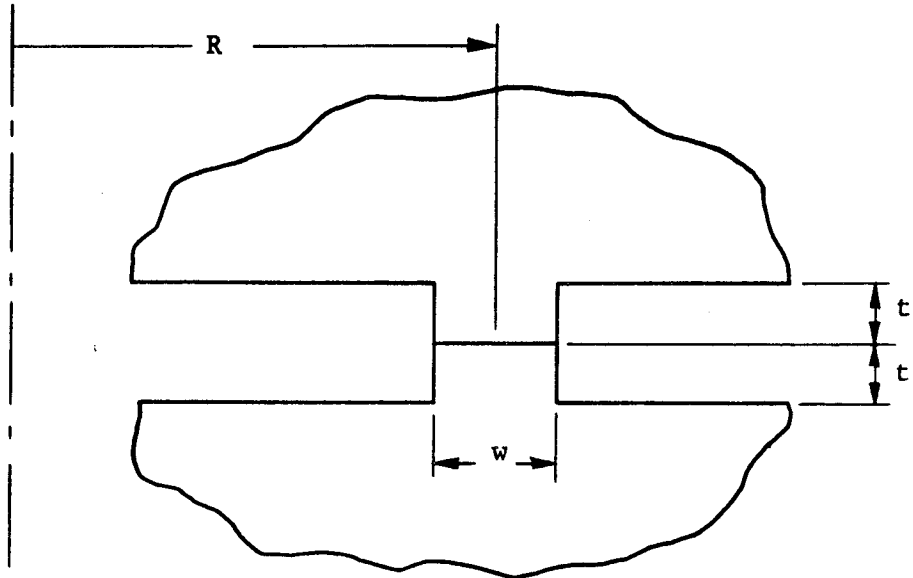
Data gained on tests with one-eighth inch wide seals. Caution should be taken when seal widths less than one-eighth inch are contemplated. Tests should be made to determine leakage-stress relationships.

7.1.1.3

CLASSIFICATION: Circumferentially Machined Surfaces

MATERIAL: Any structural connector material. Information based on tests with 347 stainless steel and 2024 T4 aluminum.

CONFIGURATION:



TEMPERATURE LIMITATIONS: No inherent limitations, limitations dependent on material used. Limitations will be the same as those on the structural members.

SURFACE CHARACTERISTICS: Approximately 75 microinches, CLA, machined with 115° included angle tool. Concentric wedges spaced 0.001 inch apart.

SEALING CHARACTERISTICS: At an internal pressure of approximately 1000 psi, system will seal to less than 10^{-6} atm cc/sec at a stress level of approximately 1.3 times the yield strength during the initial use of the system. Sealing results from localized plastic deformation. System quite insensitive to load removal. Little noticeable gross surface deformation subsequent to initial use. Successive reassemblies require stress levels above twice the yield strength. Accurate estimate of stress required for each reuse impossible to ascertain.

ADVANTAGES:

1. Insensitive to load removal.
2. No separate gasket required.
3. Same temperature limitations as connector structural parts.

DISADVANTAGES:

1. Not reusable at planned stress levels.

COMMENTS:

Sealing results from successive microscopic knife edges. Tolerances preclude knife edges being pressed together absolutely concentrically. Repetitive microscopic incomplete seals result. Caution, therefore, must be used when reducing width, since seal is effected by a multitude of redundancies. Data gathered from tests where width, w , = one-eighth inch, hence 125 knife edges across seal.

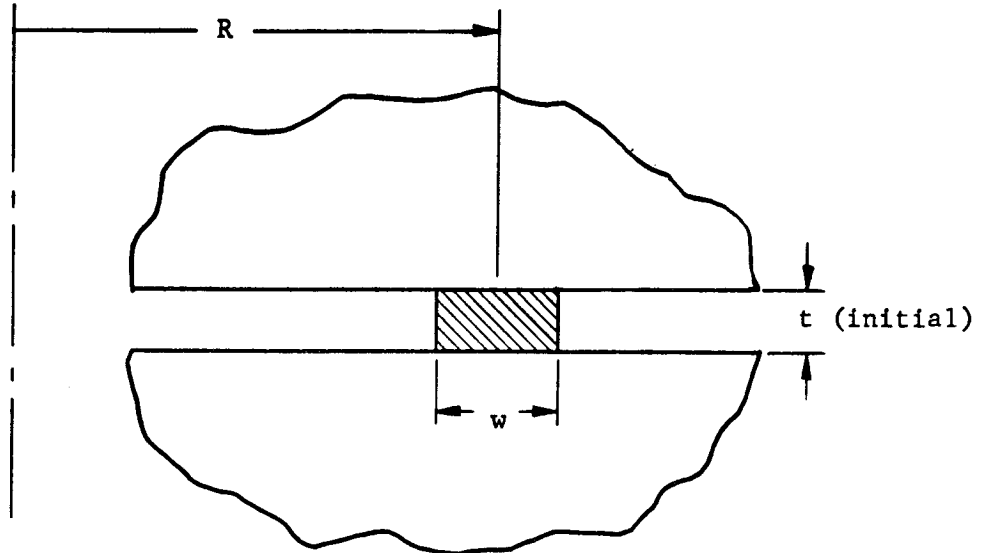
7.1.2 Flat Metal Gaskets

7.1.2.1

CLASSIFICATION: Structural Sealing Surfaces Diamond Burnished

MATERIAL: Soft metal gaskets. "Rigid" structural sealing surfaces.

CONFIGURATION:



TEMPERATURE LIMITATIONS:

Determined by creep properties of gasket material.

SURFACE SPECIFICATIONS:

Gaskets - none. Sealing surfaces diamond burnished, approximately four microinches root-mean-square.

SEALING CHARACTERISTICS:

At an internal pressure of 1000 psi, a stress level of 1.96 times the yield strength of the gasket material will insure sealing down to a level of 10^{-6} atm cc/sec. Since the sealing is effected by gross plastic deformation of the gaskets, the system is fairly insensitive to load removal. For extremely soft materials (with low yield strengths), it is impossible to apply extremely low stresses to the system and still maintain high internal pressures due to end loads caused by internal pressure. Thus, excessively high stresses must be applied initially.

ADVANTAGES:

1. Simplicity of design.
2. Upon reuse with new gasket, sealing stresses can be planned.

DISADVANTAGES:

1. Special machining techniques on structural sealing surfaces required.
2. Separate gasket (not reuseable) required.
3. More sensitive to load removal than surfaces with rougher finishes.

COMMENTS:

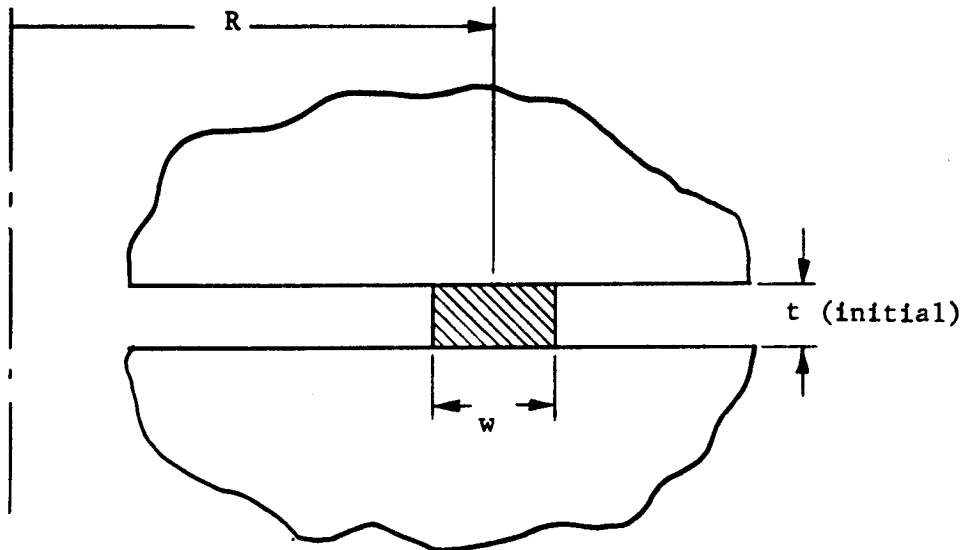
Data based on tests of seal width initially one-eighth inch.

7.1.2.2

CLASSIFICATION: Structural Sealing Finishes Circumferentially Machined

MATERIAL: Soft metal gaskets. "Rigid" structural sealing surfaces.

CONFIGURATION:



TEMPERATURE LIMITATIONS: Determined by creep properties of gasket material.

SURFACE CHARACTERISTICS: Gasket - none. Sealing surfaces circumferentially machined - approximately 100 microinches root-mean-square

SEALING CHARACTERISTICS: With internal pressure of 1000 psi, system will seal to less than 10^{-6} atm cc/sec at an applied stress level of 1.46 times the yield strength of the gasket material. The structural material must possess a yield strength greater than the applied stress. For sealing surfaces circumferentially machined with an excessively rougher characteristic, the required sealing stresses will rise considerably.

ADVANTAGES:

1. Stress levels can be predicted if a new gasket is used each time.
2. Fairly insensitive to load removals since the sealing is effected by plastic flow of the gasket material.

DISADVANTAGES:

1. Requires separate gasket.

COMMENTS: Data based on tests with one-eighth inch wide seal. For seal width less than one-eighth inch, adequate tests should be performed to insure sufficient redundancy of microscopic seals caused by the successive knife edges (individual asperities).

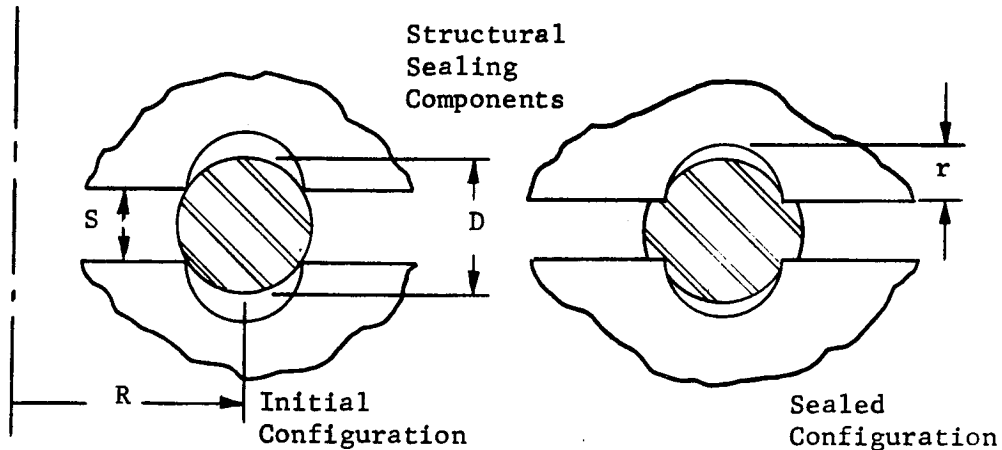
7.1.3 Shaped Metal Gaskets and Sealing Surfaces

7.1.3.1

CLASSIFICATION: Metal Shear O-Ring

MATERIAL: Gasket - soft copper (other soft metal such as aluminum, nickel, etc.). Recesses "rigid" structural material.

CONFIGURATION:



TEMPERATURE LIMITATIONS: Determined by creep properties of O-ring material.

LOAD DEFLECTION CHARACTERISTICS: (for copper at room temperature): See Figure 7.2

SEALING CHARACTERISTICS: (for copper at room temperature): See Figure 7.3

ADVANTAGES:

1. Utilizes principle of shear deformation.
2. Low sealing loads.
3. Insensitive to load removal if initially loaded well above initial sealing stress.

DISADVANTAGES:

1. Requires close tolerances to insure positioning of O-ring in recesses, particularly serious at large values of r .
2. Requires separate gasket.

COMMENTS:

1. Data based on tests where $R = 0.5$ inch, $r = 0.02$ inch, $D = 0.073$ inch.
2. Structure recess material should have yield strength at least three times higher than O-ring material.

Figure 7.2. Load Deflection Characteristics for Typical Metal Shear O-Ring Seal

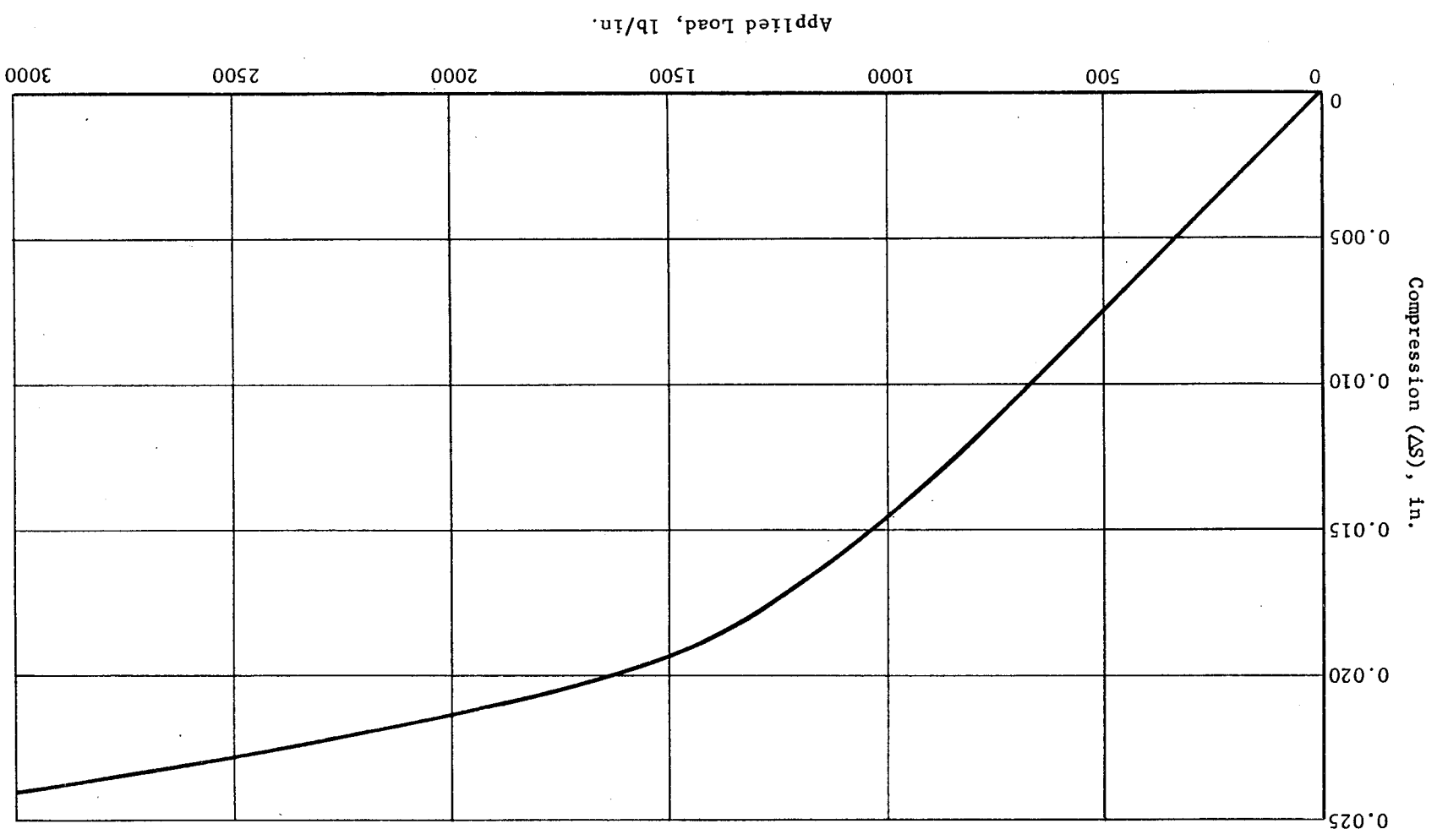
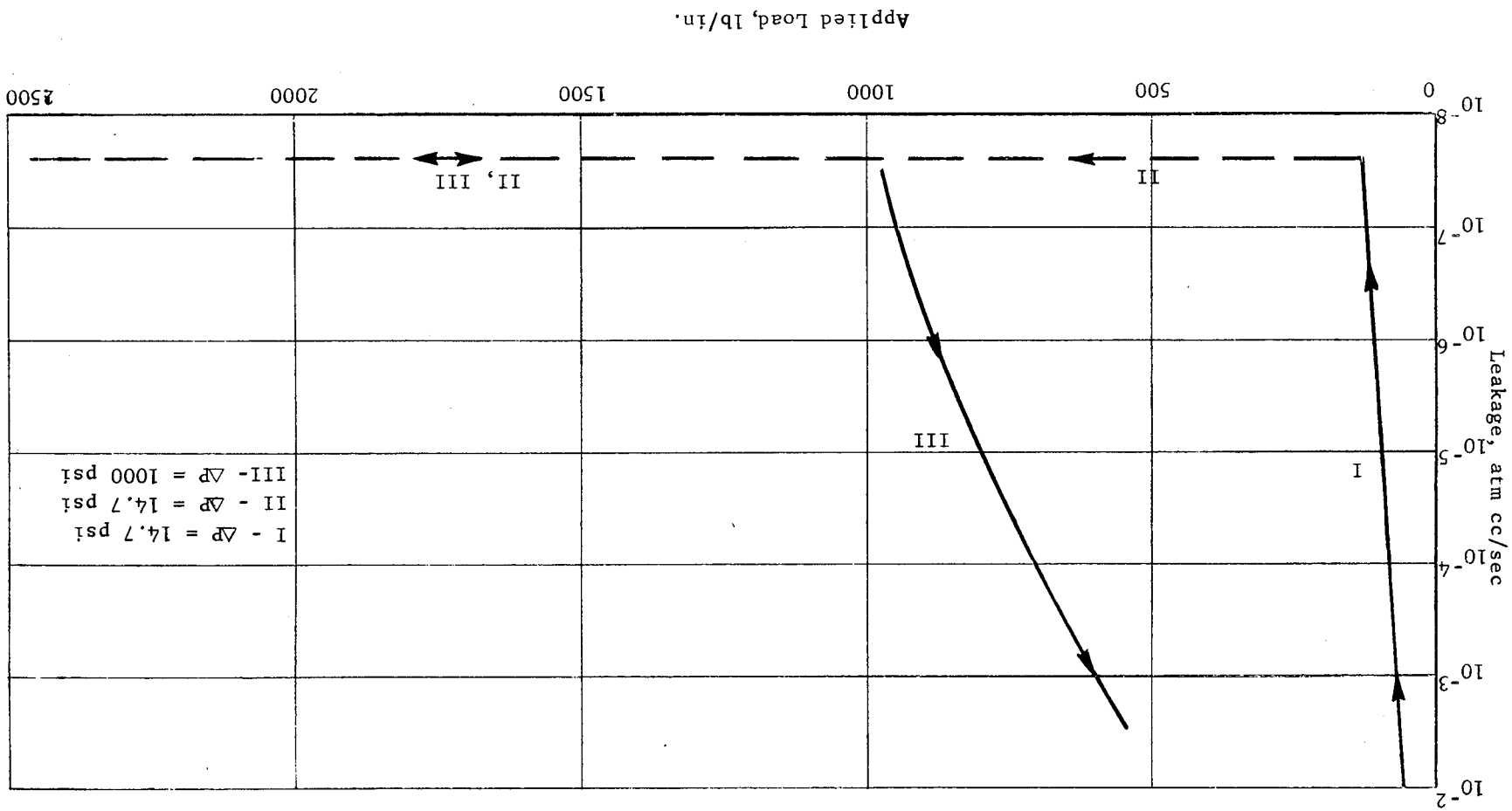


Figure 7.3. Typical Leakage - Applied Load Response for Metal Shear O-Ring Seal

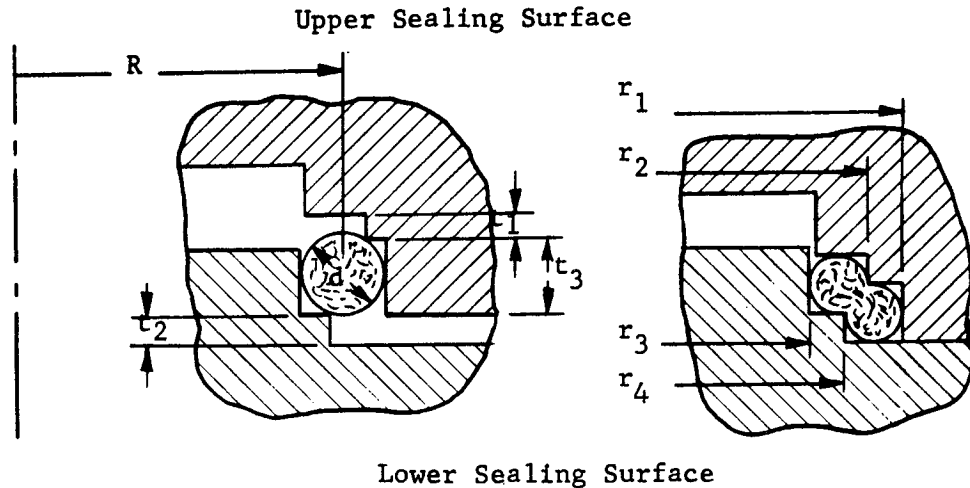


7.1.3.2

CLASSIFICATION: Modified Shear O-Ring

MATERIAL: Soft copper (other soft metal such as aluminum, nickel, etc.). Structural connector material used for recesses.

CONFIGURATION: Initial Configuration Sealed Configuration



TEMPERATURE LIMITATIONS: Determined by creep properties of O-ring material.

LOAD DEFLECTION CHARACTERISTICS: See Figure 7.4.

SEALING CHARACTERISTICS: After subjecting seal to an initial load of 1400 pounds per inch of periphery, no measurable leakage (less than 10^{-7} atm cc/sec) can be measured at an internal pressure of 1750 psi, until the load is dropped down to 200 pounds per inch of periphery (room temperature test).

- ADVANTAGES:
1. Shear deformation of the gasket is effected.
 2. The gasket is completely contained by the flanged faces.
 3. The flanged faces, being in full contact after assembly, prescribe the amount of gasket deformation.
 4. The knife edges, being at an angle to the seal center-line, make the seal less sensitive to relative axial movements of the flange faces.
 5. The O-ring and flanges are positively positioned during assembly.
 6. The knife edges on the flanges are protected from damage as they do not protrude above the flange faces.

DISADVANTAGES:

1. The system requires a new O-ring for each reassembly.

COMMENTS:

Data applies to a copper O-ring 1-1/16 inch in major diameter, 2R, and 1/16 inch in minor diameter, d.

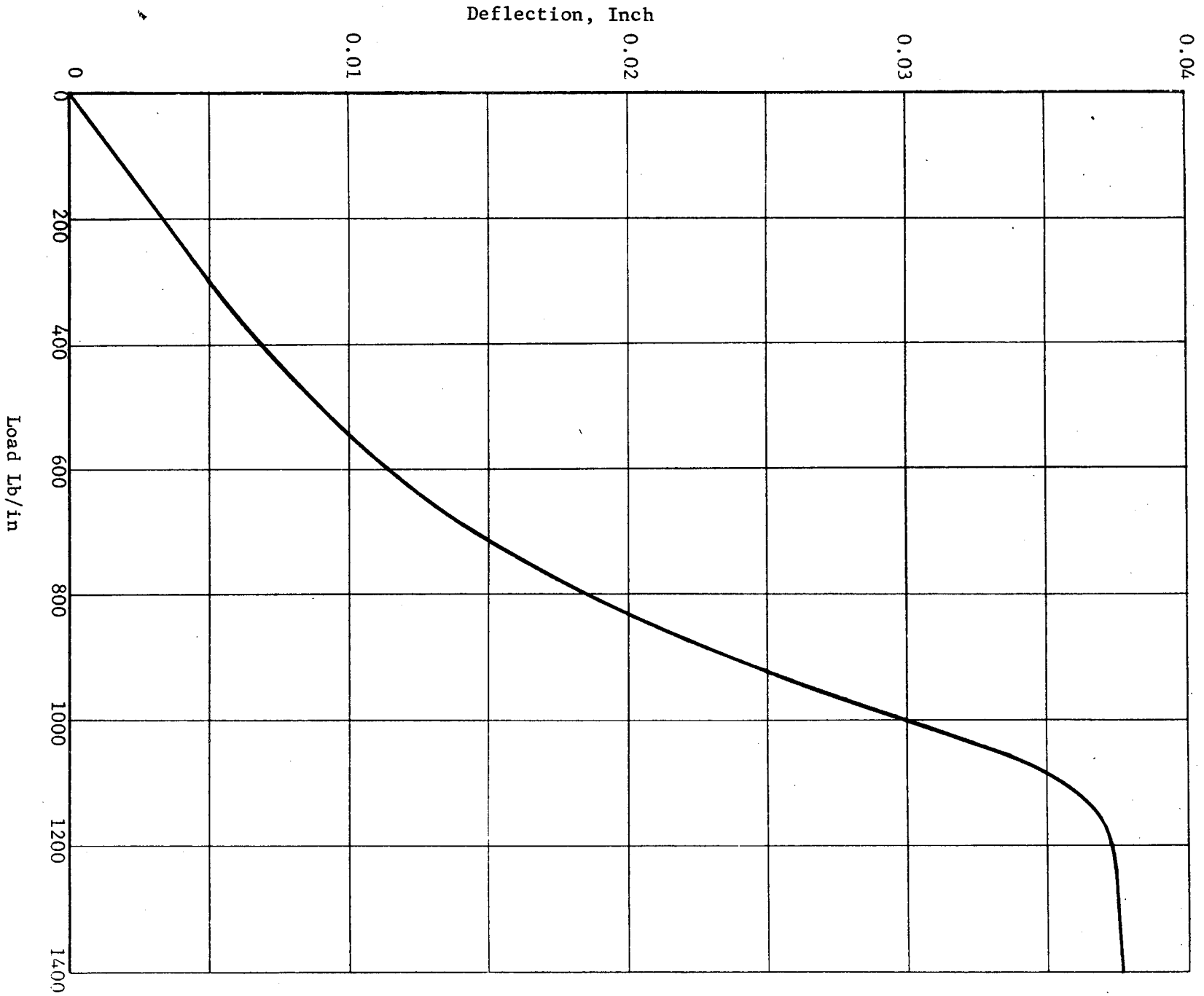


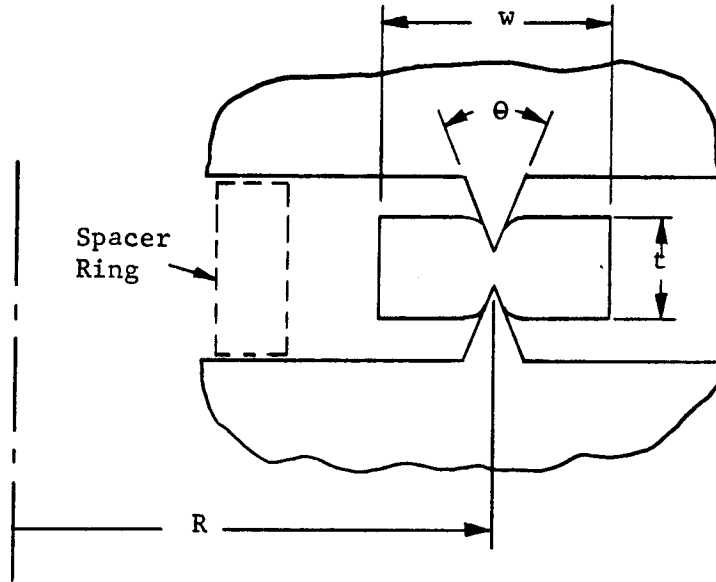
Figure 7.4. Load-Deflection Curve for Copper O-ring

7.1.3.3

CLASSIFICATION: Knife Edge Seal

MATERIAL: Gasket - 2S aluminum (copper, nickel, etc.). Knife edges are made from connector structural material

CONFIGURATION:
(Typical)



TEMPERATURE LIMITATIONS: Determined by creep properties of gasket material.

LOAD DEFLECTION CHARACTERISTICS: (2S aluminum, gasket, room temperature). Figures 7.5 and 7.6.

SEALING CHARACTERISTICS: (2S aluminum, gasket, room temperature) Where no spacer ring was used, and only a single load path existed through the gasket, no measurable leakage (less 10^{-7} atm cc/sec) is evident at a gasket load of 300 pounds per inch until the internal pressure reaches 1100 psi, at which point the leakage increases drastically. Where a spacer ring is used to fix the amount of gasket deformation, at an applied load of 500 pounds per inch, no measurable leakage is evident until the pressure increases to 1650 psi, at which time the leakage increases drastically. In that the knife edge seal can have many variations and configurations, the values cited herein are deemed typical values.

- ADVANTAGES:
1. Shear deformation of a gasket is used.
 2. Low sealing loads are required.
 3. Generally insensitive to load removal.
 4. Either single load path or double load paths can be used.
 5. Gasket geometries are simple and inexpensive to construct.

DISADVANTAGES:

1. New gasket is required upon each reuse.
2. The knife edges, being high relief, are prone to accidental scratching.

COMMENTS:

Data based on tests of systems with a nominal diameter, 2R, of one inch, with 60° included angle for knife edges, and gasket dimensions of t = 0.16 inch and width = 0.14 inch.

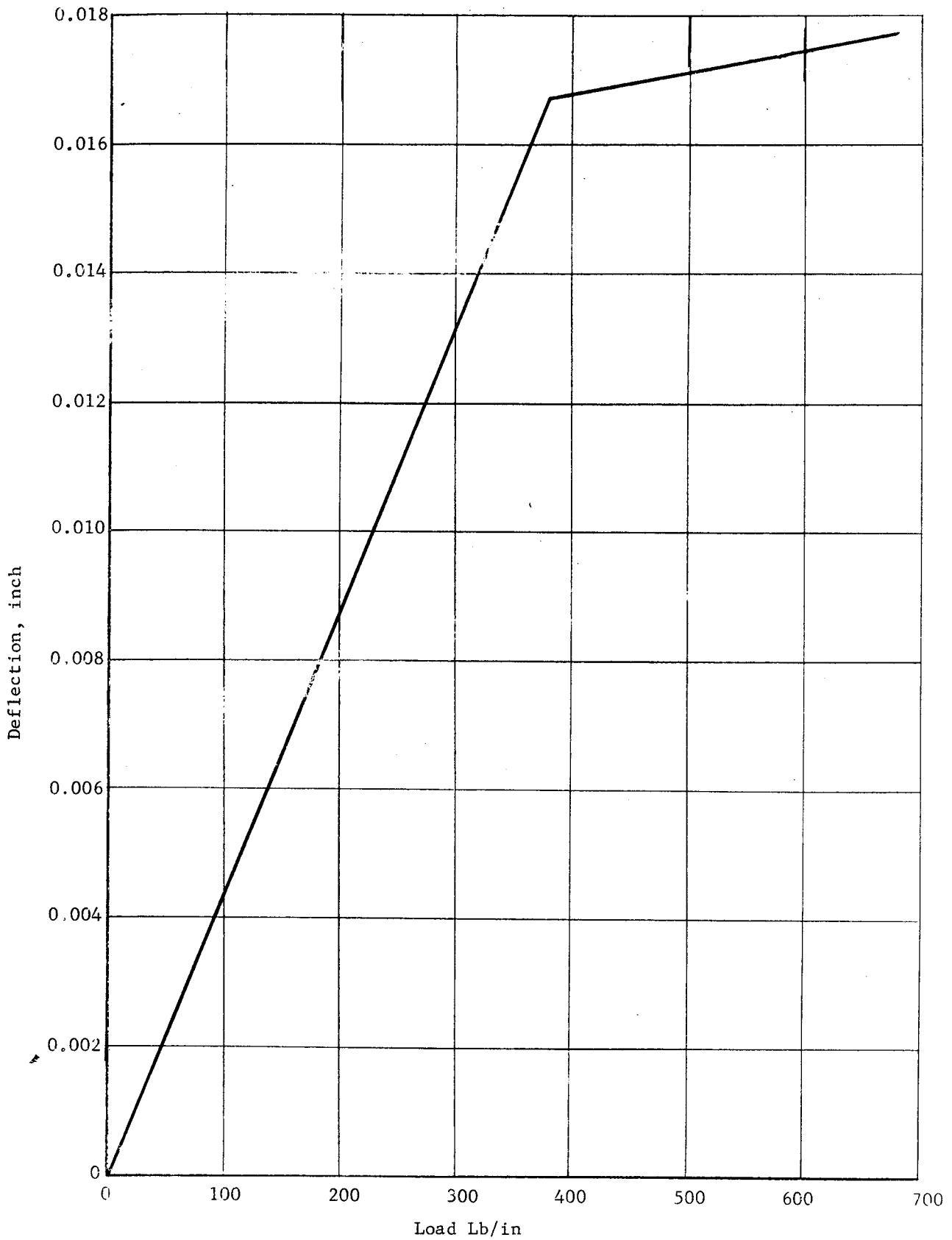


Figure 7. 5. Knife-Edge Seal Load-Deflection Curve for Aluminum Gasket with Inner Spacer Ring

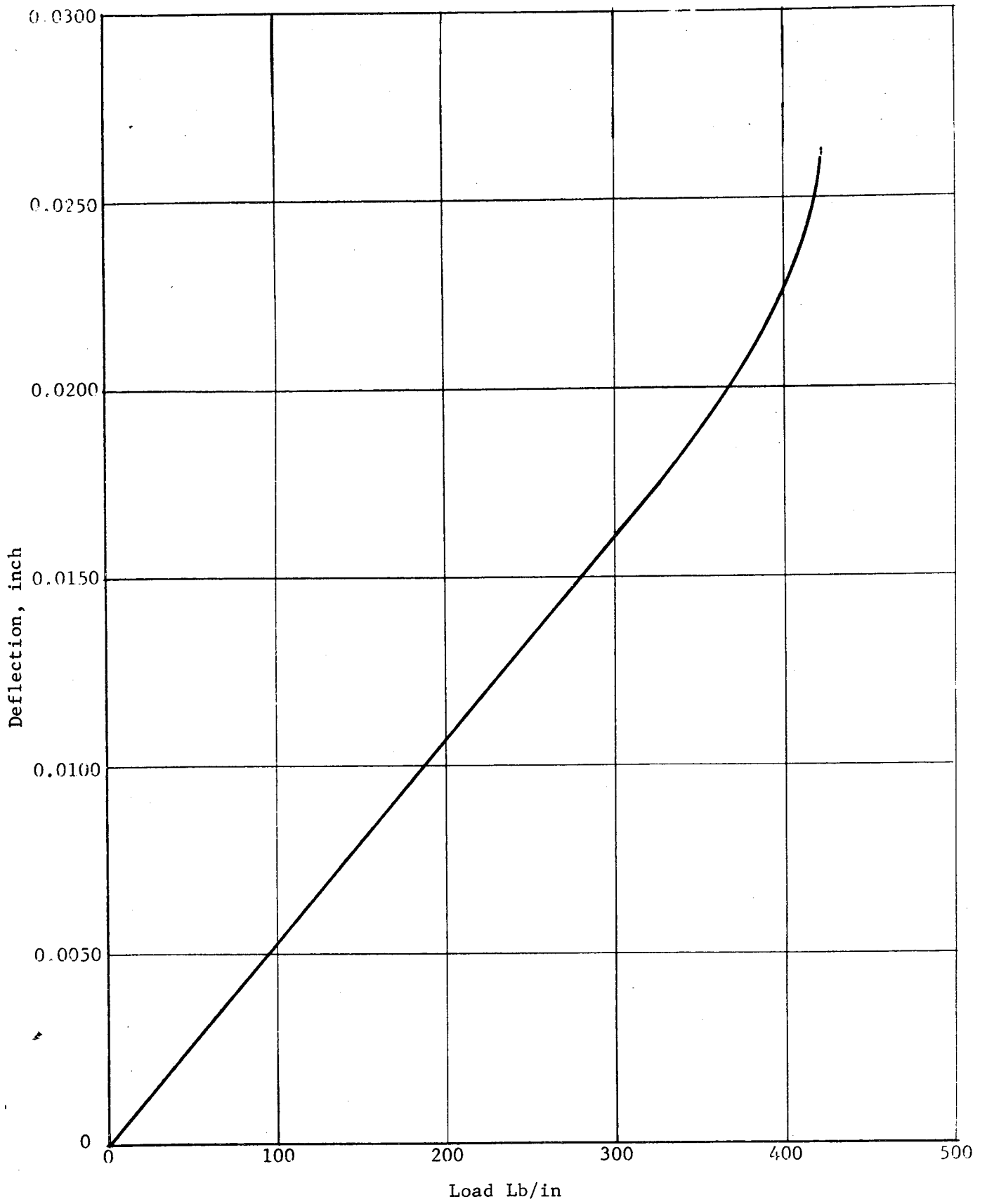


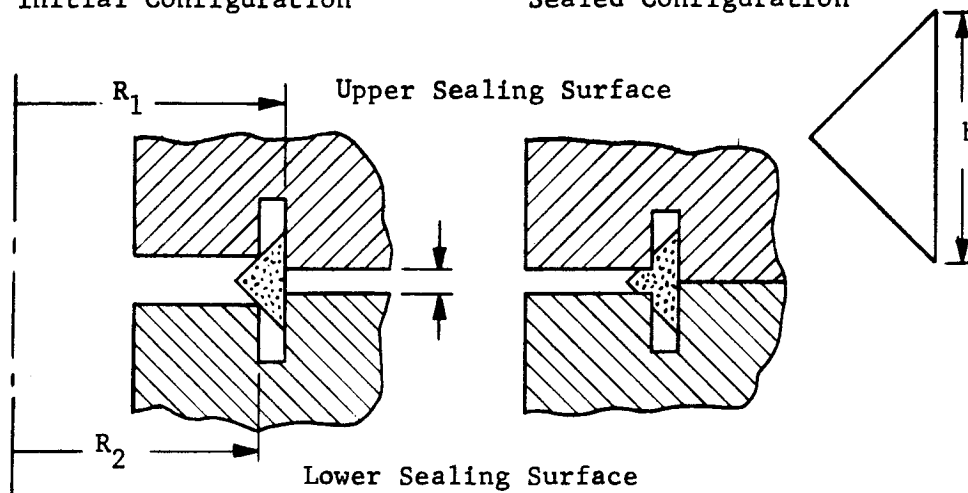
Figure 7. 6. Knife-Edge Seal Load-Deflection Curve for Aluminum Gasket Without Spacer Ring

7.1.3.4

CLASSIFICATION: Triangle Seal

MATERIAL: Gasket - 2S aluminum (copper, nickel, etc.). Knife edges constructed from connector structural material.

CONFIGURATION: Initial Configuration Sealed Configuration



TEMPERATURE LIMITATIONS: Determined by creep properties of gasket material.

LOAD DEFLECTION CHARACTERISTICS: (2S aluminum, room temperature): See Figure 7.7.

SEALING CHARACTERISTICS: (2S aluminum, room temperature): After 950 pounds per inch has been applied to the seal (thus causing a dual load path to exist) at an internal pressure of 1800 psi, the load can be reduced to 300 pounds per inch before leakage is evident. At this load, leakage increases drastically.

- ADVANTAGES:
1. Shear deformation of the gasket is utilized.
 2. Since the internal pressure pushes the gasket radially outward into the knife edges, the gasket is pressure energized.
 3. Desired amount of gasket deformation can be specified due to the dual load paths called for in the design.
 4. Knife edges, being at an angle to the seal centerline, make the seal insensitive to axial movement of the flange faces.
 5. Gasket flanges are positively positioned during assembly.
 6. Knife edges are protected from damage and they do not protrude above the flange faces.
 7. Gasket is contained by the flanges.

DISADVANTAGES:

1. Each reassembly requires a new gasket.

COMMENTS:

Data based on a sealing system having a nominal diameter of one inch.

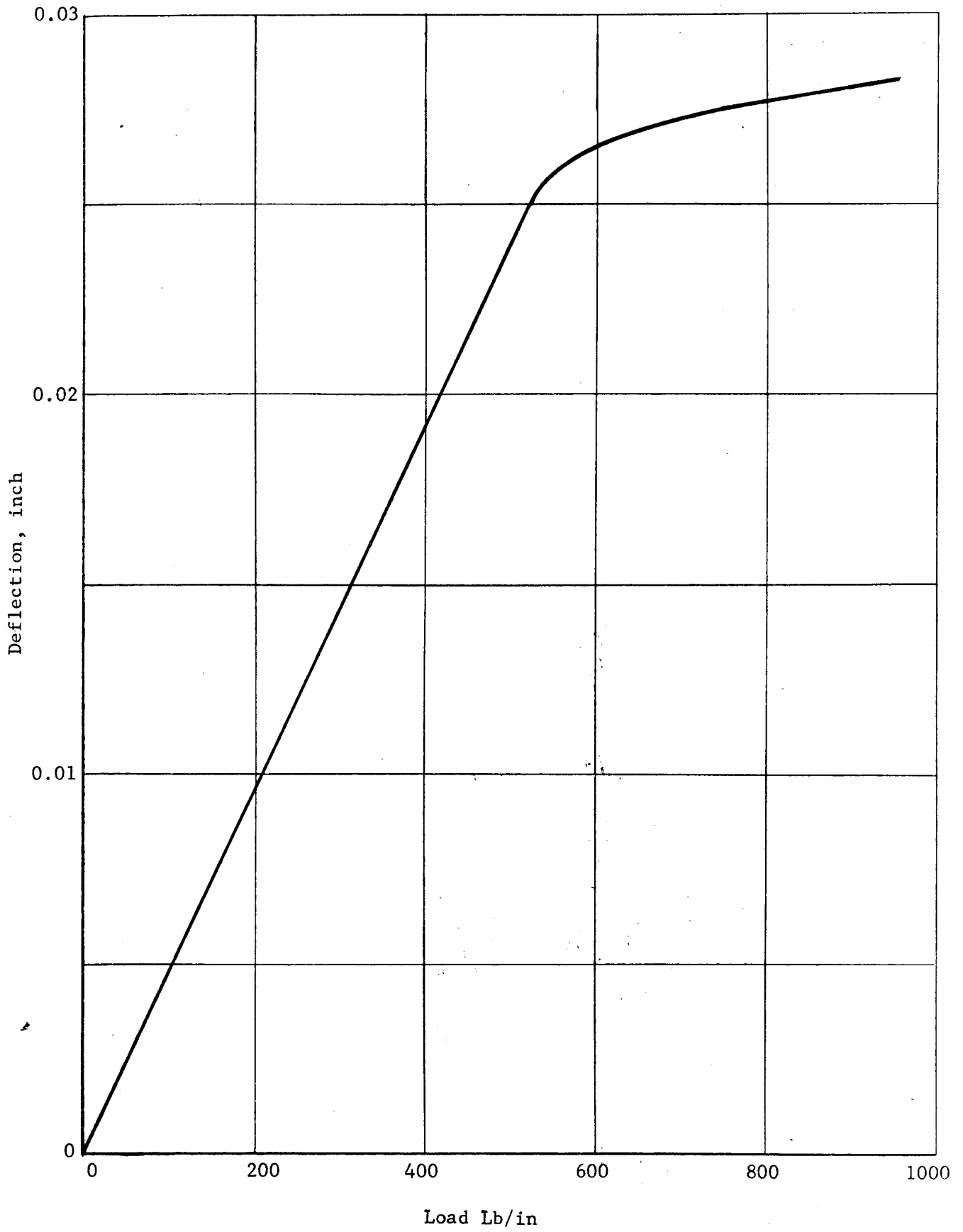


Figure 7.7. Triangle Seal Load-Deflection Curve for Aluminum Gasket

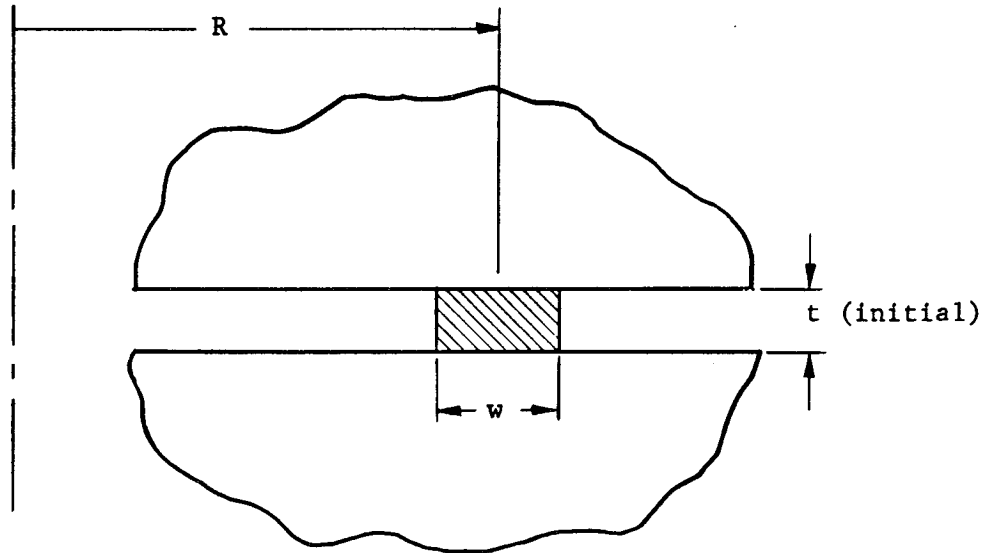
7.1.4 Plastic Gaskets

7.1.4.1 Flat Plastic Gasket on Flat Metal Structural Surfaces

CLASSIFICATION:

MATERIAL: KEL-F81 (Chlorotrifluoroethylene)

CONFIGURATION:



TEMPERATURE LIMITATIONS: -400°F to +400°F

SEALING CHARACTERISTICS: For the dimensions tested, KEL-F gaskets sealed to below 10^{-6} atm cc/sec helium at stress levels less than 4000 psi. The degree of sealing is independent of the surface finish of the metal flanges on which the gasket lies.

ADVANTAGES:

1. Low sealing stress
2. Mating independent of surface finish
3. Once sealed, leakage primarily due to diffusion. Hence fairly insensitive to increase in pressure (mating at interface between metal plastic fairly complete).
4. If loaded well above minimum sealing stress, fairly insensitive to reduction of load.

DISADVANTAGES:

1. Some cold flow deformation
2. Some gas diffusion

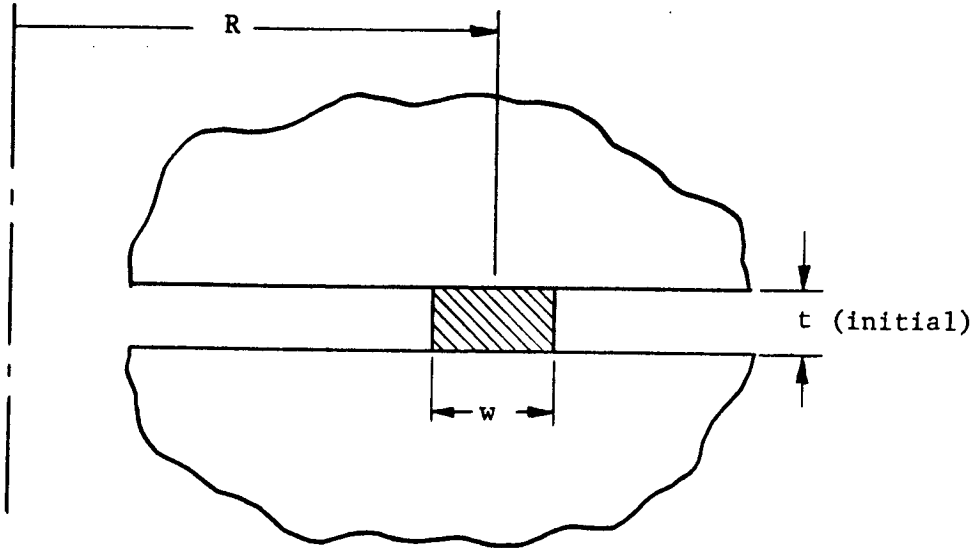
COMMENTS: Data gained on gaskets 1/8 inch wide. See Teflon TFE sheet for typical cold flow data.

7.1.4.2

CLASSIFICATION: Plastic Flat Gasket

MATERIAL: Teflon-TFE (tetrafluoroethylene)

CONFIGURATION:



TEMPERATURE LIMITATIONS: -450°F to +500°F

SEALING CHARACTERISTICS: System will seal down to gas diffusion leakage rate with stress levels as low as 1000 psi at internal pressures of 1000 psi, based on the geometry used. Sealing stress is insensitive to surface finish of flanges.

- ADVANTAGES:
1. Low sealing stress
 2. Extremely good mating at surface, independent of surface finish
 3. Insensitive to reduction of load

- DISADVANTAGES:
1. Cold flow deformation
 2. Containment must be provided to keep gasket from blowing out (see cold flow deformation below).
 3. Porous, gas diffusion may be excessive.

COLD FLOW DEFORMATION: Teflon TFE is used with a rough metal surface, and the gasket thickness is reduced such that it is not thicker than four or five times the peak-to-peak height of the asperities of the metal surfaces. The cold flow can be reduced considerably. The width to thickness should be at least ten to one.

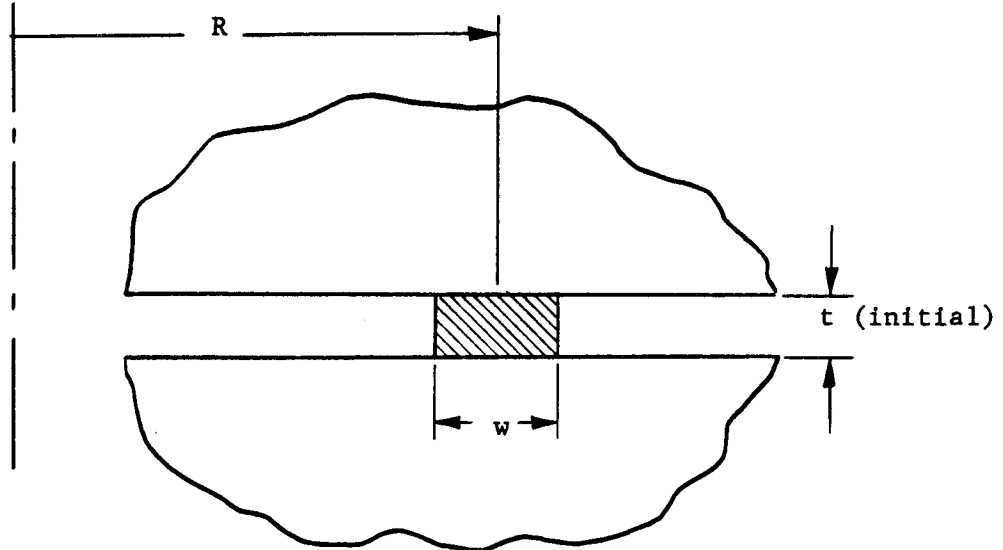
COMMENTS: Data gained from tests with one-eighth inch gaskets.

7.1.4.3

CLASSIFICATION: Plastic Flat Gasket

MATERIAL: Teflon FEP (fluorinated ethylene-propylene)

CONFIGURATION:



TEMPERATURE LIMITATION: -450°F to +400°F

SEALING CHARACTERISTICS: System will seal down to 10^{-6} atm cc/sec at low pressures at stress levels less than 2000 psi. Leakage thereafter is essentially due to gas diffusion. Mating at interfaces is nearly complete.

ADVANTAGES:

1. Low sealing stress
2. Rating independent of surface finish
3. Insensitive to reduction of load

DISADVANTAGES:

1. Large cold flow deformation
2. In general, restraint must be provided to keep gasket from blowing out. (See Teflon-TFE data.)
3. Gas diffusion problem

COMMENTS: Data gained from one-eighth inch gasket width samples.

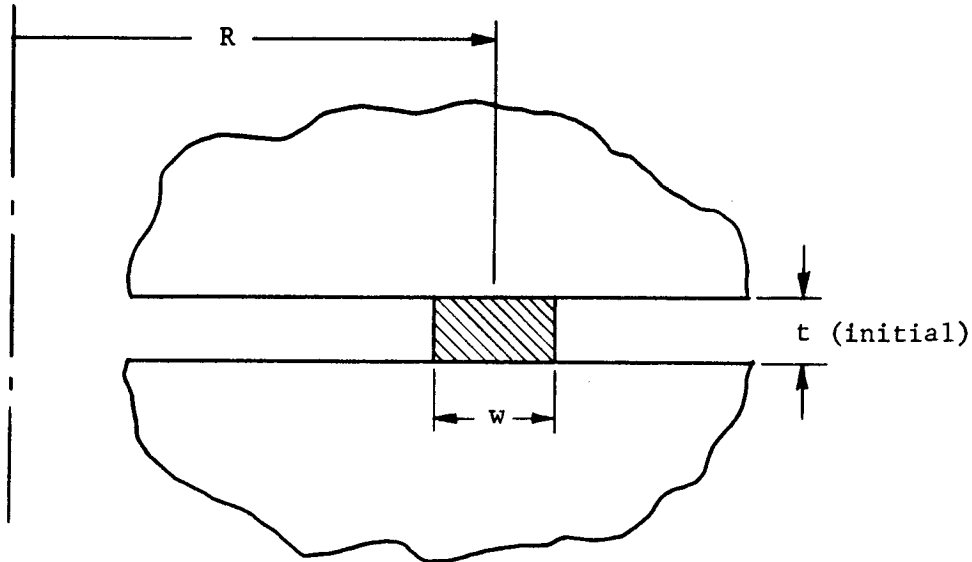
7.1.5 Elastomeric Gaskets

7.1.5.1

CLASSIFICATION: Elastomeric Flat Gaskets

MATERIAL: Neoprene, Viton-A, and Hypalon

CONFIGURATION:



TEMPERATURE
LIMITATION:

Near room temperature, dependent on fluid contained.

SEALING
CHARACTERISTICS:

Each material, based on the geometry and dimensions tested, will seal helium to a rate of 10^{-6} atm cc/sec at a stress level of 575 psi, at internal pressures of 1000 psi. Stress level is independent of surface finish on the metal mating surfaces.

ADVANTAGES:

1. Extremely low sealing stresses
2. Insensitive to flange surface finish
3. Almost complete mating between elastomer and metal surface, resulting in leakage by diffusion only.
4. Insensitive to reduction in stress level.
5. Low gas diffusion rate.

DISADVANTAGES:

1. Constraint must be provided to keep gasket in place.

COMMENTS:

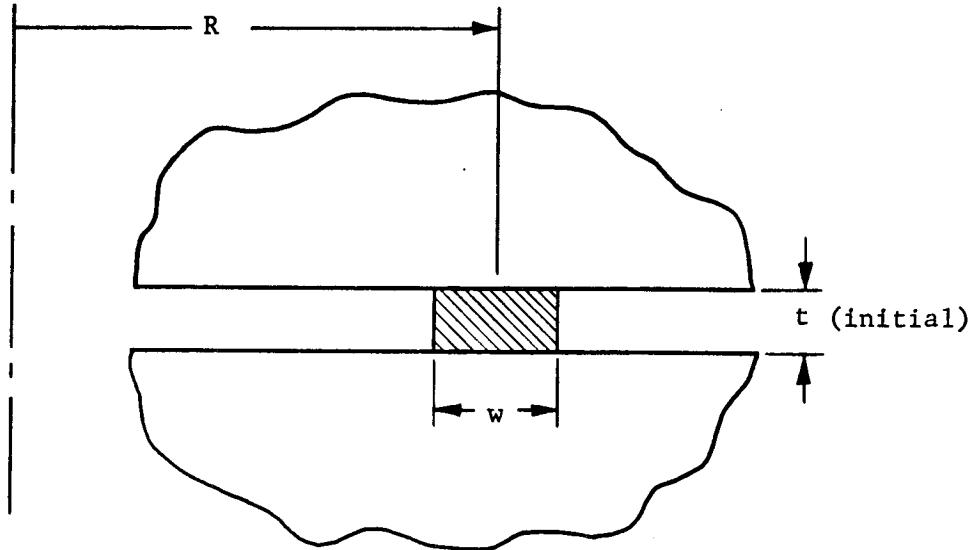
Data gained from tests on samples one-eighth inch wide.

7.1.5.2

CLASSIFICATION: Elastomeric Flat Gaskets

MATERIAL: Silicone rubber

CONFIGURATION:



TEMPERATURE LIMITATION:

Near room temperature, dependent on fluid contained.

SEALING CHARACTERISTICS:

Seals to gas diffusion level with a nominal gasket stress of 575 psi, at internal pressures of 1000 psi.

ADVANTAGES:

1. Very low sealing stress
2. Insensitive to flange surface finish
3. Insensitive to reduction in load

DISADVANTAGES:

1. Constraint must be provided to keep gasket from blowing out.
2. Large gas diffusion rate.

COMMENTS:

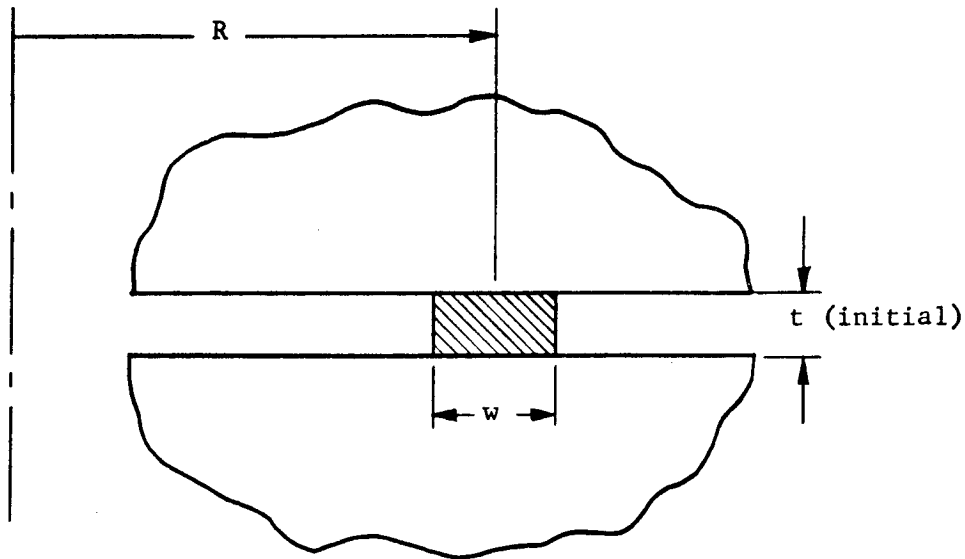
Data presented gained from gasket widths of one-eighth inch.

7.1.6 Miscellaneous

7.1.6.1

CLASSIFICATION: Metal-Asbestos Spiral Wound Gasket

CONFIGURATION:



TEMPERATURE LIMITATION:

Above 500°F

SEALING CHARACTERISTICS:

When mated with 32 microinch seal, circumferentially machined, flat metal surface, 3000 psi periphery are required to reduce the flow rate to below 10^{-6} atm cc/sec at an internal pressure of 1000 psi. Such a stress level is beyond the flexibility limit of the gasket. At a stress level of 2000 pounds per linear inch, the leakage rate with a 500 psi internal pressure is 10^{-4} atm cc/sec. At the latter stress level, the gasket is not completely flexible.

ADVANTAGES:

1. High temperature characteristics.
2. No special metal surface preparation.
3. Some flexibility, thus moderately insensitive to reduction of load.

DISADVANTAGES:

1. Incomplete sealing at interface, thus moderately high leakage level.

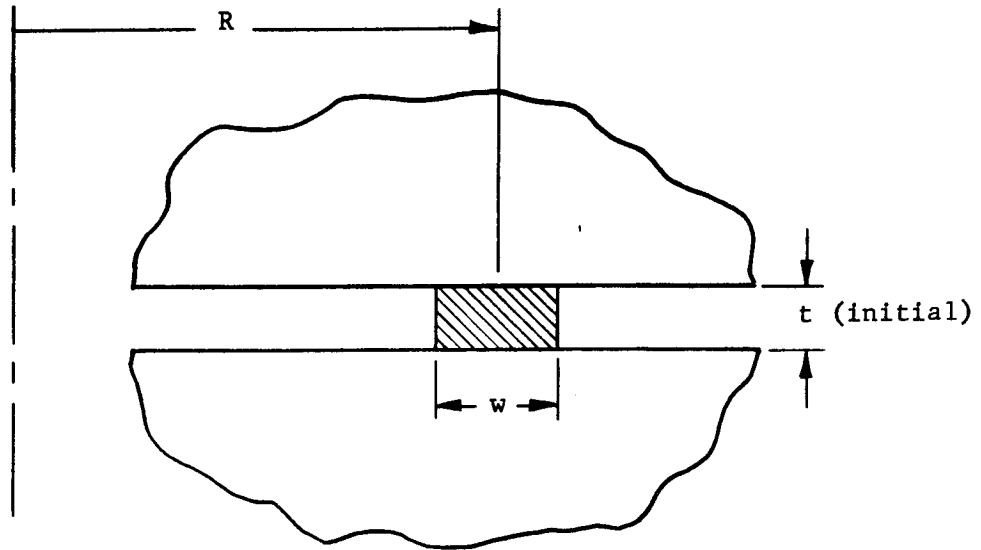
COMMENTS:

Data based on tests with gasket one-eighth inch thick, a mean diameter of one inch, and a gasket width of one-eighth inch.

7.1.6.2

CLASSIFICATION: Flat Fluorolube Impregnated Asbestos Gasket

CONFIGURATION:



TEMPERATURE
LIMITATION:

Cryogenic to room temperature

SEALING
CHARACTERISTICS:

When mated with a circumferentially machined surface with a 32 microinch finish, CLA, the system will seal to 10^{-5} atm cc/sec with a normally applied stress of 4300 psi at an internal pressure of 1100 psi.

ADVANTAGES:

1. Cryogenic use
2. Fluorolube liquid causes intimate mating at metal interface.
3. Simple to use.

DISADVANTAGES:

1. Fluorolube flows from the gasket under high stress.
2. Little flexibility in gasket.

COMMENTS:

Data based on tests on gaskets one-eighth inch wide.